Electronic Supplementary Material (ESI) for Chemical Science.

Supporting Information

Mono-*N*-Protected Amino Acid Ligands Stabilize Dimeric Palladium(II) Complexes of Importance to C-H Functionalization

Joseph J. Gair,[1] Brandon E. Haines,[2] Alexander S. Filatov,[1] Djamaladdin G. Musaev,[2]* and Jared C. Lewis[1]*

[1]Department of Chemistry, The University of Chicago, Chicago Illinois, 60637, United States

[2]Cherry L. Emerson Center for Scientific Computation, Emory University, 1515 Dickey Drive, Atlanta Georgia 30322, United States

E-mail: jaredlewis@uchicago.edu , dmusaev@emory.edu

Supporting information 1 of 4: Synthesis, characterization, experimental details

Supporting information 2 of 4: Computational Analysis

Supporting information 3 of 4: Annotated NMR spectra

Supporting information 4 of 4: Annotated mass spectra

Section S1.0: Methods and Materials

All commercially available reagents were used as received unless otherwise noted. Mono-protected amino acids were purchased from Chem-Impex. Thallium acetylacetonate (acac) was purchased from Strem. Palladium(II) acetate was purchased from Pressure Chemical. 2-(trifluoromethyl)pheny acetic acid was purchased from TCI. 2-(trifluoromethyl)benzyl bromide was purchased from Matrix Scientific. *N*,*N*-dimethylbenzylamine was purchased from Acros. 1,4-bis(trifluoromethyl)benzene were purchased from Alfa-Aesar. Iodobenzene dichloride was prepared by a reported procedure.[1]

All preparative reactions were conducted under air with solvents stored in air except where noted. In instances where anhydrous solvents were used, they were obtained from an Inert solvent purification system (1 hour sparge with nitrogen followed by passage over two columns of activated alumina). CD_2Cl_2 and $CDCl_3$ were dried by stirring over CaH_2 under nitrogen overnight followed by vacuum transfer into a Teflon sealed container and three cycles of freeze pump thaw. NMR tube reactions were set up in an inert atmosphere glovebox under circulating nitrogen either in a J. Young tube or an NMR tube with a rubber septum.

NMR spectra were acquired on a Bruker DRX-500 MHz spectrometer at ambient temperature unless otherwise specified. Chemical shifts are reported in ppm and coupling constants are reported in Hz. MPAA complexes with chiral MPAA's exist as nearly equal mixture of diastereomers in solution. Each of these mixtures had several baseline separated ^{1}H and ^{13}C resonances which enabled assignment of the connectivity of the MPAA and substrate fragments; however, the absolute stereochemistry each of the diastereomers could not be assigned by NMR. As such, each ^{1}H and ^{13}C signal is annotated by its connectivity rather than absolute stereochemistry in the spectra and chemical shifts listed below and more upfield of the two diastereomeric resonances is labeled with an apostrophe in the naming scheme below. Moreover, each annotated spectra is accompanied by a chemdraw representation of one of the two diastereomers for simplicity.

All NMR tube kinetics reactions were set up in dried degassed solvents in an inert atmosphere glovebox with stock solutions prepared in volumetric flasks and dispensed with gas tight syringes. In order to obtain kinetic data as near to the start of the reaction as possible, samples were prepared without palladium inside the glovebox, one sample was removed from the glovebox with a gas tight syringe containing the appropriate volume of the palladium stock solution. The sample was brought to the NMR spectrometer, locked, shimmed, ejected from the spectrometer, injected with the palladium stock solution through a rubber septum, shaken vigorously, lowered into the spectrometer, and data acquisition began as soon as a stable lock signal was obtained (typically less than 40 seconds after injection).

Section S1.1: Synthesis of Pd(dmba) complexes

Synthesis of [Pd(dmba)(OAc)]$_2$ (4)

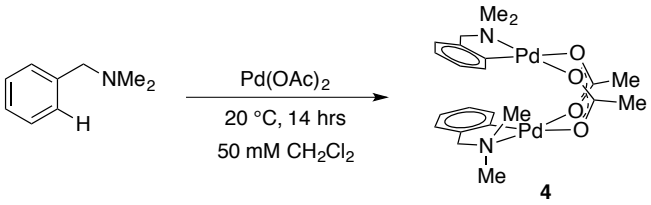

4 [Pd(dmba)(OAc)]$_2$ was prepared by a reported procedure[2] to give yellow crystals which matched the reported ^{1}H NMR of **4** [Pd(dmba)(OAc)]$_2$.

Jones, T. C.; Nielson, A. J.; Rickard, C. E. *Australian Journal of Chemistry* **1984**, *37*, 2179.

Synthesis of [Pd(dmba)(Cl)]$_2$ (S1)

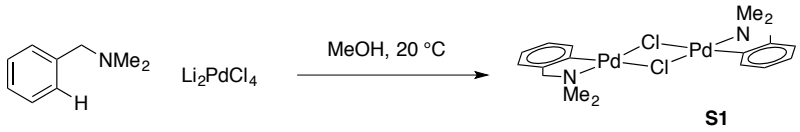

S1 [Pd(dmba)(Cl)]$_2$ was prepared by a reported procedure[3,4] to give a yellow powder which matched the ^{1}H NMR o**f S1** [Pd(dmba)(Cl)]$_2$.

Cope, A. C.; Friedrich, E. C. J. Am. Chem. Soc. 1968, 90 (4), 909.

Pfeffer, M. Inorganic Syntheses 1989, 26, 211.

Synthesis of Pd(dmba)(acac) (S2)

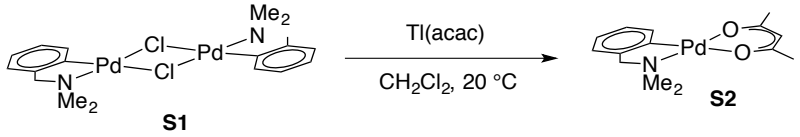

S2 Pd(dmba)(acac) was prepared by a reported procedure[5] to give a yellow powder which matched the ^{1}H NMR o**f S2** Pd(dmba)(acac).

Diaz-de-Villegas. Journal of Organometallic Chemistry 1995, 490, 35.

Synthesis of [Pd(dmba)(NAc-Gly)]$_2$ (2) from S1

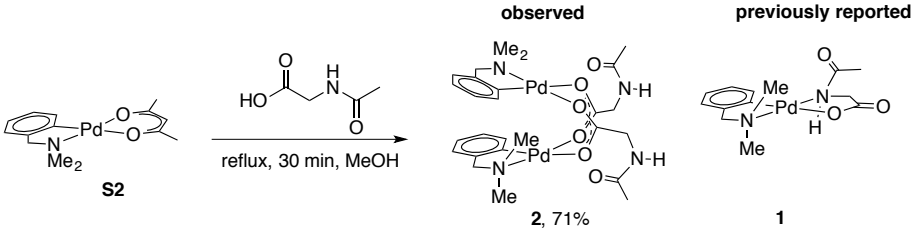

Complex **2** was prepared by a known procedure,[5] in which the products were assigned as the monomeric complex **1.** When the procedure was repeated, a complex with ^{1}H and ^{13}C NMR spectra matching those reported in the literature was obtained, but extensive characterization revealed that the structure in solution is **2**. Single crystals of complex **2** were obtained vapor diffusion of diethyl ether in to a concentrated of **2** in CH_2Cl_2 at 4 °C.

Diaz-de-Villegas. Journal of Organometallic Chemistry 1995, 490, 35.

Synthesis of 2 by C-H activation

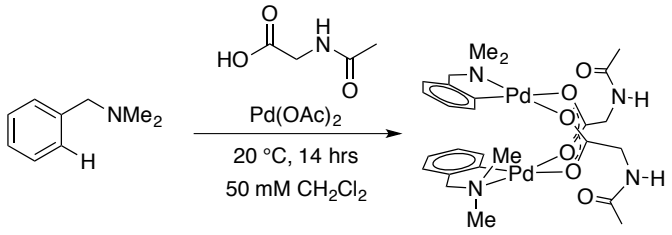

2, 57%

A 20 mL scintillation vial was charged with NAc-Gly (0.65 mmol, 76.1 mg, 1 equiv.), a stir bar, and 10 mL of methanol. The solution was stirred until the MPAA dissolved completely. To the MPAA solution was added solid $Pd(OAc)_2$ (0.65 mmol, 150 mg, 1 equiv.) and a solution of dmba (90 mg, 0.65 mmol, 1 equiv.) in 3 mL MeOH. The orange suspension gradually turned to a yellow solution and developed the smell of acetic acid. The solution was stirred for 14 hours at room temperature after which a 200 µL aliquot was concentrated in vacuo and to analyzed by ^{1}H NMR which revealed complete consumption of starting material and a 3:1 mixture of the desired product and a mixed MPAA/acetate complex. The remaining methanol solution was concentrated in vacuo and suspended in 3 mL toluene to azeotropically remove residual acetic acid in vacuo. The yellow solids were washed on a medium frit with 3x3mL diethyl ether to remove any remaining free acetic acid. The yellow solids were washed through the frit with 5x2 mL CH_2Cl_2 to remove any NAc-Gly. The CH_2Cl_2 solution was concentrated to 5mL, layered with 10 mL of diethyl ether, and stored over night at 4 °C. Decanting the supernatant afforded yellow solids that were not pure, but enriched in **2** by ^{1}H NMR. The enriched yellow solids were washed over a 1 cm pad of celite in a Pasteur pipette with 5x1 mL CH_2Cl_2, layered with 10 mL diethyl ether, and stored over night at 4 °C. The supernatant was decanted to afford 55.4 mg (23% yield) of pure **2** which matched the reported ^{1}H and ^{13}C NMR. The supernatant was concentrated by slow evaporation and layered with diethyl ether to afford an additional 77.1 mg of pure material to give a total of 132.5 mg (57% yield).

Section S1.2: Synthesis of Pd(CF_3-dmba) complexes

Synthesis of [Pd(CF_3-dmba)(OAc)]$_2$ (9)

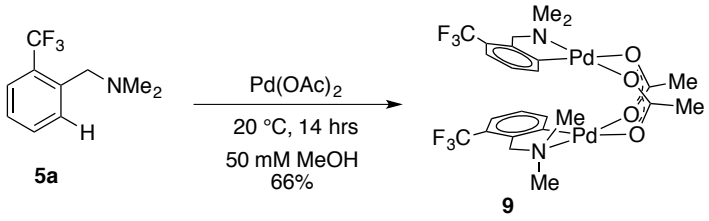

$Pd(OAc)_2$ (112 mg, 0.5 mmol, 1 equiv.) was weighed into a 20 mL scintillation vial, dissolved in 10 mL CH_2Cl_2, and treated with CF_3-dmba (**5a**) (101 mg, 92 µL, 0.5 mmol, 1 equiv.) at 20 °C. After 14 hours, the solvent was removed under reduced pressure, and the solids filtered over a pad of celite with diethyl ether 3x3mL, which was allowed to evaporate to ca. 1 mL under ambient conditions and layered with 5 mL pentane. After 14 h at 4 °C, the supernatant was decanted to afford 112 mg (66 % yield) of yellow crystals of [Pd(CF_3-dmba)(OAc)]$_2$ (**9**). **^{1}H NMR (500 MHz, CD_2Cl_2)** δ 2.06 (s, 6 H, NMe toward pi face), 2.07 (s, 6 H, OAc-CH_3), 2.78 (s, 6 H, NMe away from pi face), 3.48 (m, 4 H, benzylic CH_2), 7.08 (t, J=7.70 Hz, 2 H, meta to Pd), 7.28 (d, J=7.60 Hz, 2 H, ortho to Pd), 7.34 (d, J=7.65 Hz, 2 H, para to Pd). **^{13}C NMR (126 MHz, CD_2Cl_2)** δ 24.25 (s, OAc-CH_3), 51.12 (s, NMe toward pi face), 52.55 (s, NMe away from pi face), 70.11 (s, benzylic CH_2), 121.47 (m, CH para to Pd), 124.01 (q, J=273.36 Hz, CF_3), 124.08 (q, J=32.59 Hz, ipso to CF_3), 124.72 (s, CH meta to Pd), 135.83 (s, CH ortho to Pd), 143.73 (s, aromatic quaternary), 146.59 (s, aromatic quaternary), 180.88 (s, OAc-$\underline{C}O_2$). **^{19}F NMR (470 MHz, CD_2Cl_2)** δ -61.917

Synthesis of [Pd(CF_3-dmba)(NAc-Gly)]$_2$ (6a)

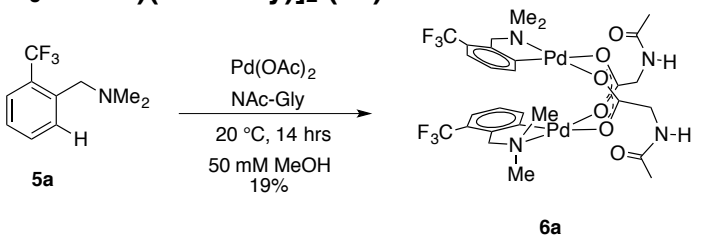

A 20 mL scintillation vial was charged with NAc-Gly (0.65 mmol, 76.1 mg, 1 equiv.), a stir bar, and 10 mL of methanol. The solution was stirred until the MPAA dissolved completely. To the MPAA solution was added solid $Pd(OAc)_2$ (0.65 mmol, 150 mg, 1 equiv.) and a solution of CF_3-dmba (132 mg, 0.65 mmol, 1 equiv.) in 3 mL MeOH. The orange suspension gradually turned to a yellow solution and developed the smell of acetic acid. The solution was stirred for 14 hours at room temperature after which a 200 µL aliquot was concentrated in vacuo and to analyzed by ^{19}F NMR which revealed complete consumption of starting material and 81% conversion to the desired product **6a** and 19% of mixed MPAA/ acetate complex **10**. Methanol was removed under a stream of nitrogen. The yellow solids were suspended in diethyl ether and transferred to a medium porosity frit where they were washed with 3x3mL diethyl ether to remove any free acetic acid. The yellow solids were washed through the frit with 5x2 mL 50:50 PhMe:CH_2Cl_2 to remove any NAc-Gly. The yellow PhMe:CH_2Cl_2 solution was layered with 5 mL diethyl ether, and stored over night at -35 °C. Decanting the supernatant afforded 53 mg (19% yield) of pure **6a**. Further crystallization of the precipitate resulted in material contaminated with 5-20% of the mixed acetate

MPAA complex **10**. Single crystals were grown from a concentrated solution of **6a** in CH_2Cl_2 layered with an equal volume of styrene oxide at -35 °C.

^{1}H NMR (500 MHz, CD_2Cl_2) δ 2.06 (s, 6 H, NAc-CH_3), 2.07 (s, 6 H, NMe toward pi face), 2.80 (s, 6 H, NMe away from pi face), 3.51 (m, 4 H, benzylic CH_2's), 3.94 (dd, J_{NH}=5.40, J_{HH}=17.79 Hz, 2 H, NAc-Gly C$\underline{H}^A$H^B), 4.05 (dd, J_{NH}=5.40, J_{HH}=17.79 Hz, 2 H, NAc-Gly CH$^A\underline{H}^B$), 6.38 (t, J_{NH}=5.40, 2 H, NH), 7.10 (t, J=7.72 Hz, 2 H, CH meta to Pd), 7.22 (d, J=7.15 Hz, 2 H, CH ortho to Pd), 7.37 (d, J=7.70 Hz, 2 H, para to Pd). **^{13}C NMR (126 MHz, CD_2Cl_2)** δ 22.92 (s, NAc-CH_3), 44.00 (s, Gly-CH_2), 51.50 (s, NMe toward pi face), 52.72 (s, NMe away from pi face), 70.29 (s, benzylic CH_2), 121.95 (m, CH para to Pd), 123.87 (q, J=273.39 Hz, CF_3), 124.31 (q, J=31.57 Hz, ipso to CF_3), 125.10 (s, CH meta to Pd), 135.53 (s, CH ortho to Pd), 143.65 (s, C aromatic quaternary), 145.44 (s, C aromatic quaternary), 169.77 (s, NAc-Gly $\underline{C}$(O)N),178.97 (s, NAc-Gly $\underline{C}O_2$). **^{19}F NMR (470 MHz, CD_2Cl_2)** δ -62.1103

Treating mixtures of **6a** and **10** in acetone with with an excess of aqueous lithium chloride generally afforded good conversion to the chloride bridged dimer **8**.[6]

Hiraki, K.; Fuchita, Y.; Pfeffer, M. 6-Membered Cyclopalladated Complexes of 2-benzylpyridine; Inorganic Syntheses, Vol 28, pp 208-211, 1989.

Synthesis of [Pd(CF_3-dmba)(NAc-Ala)]$_2$ (6b)

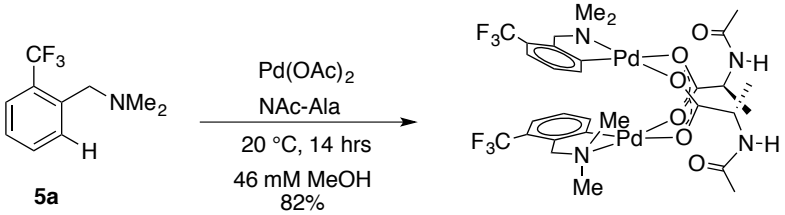

5a **6b**

A 200 mL round bottom flask was charged with NAc-Ala (2.29 mmol, 300 mg, 1 equiv.), a stir bar, and 40 mL of methanol. The solution was stirred until the MPAA dissolved completely. To the MPAA solution was added solid $Pd(OAc)_2$ (2.20 mmol, 514 mg, 1 equiv.) and a solution of CF_3-dmba (2.29 mmol, 465 mg, 1 equiv.) in 10 mL MeOH. The orange suspension gradually turned to a yellow solution and developed the smell of acetic acid. The solution was stirred for 14 hours at room temperature after which a 200 µL aliquot was concentrated in vacuo and to analyzed by ^{19}F NMR which revealed complete consumption of starting material and 91% conversion to the desired product **6b**. Methanol was removed under a stream of nitrogen. The yellow solid was filtered over a medium porosity frit with 4x3 mL CH_2Cl_2. The yellow solution was allowed to slowly evaporate to ca. 5 mL and crystallized by slow diffusion of diethyl ether (5 mL) at -35 °C to give 825 mg (82% yield) of **6b**. Single crystals suitable for x-ray diffraction were grown by slow evaporation of a 5 mM solution of **6b** in acetonitrile under ambient conditions.

^{1}H NMR (500 MHz, CD_2Cl_2) δ 1.33 (t, J=6.55 Hz, 6 H, Ala CH_3 + Ala CH_3'), 2.00 (s, 3 H, NAc CH_3'), 2.04 (s, 3 H, NAc CH_3), 2.05 (s, 3 H, NMe upfield'), 2.07 (s,1 3 H, NMe upfield), 2.81 (s, 3 H, NMe downfield'), 2.81 (s, 3 H, NMe downfield), 3.53 (m, 4 H, benzylic CH_2 + benzylic CH_2'), 4.39 (m, 1 H, Ala methine'), 4.45 (m, 1 H, Ala methine), 6.24 (d, J=7.00 Hz, 1 H, NH'), 6.28 (d, J=6.75 Hz, 1 H, NH), 7.09 (m, 2 H, CH meta to Pd + CH meta to Pd'), 7.17 (d, J=7.60 Hz, 1 H, CH ortho to Pd'), 7.24 (d, J=7.75 Hz, 1 H, CH ortho to Pd), 7.37 (d, J=7.75 Hz, 2 H, CH para to Pd + CH para to Pd'). **^{13}C NMR (126 MHz, CD_2Cl_2)** δ 18.87 (s, Ala CH_3'), 18.99 (s, Ala CH_3), 23.05 (s, NAc CH_3 + NAc CH_3'), 50.69 (s, Ala CH'), 50.72 (s, Ala CH), 51.51 (s, NMe toward pi face + NMe toward pi face'), 52.75 (s, NMe away from pi face'), 52.79 (s,

NMe away from pi face), 70.26 (s,1 benzylic CH_2 + benzylic CH_2'), 121.81 (m, CH para to Pd + CH para to Pd'), 123.91 (q, J=273.27 Hz, CF_3 + CF_3'), 124.25 (q, J=31.26 Hz, C ipso to CF_3'), 124.27 (q, J=31.38 Hz, C ipso to CF_3), 124.96 (s, CH meta to Pd'), 125.02 (s, CH meta to Pd), 135.55 (s, CH ortho to Pd'), 135.65 (s, CH ortho to Pd), 143.65 (s, quaternary aromatic), 143.68 (s, quaternary aromatic), 145.77 (s, quaternary aromatic), 145.84 (s, quaternary aromatic), 168.96 (s, C(O)N'), 169.00 (s, C(O)N), 181.73 (s, CO_2'), 181.79 (s, CO_2) **^{19}F NMR (470 MHz, CD_2Cl_2)** δ -61.975 (s), -61.986 (s).

Synthesis of $[Pd(CF_3\text{-dmba})(NAc\text{-Leu})]_2$ (6c)

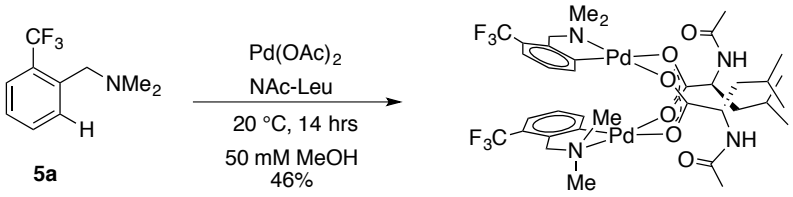

5a **6c**

A 20 mL scintillation vial was charged with NAc-Leu (0.5 mmol, 86.5 mg, 1 equiv.), a stir bar, and 8 mL of methanol. The solution was stirred until the MPAA dissolved completely. To the MPAA solution was added solid $Pd(OAc)_2$ (0.5 mmol, 112 mg, 1 equiv.) and a solution of CF_3-dmba (102 mg, 0.5 mmol, 1 equiv.) in 2 mL MeOH. The orange suspension gradually turned to a yellow solution and developed the smell of acetic acid. The solution was stirred for 14 hours at room temperature after which a 200 µL aliquot was concentrated in vacuo and to analyzed by ^{19}F NMR which revealed complete consumption of starting material and 62% conversion to **6c**. Methanol was removed under a stream of nitrogen and the yellow solid filtered through a medium porosity frit with benzene (4x 3 mL). The yellow benzene solution was concentrated to c.a. 5 mL under a stream of nitrogen and layered with 5 mL of pentane. After 14 h of slow diffusion of pentane into the benzene solution, the supernatant was decanted and the solids washed with pentane to afford 106 mg (46%yield) **6c**. Single crystals suitable for x-ray diffraction were grown by layering 1 mL of 10 mM **6c** in CH_2Cl_2 with 1 mL PhMe followed by 2 mL n-heptane.

NMR (500 MHz, CD_2Cl_2) δ 0.98 (m, 12 H, Leu CH_3's), 1.51 (m, 4 H, Leu CH_2's), 1.68 (m, 2 H, Leu CH's), 2.00 (s, 3 H, NAc CH_3'), 2.04 (s, 3 H, NMe toward pi face'), 2.07 (s, 3 H, NAc CH_3), 2.07 (s, 3 H, NMe toward pi face), 2.78 (s, 3 H, NMe away from pi face'), 2.80 (s, 3 H, NMe away from pi face), 3.52 (m, 4 H, benzylic CH_2 + benzylic CH_2'), 4.44 (m, 1 H, Leu Hα'), 4.53 (m, 1 H, Leu Hα), 5.95 (d, J=8.55 Hz, 1 H, NH'), 6.04 (d, J=8.35 Hz, 1 H, NH), 7.10 (m, 3 H, CH ortho to Pd' + CH's meta to Pd), 7.28 (d, J=7.45 Hz, 1 H, CH ortho to Pd), 7.35 (d, J=7.50 Hz, 2 H, CH para to Pd + CH para to Pd') **^{13}C NMR (126 MHz, CD_2Cl_2)** δ 21.59 (s, Leu CH_3'), 22.91 (s, Leu CH_3), 22.94 (s, Leu CH_3), 23.04 (s, NAc CH_3'), 23.06 (s, NAc CH_3), 25.00 (s, Leu CH'), 25.02 (s, Leu CH), 42.41 (s, Leu CH_2'), 42.47 (s, Leu CH_2), 51.54 (s, NMe toward pi face'), 51.60 (s,NMe toward pi face), 52.68 (s, NMe away from pi face'), 52.74 (s, NMe away from pi face), 53.39 (s, Leu Cα'), 53.43 (s, Leu Cα), 70.27 (s, benzylic CH_2'), 70.29 (s, benzylic CH_2'), 121.74 (m, CH para to Pd + CH para to Pd'), 123.92 (q, J=273.34 Hz, CF_3'), 123.93 (q, J=273 Hz, CF_3), 124.15 (q, J=31.38 Hz, C ipso to CF_3'), 124.22 (q, J=31.10 Hz, C ipso to CF_3'), 124.82 (s, CH meta to Pd'), 124.98 (s, CH meta to Pd), 135.48 (s, CH ortho to Pd'), 135.84 (s, CH ortho to Pd), 143.61 (s, aromatic quaternary), 143.73 (s, aromatic quaternary),145.91 (s, aromatic quaternary), 146.02 (s, aromatic quaternary), 169.23 (s, C(O)N'),169.25 (s, C(O)N), 181.87 (s, CO_2'),181.90 (s, CO_2) **^{19}F NMR (470 MHz, CD_2Cl_2)** δ -61.944, -61.976

Synthesis of $[Pd(CF_3\text{-dmba})(NAc\text{-Ile})]_2$ (6d)

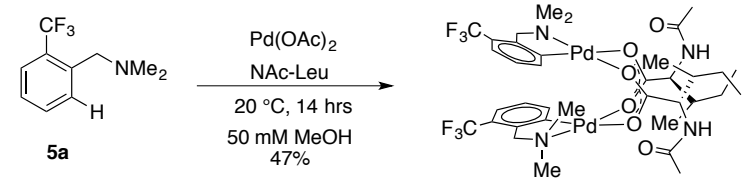

A 20 mL scintillation vial was charged with NAc-Ile (0.5 mmol, 86.5 mg, 1 equiv.), a stir bar, and 8 mL of methanol. The solution was stirred until the MPAA dissolved completely. To the MPAA solution was added solid $Pd(OAc)_2$ (0.5 mmol, 112 mg, 1 equiv.) and a solution of CF_3-dmba (102 mg, 0.5 mmol, 1 equiv.) in 2 mL MeOH. The orange suspension gradually turned to a yellow solution and developed the smell of acetic acid. The solution was stirred for 14 hours at room temperature after which a 200 µL aliquot was concentrated in vacuo and to analyzed by ^{19}F NMR which revealed complete consumption of starting material and 69% conversion to **6d**. Methanol was removed under a stream of nitrogen and the yellow solids were suspended in 2 mL diethyl ether. The suspension was transferred to a medium porosity frit and washed 2x 2 mL diethyl ether to remove residual acetic acid (note, the diethyl ether filtrate contains a substantial quantity of **6d**). The yellow solids on the frit were washed into a separate flask with 5 x 1 mL CH_2Cl_2 and precipitated by slow diffusion with 10 mL pentane at room temperature to afford 103.2 mg (47% yield) of **6d**.

^{1}H NMR (500 MHz, CD_2Cl_2) δ 0.89 (m, 6H, Ile Me + Me'), 0.95 (m, 6H, Ile Et-CH_3 + Et-CH_3'), 1.18 (m, 2H, Ile Et-CH^a_2 + Et-CH^a_2'), 1.44 (m, 2H, Ile Et-CH^b_2 + Et-CH^b_2'), 1.87 (m, 2H, Ile CH + CH'), 2.01 (s, 3H, NAc-CH_3'), 2.03 (s, 3H, NMe' toward pi face), 2.04 (s, 3H, NMe toward pi face), 2.06 (s, 3H, NAc-CH_3), 2.78 (s, 3H, NMe' away from pi face), 2.81 (s, 3H, NMe away from pi face), 3.55 (m, 4H, benzylic CH_2's), 4.40 (dd, J=5.0, 8.9 Hz, 1 H, Ile Hα'), 4.47 (dd, J=5.0, 8.9 Hz, 1 H, Ile Hα), 6.13 (t, J=8.9 Hz, 1H, NH'), 6.21 (t, J=8.9 Hz, 1H, NH), 7.09 (m, 3H, CH's meta to Pd + CH ortho to Pd'), 7.29 (d, J=7.40 Hz, 1H, CH ortho to Pd), 7.36 (d, J=7.45 Hz, 1H, CH para to Pd + CH para to Pd') **^{13}C NMR (126 MHz, CD_2Cl_2)** δ 11.48 (s, Ile Et-CH_3'), 11.49 (s, Ile Et-CH_3), 15.40 (s, Ile Me'), 15.43 (s, Ile Me), 23.12 (s, NAc-CH_3'), 23.13 (s, NAc-CH_3), 25.17 (s, Ile Et-CH_2'), 25.21 (s, Ile Et-CH_2), 38.20 (s, Ile-CH'), 38.25 (s, Ile-CH), 51.47 (s, NMe' toward pi face), 51.71 (s, NMe' toward pi face), 52.77 (s, NMe' + NMe away from pi face), 59.13 (s, Ile Cα'), 59.31 (s, Ile Cα), 70.22 (s, benzylic CH_2'), 70.35 (s, benzylic CH_2), 121.82 (m, CH para to Pd + CH para to Pd'), 123.90 (q, J=273.57 Hz, CF_3 + CF_3'), 124.21 (q, J=32.0 Hz, C ipso to CF_3'), 124.31 (q, J=31.4 Hz, C ipso to CF_3), 124.85 (s, CH meta to Pd'), 124.99 (s, CH meta to Pd), 135.46 (s, CH ortho to Pd'), 135.82 (s, CH ortho to Pd), 143.54 (s, C aromatic quaternary), 143.68 (s, C aromatic quaternary), 145.73 (s, C aromatic quaternary), 145.77 (s, C aromatic quaternary), 169.04 (s, C(O)N'), 169.08 (s, C(O)N), 180.44 (s, CO_2'), 180.59 (s, CO_2) **^{19}F NMR (470 MHz, CD_2Cl_2)** δ -61.932, -61.967

Synthesis of $[Pd(CF_3\text{-dmba})(Cl)]_2$ (8)

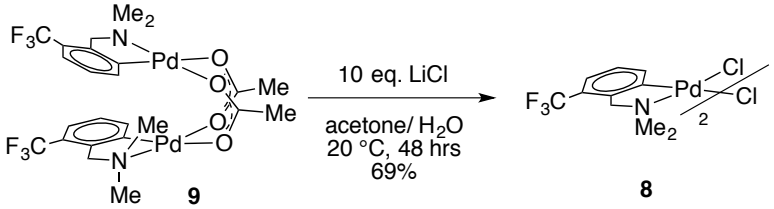

Chloride bridged dimer **8** was prepared by modification of a known procedure.[7] In 100 mL round bottom flask was with a magnetic stir bar, **9** (0.5 mmol, 382 mg, 1 equiv.) was dissolved in 20 mL acetone. The acetone solution was treated with 10 mL of aqueous lithium chloride (5.0 mmol, 212 mg, 10 equiv.) and flask was sealed with a rubber septum. After two days at room temperature, acetone was removed under reduced pressure to afford a yellow solid which was washed with 3x10 mL water. The yellow solid was washed through a medium porosity frit with diethyl ether, which was concentrated to c.a. 3 mL under a stream of nitrogen and layered with pentane to afford 475 mg (69% yield) of **8** as a mixture of two isomers (as has been previously noted for analogous chloride bridged dmba palladacycles).[7]

^{1}H NMR (500 MHz, CD_2Cl_2) δ 2.89 (s, 6 H), 2.90 (s, 6 H), 4.14 (m, 4 H), 7.04 (t, J=7.75 Hz, 2 H), 7.34 (d, J=7.70 Hz, 2 H), 7.40 (m, 2 H) **^{13}C NMR (126 MHz, CD_2Cl_2)** δ 52.86 (s), 53.05 (s), 70.98 (s), 71.21 (s), 121.82 (q, J=5.12 Hz), 123.98 (q, J=273.21 Hz), 124.13 (q, J=31.19 Hz), 124.91 (s), 125.03 (s), 136.76 (s), 137.09 (s), 144.06 (m), 145.38 (s) **^{19}F NMR** (470 MHz, CD_2Cl_2) δ -61.646 (s), -61.682 (s)
Milani, J.; Pridmore, N. E.; Whitwood, A. C.; Fairlamb, I. J. S.; Perutz, R. N. Organometallics 2015, 34 (17), 4376.

Synthesis of Pd(CF_3-dmba)(acac) (7)

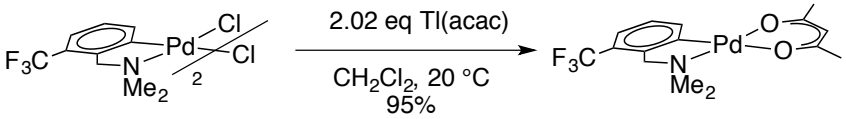

8 **7**

The acac complex **7** was prepared by modification of a known procedure.[5] In an inert atmosphere glove box, a 20 mL scintillation vial equipped with a magnetic stirrer was dissolved complex **8** (306 mg, 0.445 mmol, 1 equiv.) in 5 mL CH_2Cl_2. To this solution was added solid thallium acetonylacetonate (0.898 mmol, 273 mg, 2.02 equiv.). A white solid precipitated immediately and the suspension was stirred for 1 hour after which the suspension was passed over a medium porosity frit, washed with CH_2Cl_2 3x 3 mL and concentrated under reduced pressure to afford **7** 345 mg (95% yield).

^{1}H NMR (500 MHz, CD_2Cl_2) δ 2.01 (s,3 H), 2.05 (s,3 H), 2.87 (s,6 H), 4.10 (s,2 H), s,1 H), 7.11 (t, J=7.63 Hz, 1 H), 7.32 (d, J=7.70 Hz, 1 H), 7.53 (d, J=7.65 Hz, 1 H) **^{13}C NMR (126 MHz, CD_2Cl_2)** δ 27.22 (s), 27.77 (s), 51.85 (s), 71.16 (q, J=2.05 Hz), 99.92 (s), 121.18 (q, J=5.34 Hz), 123.38 (q, J=30.56 Hz), 124.48 (q, J=271.15 Hz), 134.66 (m), 144.09 (m), 148.98 (s), 186.26 (s), 188.45 (s) **^{19}F NMR (470 MHz, CD_2Cl_2)** δ -61.541
Diaz-de-Villegas. Journal of Organometallic Chemistry 1995, 490, 35.

Section S1.3: Synthesis of substrate and authentic standards

Synthesis of CF_3-dmba (5a)

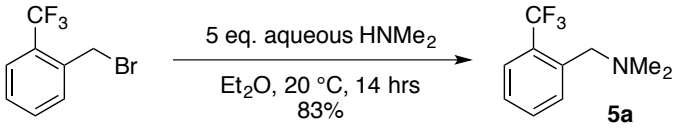

5a

5a was prepared by a previously reported procedure with minor modification.[8] To a 500 mL round bottom flask equipped with a magnetic stir bar was added the benzylic bromide (100.4 mmol, 24g, 1 equiv.) and 100 mL diethyl ether. To the ethereal solution was added aqueous dimethylamine (502 mmol, 56.5g (40 wt%), 5 equiv.). The heterogeneous mixture was stirred for 14 h at room temperature, after which the organic phase was separated and extracted 3 times with 10 wt% aqueous citric acid. The combined aqueous phases were treated with 15 wt% aqueous sodium hydroxide and extracted 3 times with diethyl ether. The ethereal extracts were concentrated under reduced pressure and the clear liquid was further purified by short path distillation (0.08 mmHg, 60 °C) into a receiving flask cooled to -10 °C to afford 16.86g (83% yield) of **5a**.

^{1}H NMR (**500 MHz, CD_2Cl_2)** δ 2.31 (s, 6H, NMe_2), 3.64 (s, 2H, CH_2), 7.39 (t, J=7.63 Hz, H^c), 7.59 (t, J=7.58 Hz, H^b), 7.68 (d, J=7.85 Hz, H^d), 7.85 (d, J=7.80 Hz, H^a) **^{13}C NMR (126 MHz, CD_2Cl_2)** δ 45.29 (s, NMe_2), 59.51 (q, J=1.72 Hz, CH_2), 124.63 (q, J=271.19 Hz, CF_3), 125.50 (q, J=5.89 Hz, CH ortho to CF_3), 126.65 (s, CH para to CH_2), 128.22 (q, J=29.97 Hz, C ipso to CF_3), 130.52 (s, CH ortho to CH_2), 131.78 (m, CH para to CF_3), 138.69 (q, J=1.47 Hz, C ipso to CH_2) **^{19}F NMR** (470 MHz, $CDCl_3$) δ -59.04
Tayama, E.; Kimura, H. Angew. Chem. Int. Ed. 2007, 46 (46), 8869.

Synthesis of Cl-CF_3-dmba (5b)

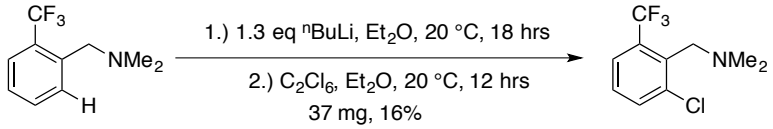

5a **5b**

A 25 mL round bottom flask equipped with a magnetic stir bar and septum was evacuated and refilled with nitrogen 3 times. To the flask, under nitrogen, was added **5a** (1 mmol, 203 mg, 1 equiv.) and 2.5 mL anhydrous diethyl ether. To the ethereal solution, n-butyl lithium (1.3 mmol, 0.845 mL (1.54M), 1.3 equiv.) was added drop-wise. The mixture was stirred under nitrogen for 18 hours at room temperature. Hexachloroethane (1.3 mmol, 308 mg, 1.3 equiv.) was added drop-wise under nitrogen as a solution in 5 mL anhydrous diethyl ether. The mixture was stirred for 12 hours under nitrogen and quenched under air with 2 grams of silica gel slurried in 5 mL of diethyl ether. The volatiles were removed under reduced pressure and the solids were loaded onto a silica gel column. Eluting with a gradient from 1-5% diethyl ether in hexanes gave two pure fractions which were combined and concentrated to give **5b** 37 mg (16% yield).

^{1}H NMR (500 MHz, $CDCl_3$) δ (s, 6H, NMe_2), 3.70 (s, 2H, CH_2), 7.34 (t, J=8.0 Hz, CH meta to CF_3), 7.61 (d, J=8.0 Hz, CH para to CF_3 + CH ortho to CF_3) **^{13}C NMR (126 MHz, $CDCl_3$)** δ 45.33 (s, NMe_2), 56.38 (s, CH_2), 123.82 (q, J=274.71 Hz, CF_3), 124.79 (q, J=6.05 Hz, CH ortho to CF_3), 128.19 (s, CH meta to CF_3),131.47 (q, J=29.73 Hz, C ipso to CF_3), 133.68 (s, CH para to CF_3), 136.04 (s, aromatic C quaternary),138.16 (s, aromatic C quaternary) **^{19}F NMR (470 MHz, $CDCl_3$)** δ -57.26

Synthesis of Br-CF_3-dmba (5c)

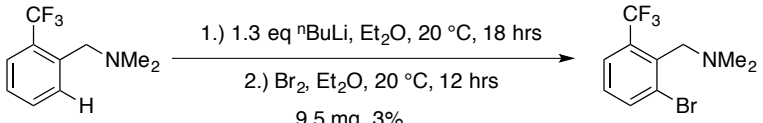

5a **5c**

A 25 mL round bottom flask equipped with a magnetic stir bar and septum was evacuated and refilled with nitrogen 3 times. To the flask, under nitrogen, was added **5a** (1 mmol, 203 mg, 1 equiv.) and 2.5 mL anhydrous diethyl ether. To the ethereal solution, n-butyl lithium (1.3 mmol, 0.845 mL (1.54M), 1.3 equiv.) was added drop-wise. The mixture was stirred under nitrogen for 18 hours at room temperature. Bromine (1.3 mmol, 208 mg, 67µL, 1.3 equiv.) was added drop-wise under nitrogen. The mixture was stirred for 12 hours under nitrogen, quenched with 1 mL water, and acidified with 5 mL 2M HCl. The aqueous fraction was basified with 2M NaOH and extracted 3x with 5 mL diethyl ether. To the ethereal extracts was added 2g of celite and the solvent was removed under reduced pressure. The celite pad was loaded on a silica gel column which was eluted with a gradient from 1-10% diethyl ether in hexanes. Three pure fractions were obtained as assayed by GCMS and were combined to give **5c** 9.5 mg (3% yield).

^{1}H NMR (500 MHz, $CDCl_3$) δ 2.31 (s, 6H, NMe_2), 3.70 (s, 2H, CH_2), 7.25 (t, J=7.9 Hz, 1 H), 7.66 (d, J=7.9 Hz, 1 H), 7.82 (d, J=7.9 Hz, 1 H) **^{13}C NMR (126 MHz, $CDCl_3$)** δ 45.17 (s, NMe_2), 58.55 (s, CH_2), 123.44 (q, J=32.12 Hz, C ipso to CF_3), 123.70 (q, J=280.88 Hz, CF_3), 125.41 (q, J=6.02 Hz, CH ortho to CF_3), 128.37 (s, aromatic C quaternary), 128.69 (s, aromatic C quaternary), 128.81 (s, aromatic C quaternary), 137.20 (s, aromatic CH) **^{19}F NMR (470 MHz, $CDCl_3$)** δ -57.12

Synthesis of I-CF_3-dmba (5d)

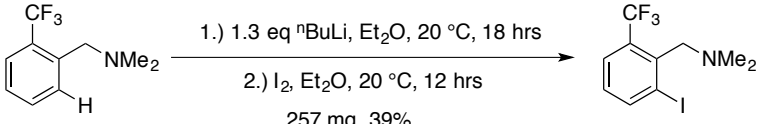

5a **5d**

A 25 mL round bottom flask equipped with a magnetic stir bar and septum was evacuated and refilled with nitrogen 3 times. To the flask, under nitrogen, was added **5a** (2 mmol, 406 mg, 1 equiv.) and 5 mL anhydrous diethyl ether. To the ethereal solution, n-butyl lithium (2.6 mmol, 1.69 mL (1.54M), 1.3 equiv.) was added drop-wise. The mixture was stirred under nitrogen for 18 hours at room temperature. Iodine (2.6 mmol, 660 mg, 1.3 equiv.) was added drop-wise under nitrogen as a solution in 5 mL anhydrous diethyl ether. The mixture was stirred for 12 hours under nitrogen and quenched under air with 2 grams of silica gel suspended in 5 mL of diethyl ether. The volatiles were removed under reduced pressure and the solids were loaded onto a silica gel column. Eluting with a 5% triethylamine in hexanes gave two pure fractions which were combined and concentrated to give **5d** 257 mg (39% yield).

^{1}H NMR (500 MHz, $CDCl_3$) δ 2.29 (s, 6H, NMe_2), 3.64 (s, 2H, CH_2), 7.05 (t, J=7.9 Hz, 1 H), 7.67 (d, J=7.9 Hz, 1 H), 8.12 (d, J=7.9 Hz, 1 H) **^{13}C NMR (126 MHz, $CDCl_3$)** δ 44.80 (s, NMe_2), 61.93 (d, J=1.48 Hz, CH_2), 104.27 (q, J=4.1 Hz, aromatic quaternary), 123.72 (q, J=275.04 Hz, CF_3), 125.97 (q, J=6.10 Hz, CH ortho to CF_3), 128.39 (s,1 CH meta to CF_3), 130.56 (q, J=29.82 Hz, C ipso to CF_3), 140.06 (s, aromatic quaternary), 144.27 (d, J=1.01 Hz, CH para to CF_3) **^{19}F NMR (470 MHz, $CDCl_3$)** δ -56.94

Section S1.4: Attempted bridge splitting equilibrium experiments

It has been reported[9-11] that carboxylate bridged palladacycles can undergo a bridge splitting reaction in the presence of nitrogen donor. We sought to assess whether in the presence of excess substrate, the MPAA complex **6a** underwent a similar bridge splitting reaction. Surprisingly, **6a** showed no sign of reaction when treated with as much as 100 eq. of **5a**. The last spectrum in each series is **5a** with no Pd, to show that the new small new peaks visible when **6a** is treated with 100 eq. **5a** are from minor (<0.5%) impurities in **5a**, not from new species in equilibrium with **6a**.

Deprez, N. R.; Sanford, M. S. J. Am. Chem. Soc. 2009, 131 (31), 11234.
Powers, D. C.; Xiao, D. Y.; Geibel, M. A. L.; Ritter, T. J. Am. Chem. Soc. 2010, 132 (41), 14530.
Ryabov, A. D. Inorg. Chem. 1987, 26, 1252.

stacked ^{19}F NMR spectra

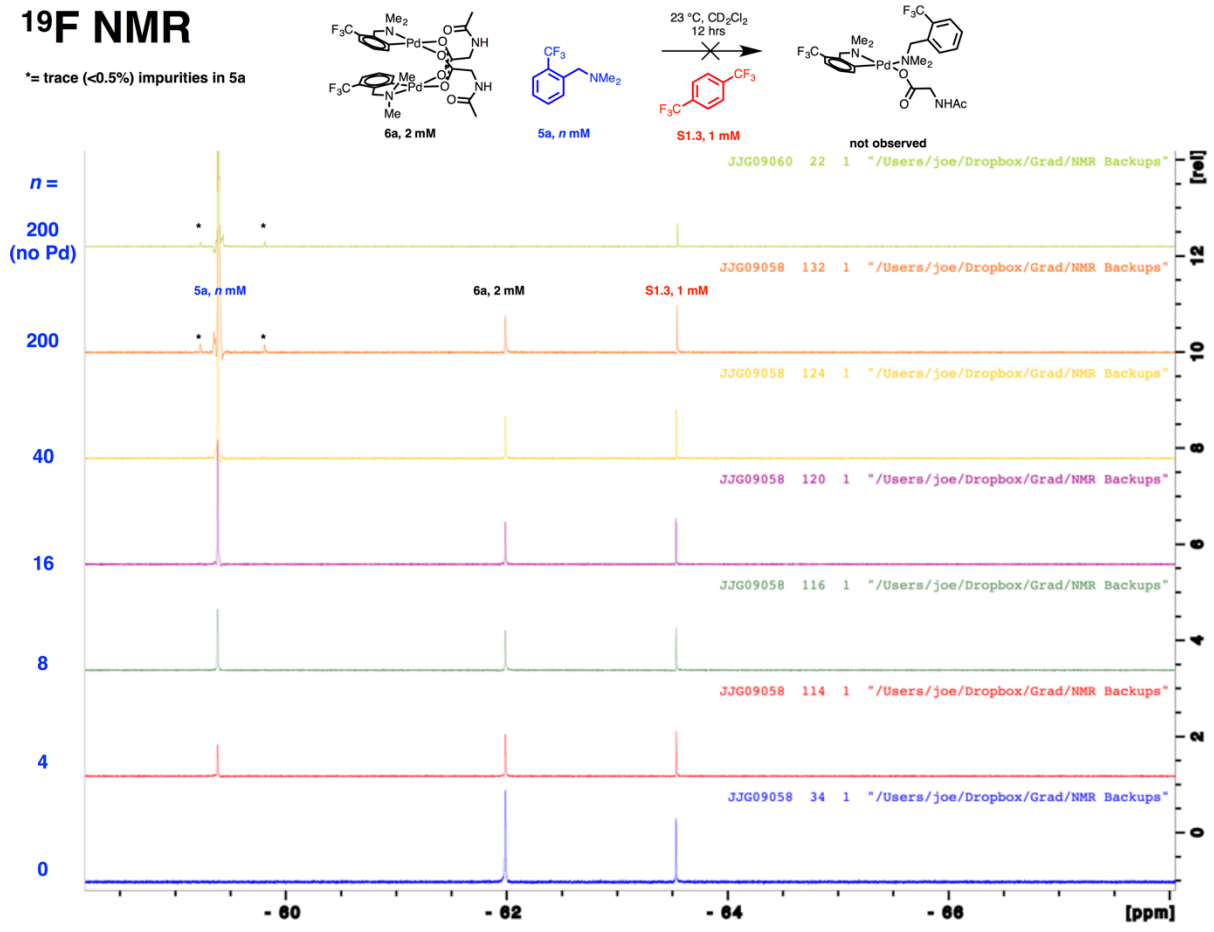

stacked ^{1}H NMR spectra

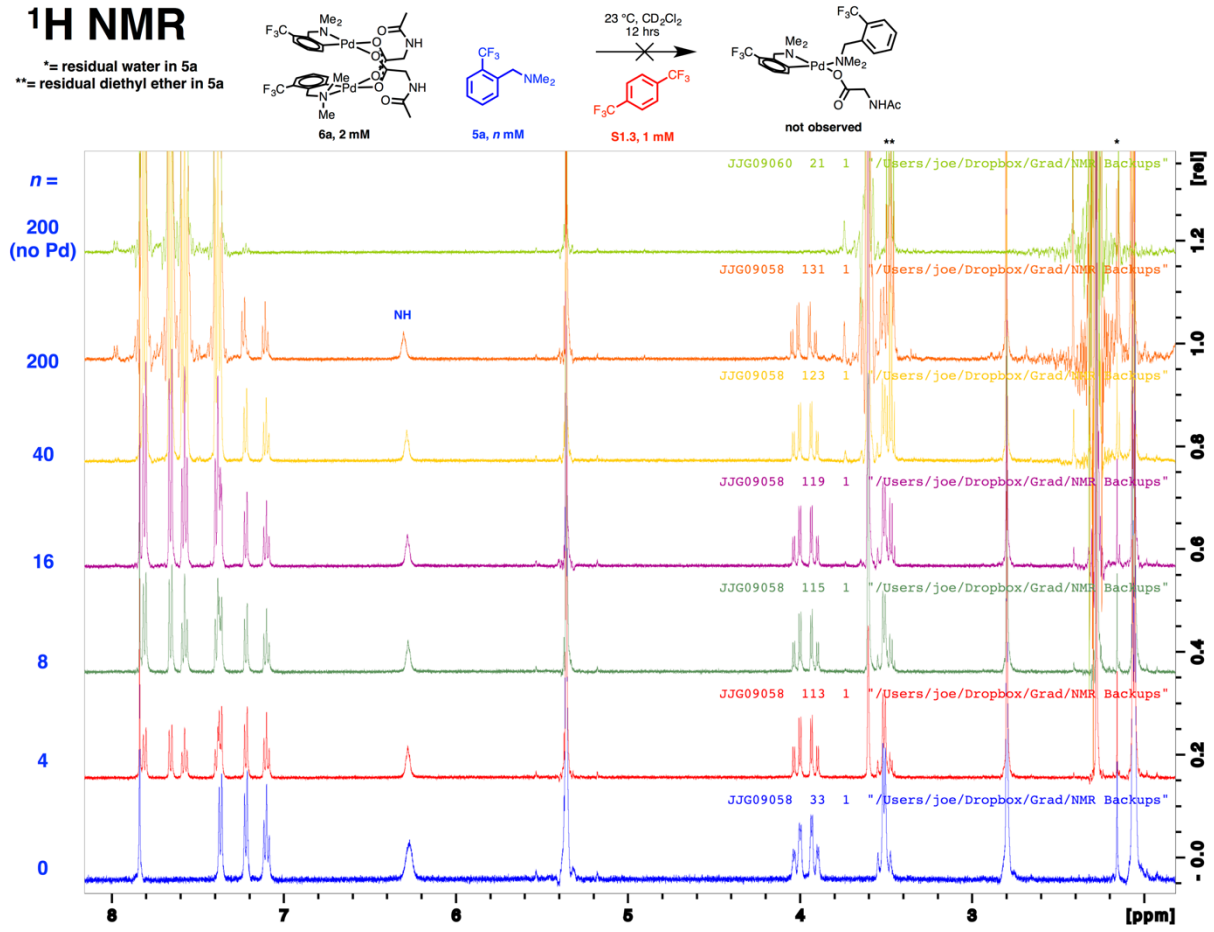

Notably, in the presence of a large excess of a strong[12] hydrogen bond acceptor (tertiary amine **5a**), there is no change in the chemical shift of the MPAA amide N-H. This is consistent with (although not sufficient to prove) intramolecular hydrogen-bonding between the two MPAA's (AcN-H···O) that is strong enough to not be perturbed in the presence of a large excess a stronger hydrogen bond acceptor.

Laurence, C.; Legros, J.; Nicolet, P.; Vuluga, D.; Chantzis, A.; Jacquemin, D. J Phys Chem B 2014, 118 (27), 7594.

Section S1.5: looking for species in equilibrium with MPAA complexes

variable concentration UV-vis of 6a in CH_2Cl_2

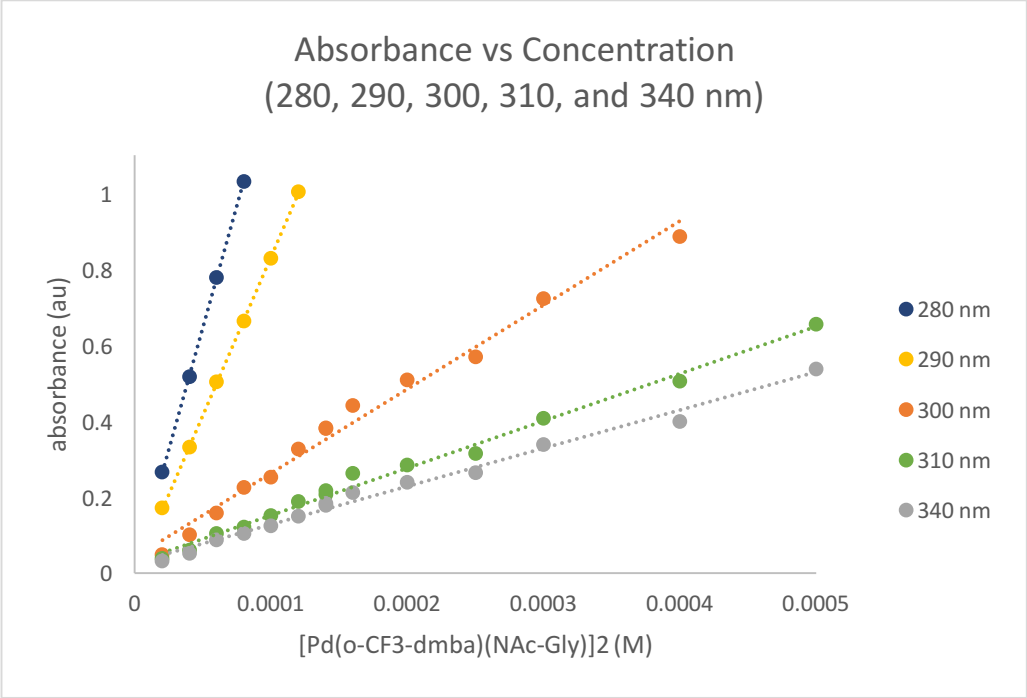

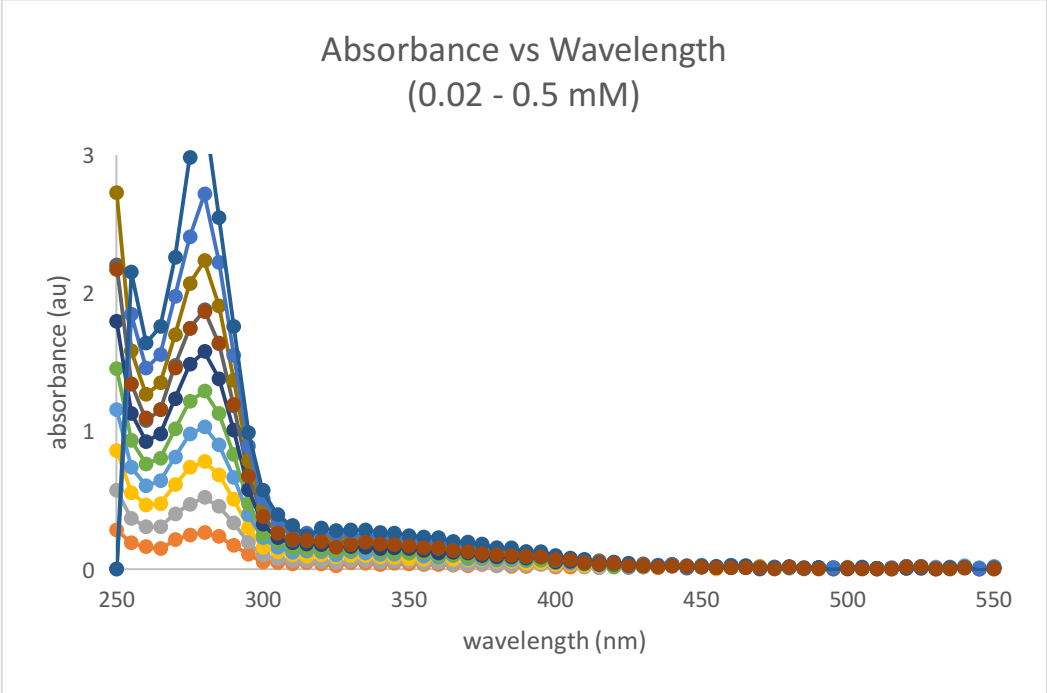

The possibility of dissociation of **6a** into two putative monomers (or equilibrium with another species) at low concentrations was not observed based on linear, concentration-dependent UV-Vis spectra from 0.02-0. 5 mM in CH_2Cl_2.

variable concentration ^{19}F NMR of 6b in CD_2Cl_2

Solutions of **6b** from 3-39 mM (with 2.2 mM 1,4-bis(trifluoromethyl)benzene) were monitored by ^{19}F NMR to look for possible aggregation at high concentration or dissociation to putative monomeric species at low concentration. Over the range of concentrations monitored, no evidence for any species in equilibrium with **6b** was observed.

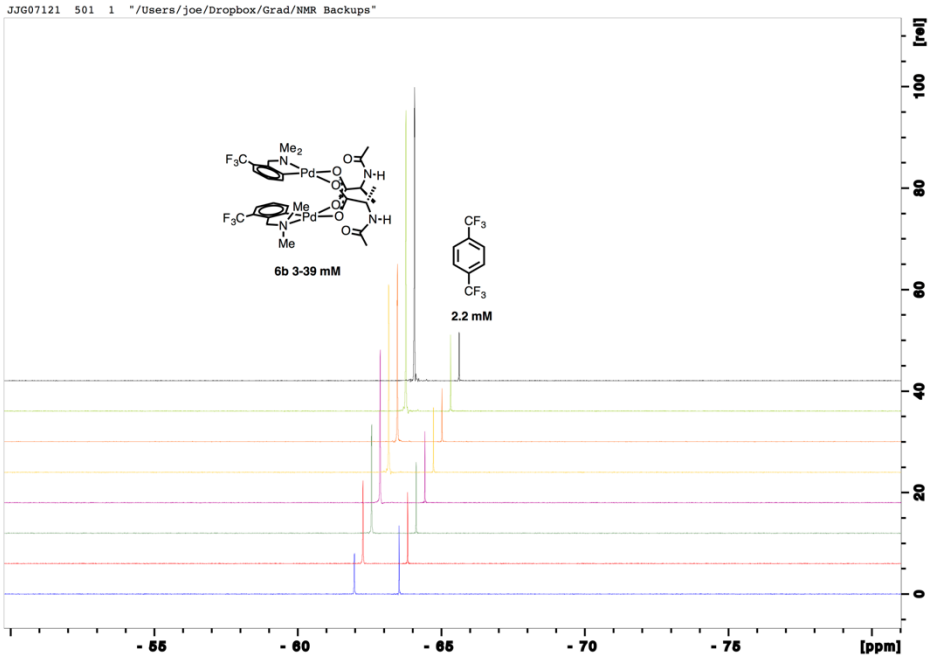

low temperature ^{1}H NMR of 6a in CD_2Cl_2

In an attempt to observe species that might be in rapid exchange on the NMR time scale at room temperature, a sample of **6a** in CD_2Cl_2 was cooled from 15 °C down to -40 °C in the NMR spectrometer using a variable temperature probe, which revealed substantial changes in chemical shift and peak shape, especially for the amide N-H (indicated by a colored line at each temperature). Vertical black lines are guides to visualize small changes in chemical shift. These changes could be indicative of a dynamic process (eg carboxylate exchange or rotation about C-C or C-N bonds in the MPAA), but no distinct new species were observed.

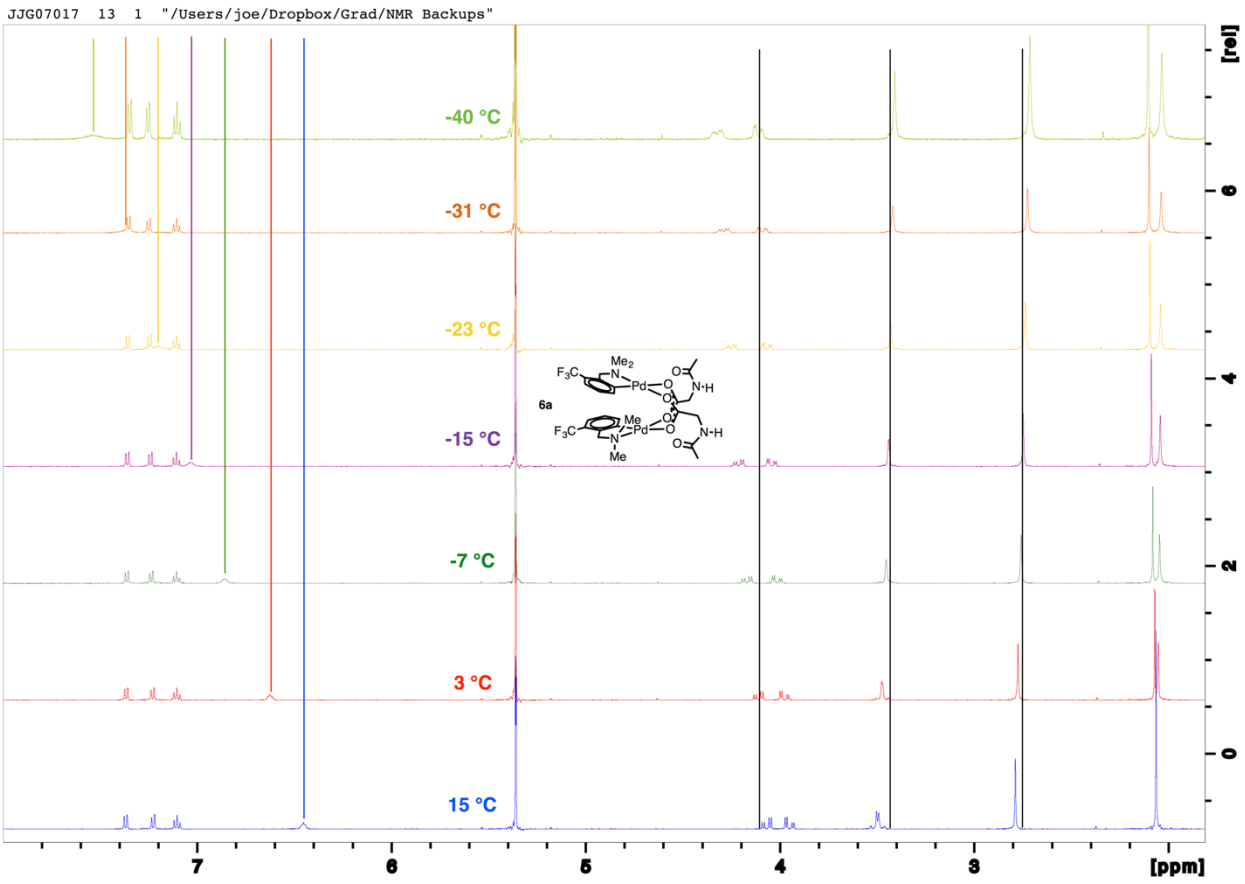

high temperature ^{1}H NMR of 6a in 1,1,2,2-tetrachloroethane-d_2

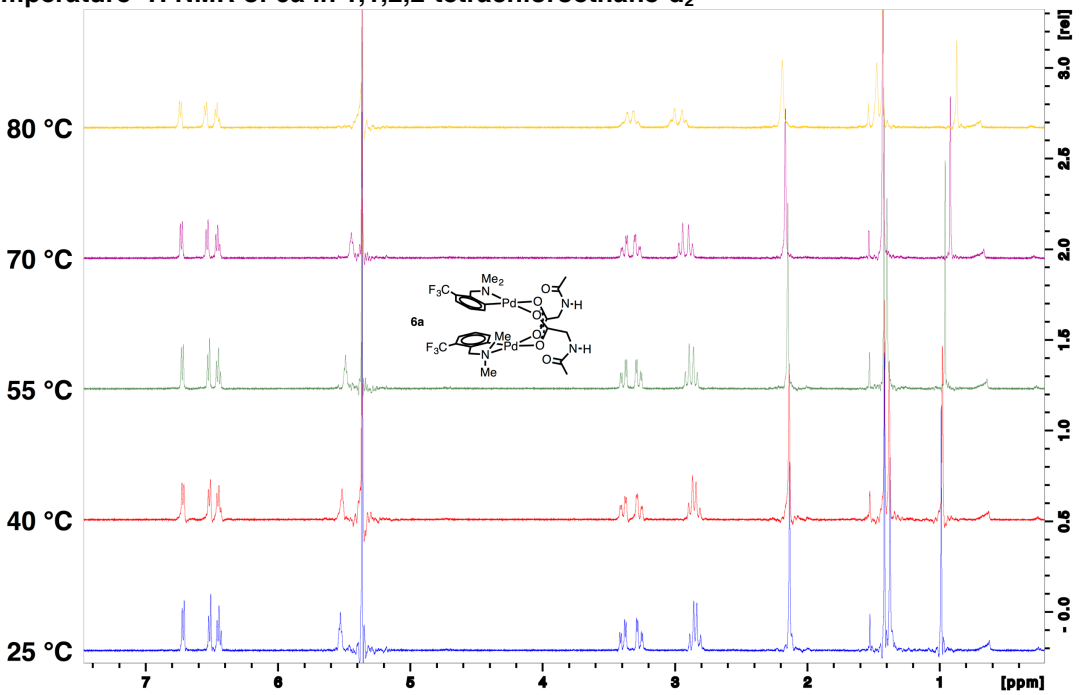

high temperature ^{19}F NMR of 6a in 1,1,2,2-tetrachloroethane-d_2

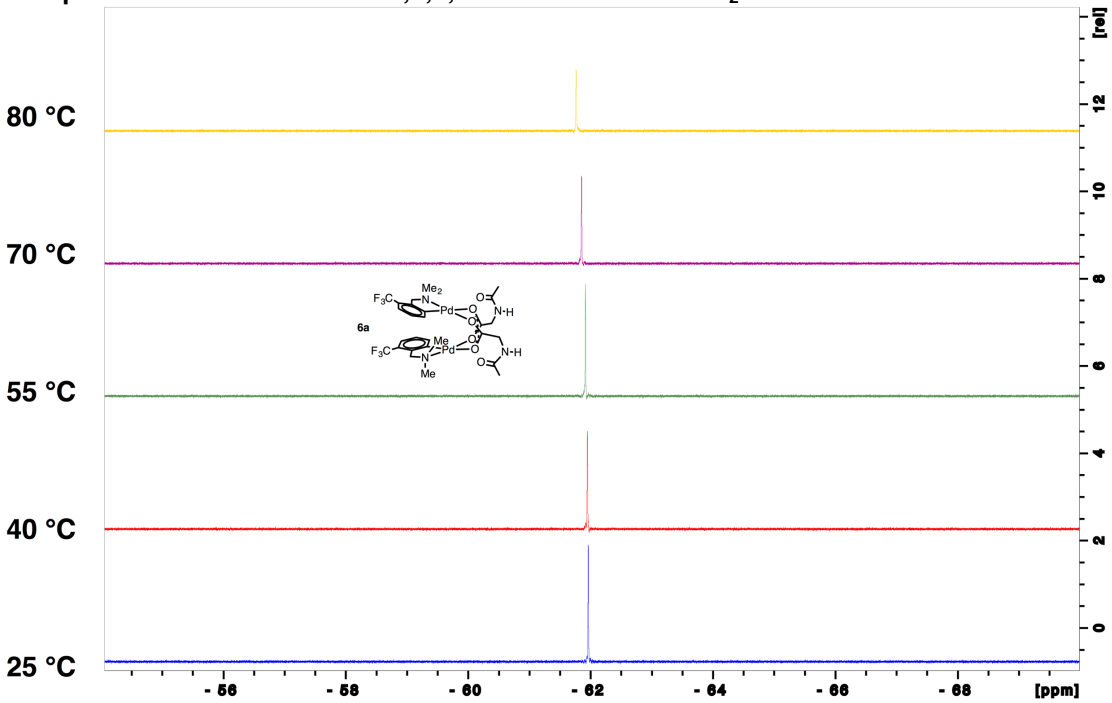

^{1}H NMR of homodimers 6a and 2 compared to mixture with heterodimer

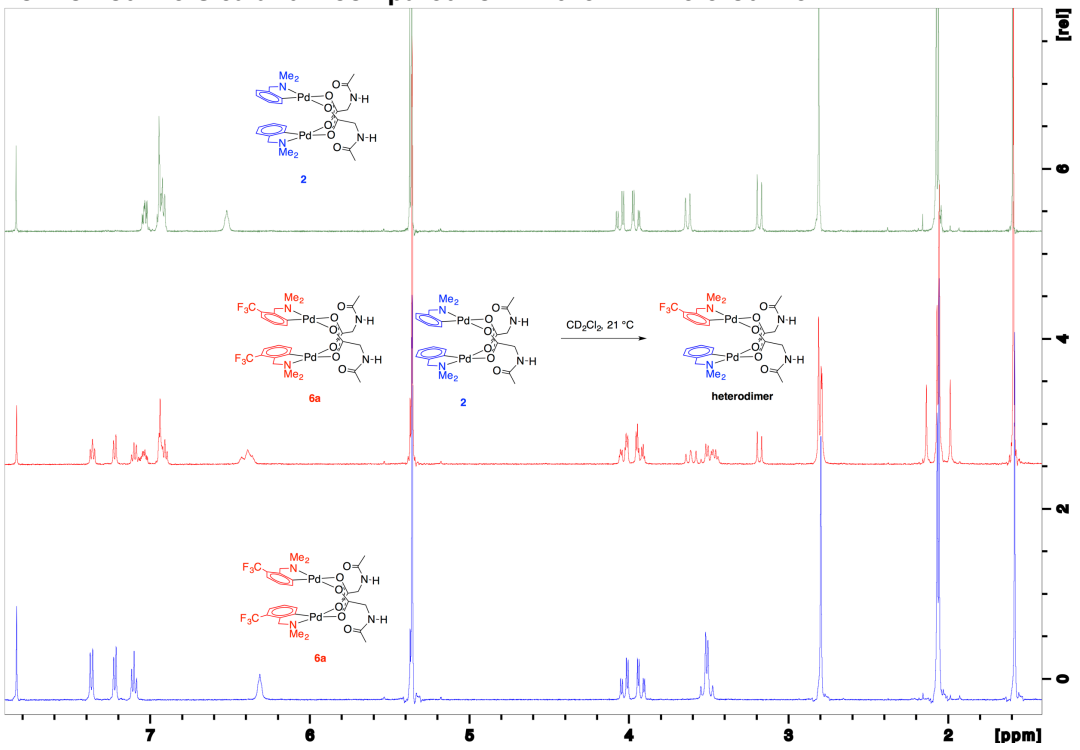

^{19}F NMR reaction progress of equilibration homodimers 6a and 2 to heterodimer

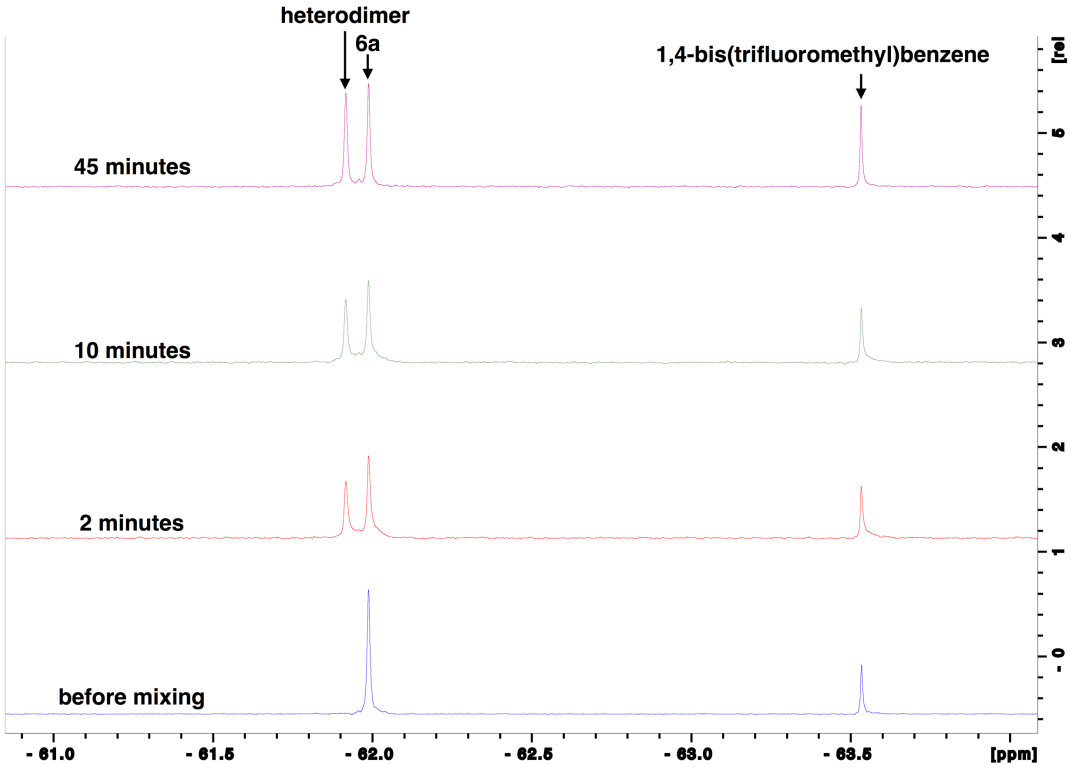

Determination of homodimer/heterodimer exchange rate constant by ^{19}F EXSY

Complex 2 (7.13 mg, 10 µmol) and 10 micromoles of **6a** (8.49 mg,10 µmol) were weighed into a 1 dram vial, dissolved in 600 µL CD_2Cl_2 and transfered to a medium walled NMR tube. The tube was attached to cajon adaptor, degassed by 3 cycles of freeze pump thaw, and flame sealed. The sample was analyzed by ^{19}F EXSY with mixing times (t_m) varying from 100-800 ms. The volumes of the diagonal and cross peaks were used to solve for the rate constant (k) according to equation (1).

$$(\mathbf{1}) \qquad k = \frac{1}{t_m} ln \frac{r+1}{r-1}$$

where

$$(\mathbf{2}) \qquad r = 4X_A X_B \frac{I_{AA} + I_{BB}}{I_{AB} + I_{BA}} - (X_A - X_B)^2$$

and I_{AA} and I_{BB} correspond to the volumes of the three dimensional peak on the diagonals and I_{AB} and I_{BA} correspond to the volumes under the three dimensional cross peaks. Rate constants across the range of mixing times were in good agreement and were used to calculate $\Delta G^{\ddagger}_{exchange}$ by the Eyring equation (3).

$$(\mathbf{3}) \qquad \Delta G^{\ddagger}_{exchange} = RT\left(ln\frac{k_b T}{h} - ln\, k\right)$$

Rate constants and $\Delta G^{\ddagger}_{exchange}$ by ^{19}F EXSY at various t_m

t_m (ms)	100	200	400	600	800	average
k (1/ms)	71	50	54	51	48	54
$\Delta G^{\ddagger}_{exchange}$ (kcal/mol)	19.2	19.3	19.2	19.2	19.2	19.2

Method of continuous variation (Job Plot) with homodimers 6a and 2 to heterodimer

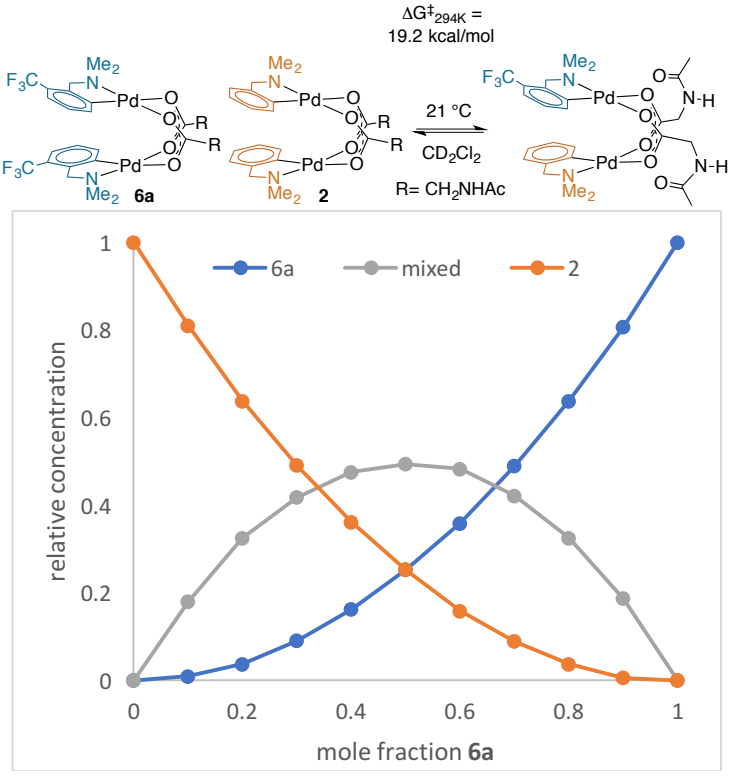

Section S1.6: Pulse gradient spin echo experiments

PGSE experimental description

PGSE[17] data were obtained on a Bruker DRX-500 spectrometer using the Stejskal-Tanner method. Two pulsed field gradients with duration δ = 4 ms separated by a delay time Δ = 0.0151 s were incorporated into a spin echo sequence with with one before and the other after the 180 ° pulse. The gradient was calibrated with a sample of 2% H_2O in D_2O with a 2 mm teflon disk. ^1H NMR spectra were acquired in CD_2Cl_2 at 294K without sample spinning. For each sample the gradient strength (G) was varied between 0 and 30 G/cm while keeping all other variables constant. The most upfield N-methyl resonance of each spectrum was integrated. The relative integrals are related to diffusion coefficient D by equation (1) (I_G = integral of a peak with applied gradient G, I_0 is the integral of the the peak with no gradient). According to equation (1) the slope of a plot of plot of $\ln(I_G / I_0)$ vs G^2 is proportional to the diffusion coefficient and thus inversely proportional to the hydrodynamic radius by the Stokes-Einstein equation (2). Relative diffusion coefficients were determined with respect to complex **7** by dividing the slope of the plots $\ln(I_G / I_0)$ vs G^2 for each sample by the slope of the plot for complex **7**. Relative hydrodynamic radii were thus given by the inverse of relative diffusion coefficients. Relative hydrodynamic volumes were determined from relative hydrodynamic radii by equation (3).

(1) $\ln(I_G / I_0) = -[\gamma^2 \delta^2 G^2 (\Delta - \delta/3)] D$
Where γ is the proton gyromagnetic ratio (2.675×10^8 $T^{-1}s^{-1}$).

(2) $D = (k_B T)/(6 \pi \eta r)$
Where k_B is the Boltzmann constant; η is the viscosity of the solvent, T is temperature, r is the hydrodynamic radius of the molecule (approximated as a sphere).

(3) $V = 4 \pi r^3$

Good fits were found for each linear regression (R^2 = 0.9948-0.9996) made up of measurements at 10 different field strengths for each complex. The points at zero field strength were found to be anomalously variable and were not included in the fit used to determined the slope. Plots are normalized to give a y intercept near 0 to facilitate visualizing differences in slope.

Table of PGSE results

number	**7**	**7**	**8**	**9**	**6a**	**6b**	**6c**	**6d**
ligand	acac	acac	Cl	OAc	NAc-Gly	NAc-Ala	NAc-Leu	NAc-Ile
conc. (mM)	10	5	5	5	5	5	5	5
slope	-17.63	-17.63	-14.15	-13.22	-11.36	-11.40	-11.20	-10.49
D_{rel}	1.00	1.00	0.80	0.75	0.64	0.65	0.64	0.60
r_{rel}	1.00	1.00	1.25	1.33	1.55	1.55	1.58	1.68
V_{rel}	**1.0**	**1.0**	**1.9**	**2.4**	**3.7**	**3.7**	**3.9**	**4.8**

Plot of PGSE slopes

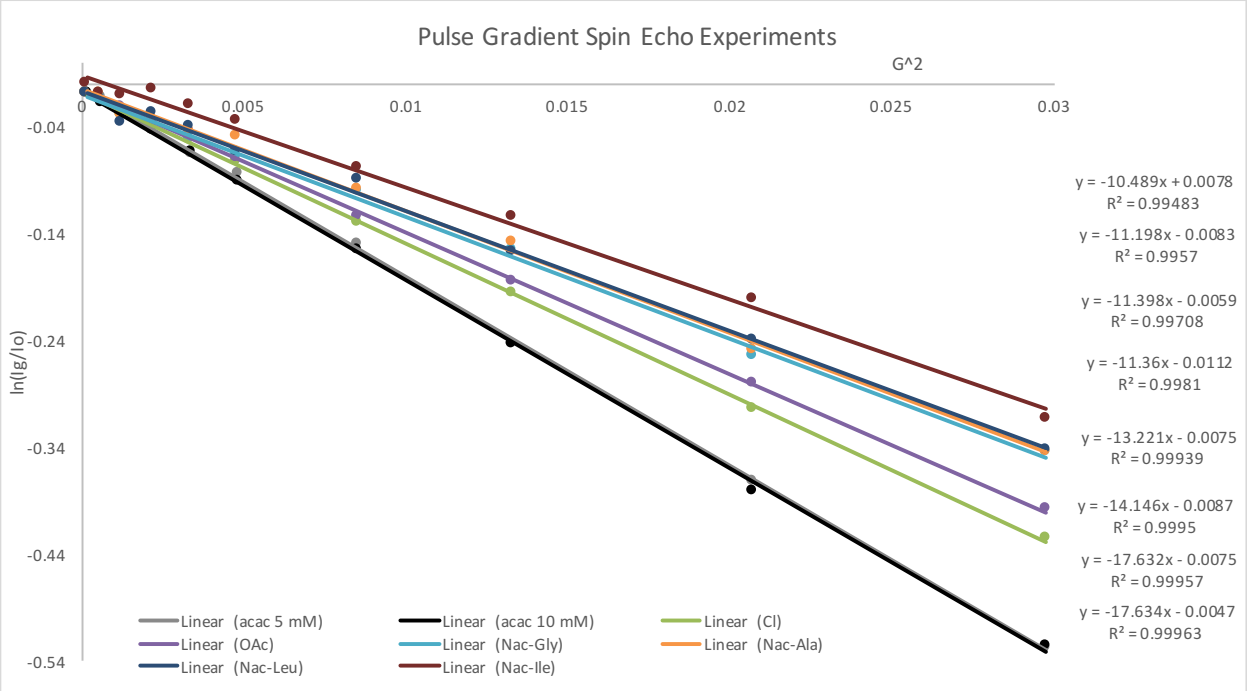

Section S1.7: Effect of MPAA and base on rate of cyclopalladation

reaction summary

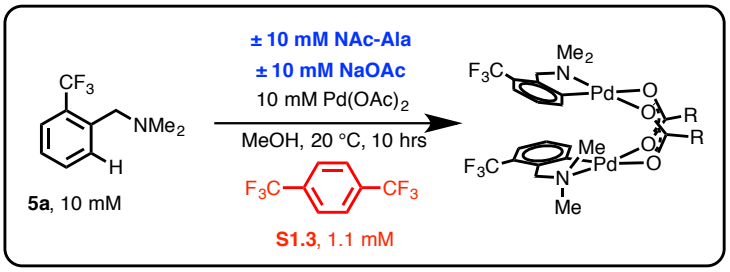

reaction #	[Pd]	[5a]	[S1.3]	[NAc-Ala]	[NaOAc]
1	10 mM	10 mM	9.1 mM	0 mM	0 mM
2	10 mM	10 mM	9.1 mM	10 mM	0 mM
3	10 mM	10 mM	9.1 mM	0 mM	10 mM
4	10 mM	10 mM	9.1 mM	10 mM	10 mM

experimental set up

Reactions for determining initial rates of cyclopalladation were prepared in four NMR tubes under air in parallel. Compounds were added using stock solutions prepared in volumetric flasks and dispensed from gas tight syringes. To each tube was added either 100 µL of 80 mM NAc-Ala, 100 µL of 80 mM NaOAc, both, or neither according to the table above. The each tube was diluted with an appropriate volume of methanol to bring the total volume to 200 µL. A stock solution of palladium acetate in methanol-d_4 (16 mM) was prepared immediately before use (palladium acetate is known to slowly decompose in solutions of methanol).[13] The palladium(II) acetate stock solution (500 µL) was added to all four tubes and the tubes were immediately flash frozen in liquid nitrogen. Each tube was initiated separately to allow for continuous monitoring during the initial rate portion of the reaction. To initiate, each tube was removed from the liquid nitrogen bath, allowed to thaw for 10 minutes at room temperature, at which time 100 µL of a stock solution of **5a** 80 mM and 8.8 mM **S1.3** in methanol was added, the tube was shaken to mix, and a stopwatch was started. The sample was walked to the NMR spectrometer and the delay time between initiation and data acquisition was noted. Spectra were acquired at 17 second intervals during the initial rates portion of the reaction and the reactions were monitored periodically until all starting material was consumed. Starting material and product concentrations were determined with respect to 1.1 mM **S1.3** internal standard. Error bars are the standard deviation of the slope of linear regression fit.

Bakhmutov, V. I.; Berry, J. F.; Cotton, F. A.; Ibragimov, S. Dalton Trans., 2005, 1989-1992

bar graph comparing initial rates of starting material consumption

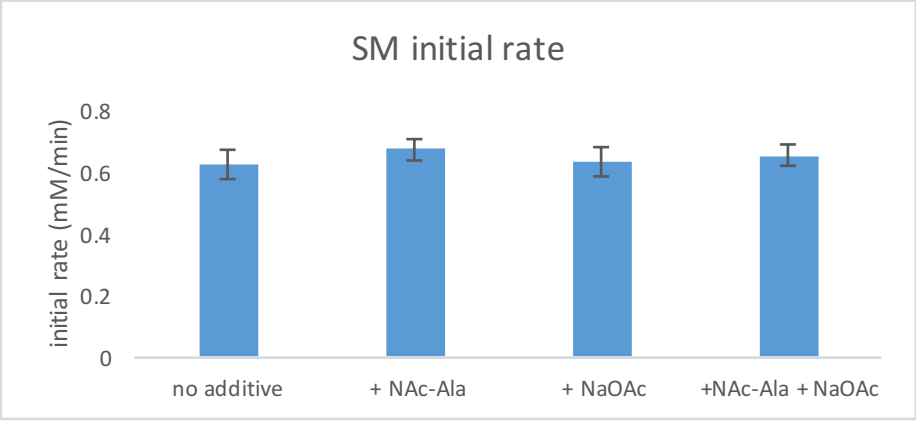

bar graph comparing initial rates of product formation

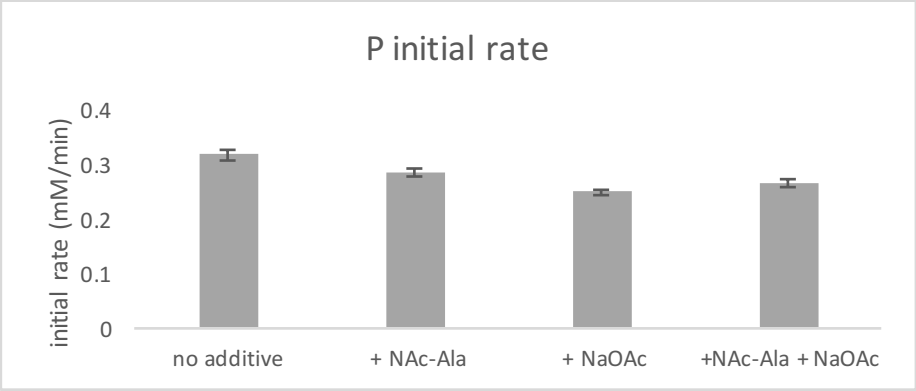

overlaid plots of reaction progress in initial rates portion of reaction

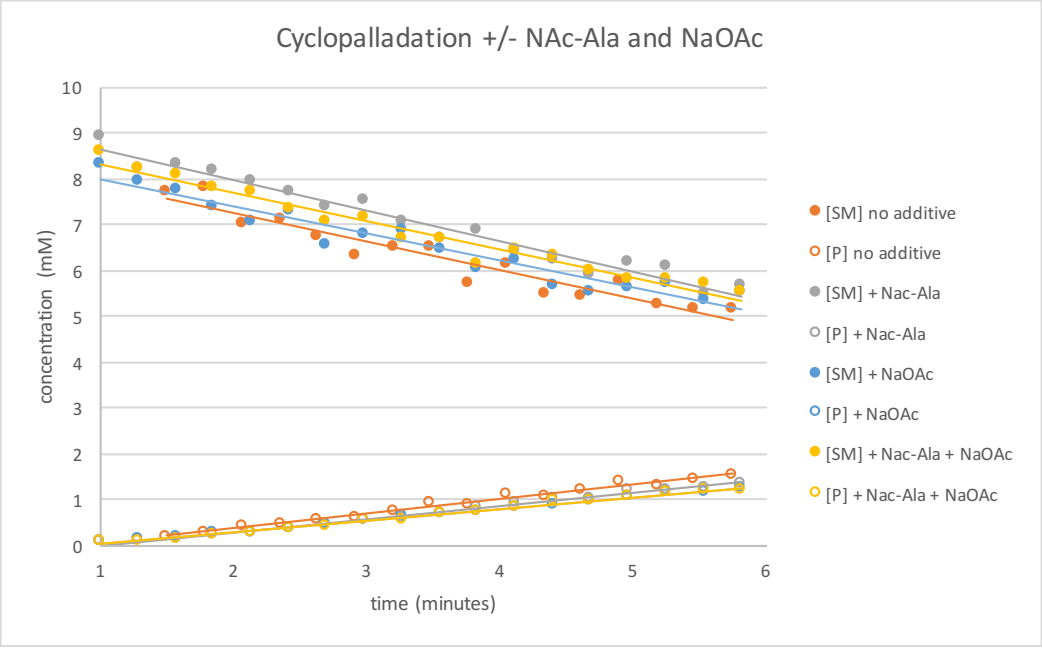

overlaid plots of reaction progress in first 60 minutes of reaction

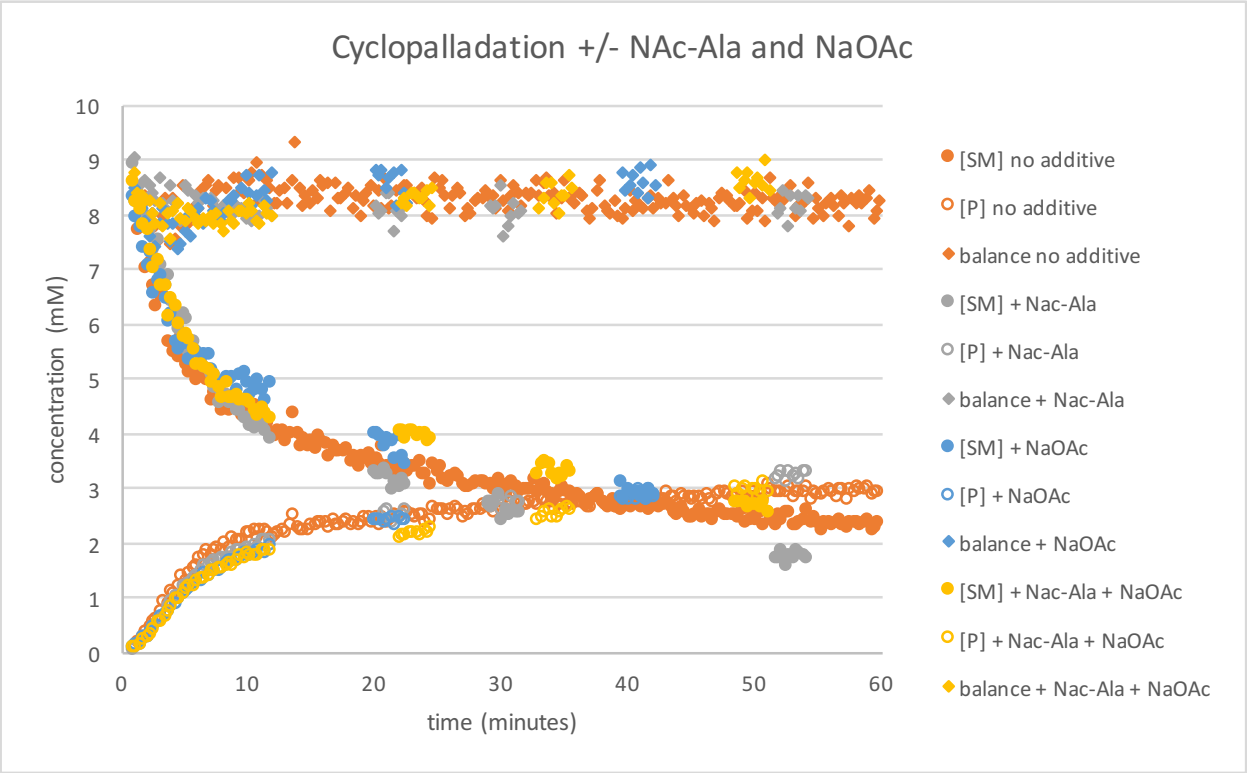

overlaid plots of reaction progress over full reaction

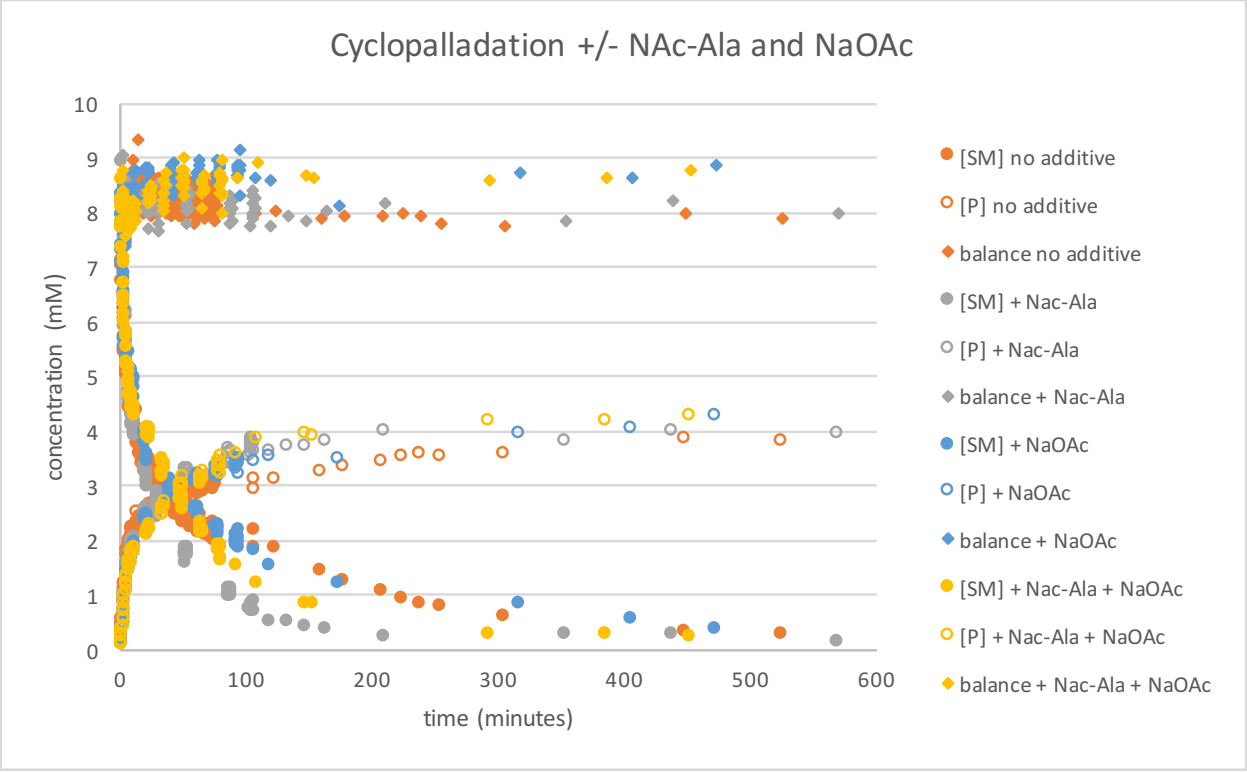

stacked spectra with no additive

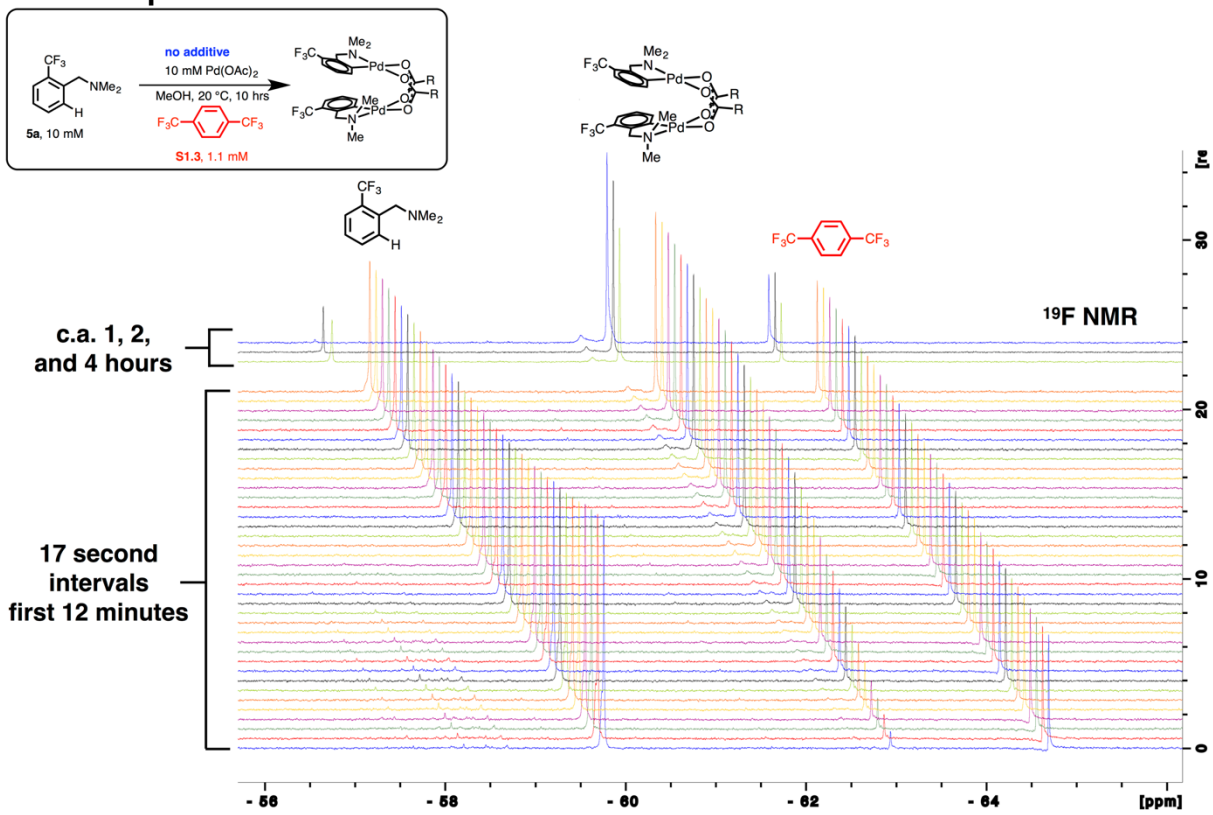

stacked spectra with MPAA additive

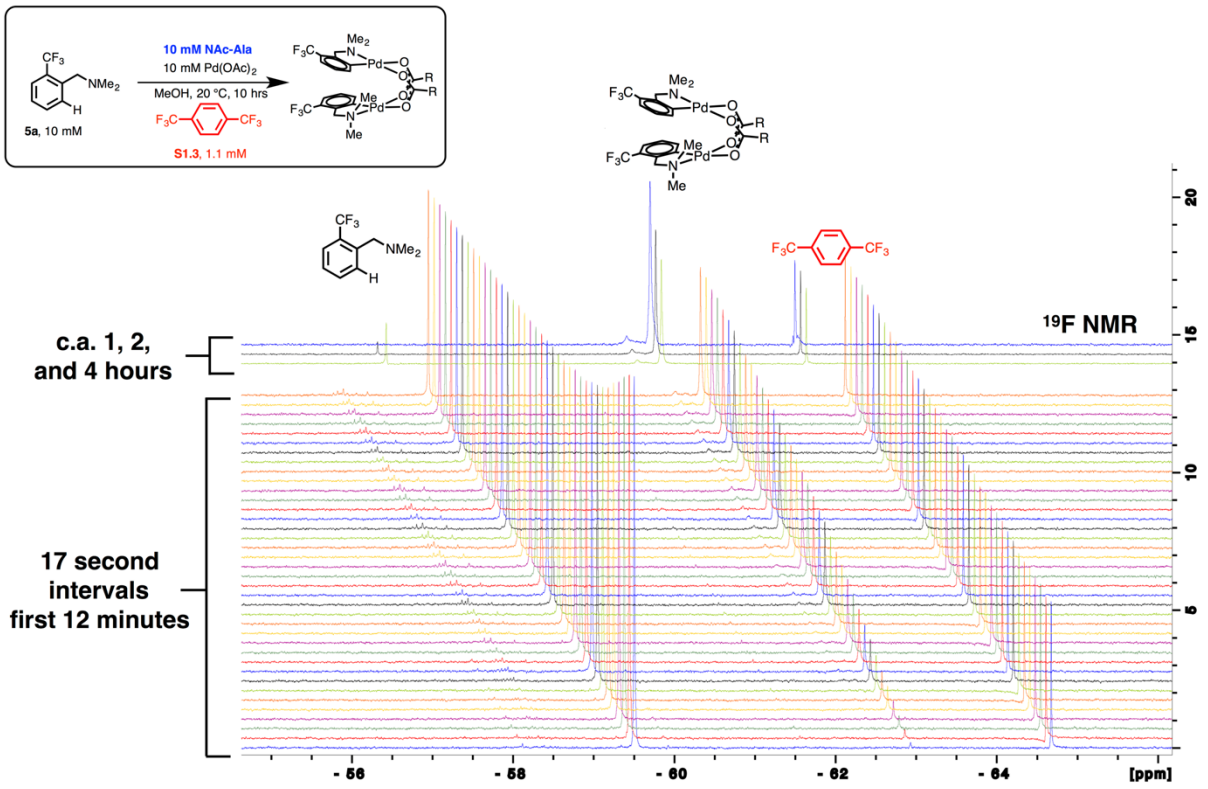

stacked spectra with sodium acetate

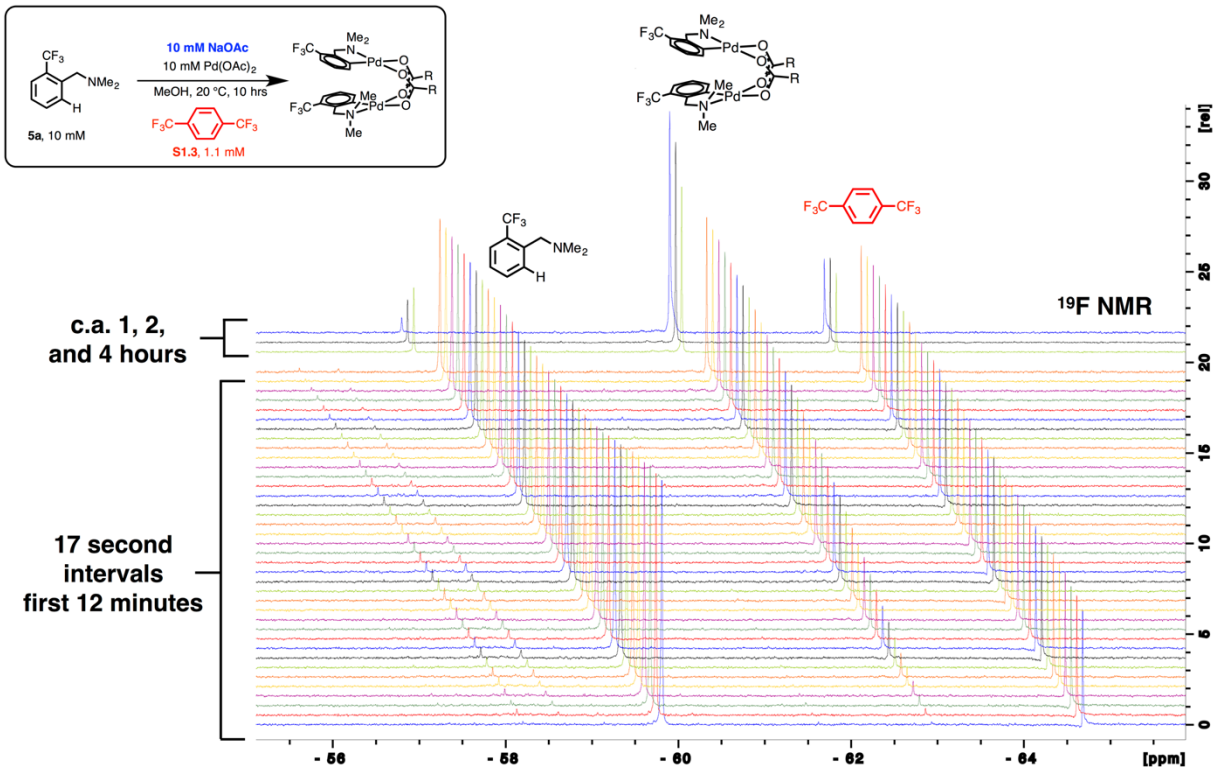

stacked spectra with MPAA additive and sodium acetate

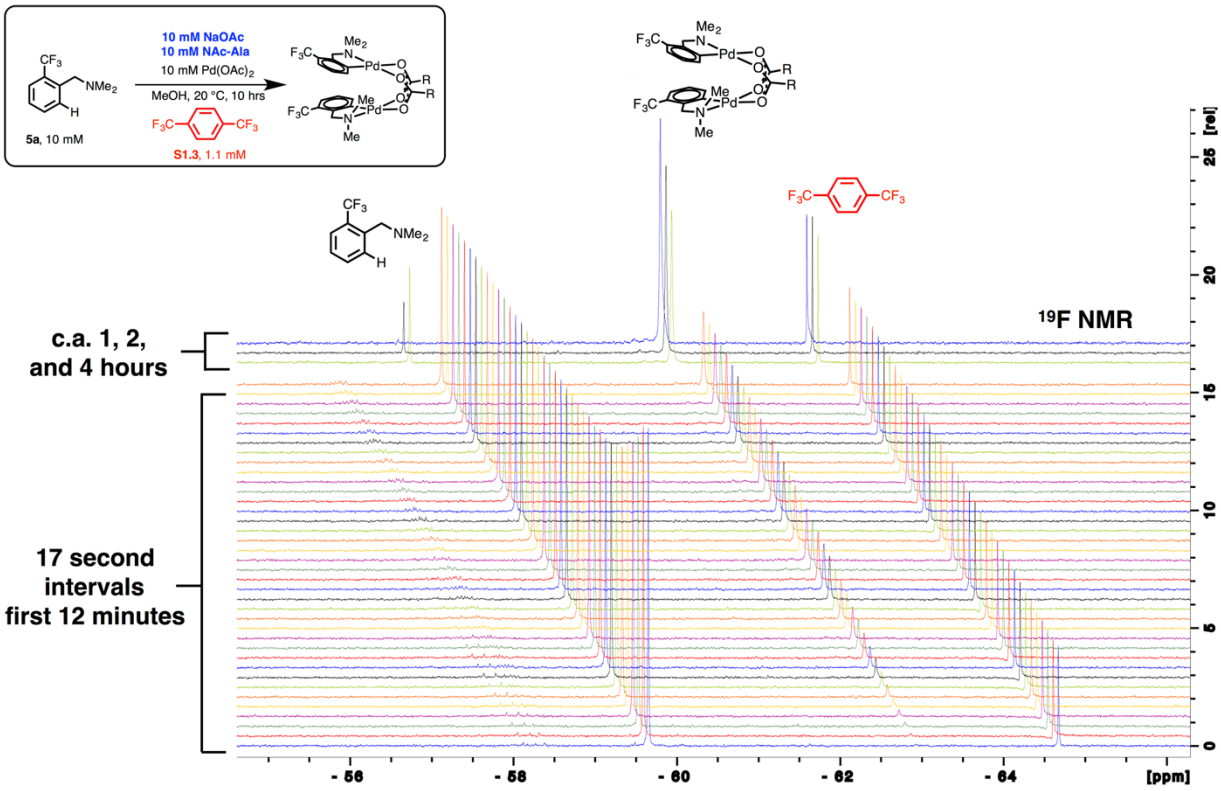

Section S1.8: Acetate/MPAA exchange equilibria

procedure for displacing acetate with MPAAs

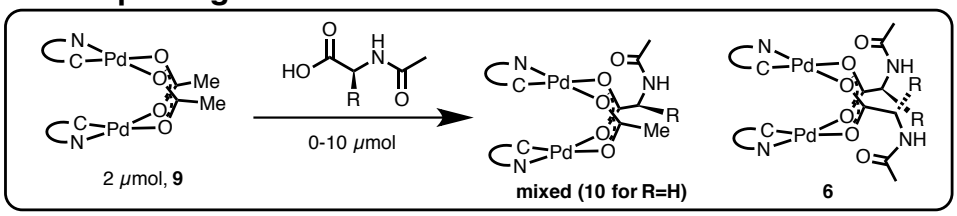

To 8 vials in parallel was added by gas tight syringe a stock solution in methanol of MPAA (15 mM) (MPAA = NAc-Gly, NAc-Ala, or NAc-Ile). Each vial was diluted with (800-*n*) µL methanol to bring the total volume to 800 µL. To each vial was added a stock solution of **9** (10 mM, 200 µL, 2 µmol). The vials were capped, shaken, and left for 8 hours at room temperature at which time the caps were loosened, the samples were flash frozen in liquid nitrogen, and frozen methanol was removed at room temperature in a vacuum chamber. To each of the vials was added a stock solution in CD_2Cl_2 of internal standard **S1.3** (20 mM, 50 µL, 1 µmol) followed by 600 µL of CD_2Cl_2. The samples were dissolved by agitation with a glass pipette and transferred to an NMR tube for analysis by ^{19}F NMR.

Exchange equilibria were conducted in methanol because methanol is required to prepare sufficiently concentrated stock solutions of MPAAs; however, the ^{19}F NMR spectra of the complexes in equilibrium are broad and overlapping in methanol. Thus, the reactions were conducted in methanol and analyzed in CD_2Cl_2, which results in resolvable peaks in ^{19}F NMR spectra of **6a**, **9**, and **10**, but prevents determination of quantitative equilibrium constants.

vial #	1	2	3	4	5	6	7	8
n	0	133	200	267	333	400	533	667
[MPAA] (mM)	0	2	3	4	5	6	8	10
[9] (mM)	2	2	2	2	2	2	2	2

Figure S1.1: ^{19}F NMR comparison of acetate displaced by MPAAs

Note that for NAc-Gly the there is always some small amount of starting material **9** and mixed complex **10** present, even with excess MPAA. In contrast, NAc-Ala and NAc-Ile drive the equilibrium to no observable starting material (**9**) and very little or no mixed complex, indicating more MPAA bound.

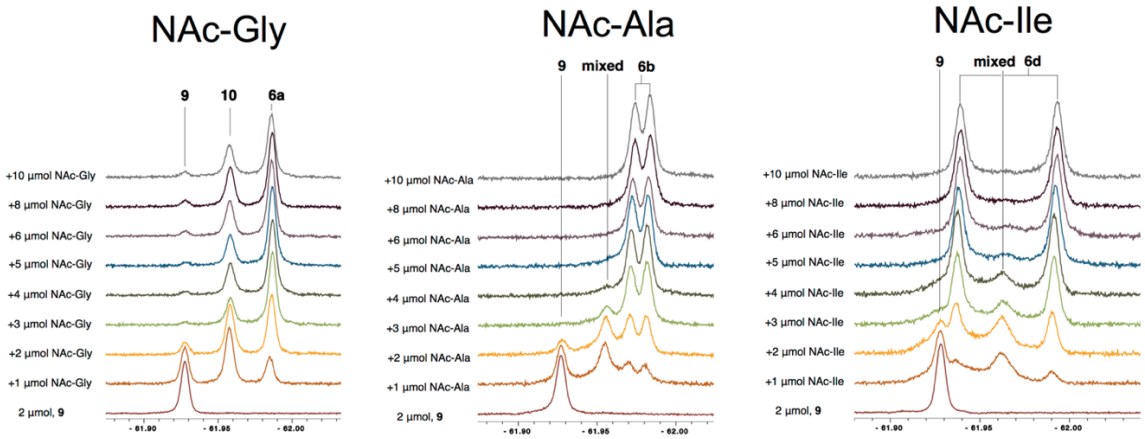

procedure for displacing NAc-Gly with acetate

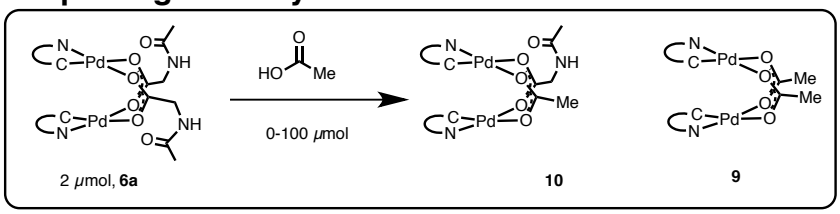

To each of 11 vials in parallel was added by gas tight syringe a stock solution in methanol of acetic acid (200 mM, *n* µL, 0.2*n* µmol) (MPAA = NAc-Gly, NAc-Ala, or NAc-Ile). Each vial was diluted with (500-*n*) µL methanol to bring the total volume to 500 µL. To each vial was added a stock solution of **6a** (4 mM, 500 µL, 2 µmol). The vials were capped, shaken, and left for 8 hours at room temperature at which time the caps were loosened, the samples were flash frozen in liquid nitrogen, and frozen methanol was removed at room temperature in a vacuum chamber. To each of the vials was added a stock solution in CD_2Cl_2 of internal standard **S1.3** (20 mM, 50 µL, 1 µmol) followed by 600 µL of CD_2Cl_2. The samples were dissolved by agitation with a glass pipette and transferred to an NMR tube for analysis by ^{19}F NMR.

vial #	1	2	3	4	5	6	7	8	9	10	11
n	0	5	10	15	20	25	40	50	100	250	500
[AcOH] (mM)	0	1	2	3	4	5	8	10	20	50	100
[6a] (mM)	2	2	2	2	2	2	2	2	2	2	2

comparing ^{19}F NMR spectra of forward and reverse carboxylate exchange

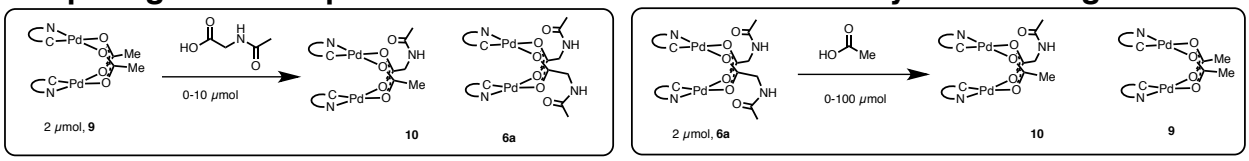

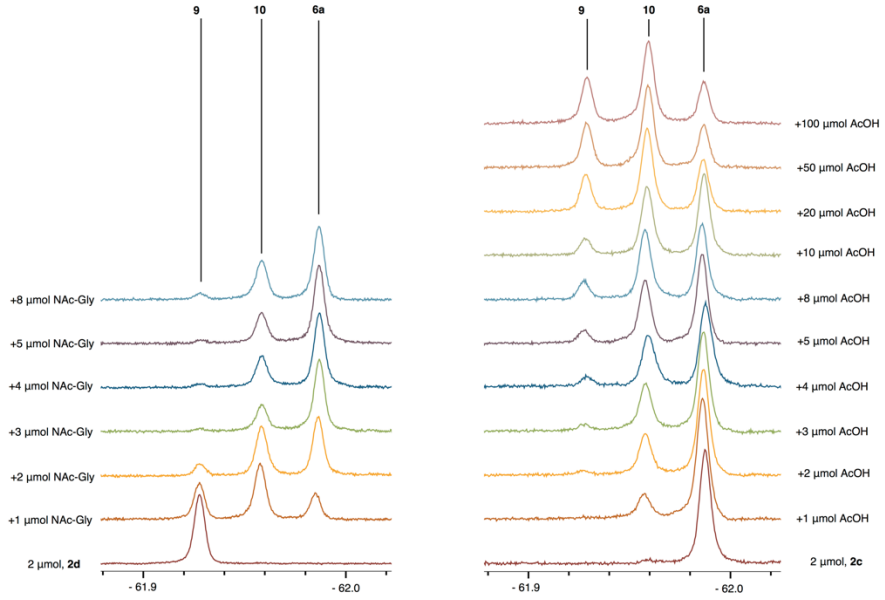

Section S1.9: Scope of MPAA palladacycle functionalization

Yields of stoichiometric palladacycle functionalization reactions are reported with respect to one equivalent of dimeric complex as has been the practice in recent papers on C-H activation and C-H functionalization with acetate bridged palladacycles.[1,10,14,15]

Powers, D. C.; Xiao, D. Y.; Geibel, M. A. L.; Ritter, T. *J. Am. Chem. Soc.* **2010**, *132* (41), 14530.
Powers, D. C.; Geibel, M. A. L.; Klein, J. E. M. N.; Ritter, T. *J. Am. Chem. Soc.* **2009**, *131* (47), 17050.
Powers, D. C.; Benitez, D.; Tkatchouk, E.; Goddard, W. A., III; Ritter, T. *J. Am. Chem. Soc.* **2010**, *132* (40), 14092.
Powers, D. C.; Ritter, T. *Nature Chemistry* **2009**, *1* (4), 302.

Iodination

To an NMR tube was added a stock solution in CD_2Cl_2 of **6b** (7.5 mM, 500 µL, 3.75 µmol), followed by a stock solution in CH_2Cl_2 of **S1.3** (30 mM, 50 µL, 1.5 µmol), followed by a stock solution in CH_2Cl_2 of iodine (37.5 mM, 200 µL, 7.5 µmol, 2 equiv.). The tube was capped, shaken, and left at room temperature for 17 h at which time it was analyzed by ^{19}F NMR and the concentration of the desired product was determined with respect to **S1.3**. The formation of the **5d** was confirmed by spiking independently synthesized **5d** into the mixture. GCMS analysis of the reaction mixture showed one major product which had the same m/z and retention time as independently synthesized **5d**.

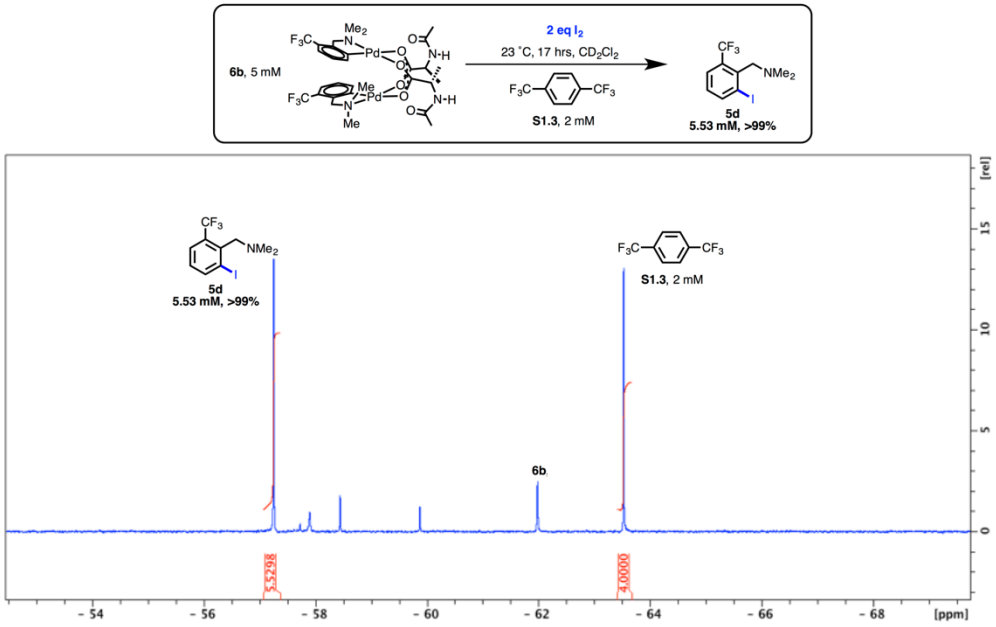

Bromination

To an NMR tube was added a stock solution in CD_2Cl_2 of **6b** (7.5 mM, 500 µL, 3.75 µmol), followed by a stock solution in CH_2Cl_2 of **S1.3** (30 mM, 50 µL, 1.5 µmol), followed by a stock solution in CH_2Cl_2 of bromine (22.5 mM, 200 µL, 4.5 µmol, 1.2 equiv.). The tube was capped, shaken, and left at room temperature for 17 h at which time it was analyzed by ^{19}F NMR and the concentration of the desired product was determined with respect to **S1.3**. GCMS analysis of the reaction mixture showed one major product which had the same m/z and retention time as independently synthesized **5c**.

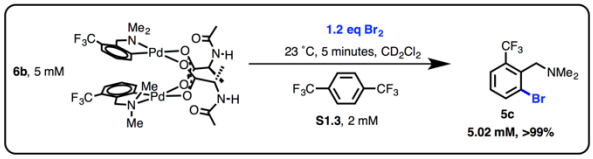

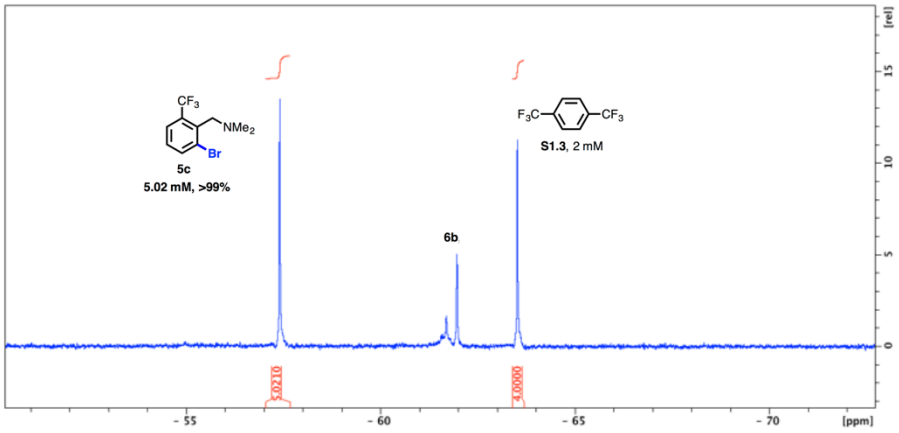

Relative rates of iodination and bromination

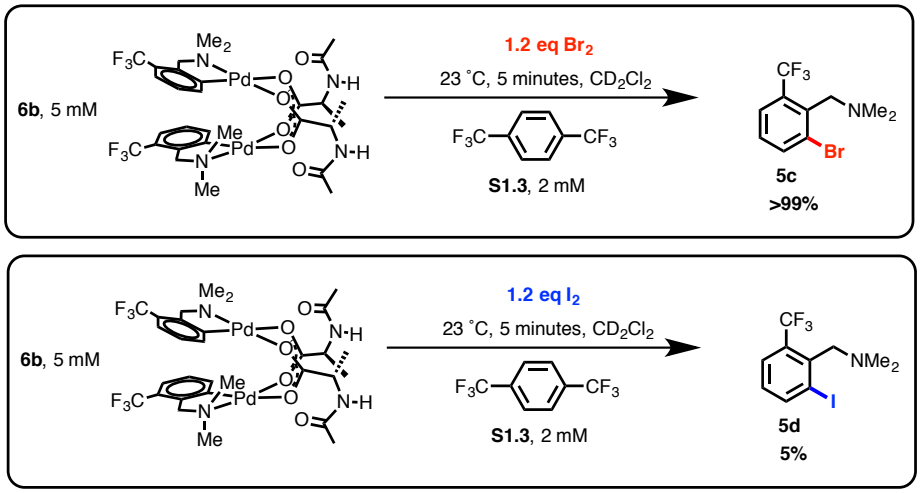

To an NMR tube was added a stock solution in CD_2Cl_2 of **6b** (7.5 mM, 500 µL, 3.75 µmol) followed by a stock solution in CH_2Cl_2 of **S1.3** (30 mM, 50 µL, 1.5 µmol). The tube was sealed with a rubber septum, brought to the NMR spectrometer, locked, and shimmed. The sample was ejected from the spectrometer, and through the rubber septum was injected a stock solution in CH_2Cl_2 of X_2 (X=Br or I) (22.5 mM, 200 µL, 4.5 µmol, 1.2 equiv.). The sample was shaken and lowered into the spectrometer immediately. The reaction was monitored by ^{19}F NMR at 15 second intervals over 20 minutes the concentration of the desired products was determined with respect to **S1.3**.

Figure S1.2: palladacycle bromination proceeds more rapidly than iodination
note that scales on y axis are different for iodination and bromination

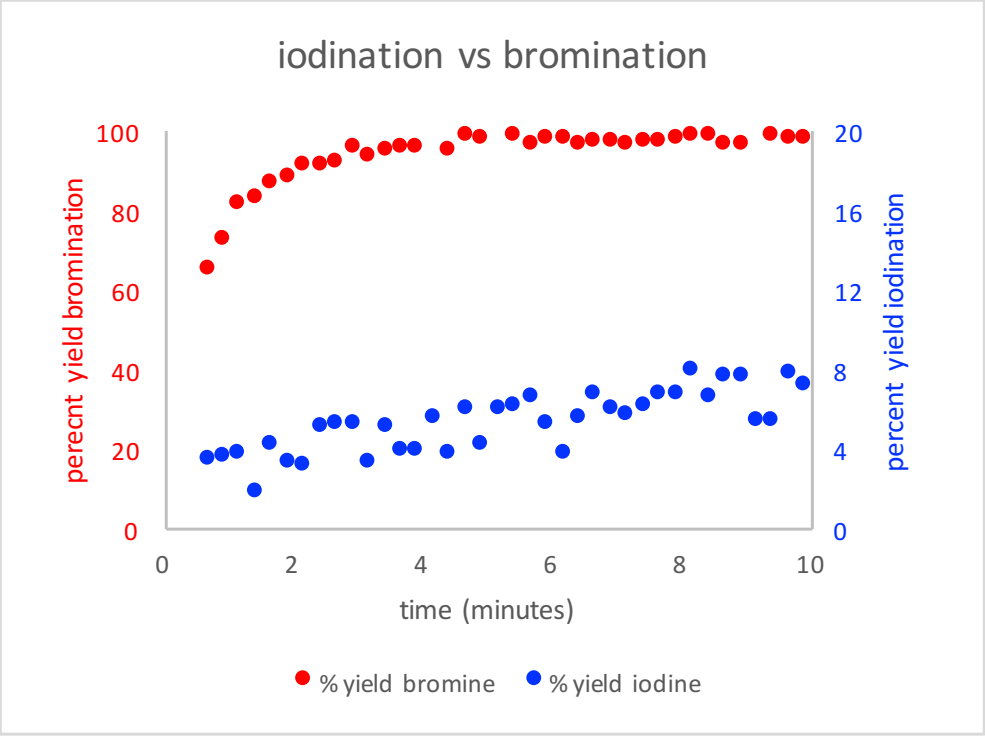

Chlorination with 2 equiv. oxidant

To an NMR tube was added a stock solution in CD_2Cl_2 of **6b** (7.5 mM, 500 µL, 3.75 µmol), followed by a stock solution in CH_2Cl_2 of **S1.3** (30 mM, 50 µL, 1.5 µmol), followed by a stock solution in CH_2Cl_2 of iodobenzene dichloride (37.5 mM, 200 µL, 7.5 µmol, 2 equiv.). The tube was capped, shaken, and left at room temperature for 30 minutes at which time it was analyzed by ^{19}F NMR and the concentration of the desired product was determined with respect to **S1.3**. GCMS analysis of the reaction mixture showed one major product which had the same m/z and retention time as independently synthesized **5b**.

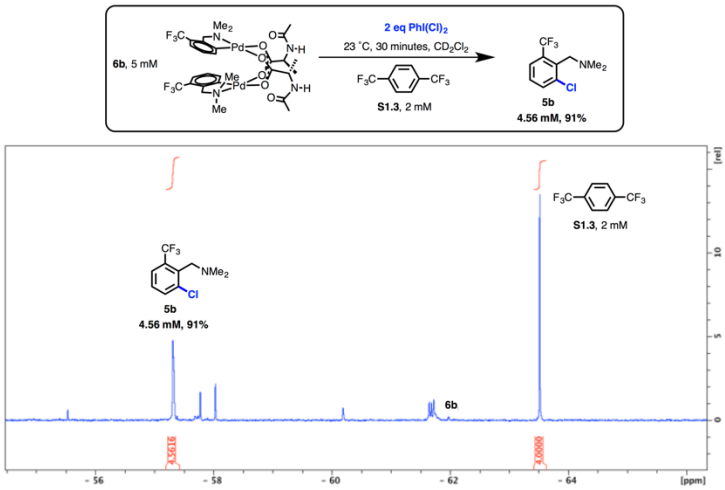

Chlorination with 5 equiv. oxidant

To an NMR tube was added a stock solution in CD_2Cl_2 of **6b** (7.5 mM, 500 µL, 3.75 µmol), followed by a stock solution in CH_2Cl_2 of **S1.3** (30 mM, 50 µL, 1.5 µmol), followed by a stock solution in CH_2Cl_2 of iodobenzene dichloride (93.75 mM, 200 µL, 18.75 µmol, 5 equiv.). The tube was capped, shaken, and left at room temperature for 30 minutes at which time it was analyzed by ^{19}F NMR and the concentration of the desired product was determined with respect to **S1.3**. Further monitoring of the reaction mixture revealed decreasing concentration of **5b** and a new species developing. The mixture was transferred to a 1 dram vial and left uncapped overnight. Slow evaporation of CH_2Cl_2 afforded singled crystals of a know coordination polymer with the formula $PdCl_2$ + HCl + $HNMe_2$. See crystallographic section for details.

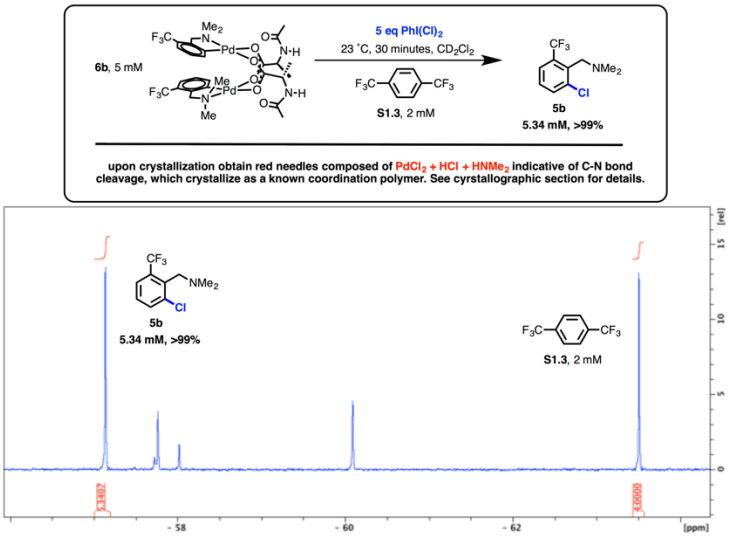

Olefination in trifluoroethanol

MPAA complex **2** (10 µmol, 7.1 mg, 1 equiv.) was weighed into a 1 mL vial and transferred as a solid into an NMR tube with a J. Young cap, vial was washed with two 250 µL portion of trifluoroethanol. Internal standard1,2,4,5-tetrachloro-benzene (10 µmol, 2.15 mg, 1 equiv.) was added to the NMR tube in the same way. n-Butyl acrylate (400 µmol, 51.3 mg, 57 µL, 40 equiv.) was added by gas tight syringe. The J. Young cap was sealed and the tube placed in an 80 °C oil bath. The reaction was monitored hourly, but precipitation of Pd black led to poor line shapes. After 4 hours, the sample was removed from the oil bath, transferred to a 20 mL scintillation vial and the volatiles were removed under reduced pressure. The reaction mixture was dissolved in $CDCl_3$ and the yield of **14** was determined by ^1H NMR (which matched the spectrum for this compound reported in the literature, see ref. 16) by integration of the most downfield proton with respect to internal standard.

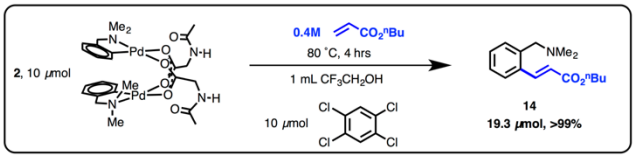

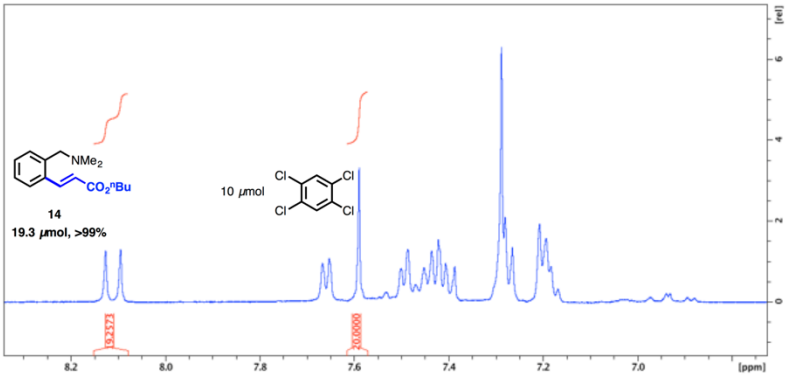

Olefination in 1,2-dichloroethane

MPAA complex **2** (10 µmol, 7.1mg, 1 equiv.) was weighed into a 1 mL vial and transferred as a solid into an NMR tube with a J. Young cap, vial was washed with two 250 µL portion of 1,2-dichloroethane. Internal standard 1,2,4,5-tetrachloro-benzene (10 µmol, 2.15 mg, 1 equiv.) was added to the NMR tube in the same way. n-Butyl acrylate (400 µmol, 51.3 mg, 57 µL, 40 equiv.) was added by gas tight syringe. The J. Young cap was sealed and the tube placed in an 80 °C oil bath. The reaction was monitored hourly, but precipitation of Pd black led to poor line shapes. After 42 hours, the sample was removed from the oil bath, transferred to a 20 mL scintillation vial and the volatiles were removed under reduced pressure. The reaction mixture was dissolved in $CDCl_3$ and the yield of **14** was determined by ^1H NMR by integration of the most downfield proton with respect to internal standard.

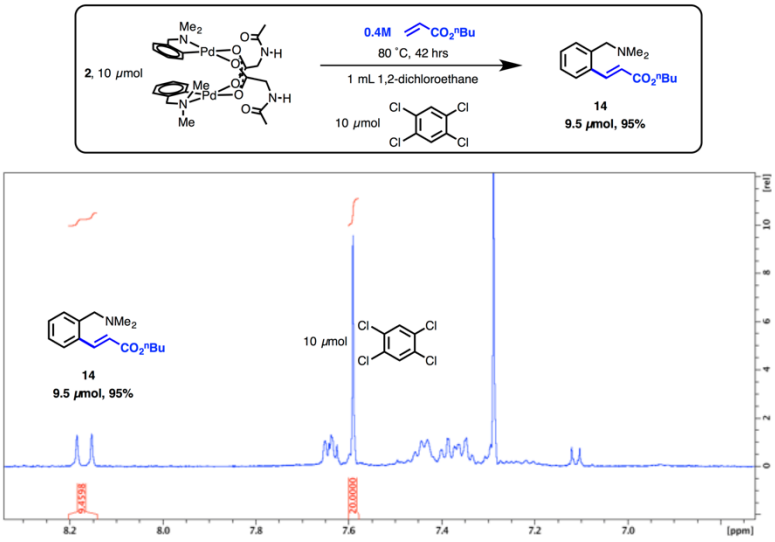

Section S1.10: Reaction of complex 2 with iodobenzene dichloride

Reaction with 1.2 equiv. iodobenzene dichloride

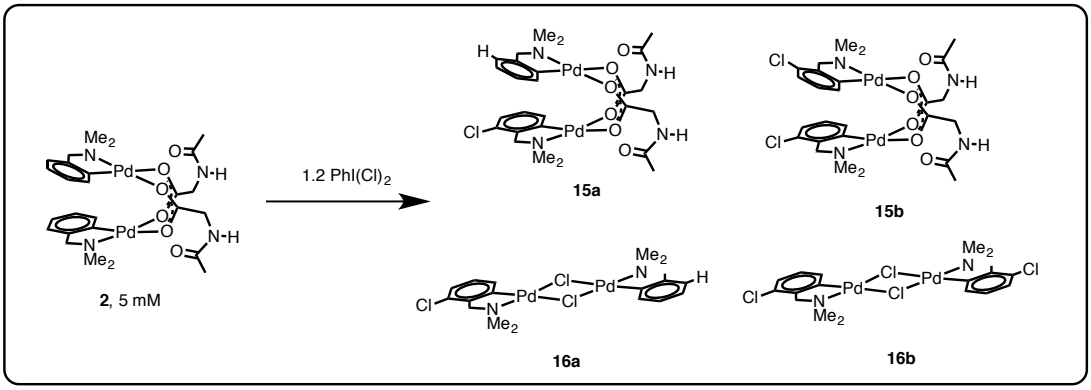

To an NMR tube was added a stock solution in CD_2Cl_2 of **2** (10 mM, 500 µL, 5 µmol, 1 equiv.) and a stock solution in CD_2Cl_2 of **S1.3** (20 mM, 50 µL, 1 µmol, 0.20 equiv.) and an additional 225 µL of CD_2Cl_2. The sample was brought to the NMR spectrometer, locked, shimmed, ejected from the instrument, injected with a stock solution in CD_2Cl_2 of iodobenzene dichloride (26.7 mM, 225 µL, 6 µmol, 1.2 equiv.), shaken, and inserted into the instrument. A spectrum was acquired every 2 minutes for the first 16 minutes of the reaction and the reaction was monitored periodically until the reaction stopped changing at 24 h. The sample was poured into a 1 dram vial which was nested in a 20 mL scintillation vial. Overnight, a small amount of yellow powder developed on the glass of the vial where the solved was evaporating. The mother liquor was poured into a separate vial and the yellow powder was analyzed and revealed a mixture of products consistent with **15a** and **15b**. The vial containing the mother liquor was nested in a 20 mL vial with 2 mL of pentane in the larger vial. Overnight, yellow, block shaped crystals suitable for x-ray diffraction grew and gave a crystal structure consistent with a mixture of mono and dichlorinated MPAA bridged palladacycles **15a** and **15b**. The yellow blocks were characterized by ^{1}H NMR was consistent with a mixture of **15a** + **15b** (see NMR of mixture). The supernatant from which the yellow blocks grew was decanted into a separate 1 dram vial and overnight, yellow needles suitable for x-ray diffraction grew as well as additional yellow blocks which were removed manually. Analysis of the yellow needles by x-ray diffraction was consistent with a mixture of non, mono, and dichlorinated chloride bridged MPAA complexes **16a** and **16b**. An NMR of the yellow needles that were characterized by x-ray diffraction were also consistent with a mixture of **16a** and **16b**.

Reaction progress by ^{1}H NMR

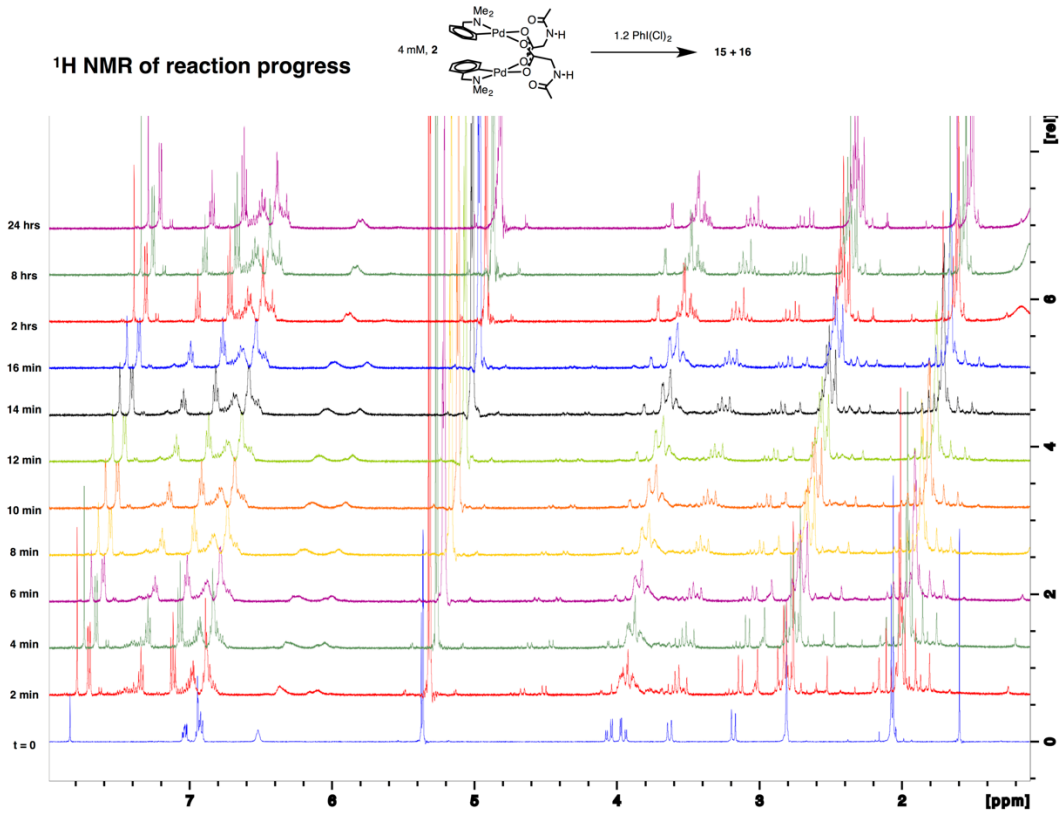

Comparison of ^{1}H NMR of MPAA complex 2 with isolated mixture of 15a and 15b

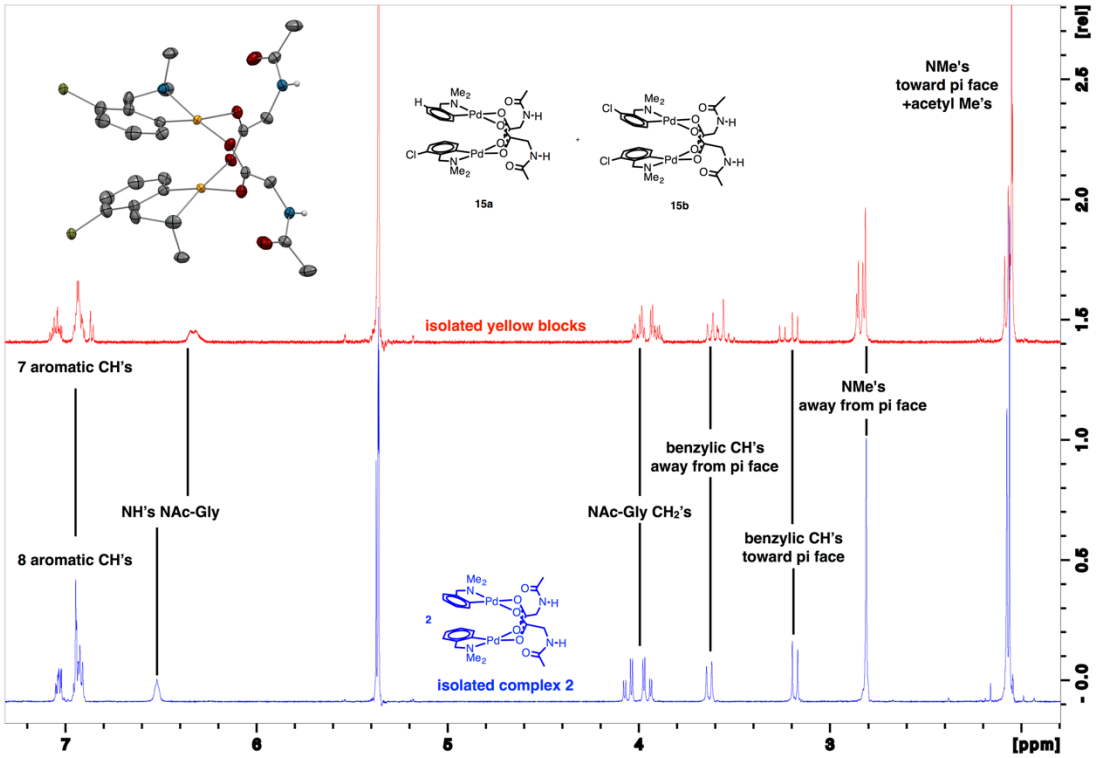

^{1}H NMR of isolated 15a and 15b

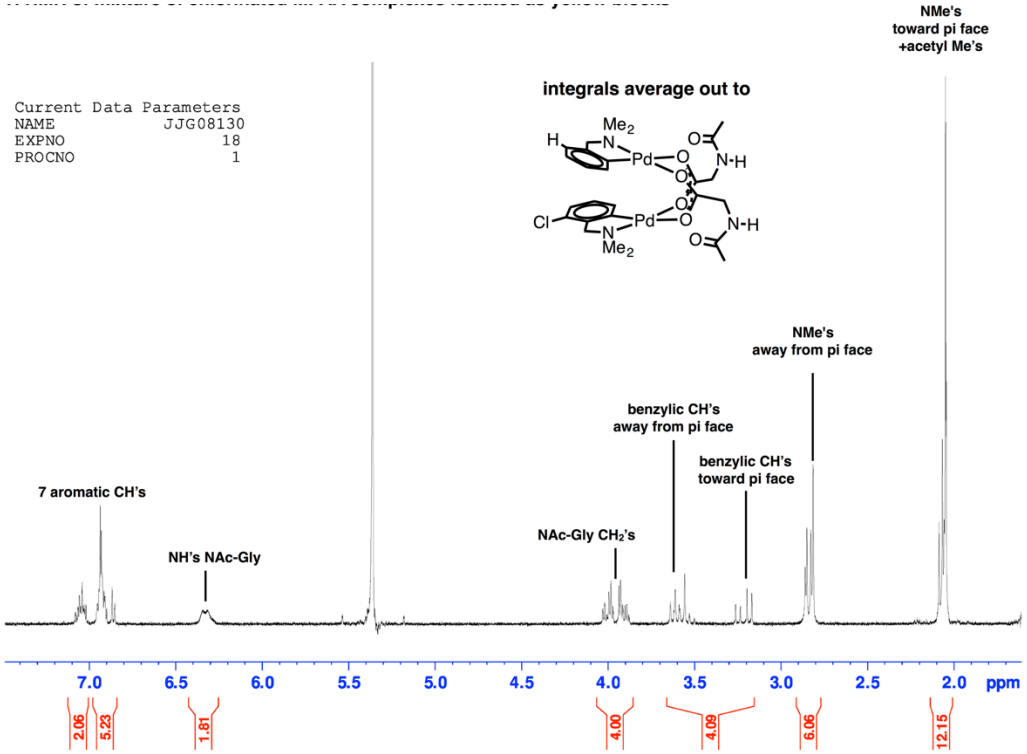

Comparison of ^{1}H NMR of complex S1.1 with isolated mixture of 16a and 16b

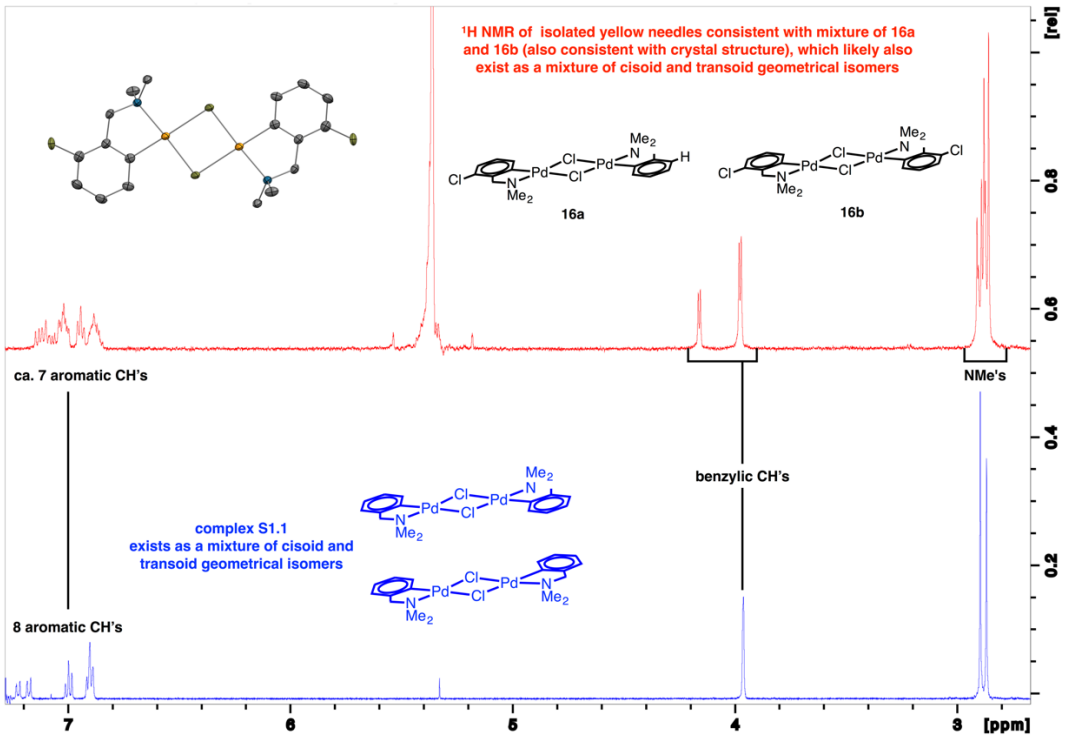

^{1}H NMR of 16a and 16b

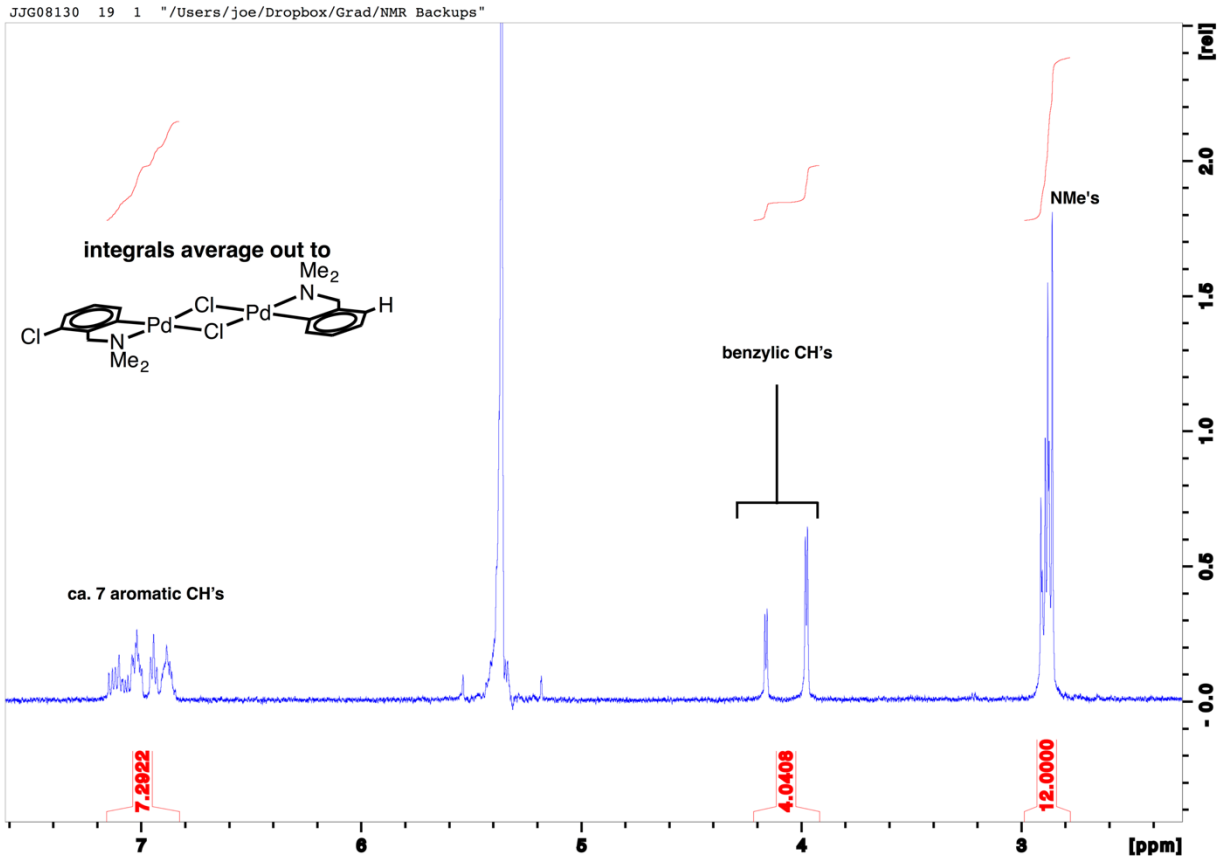

Reaction with 2.4 equiv. iodobenzene dichloride

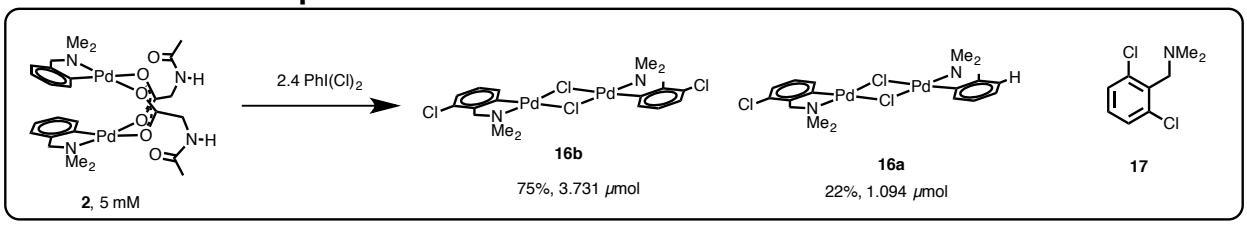

To an NMR tube was added a stock solution in CD_2Cl_2 of **2** (10 mM, 500 µL, 5 µmol, 1 equiv.), a stock solution in CD_2Cl_2 of **S1.3** (20 mM, 50 µL, 1 µmol, 0.20 equiv.), and a stock solution in CD_2Cl_2 of iodobenzene dichloride (26.7 mM, 450 µL, 12 µmol, 2.4 equiv.). The reaction was monitored over 24 hours and the yields of each complex determined by integration of the benzylic resonances with respect to internal standard (see NMR below). The sample was filtered over a 1 cm pad of celite in a Pasteur pipette with an additional 2 mL CH_2Cl_2 into a one dram vial to remove precipitated MPAA. The one dram vial was nested in a 20 mL scintillation vial with 2 mL pentane in the outer vial. Overnight, red needles suitable for x-ray diffraction grew and upon analysis by x-ray diffraction revealed the dichlorinated organic product **17** which co-crystalized as the HCl salt of tetrachloropalladate. The mother liquor was poured into a new one dram vial and was nested in a 20 mL scintillation vial with 10 mL pentane in the outer vial. Over two days at room temperature, yellow needles developed. The until cell of the needles was determined by x-ray diffraction was identical to that of the crystallized mixture of **16a** + **16b** from the previous experiment. The yellow needles were washed with pentane and analyzed by ^{1}H NMR which gave a spectrum consistent with **16b** contaminated with <10% **16a** (see NMR below).

^{1}H NMR of reaction progress

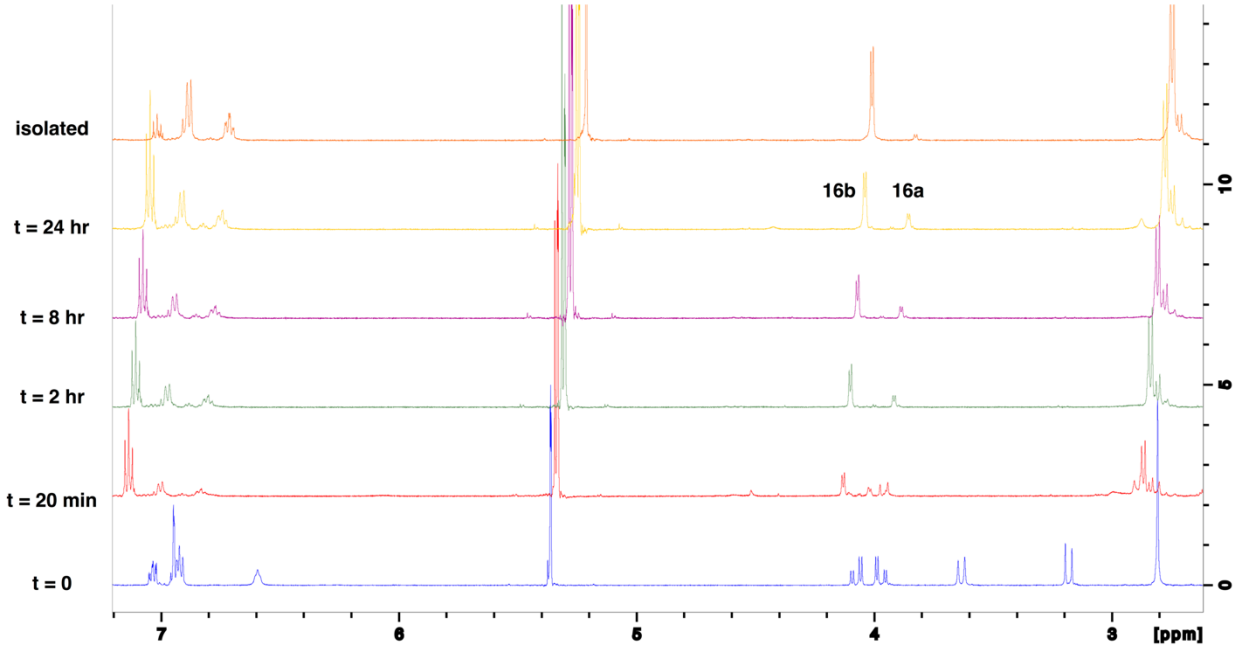

^{1}H NMR integrals used to determine yield

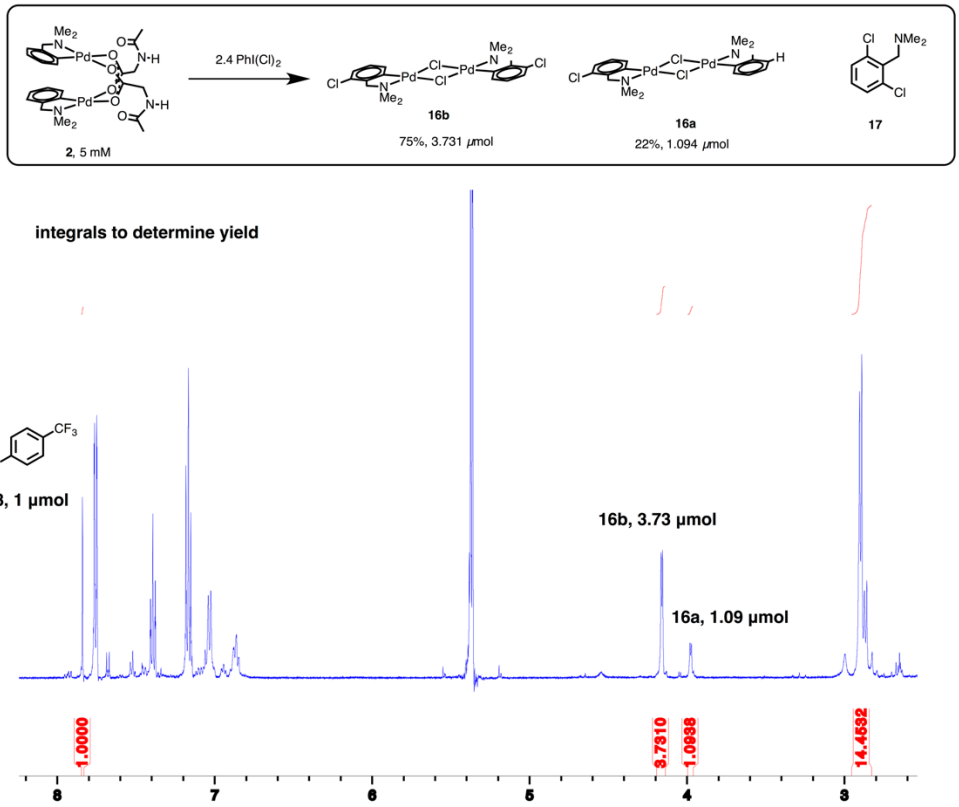

^{1}H NMR of isolated 16b

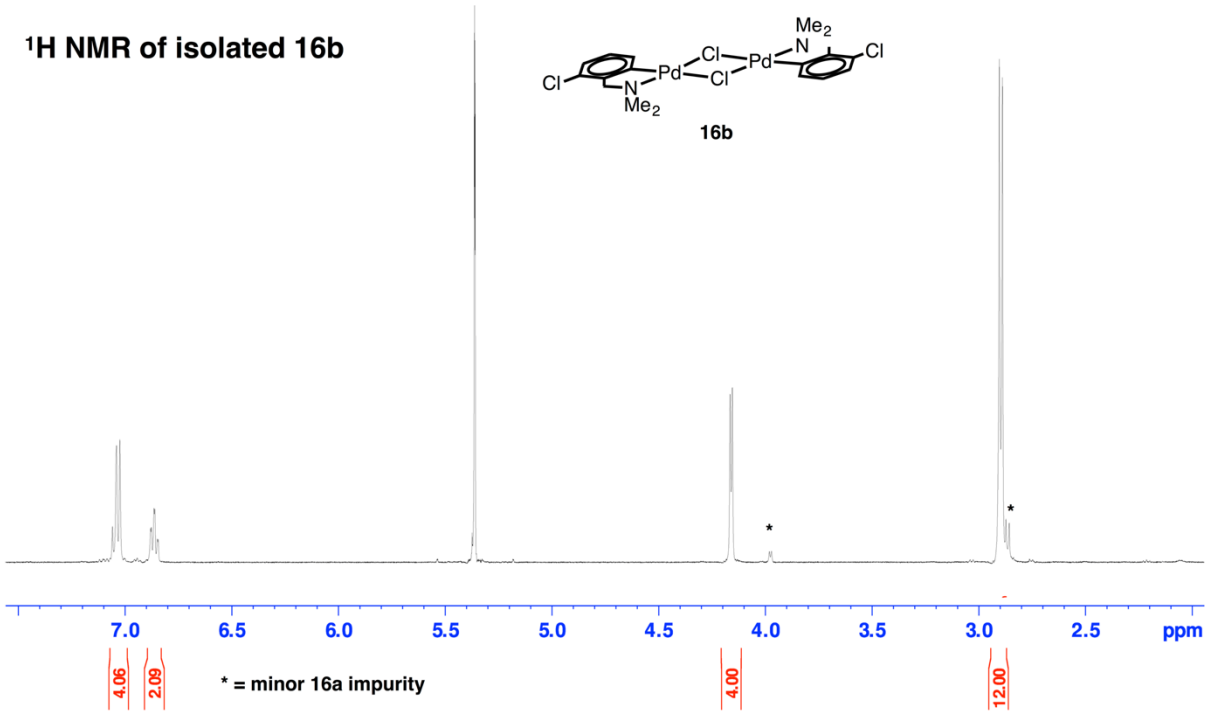

Pd(II) catalyzed olefination of dmba

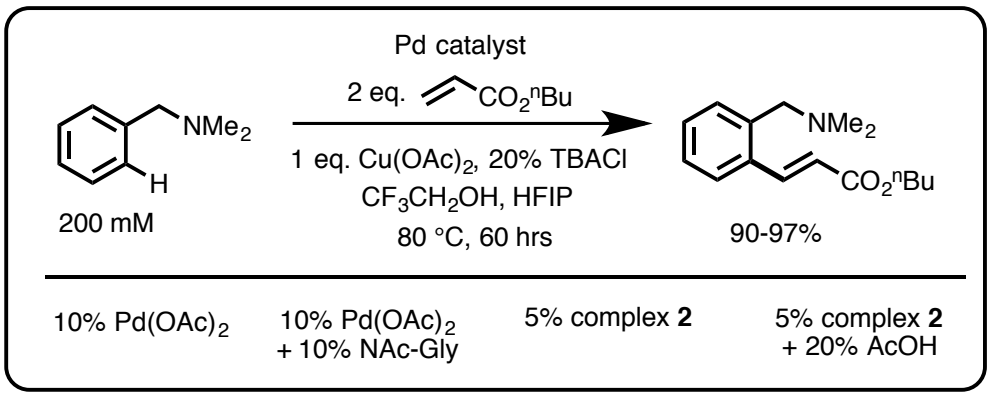

experimental set up

Four reactions were set up in 2 dram vials in parallel under air. The appropriate catalyst was weighed into each vial as a solid (acetic acid by volume as neat liquid):
vial A: Pd(II) acetate (18.0 mg, 80 μmol, 10 mol%)
vial B: Pd(II) acetate (18.0 mg, 80 μmol, 10 mol%) + NAc-Gly (9.39 mg, 80 μmol, 10 mol%)
vial C: complex **2** (28.5 mg, 40 μmol, 5 mol%)
vial D: complex **2** (28.5 mg, 40 μmol, 5 mol%) + acetic acid (9.61 mg, 9.16 μL, 160 μmol, 20%).
To each vial was added as a solid $Cu(OAc)_2$ (145 mg, 0.8 mmol, 1.0 equiv.) as a solid and a magnetic stir bar. To each vial was added 200 μL trifluoroethanol, followed by a stock solution in trifluoroethanol (800 μL) of dmba (1.0 M, 0.8 mmol, 108mg, 1 equiv.) and 1,4-bis(trifluoromethyl)-benzene (0.05 M, 0.04 mmol, 5%). To each vial was added a stock solution in trifluoroethanol of tetrabutylammonium chloride (1mL, 160mM,160 μmol, 44.5mg, 20%). To each vial was added 2 mL of hexafluoro-isopropanol. Each vial was clamped into a preheated 80 °C oil bath and stirred for 5 minutes. Reactions were initiated by addition of neat n-butyl-acrylate (1.6 mmol, 205 mg, 229 μL, 2 equiv.). Reaction progress was monitored by extracting 50 μL, quenching with 200μL 2M potassium carbonate in a 1.5 mL eppendorf tube, extracting with 800 μL $CDCl_3$, extracting starting material and products into the organic phase by shaking vigorously, filtering the organic phase over a 1 cm pad of Na_2SO_4 directly into an NMR tube, and determining yield by integration of the most downfield product resonance (8.09 ppm) with respect to 1,4-bis(trifluoromethyl)-benzene.

Figures S1.3: bar graph of initial rates of olefination with different precatalysts

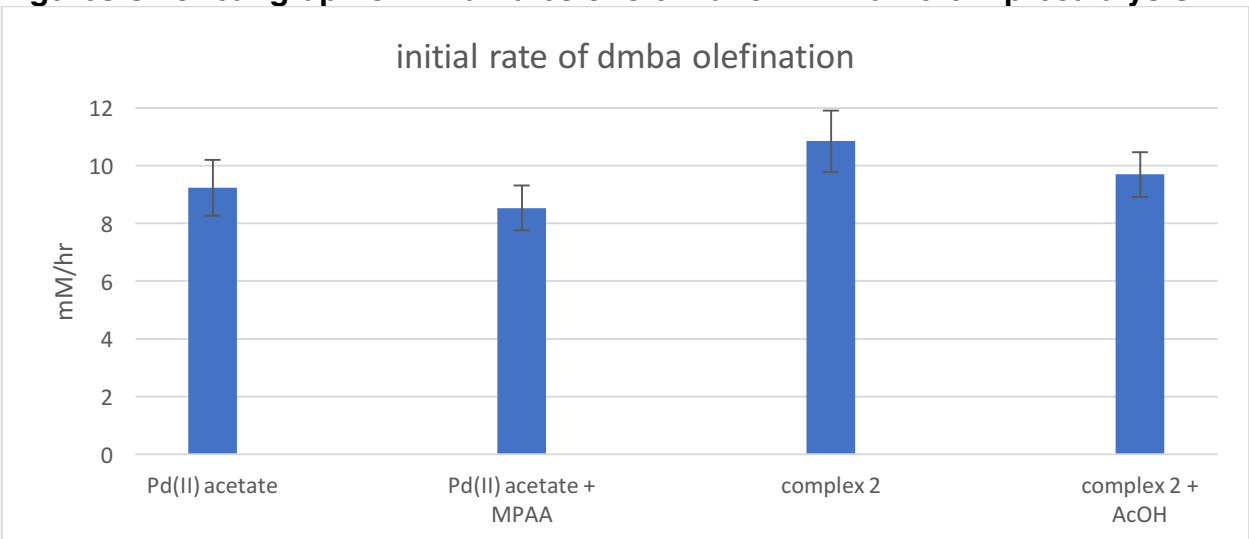

Figure S1.4: reaction progress initial rates region

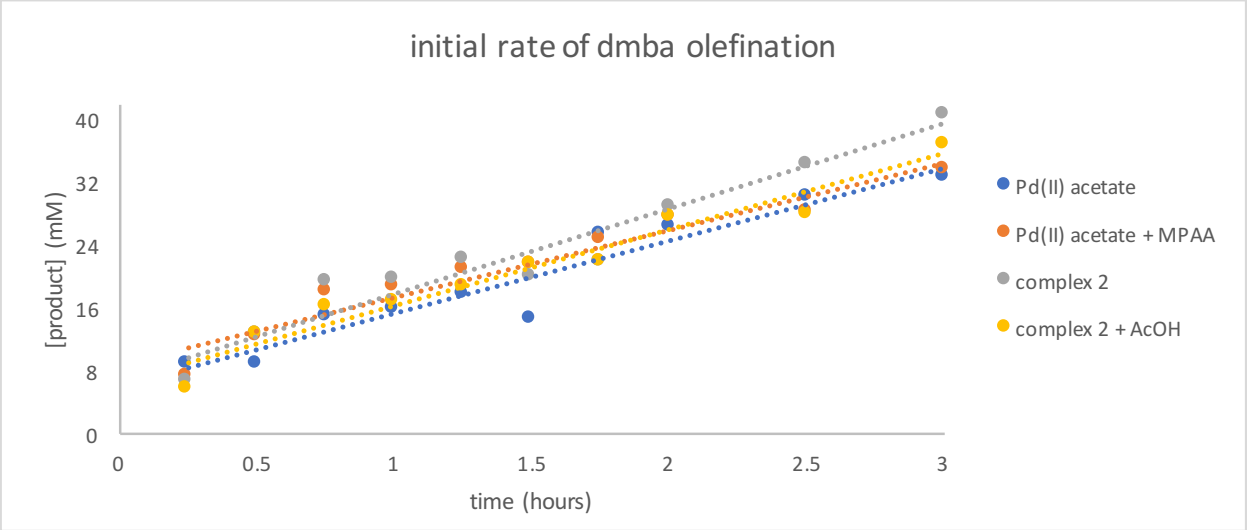

Figure S1.5: full reaction profiles

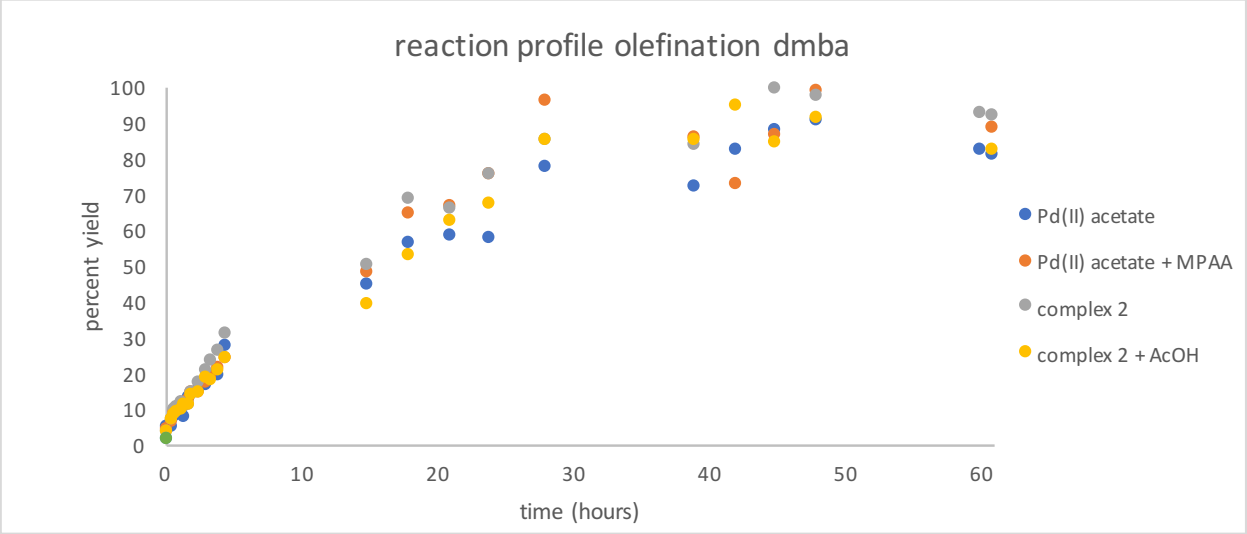

Section S1.12: Palladium catalyzed olefination of *o*-CF_3- phenyl acetic acid.

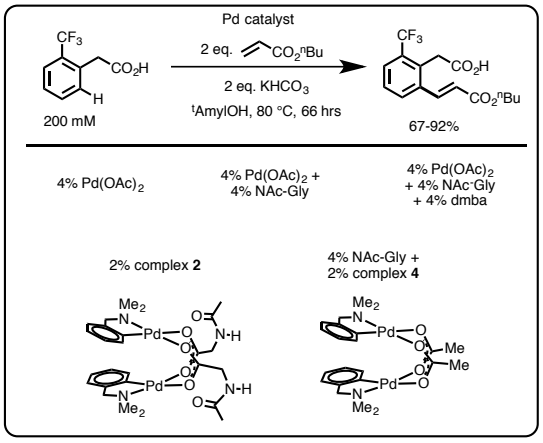

experimental set up

Five reactions were set up in 6 dram vials in parallel under air. The appropriate catalyst was weighed into each vial as a solid (dmba as a neat liquid by volume).

vial A: Pd(II) acetate (7.18 mg, 32 μmol, 4 mol%)

vial B: Pd(II) acetate (7.18 mg, 32 μmol, 4 mol%) + NAc-Gly (3.75 mg, 32 μmol, 4 mol%)

vial C: Pd(II) acetate (7.18 mg, 32 μmol, 4 mol%) + NAc-Gly (3.75 mg, 32 μmol, 4 mol%) + dmba (4.32 mg, 4.80 μL, 32 μmol, 4 mol%).

vial D: complex **2** (11.42 mg, 16 μmol, 2 mol%)

vial E: complex **4** (9.59 mg, 16 μmol, 2 mol%) + NAc-Gly (3.75 mg, 32 μmol, 4 mol%)

To each vial was added as a solid $KHCO_3$ (160 mg, 1.6 mmol, 2.0 equiv.) as a solid and a magnetic stir bar. To each vial was added 4mL of a stock solution in tert-amyl-alcohol containing 2-trifluoromethyl-phenyl-acetic acid (200 mM, 0.8 mmol, 163 mg, 1 equiv.), 1,4-bis(trifluoromethyl)-benzene (20 mM, 0.08 mmol, 17.1 mg, 10%), and n-butyl-acrylate (400 mM, 1.6 mmol, 205 mg, 2.0 equiv.). The reactions were stirred at room temperature for 5 minutes before initiating by placing in an aluminum heating block pre-heated to 80 °C. Reaction progress was monitored by extracting 50 μL, quenching with 200μL 2M aqueous HCl in a 1.5 mL eppendorf tube, adding 800 μL $CDCl_3$, extracting into the organic phase by shaking vigorously, filtering the organic phase over a 1 cm pad of Na_2SO_4 directly into an NMR tube, and determining conversion by normalizing the integrals of the starting material and product -CF_3 resonances to 100%.

Figure S1.6: reaction progress of aryl acetic acid olefination with different precatalysts

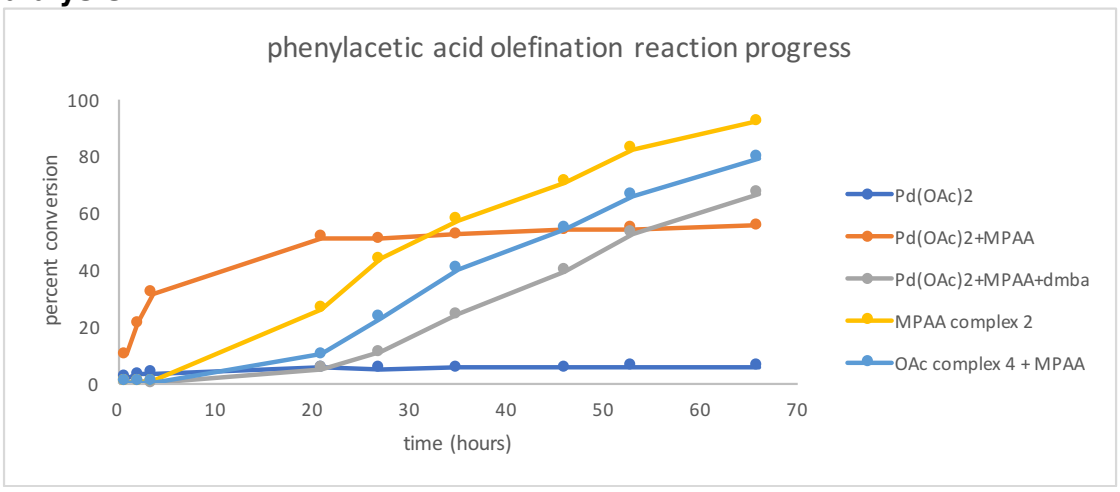

Section S1.13: Subsequent reaction of 5d in the presence of excess iodine

Preliminary observation

While conducting kinetics on the stoichiometric iodination iodination of **6b** we noticed that with extended reaction times, the iodinated product **5d** was consumed and a new product developed which we later characterized as formamidinium **S1.4**.

Stacked ^{19}F NMR of preliminary observation

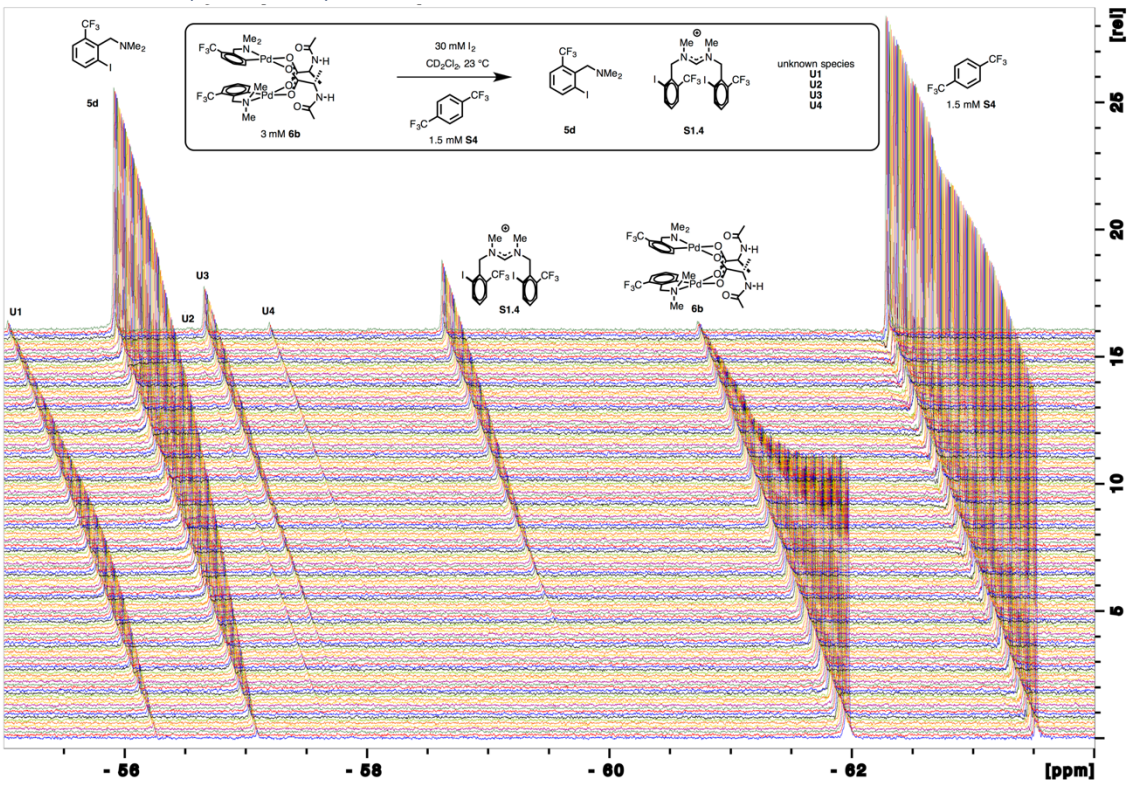

Integrated reaction profile of preliminary observation

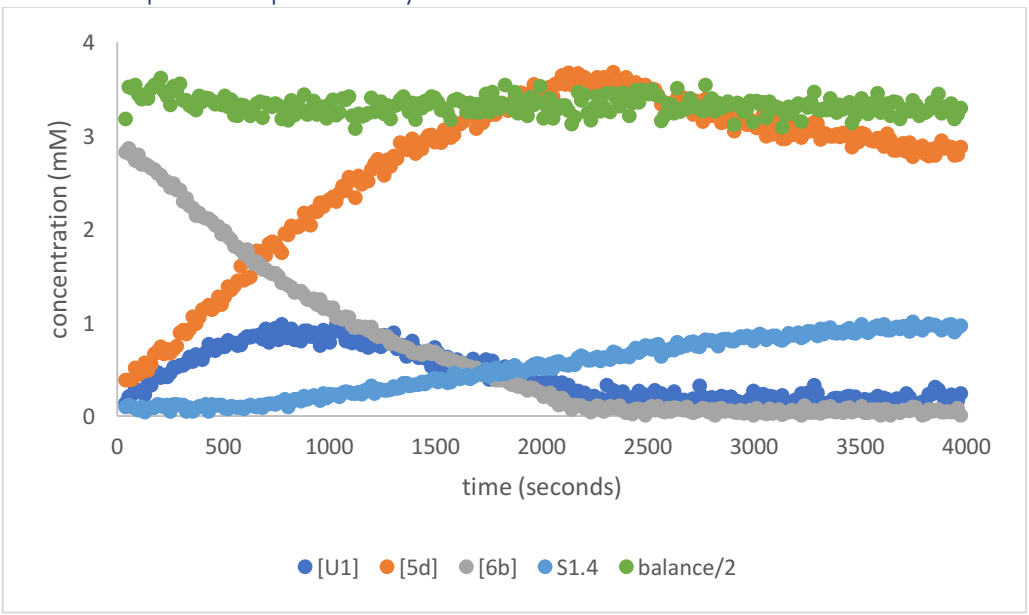

Experimental set up

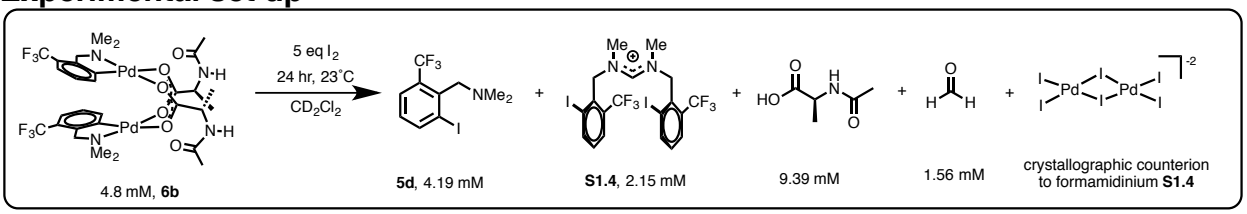

The following was performed in duplicate with one tube for spiking authentic product and the other for characterizing the reaction mixture and crystallization. To an NMR tube equipped with a J. Young cap was added a stock solution in CD_2Cl_2 of 1,4-bis(trifluoromethyl)benzene (**S1.3**) (20 mM, 50 μL, 1 μmol), a stock solution in CD_2Cl_2 of **6b** (9.6 mM, 500 μL, 4.8 μmol), and a stock solution in CD_2Cl_2 of iodine (53.3 mM, 450 μL, 24 μmol). After the iodine solution was added the sample was sealed with a J. Young cap and immediately brought to the NMR spectrometer to be monitored. The reaction was monitored periodically over 24 h (see stacked spectra below) at which time the concentrations of the species present were determined by ^{1}H NMR with respect to 1,4-bis(trifluoromethyl)benzene (**S1.3**) internal standard (see integrated spectrum of reaction mixture below). To one of the tubes was added independently synthesized **5d** (see spectra before and after spiking authentic below). The tube which did not contain spiked **5d** was connected to a U-joint and the volatiles were vacuum transferred to a third J. Young tube which was characterized by ^{1}H, ^{13}C, HMQC, and ^{19}F NMR, which revealed the presence of only formaldehyde and internal standard 1,4-bis(trifluoromethyl)benzene (**S1.3**). (Formaldehyde is the only observed product that can account for the methyl-group which must be removed from **5d** to afford formamidinium **S1.4**.) The non-volatile materials were re-dissolved by addition of 500 μL of CD_2Cl_2. The reconstituted reaction mixture was characterized by ^{1}H NMR, COSY, and ^{19}F NMR which are fully consistent with a mixture of ca. 4:2:1 NAc-Ala:**5d**:**S1.4** (see spectra below). The heterogenous mixture was filtered over a 1 cm pad of celite in a Pasteur pipette with an additional 1 mL of CH_2Cl_2 into a 1 dram vial, which was nested in a 20 mL scintillation vial. To the outer vial was added 2 mL of diethyl ether. After 24 hours at room temperature, small red-purple single crystals suitable for x-ray diffraction had grown. Analysis by x-ray diffraction revealed a ternary co-crystal with an asymmetric unit containing two equivalents of **S1.4**, two equivalents of iodine, and one equivalent of iodide bridged iodo palladate dimer ($Pd_2I_6^{2-}$). Notably, the contracted C-N bonds and the CNC angle of the fomamdidnium are consistent with an sp^2 hybridized carbon with C-N bonds of bond order >1 (see partial structure with labeled distances and angles below). Attempts to characterize pure **S1.4**, by NMR from isolated single crystals was not possible because the single crystals did not re-dissolve in CD_2Cl_2 or $CDCl_3$ after extensive sonication. Thus **S1.4** was characterized as a mixture of **S1.4**, **5d**, and NAc-Ala. A mixture enriched in **S1.4** was obtained by transferring the mother liquor from which single crystals of **S1.4** were grown to a new one dram vial nested in a 20 mL scintillation vial. To the outer vial was added 2 mL of pentane. After 24 hours at room temperature a dark precipitate had developed. The supernatant was removed and the precipitate was washed with pentane. Analysis of the precipitate by ^{1}H NMR revealed a mixture nearly free of NAc-Ala and enriched in **S1.4**. Analysis of the supernatant by ^{1}H NMR revealed a mixture of NAc-Ala, **5d**, and minor, uncharacterized impurities. The entire procedure was scaled up ten fold to obtain more material to characterize the formyl C-H by ^{13}C NMR, HMQC, and COSY (see spectra below). All of the NMR data are consistent with the assigned structure **S1.4** as observed in the solid state.

reaction progress by ^{1}H NMR

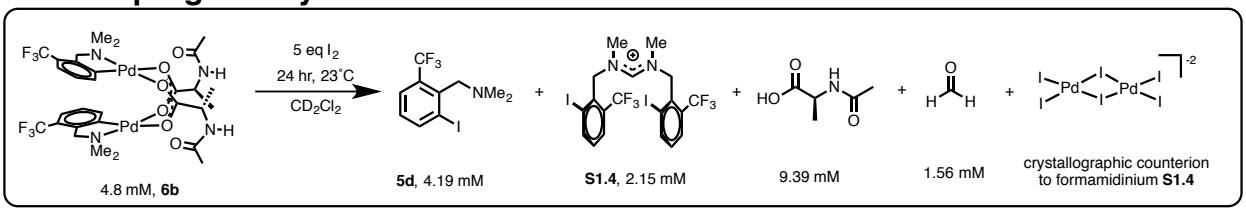

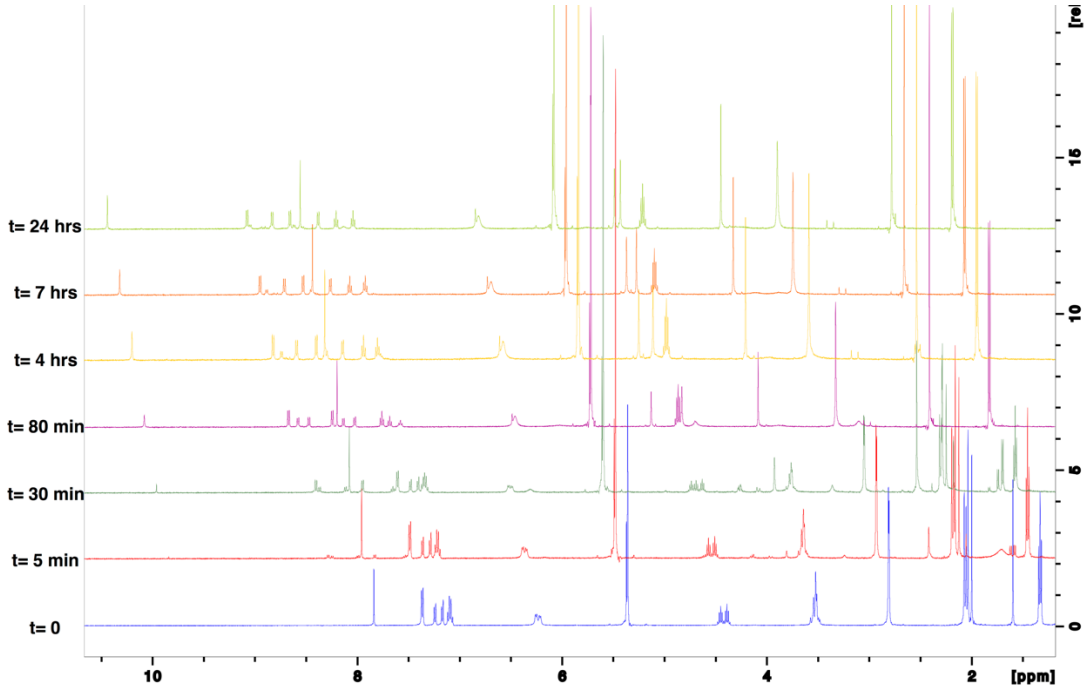

Spectra before and after spiking independently synthesized 5d

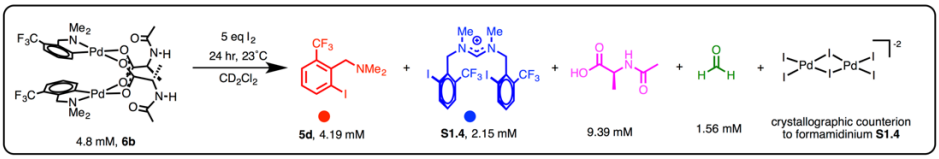

^{19}F NMR

^{1}H NMR

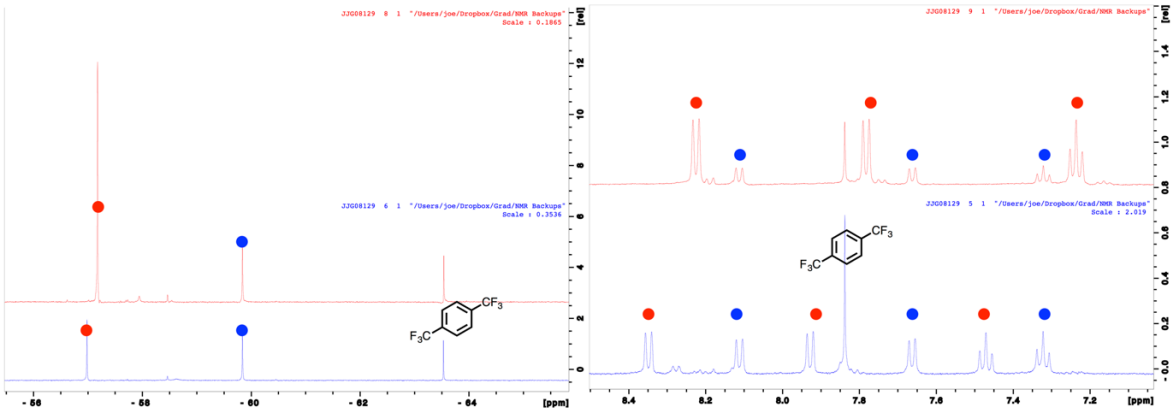

Stacked: mixture before vacuum transfer, non-volatiles, volatiles

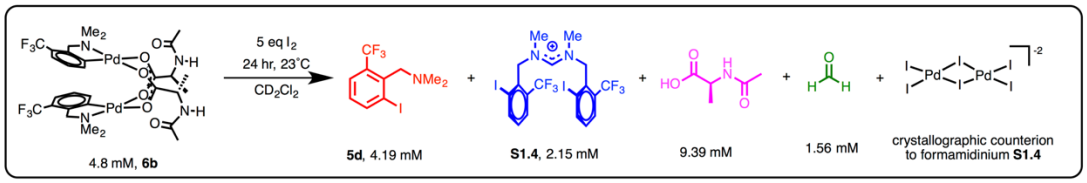

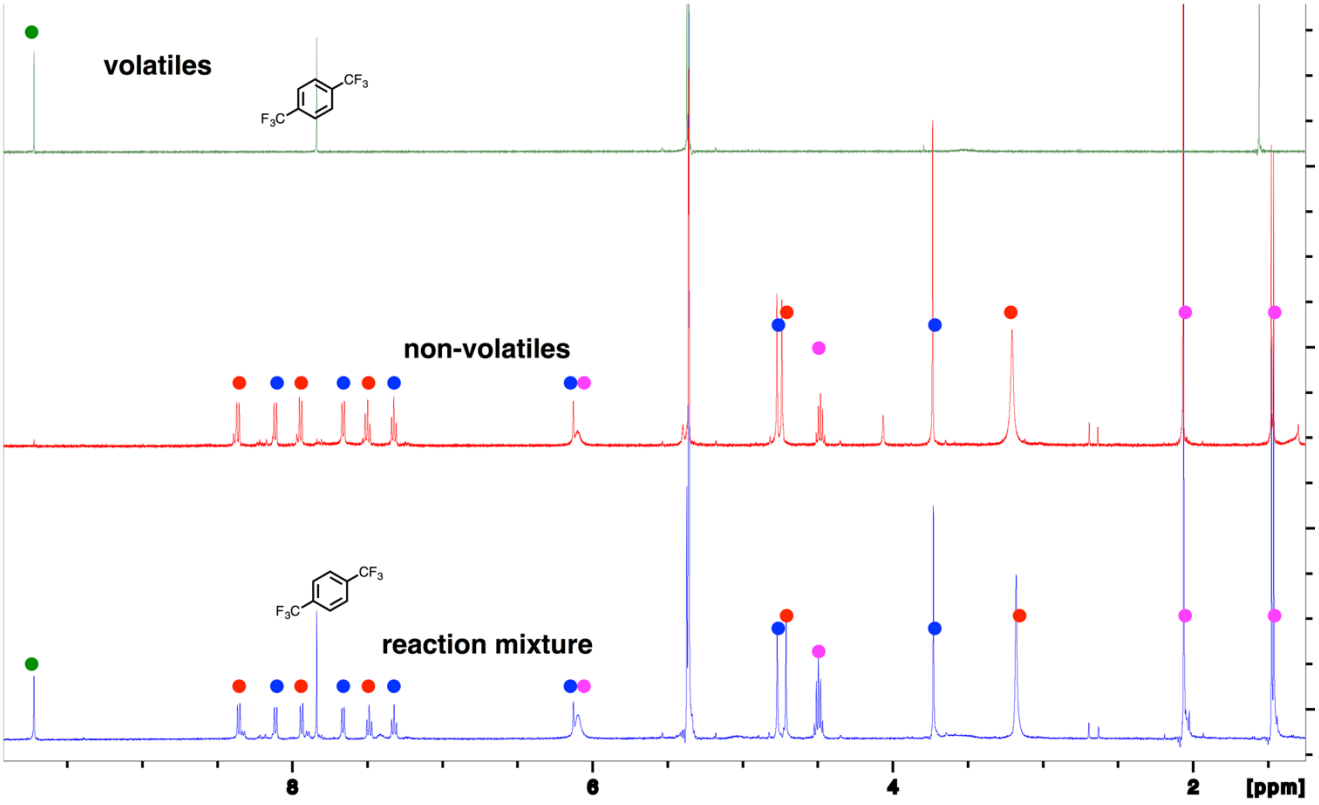

Integrated reaction mixture used to determine yield

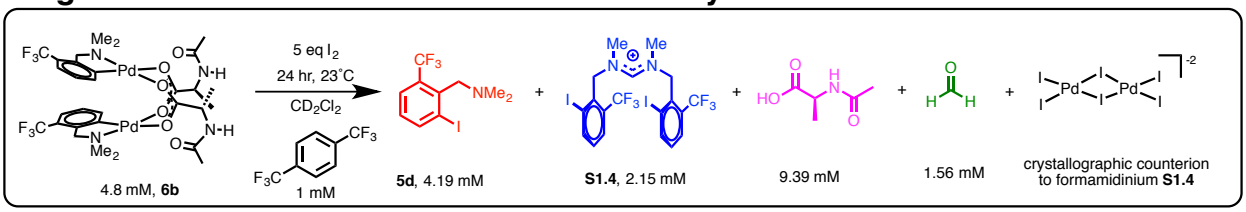

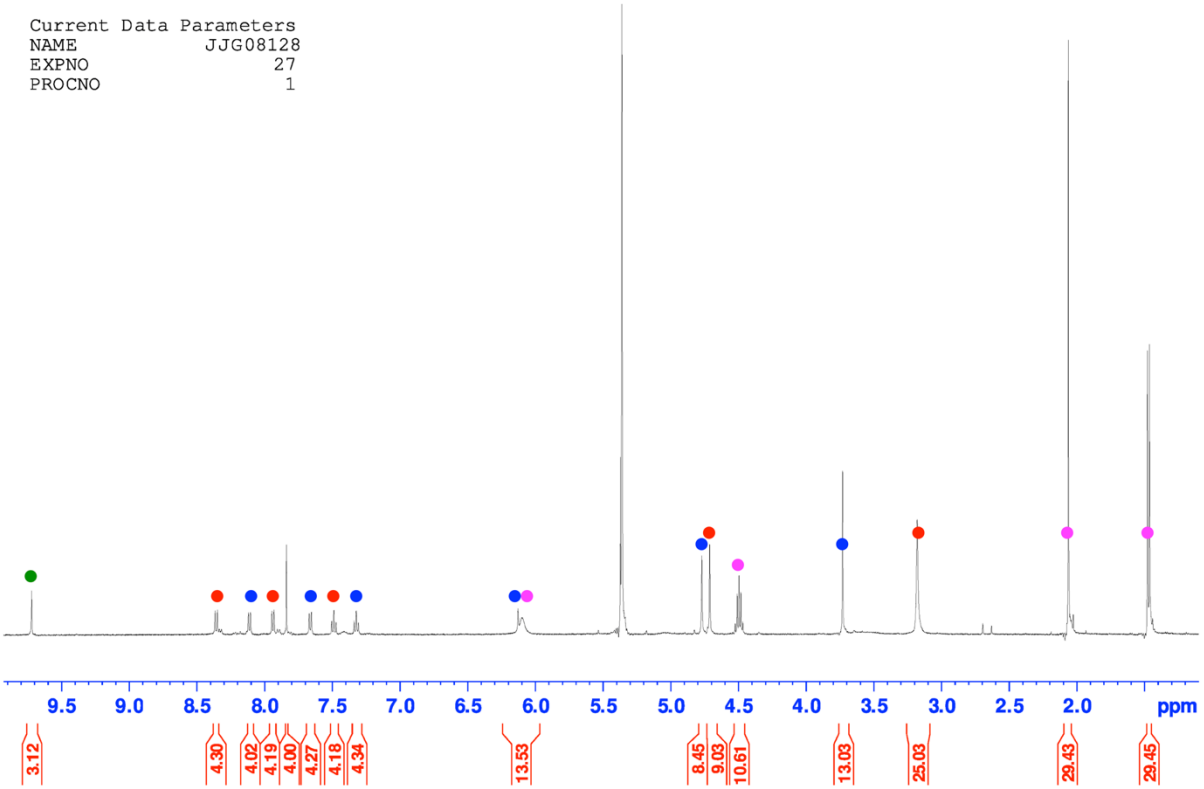

HMQC volatiles

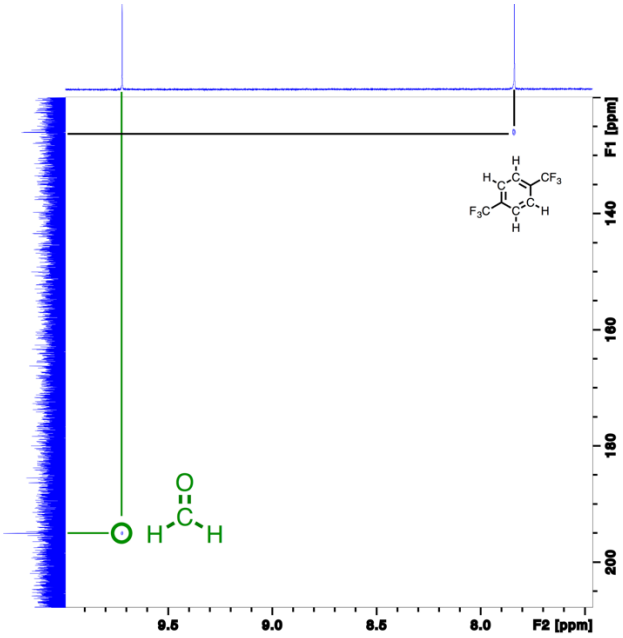

COSY reaction mixture non-volatiles

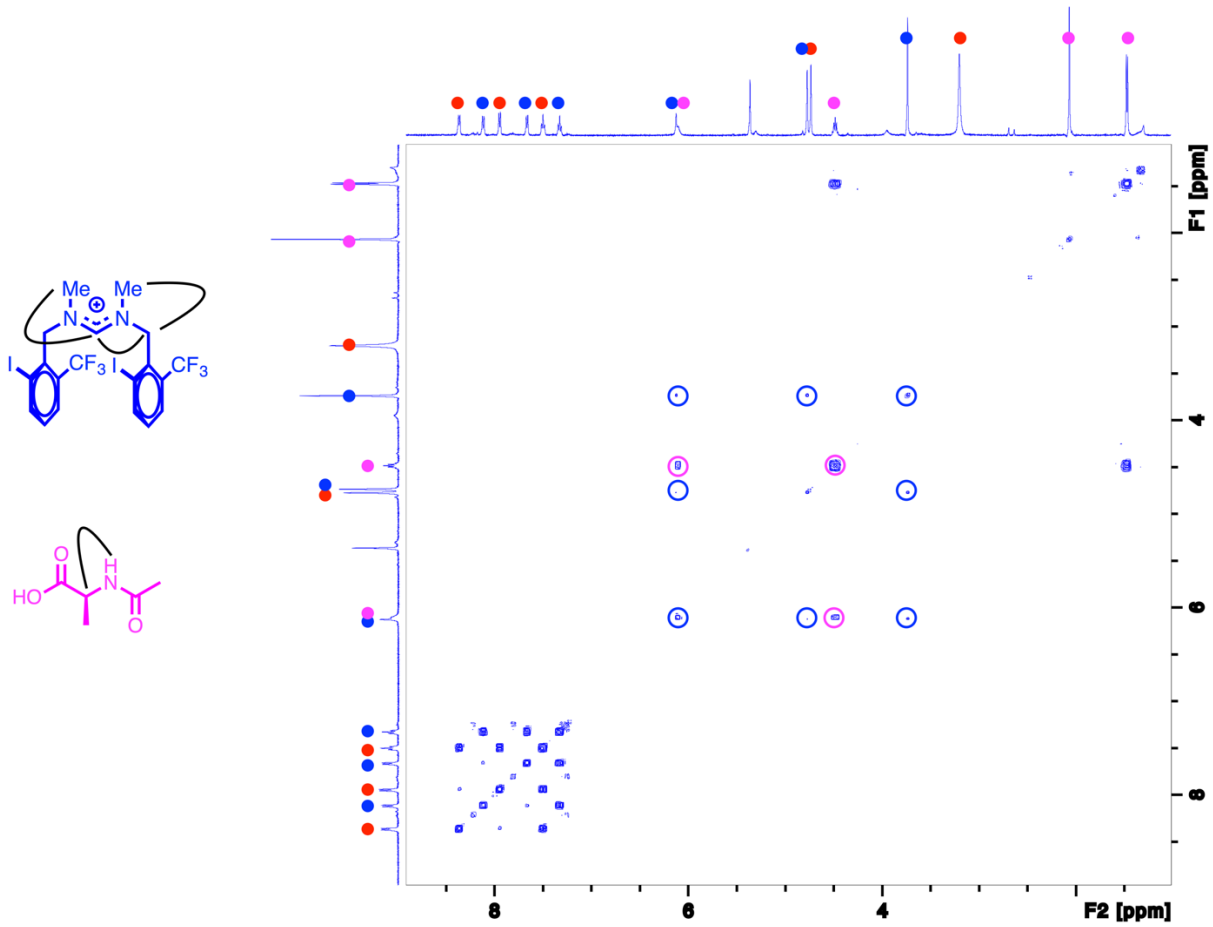

1H NMR enriched mixture integrals consistent with formamidinium

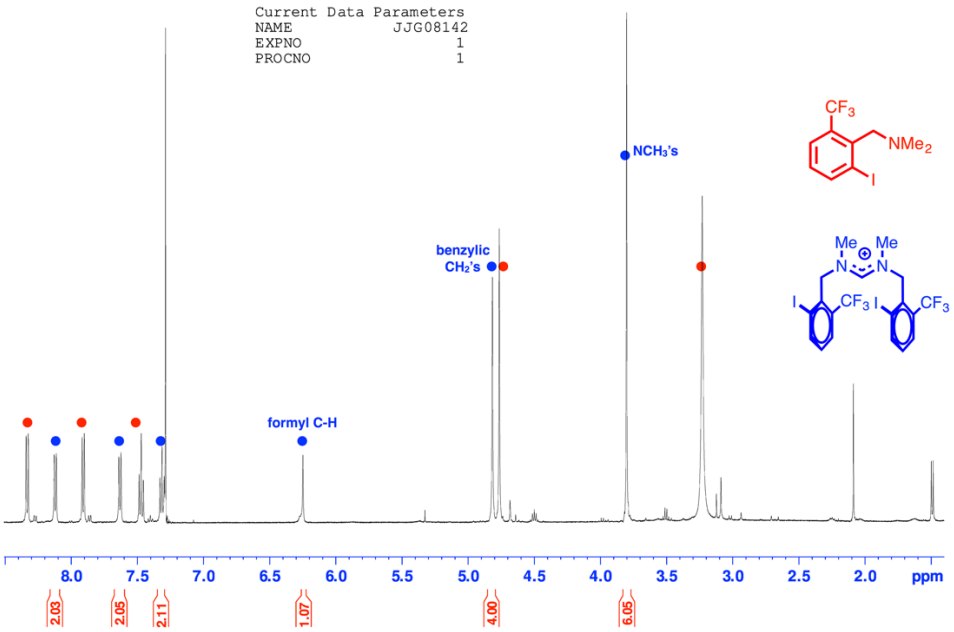

COSY enriched mixture

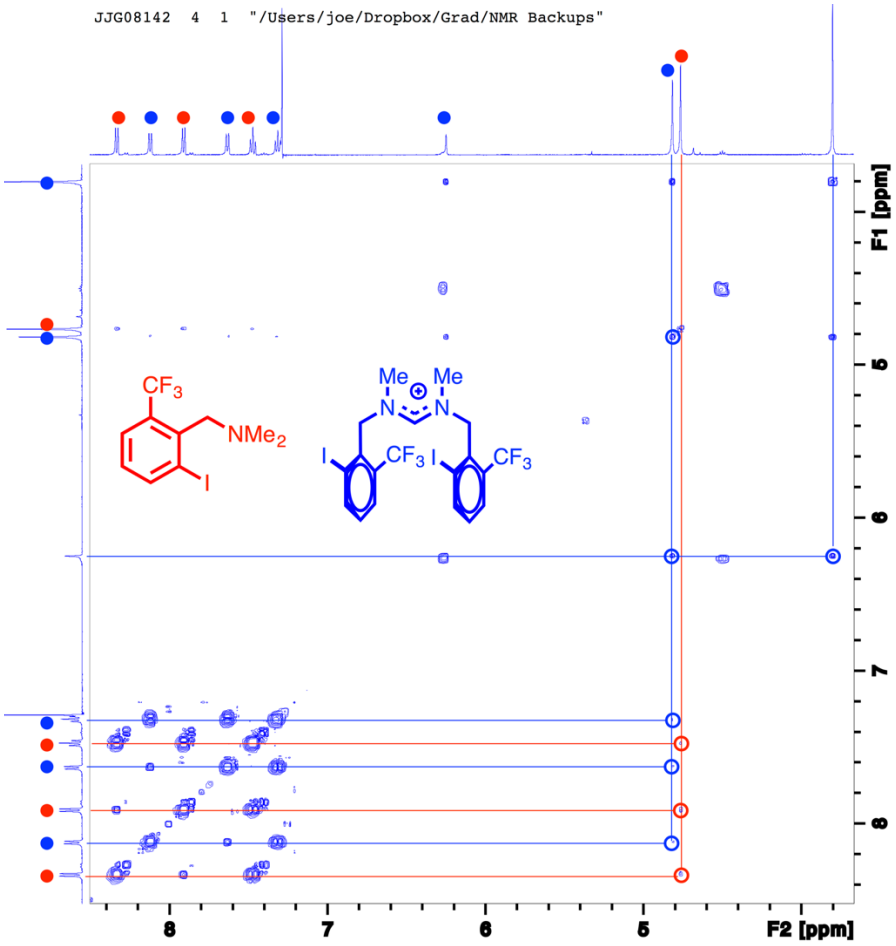

HMQC enriched mixture

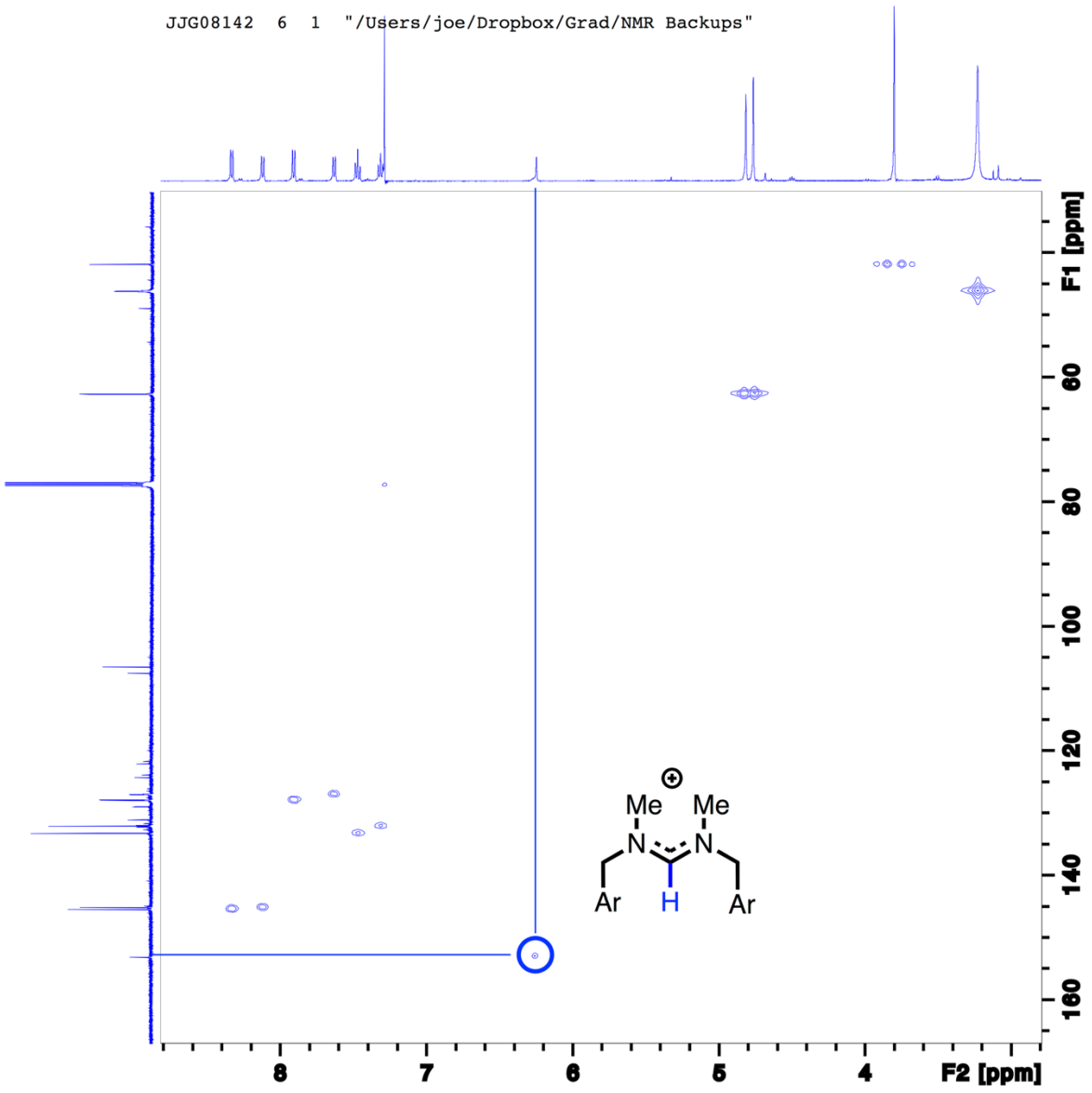

Section S1.14 Iodination Kinetics

Saturation in exogenous iodide (30 mM I_2)

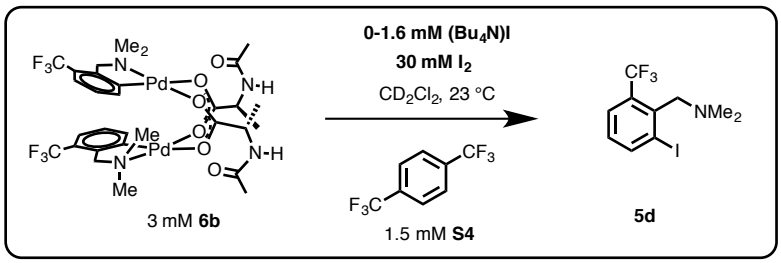

plots of reaction progress in initial rates region

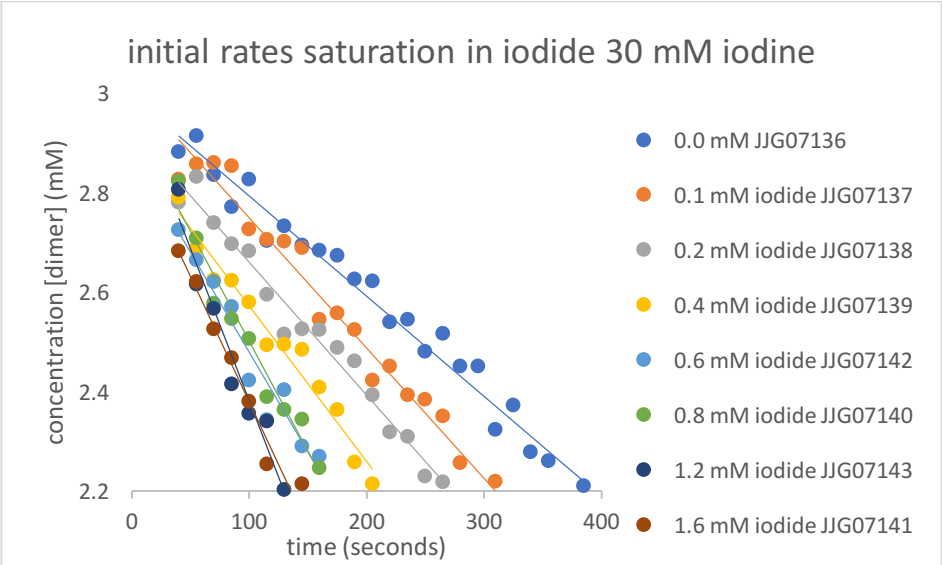

plot of initial rates vs [Bu_4NI]

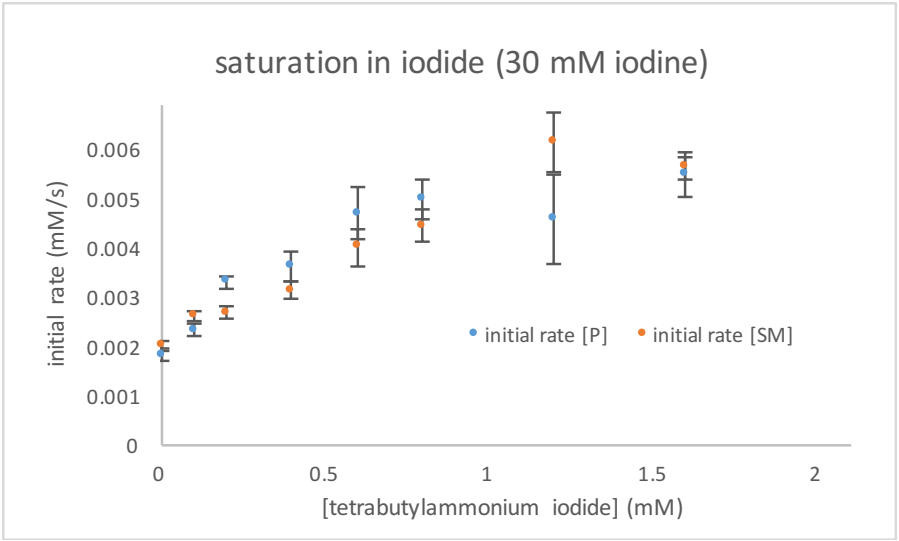

Saturation in exogenous iodide (8 mM I_2)

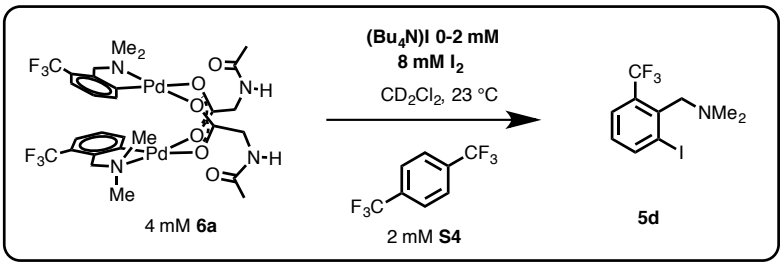

plots of reaction progress in initial rates region

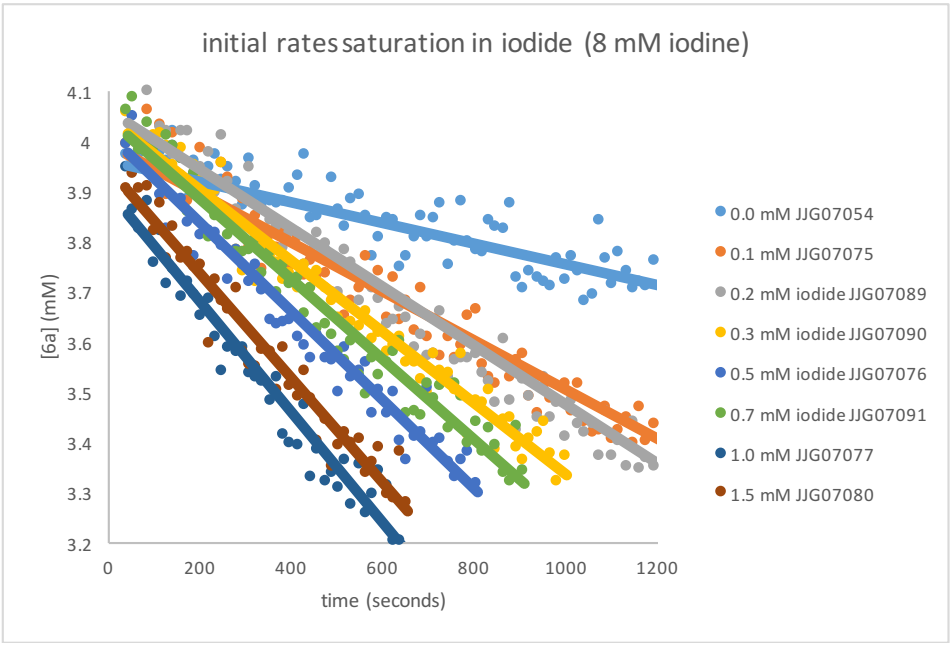

plot of initial rates vs [Bu_4NI]

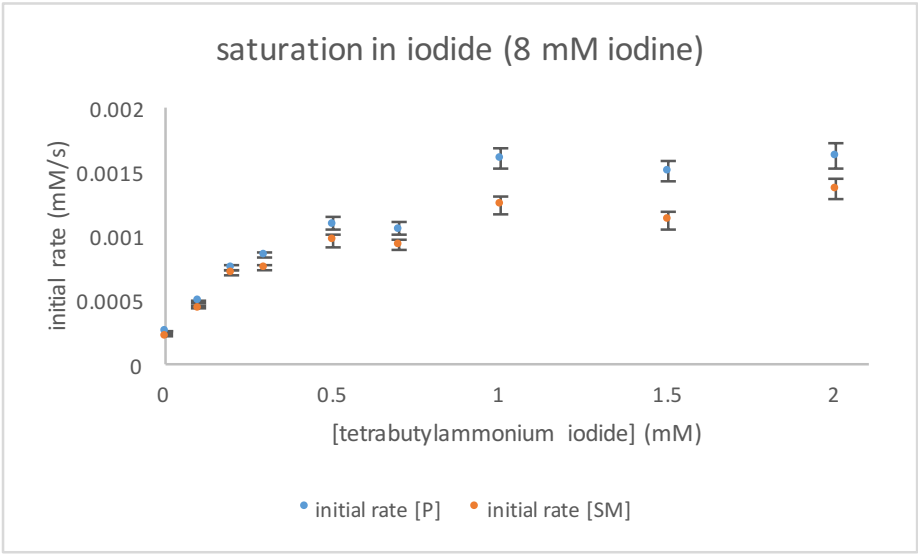

Order in I_2 in the absence of exogenous I^-

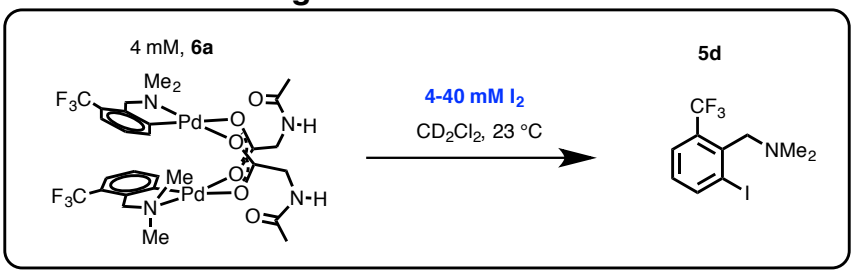

plots of reaction progress

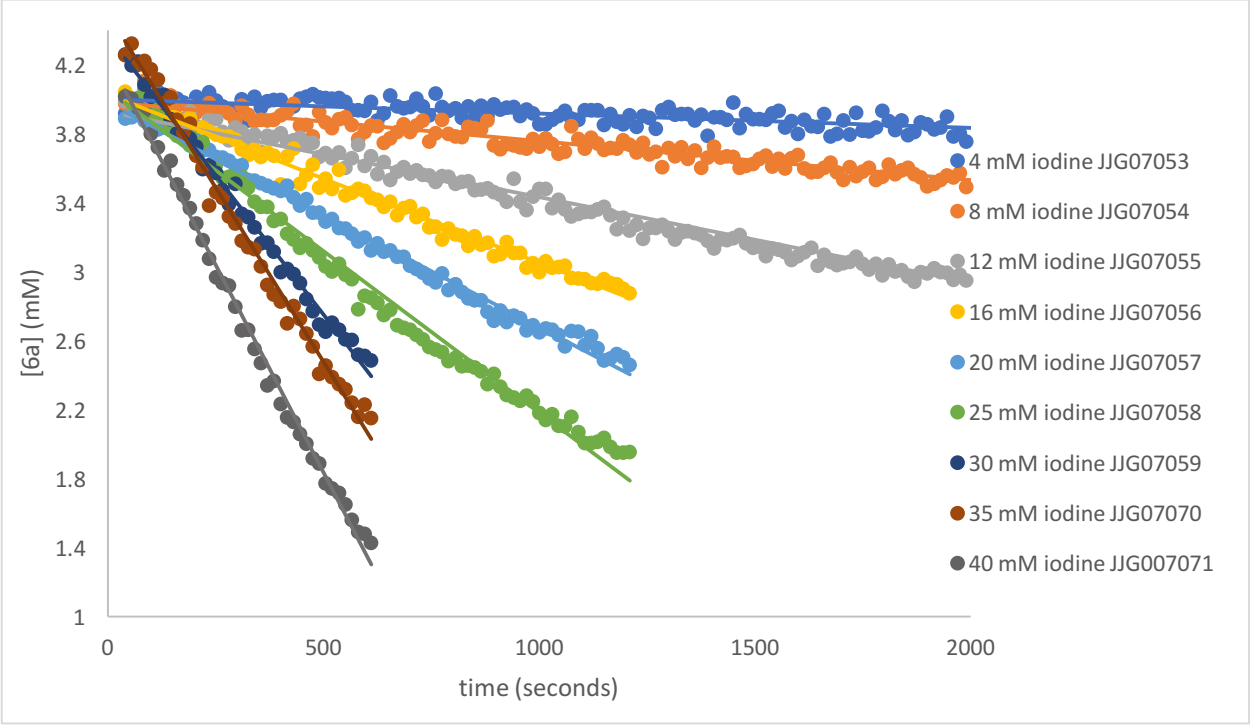

plot of initial rate versus initial [I_2]

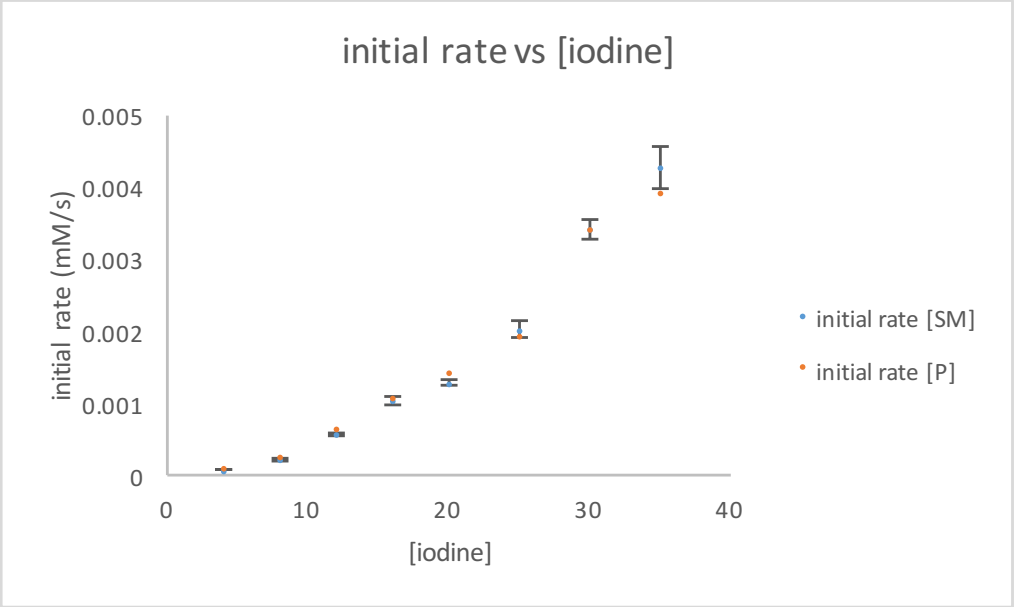

A reviewer noted that in the absence of exogenous iodide, the upward curvature in the plot of initial rate vs initial [I_2] could be a concequence of I_2 acting as weakly binding/activating ligand. In this scenario, we would expect to see second order in I_2 because one equivalent of I_2 is required for functionalization and one for activation (relative to the resting state). On the other hand, the staturation behavior observed with iodide may be a concequnce of iodide acting as a more strongly binding and activating ligand. In other words, iodide and iodine may play a similar role, but because of the differential ability of iodine and iodide to bind and activate, these effects are saturated in in different concentration regimes.

Order in I_2 in the presence of exogenous I^-

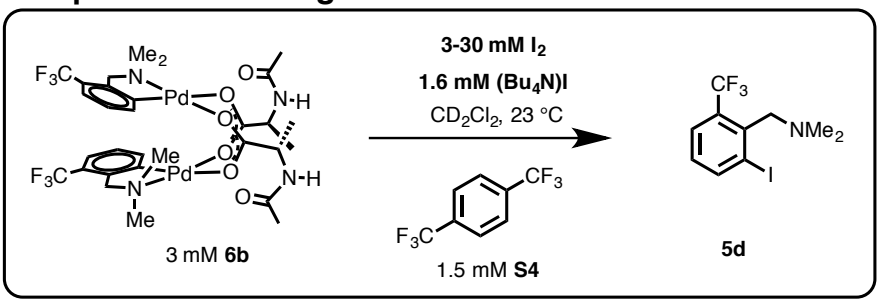

plots of reaction progress

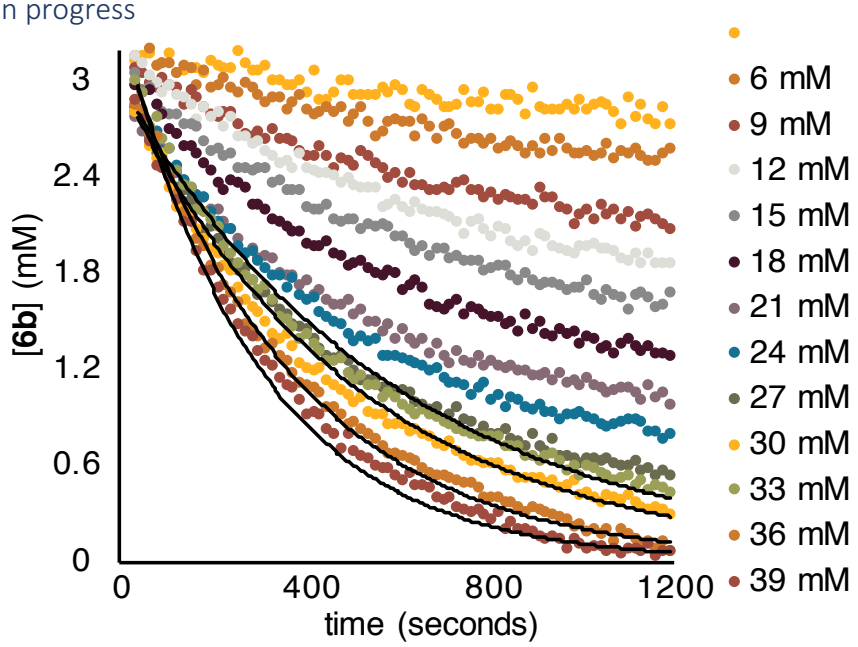

plot of initial rate versus initial [I_2]

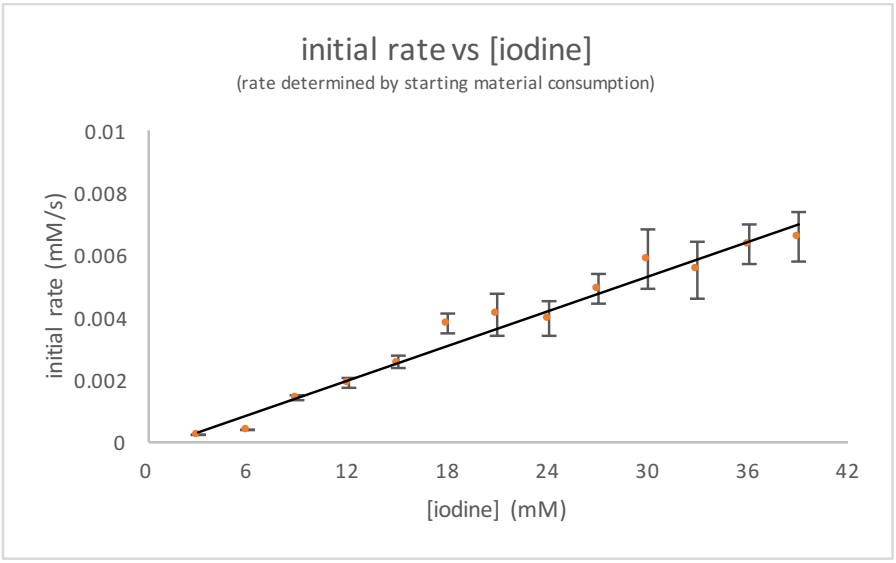

Attempt to determine order in palladium by initial rates

Because of the small changes in concentration of [6b] when using large initial [6b], initial rates determined by consumption of [6b] were too variable. Instead, we determined initial rates by the rate of product formation. However, because we know that product is eventually consumed over the course of the reaction to form formamidinium **S1.4**, it is unclear how much confidence can be place in initial rates of product formation.

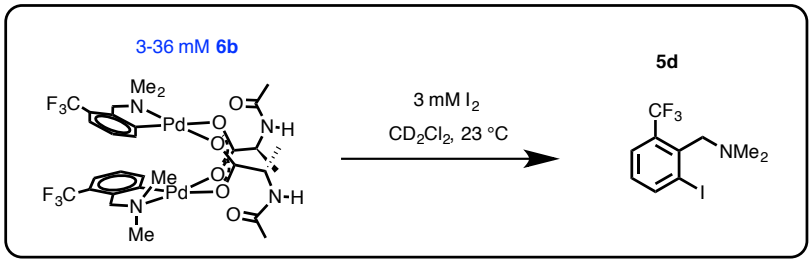

plot of initial rates versus initial [6b]

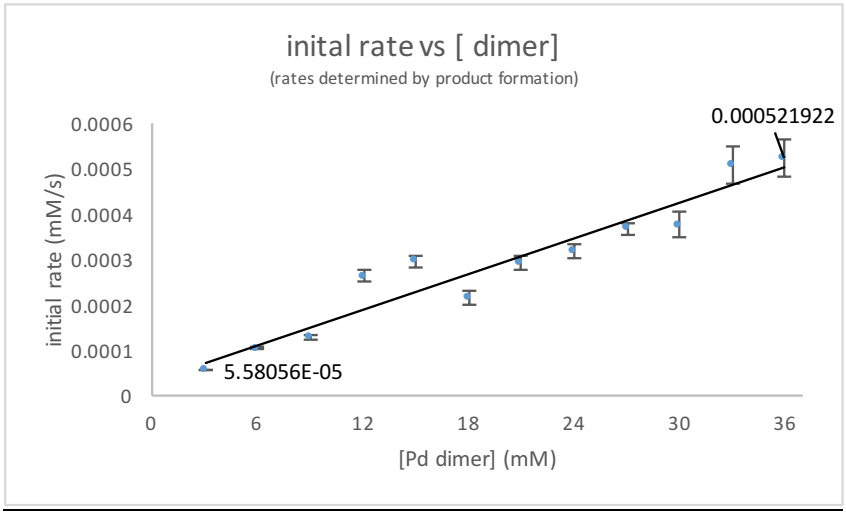

selected reaction profiles presented for clarity

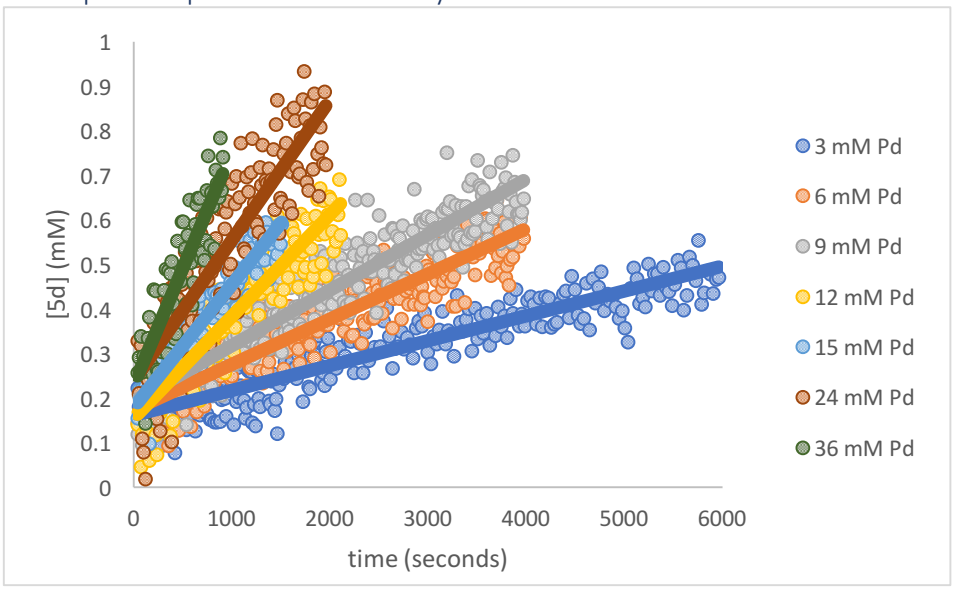

General Crystallographic Methods

The diffraction data for all structures except complex_**15** were measured at 100 K on a Bruker D8 VENTURE diffractometer equipped with a micro focus Mo-target X-ray tube (λ = 0.71073 Å) and PHOTON 100 CMOS detector. Data were collected using φ and ω scans to survey a hemisphere of reciprocal space. The diffraction data for complex_**15** were measured at 100 K on a Bruker D8 fixed-chi with APEXII detector (synchrotron radiation at λ = 0.41328 Å) located at the Advanced Photon Source, Argonne Nat'l Lab (ChemMatCARS Sector 15).[1] Data were collected using φ scans in this case. Data reduction and integration were performed with the Bruker APEX3 software package.[2] Data were scaled and corrected for absorption effects using the multi-scan procedure as implemented in SADABS.[3] The structure were refined by a full-matrix least-squares procedure using OLEX2, version 1.2.8[4] with implemented XL refinement program version 2016/6.[5] Crystallographic data and further details of the data collection and structure refinement are listed in the corresponding tables below.

All of the structures below are shown with Pd= yellow, C= grey, O= red, N= blue, F= green, Cl= green, I= purple

1. ChemMatCARS Sector 15 is principally supported by the Divisions of Chemistry (CHE) and Materials Research (DMR), National Science Foundation, under grant number NSF/CHE-1346572. Use of the Advanced Photon Source, an Office of Science User Facility operated for the U.S. Department of Energy (DOE) Office of Science by Argonne National Laboratory, was supported by the U.S. DOE under Contract No. DE-AC02-06CH11357.

2. Bruker AXS, version 2015.5-2, 2015

3. SADABS, version 2014/5, 2015, part of Bruker APEX3 software package

4. O. V. Dolomanov, L. J. Bourhis, R. J. Gildea, J. A. K. Howard and H. Puschmann. J. Appl. Cryst. (2009). 42, 339-341

5. a) Sheldrick, G. M. *Acta Cryst.* **2008**, *A64*, 112-122; b) *Sheldrick, G. M. Acta Cryst.* **2015**, *C71*, 3-8

Complex_2

molecular structure complex_2 with 50% ellipsoids

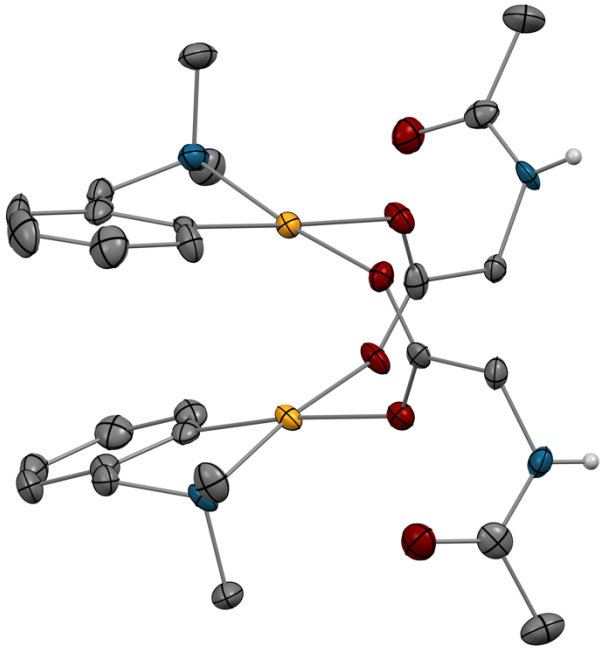

asymmetric unit complex_2 with 50% ellipsoids

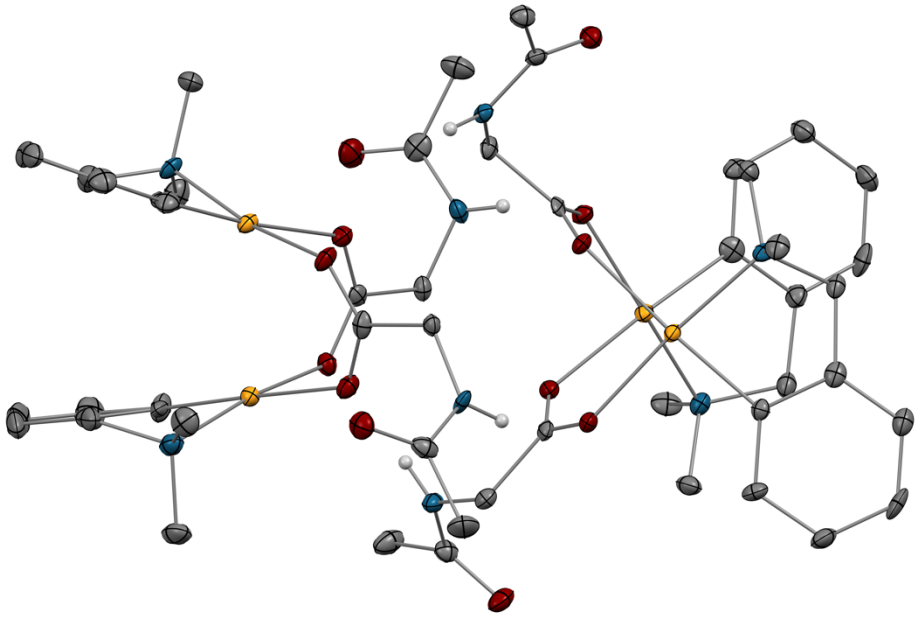

unit cell complex_2 with hydrogen bonds

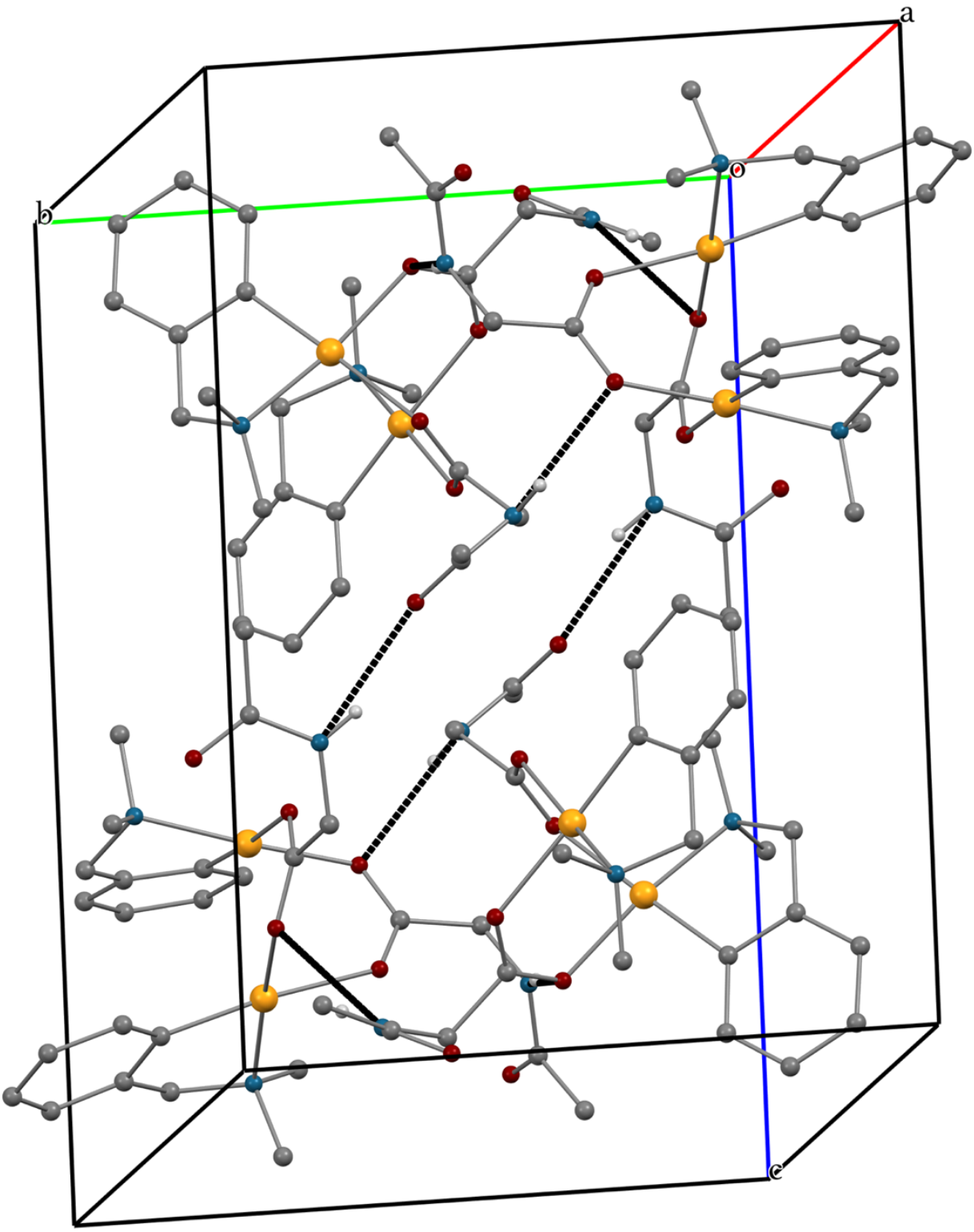

Table 1 Crystal data and structure refinement for complex_2.

Identification code	complex_2
Empirical formula	$C_{52}H_{72}N_8O_{12}Pd_4$
Formula weight	1426.77
Temperature/K	100(2)
Crystal system	triclinic
Space group	P-1
a/Å	12.609(3)
b/Å	12.998(3)
c/Å	18.154(4)
α/°	81.932(7)
β/°	84.577(7)
γ/°	82.253(7)
Volume/Å^3	2910.0(11)
Z	2
ρ_{calc}g/cm^3	1.628
μ/mm^{-1}	1.280
F(000)	1440.0
Crystal size/mm^3	0.32 × 0.22 × 0.14
Radiation	MoKα (λ = 0.71073)
2Θ range for data collection/°	4.278 to 52.864
Index ranges	$-15 \leq h \leq 15$, $-15 \leq k \leq 14$, $-22 \leq l \leq 22$
Reflections collected	35886
Independent reflections	11497 [R_{int} = 0.0649, R_{sigma} = 0.0871]
Data/restraints/parameters	11497/4/709
Goodness-of-fit on F^2	1.026
Final R indexes [I>=2σ (I)]	R_1 = 0.0510, wR_2 = 0.0998
Final R indexes [all data]	R_1 = 0.0887, wR_2 = 0.1112
Largest diff. peak/hole / e Å^{-3}	1.48/-1.04

Table 2 Fractional Atomic Coordinates (×104) and Equivalent Isotropic Displacement Parameters (Å2×103) for complex_2. U_{eq} **is defined as 1/3 of of the trace of the orthogonalised** U_{IJ} **tensor.**

Atom	*x*	*y*	*z*	U(eq)
Pd1	1956.2(3)	7644.1(3)	8145.3(2)	13.66(12)
Pd2	1592.7(3)	7695.5(3)	6542.6(2)	13.00(11)
Pd3	6707.3(4)	4320.3(4)	7285.2(2)	15.32(12)
Pd4	5063.7(4)	2918.5(4)	7813.6(2)	14.65(12)
N1	534(4)	7480(4)	8783(3)	16.0(11)
N2	1468(4)	9279(4)	6176(3)	14.5(11)
N3	5483(4)	7592(4)	6141(3)	13.4(11)
N4	2274(4)	3910(4)	8223(3)	18.4(12)
N5	7925(4)	4030(4)	7997(3)	17.3(11)
N6	5426(4)	1692(4)	7195(3)	20.8(12)
N7	3061(4)	4946(4)	5777(3)	16.9(11)
N8	4662(4)	6640(4)	8900(3)	19.0(12)
O1	3491(3)	7820(3)	7675(2)	16.1(9)
O2	3302(3)	7517(3)	6503(2)	14.9(9)
O3	5128(3)	9321(3)	6165(2)	20.8(10)
O4	2191(3)	6028(3)	7965(2)	15.1(9)
O5	1578(3)	6106(3)	6829(2)	15.7(9)
O6	676(3)	3817(3)	8884(2)	25.5(10)
O7	5667(3)	4780(3)	6466(2)	19.8(9)
O8	4249(3)	3960(3)	6950(2)	20(1)
O9	3867(3)	3701(3)	5096(2)	25.2(10)
O10	4564(3)	4002(3)	8542(2)	16.5(9)
O11	5622(3)	5204(3)	8015(2)	17.2(9)
O12	6212(4)	6054(3)	9426(2)	29.1(11)
C1	1666(5)	9077(5)	8411(3)	19.2(14)
C2	2369(5)	9792(5)	8374(3)	18.9(14)
C3	2045(5)	10797(5)	8562(3)	23.8(15)
C4	978(5)	11066(5)	8814(4)	28.4(16)
C5	267(5)	10340(5)	8881(4)	27.3(16)
C6	592(5)	9357(5)	8684(3)	19.6(14)
C7	-131(5)	8515(5)	8714(4)	21.0(14)
C8	-90(5)	6676(5)	8582(4)	21.9(14)
C9	817(5)	7171(5)	9569(3)	24.3(15)
C10	28(5)	7951(4)	6537(3)	14.7(13)
C11	-671(5)	7208(5)	6542(3)	18.5(14)
C12	-1773(5)	7519(5)	6586(4)	24.2(15)
C13	-2176(5)	8558(5)	6605(3)	25.6(16)
C14	-1480(5)	9300(5)	6569(3)	22.1(14)

C15	-380(5)	9006(5)	6537(3)	18.3(14)
C16	424(4)	9750(5)	6531(3)	17.8(13)
C17	2346(5)	9818(5)	6369(3)	19.0(14)
C18	1428(5)	9433(5)	5350(3)	21.7(14)
C19	3843(5)	7610(4)	7028(3)	13.8(13)
C20	5062(4)	7393(5)	6902(3)	15.7(13)
C21	5502(5)	8586(5)	5823(3)	16.6(13)
C22	6055(5)	8752(5)	5056(3)	21.0(14)
C23	1884(4)	5626(4)	7447(3)	14.7(13)
C24	1835(5)	4453(4)	7548(3)	16.4(13)
C25	1662(5)	3667(5)	8854(3)	18.5(14)
C26	2267(5)	3182(5)	9518(4)	29.8(17)
C27	7800(5)	3600(4)	6617(3)	18.5(14)
C28	7770(5)	3617(5)	5856(3)	21.3(14)
C29	8630(5)	3118(5)	5452(4)	26.8(16)
C30	9528(5)	2630(5)	5793(4)	27.2(16)
C31	9552(5)	2609(5)	6569(4)	26.6(16)
C32	8701(5)	3092(5)	6977(3)	20.7(14)
C33	8634(5)	3074(5)	7808(3)	20.9(14)
C34	8535(5)	4945(5)	7844(4)	25.7(15)
C35	7578(5)	3895(5)	8814(3)	28.4(16)
C36	5792(5)	1925(5)	8576(3)	18.3(14)
C37	5740(5)	1981(5)	9339(3)	23.5(15)
C38	6351(6)	1238(6)	9804(4)	35.0(18)
C39	7009(6)	429(6)	9506(4)	36.9(18)
C40	7044(5)	340(5)	8750(4)	31.5(17)
C41	6437(5)	1091(5)	8287(4)	23.3(15)
C42	6442(5)	1088(5)	7468(4)	23.8(15)
C43	5550(5)	1985(5)	6376(3)	28.0(16)
C44	4545(5)	1005(5)	7381(4)	29.8(16)
C45	4704(5)	4605(5)	6492(3)	18.7(14)
C46	4057(4)	5285(4)	5906(3)	15.5(13)
C47	3033(5)	4167(5)	5370(3)	21.2(14)
C48	1934(5)	3893(6)	5271(4)	35.1(18)
C49	4900(5)	4886(5)	8467(3)	15.6(13)
C50	4299(5)	5627(4)	8991(3)	18.1(13)
C51	5636(5)	6764(5)	9074(3)	22.8(15)
C52	5995(6)	7826(5)	8830(4)	31.8(17)

Table 3 Anisotropic Displacement Parameters (Å2×103) for complex_2. The Anisotropic displacement factor exponent takes the form: $-2\pi^2[h^2a^{*2}U_{11}+2hka^*b^*U_{12}+\ldots]$.

Atom	U_{11}	U_{22}	U_{33}	U_{23}	U_{13}	U_{12}
Pd1	11.6(2)	14.7(3)	14.1(2)	-1.11(18)	0.74(19)	-1.50(18)
Pd2	9.1(2)	14.0(3)	14.9(2)	-0.08(18)	-0.44(18)	-0.33(18)
Pd3	10.6(2)	19.7(3)	15.2(2)	0.41(19)	-2.14(19)	-1.80(19)
Pd4	12.8(2)	14.9(3)	16.2(3)	-2.41(19)	-1.09(19)	-1.05(19)
N1	13(3)	20(3)	15(3)	-2(2)	-1(2)	0(2)
N2	12(3)	18(3)	11(3)	2(2)	1(2)	-3(2)
N3	11(3)	16(3)	14(3)	-7(2)	2(2)	-2(2)
N4	14(3)	18(3)	23(3)	5(2)	-3(2)	-4(2)
N5	10(3)	26(3)	15(3)	-1(2)	-4(2)	-2(2)
N6	17(3)	22(3)	26(3)	-9(2)	0(2)	-4(2)
N7	7(3)	24(3)	19(3)	-6(2)	-4(2)	2(2)
N8	23(3)	12(3)	22(3)	-2(2)	-6(2)	2(2)
O1	12(2)	19(2)	18(2)	-4.9(18)	1.8(18)	-3.1(17)
O2	9(2)	19(2)	16(2)	-2.2(17)	-0.6(17)	-0.5(17)
O3	20(2)	19(2)	22(2)	-2.7(19)	1.9(19)	-2.3(19)
O4	13(2)	14(2)	18(2)	-1.2(17)	0.3(18)	-1.6(17)
O5	11(2)	15(2)	21(2)	-0.6(18)	-2.3(18)	-0.4(17)
O6	14(2)	34(3)	26(3)	2(2)	0(2)	-5(2)
O7	11(2)	28(3)	19(2)	2.2(18)	-3.7(18)	0.3(18)
O8	14(2)	26(3)	18(2)	1.2(19)	-2.9(19)	-0.3(19)
O9	26(3)	25(3)	24(3)	-8(2)	4(2)	-1(2)
O10	18(2)	15(2)	16(2)	-3.9(17)	0.9(18)	0.4(18)
O11	14(2)	19(2)	18(2)	-2.0(18)	-0.8(19)	-2.5(18)
O12	30(3)	29(3)	29(3)	-2(2)	-12(2)	-1(2)
C1	25(4)	24(4)	10(3)	-1(3)	-6(3)	-3(3)
C2	18(3)	23(4)	16(3)	1(3)	0(3)	-5(3)
C3	26(4)	18(4)	28(4)	-5(3)	1(3)	-5(3)
C4	30(4)	14(4)	41(4)	-8(3)	1(3)	-1(3)
C5	16(3)	36(4)	28(4)	-10(3)	0(3)	11(3)
C6	17(3)	20(4)	21(3)	-2(3)	3(3)	0(3)
C7	16(3)	21(4)	23(4)	1(3)	0(3)	3(3)
C8	23(3)	17(3)	27(4)	-4(3)	2(3)	-8(3)
C9	31(4)	28(4)	14(3)	2(3)	1(3)	-11(3)
C10	14(3)	16(3)	13(3)	-3(2)	0(3)	0(2)
C11	13(3)	24(4)	20(3)	-4(3)	1(3)	-8(3)
C12	13(3)	30(4)	31(4)	1(3)	-4(3)	-7(3)
C13	8(3)	41(5)	25(4)	-4(3)	-2(3)	7(3)
C14	18(3)	25(4)	21(4)	-1(3)	-1(3)	4(3)
C15	18(3)	23(4)	11(3)	0(3)	0(3)	1(3)

C16	15(3)	19(3)	17(3)	1(3)	0(3)	3(3)
C17	19(3)	15(3)	23(3)	1(3)	−3(3)	−3(3)
C18	21(3)	25(4)	17(3)	1(3)	2(3)	−1(3)
C19	14(3)	9(3)	16(3)	7(2)	−2(3)	1(2)
C20	15(3)	17(3)	13(3)	2(2)	−3(3)	2(3)
C21	12(3)	18(4)	21(3)	1(3)	−4(3)	−6(3)
C22	22(3)	21(4)	19(3)	0(3)	−2(3)	−5(3)
C23	10(3)	14(3)	18(3)	−2(3)	2(3)	2(2)
C24	12(3)	20(3)	17(3)	−3(3)	0(3)	−2(3)
C25	21(4)	18(3)	16(3)	2(3)	−3(3)	−4(3)
C26	21(4)	40(4)	28(4)	8(3)	−8(3)	−9(3)
C27	17(3)	13(3)	24(4)	0(3)	6(3)	−5(3)
C28	19(3)	22(4)	21(4)	3(3)	2(3)	−5(3)
C29	29(4)	27(4)	23(4)	2(3)	3(3)	−7(3)
C30	20(4)	20(4)	40(4)	−7(3)	8(3)	−1(3)
C31	15(3)	23(4)	41(4)	−5(3)	−4(3)	3(3)
C32	19(3)	17(3)	27(4)	−2(3)	−2(3)	−3(3)
C33	18(3)	18(4)	26(4)	−1(3)	−5(3)	0(3)
C34	21(4)	16(4)	41(4)	−3(3)	−2(3)	−6(3)
C35	26(4)	38(4)	21(4)	−4(3)	−9(3)	1(3)
C36	9(3)	14(3)	31(4)	4(3)	−4(3)	−3(2)
C37	19(3)	26(4)	23(4)	0(3)	−4(3)	5(3)
C38	39(4)	33(4)	30(4)	4(3)	−3(3)	−1(4)
C39	33(4)	35(5)	36(5)	13(3)	−8(4)	7(3)
C40	24(4)	16(4)	48(5)	3(3)	5(3)	7(3)
C41	18(3)	15(3)	35(4)	−2(3)	7(3)	−4(3)
C42	18(3)	16(3)	37(4)	−7(3)	5(3)	0(3)
C43	31(4)	31(4)	24(4)	−12(3)	0(3)	−3(3)
C44	25(4)	25(4)	44(4)	−16(3)	4(3)	−11(3)
C45	20(4)	21(4)	15(3)	−8(3)	−3(3)	5(3)
C46	14(3)	13(3)	19(3)	−5(2)	−2(3)	2(2)
C47	28(4)	18(4)	19(3)	2(3)	−6(3)	−7(3)
C48	27(4)	32(4)	50(5)	−9(4)	−10(4)	−12(3)
C49	15(3)	16(3)	17(3)	−1(3)	−9(3)	0(3)
C50	18(3)	15(3)	20(3)	−4(3)	−3(3)	4(3)
C51	25(4)	31(4)	14(3)	−9(3)	0(3)	−2(3)
C52	40(4)	25(4)	33(4)	−7(3)	−1(3)	−14(3)

Table 4 Bond Lengths for complex_2.

Atom	Atom	Length/Å	Atom	Atom	Length/Å
Pd1	Pd2	2.9780(9)	O6	C25	1.230(7)
Pd1	N1	2.059(5)	O7	C45	1.260(7)
Pd1	O1	2.068(4)	O8	C45	1.252(7)
Pd1	O4	2.148(4)	O9	C47	1.239(7)
Pd1	C1	1.968(6)	O10	C49	1.262(7)
Pd2	N2	2.062(5)	O11	C49	1.240(7)
Pd2	O2	2.131(4)	O12	C51	1.237(7)
Pd2	O5	2.060(4)	C1	C2	1.359(8)
Pd2	C10	1.957(6)	C1	C6	1.414(8)
Pd3	Pd4	2.9473(8)	C2	C3	1.395(9)
Pd3	N5	2.062(5)	C3	C4	1.395(9)
Pd3	O7	2.050(4)	C4	C5	1.372(9)
Pd3	O11	2.146(4)	C5	C6	1.374(9)
Pd3	C27	1.975(6)	C6	C7	1.508(8)
Pd4	N6	2.054(5)	C10	C11	1.391(8)
Pd4	O8	2.164(4)	C10	C15	1.398(8)
Pd4	O10	2.063(4)	C11	C12	1.392(8)
Pd4	C36	1.961(6)	C12	C13	1.381(9)
N1	C7	1.482(7)	C13	C14	1.379(9)
N1	C8	1.491(7)	C14	C15	1.387(8)
N1	C9	1.491(7)	C15	C16	1.491(8)
N2	C16	1.502(7)	C19	C20	1.527(8)
N2	C17	1.480(7)	C21	C22	1.498(8)
N2	C18	1.490(7)	C23	C24	1.519(8)
N3	C20	1.433(7)	C25	C26	1.503(8)
N3	C21	1.342(7)	C27	C28	1.383(8)
N4	C24	1.444(7)	C27	C32	1.403(8)
N4	C25	1.344(8)	C28	C29	1.388(9)
N5	C33	1.490(8)	C29	C30	1.377(9)
N5	C34	1.483(7)	C30	C31	1.408(9)
N5	C35	1.499(8)	C31	C32	1.376(9)
N6	C42	1.498(8)	C32	C33	1.500(8)
N6	C43	1.481(8)	C36	C37	1.392(9)
N6	C44	1.502(8)	C36	C41	1.398(8)
N7	C46	1.434(7)	C37	C38	1.391(9)
N7	C47	1.340(8)	C38	C39	1.388(10)
N8	C50	1.435(8)	C39	C40	1.390(10)
N8	C51	1.331(8)	C40	C41	1.392(9)
O1	C19	1.269(7)	C41	C42	1.487(9)
O2	C19	1.251(7)	C45	C46	1.511(8)

O3	C21	1.230(7)	C47	C48	1.510(9)
O4	C23	1.252(7)	C49	C50	1.527(8)
O5	C23	1.273(7)	C51	C52	1.506(9)

Table 5 Bond Angles for complex_2.

Atom	Atom	Atom	Angle/°	Atom	Atom	Atom	Angle/°
N1	Pd1	Pd2	109.24(13)	C49	O10	Pd4	122.6(4)
N1	Pd1	O1	170.27(17)	C49	O11	Pd3	127.7(4)
N1	Pd1	O4	92.66(17)	C2	C1	Pd1	127.7(5)
O1	Pd1	Pd2	80.49(11)	C2	C1	C6	118.3(6)
O1	Pd1	O4	90.14(15)	C6	C1	Pd1	114.0(4)
O4	Pd1	Pd2	75.56(10)	C1	C2	C3	121.7(6)
C1	Pd1	Pd2	109.00(16)	C4	C3	C2	119.1(6)
C1	Pd1	N1	82.3(2)	C5	C4	C3	119.8(6)
C1	Pd1	O1	94.4(2)	C4	C5	C6	120.5(6)
C1	Pd1	O4	174.0(2)	C1	C6	C7	114.8(5)
N2	Pd2	Pd1	101.66(13)	C5	C6	C1	120.5(6)
N2	Pd2	O2	93.90(17)	C5	C6	C7	124.7(6)
O2	Pd2	Pd1	78.61(10)	N1	C7	C6	108.8(5)
O5	Pd2	Pd1	83.63(11)	C11	C10	Pd2	127.0(4)
O5	Pd2	N2	173.32(16)	C11	C10	C15	119.8(5)
O5	Pd2	O2	91.15(15)	C15	C10	Pd2	113.2(4)
C10	Pd2	Pd1	103.15(16)	C10	C11	C12	119.4(6)
C10	Pd2	N2	82.4(2)	C13	C12	C11	120.7(6)
C10	Pd2	O2	176.1(2)	C14	C13	C12	119.8(6)
C10	Pd2	O5	92.5(2)	C13	C14	C15	120.5(6)
N5	Pd3	Pd4	109.42(14)	C10	C15	C16	116.4(5)
N5	Pd3	O11	94.55(17)	C14	C15	C10	119.7(6)
O7	Pd3	Pd4	80.55(11)	C14	C15	C16	123.9(6)
O7	Pd3	N5	169.96(18)	C15	C16	N2	107.9(5)
O7	Pd3	O11	88.76(15)	O1	C19	C20	115.3(5)
O11	Pd3	Pd4	76.65(11)	O2	C19	O1	127.2(5)
C27	Pd3	Pd4	108.48(17)	O2	C19	C20	117.3(5)
C27	Pd3	N5	82.6(2)	N3	C20	C19	115.0(5)
C27	Pd3	O7	93.4(2)	N3	C21	C22	116.9(5)
C27	Pd3	O11	174.7(2)	O3	C21	N3	120.9(6)
N6	Pd4	Pd3	104.83(14)	O3	C21	C22	122.1(5)
N6	Pd4	O8	94.95(18)	O4	C23	O5	126.6(5)
N6	Pd4	O10	171.37(18)	O4	C23	C24	118.9(5)
O8	Pd4	Pd3	79.43(11)	O5	C23	C24	114.5(5)
O10	Pd4	Pd3	83.42(11)	N4	C24	C23	113.7(5)
O10	Pd4	O8	89.00(15)	N4	C25	C26	115.4(5)
C36	Pd4	Pd3	101.95(16)	O6	C25	N4	122.3(5)
C36	Pd4	N6	82.8(2)	O6	C25	C26	122.4(6)
C36	Pd4	O8	177.6(2)	C28	C27	Pd3	126.2(5)
C36	Pd4	O10	93.1(2)	C28	C27	C32	120.1(6)

C7	N1	Pd1	107.6(4)	C32	C27	Pd3	113.5(4)
C7	N1	C8	109.5(5)	C27	C28	C29	119.6(6)
C7	N1	C9	109.7(5)	C30	C29	C28	121.1(6)
C8	N1	Pd1	115.1(4)	C29	C30	C31	119.0(6)
C8	N1	C9	108.2(5)	C32	C31	C30	120.4(6)
C9	N1	Pd1	106.5(4)	C27	C32	C33	116.0(5)
C16	N2	Pd2	106.2(3)	C31	C32	C27	119.7(6)
C17	N2	Pd2	115.0(3)	C31	C32	C33	124.2(6)
C17	N2	C16	108.9(5)	N5	C33	C32	107.8(5)
C17	N2	C18	108.8(4)	C37	C36	Pd4	127.4(5)
C18	N2	Pd2	108.4(4)	C37	C36	C41	119.2(6)
C18	N2	C16	109.4(4)	C41	C36	Pd4	113.4(5)
C21	N3	C20	119.1(5)	C38	C37	C36	120.5(6)
C25	N4	C24	122.9(5)	C39	C38	C37	119.7(7)
C33	N5	Pd3	108.0(3)	C38	C39	C40	120.7(6)
C33	N5	C35	109.4(5)	C39	C40	C41	119.3(6)
C34	N5	Pd3	106.4(4)	C36	C41	C42	115.7(6)
C34	N5	C33	109.5(5)	C40	C41	C36	120.6(6)
C34	N5	C35	107.5(5)	C40	C41	C42	123.7(6)
C35	N5	Pd3	115.8(4)	C41	C42	N6	109.4(5)
C42	N6	Pd4	106.2(4)	O7	C45	C46	114.1(5)
C42	N6	C44	108.2(5)	O8	C45	O7	127.1(5)
C43	N6	Pd4	115.6(4)	O8	C45	C46	118.8(5)
C43	N6	C42	110.2(5)	N7	C46	C45	116.4(5)
C43	N6	C44	109.0(5)	N7	C47	C48	116.2(6)
C44	N6	Pd4	107.4(4)	O9	C47	N7	121.4(6)
C47	N7	C46	121.5(5)	O9	C47	C48	122.4(6)
C51	N8	C50	121.5(5)	O10	C49	C50	113.7(5)
C19	O1	Pd1	124.4(4)	O11	C49	O10	127.5(6)
C19	O2	Pd2	125.4(4)	O11	C49	C50	118.8(5)
C23	O4	Pd1	128.2(4)	N8	C50	C49	114.2(5)
C23	O5	Pd2	122.4(4)	N8	C51	C52	116.3(6)
C45	O7	Pd3	126.7(4)	O12	C51	N8	122.2(6)
C45	O8	Pd4	123.4(4)	O12	C51	C52	121.4(6)

Complex_6b

asymmetric unit complex_6b with 40% ellipsoids

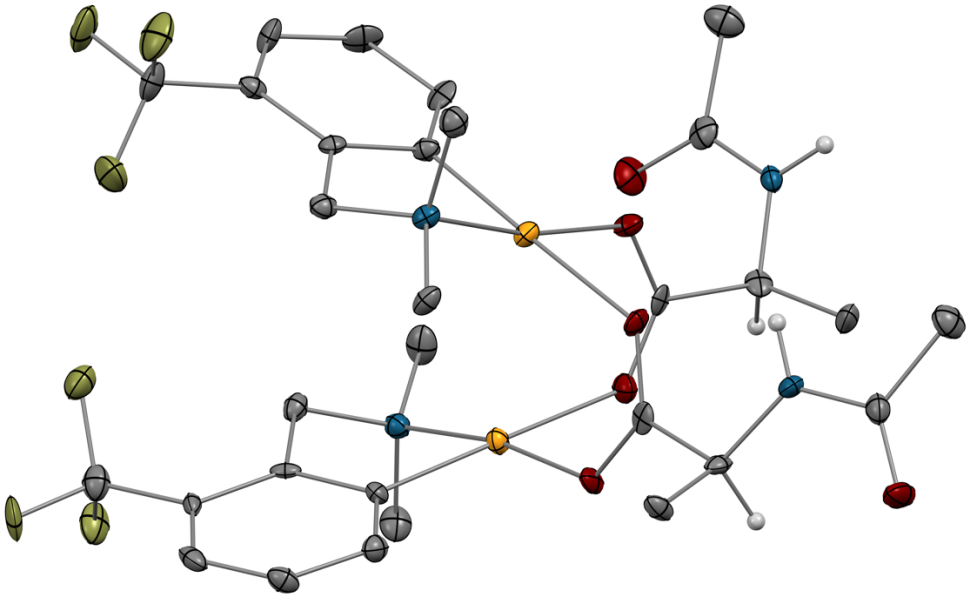

asymmetric unit complex_6b with co-crystallized, hydrogen bonding acetonitrile

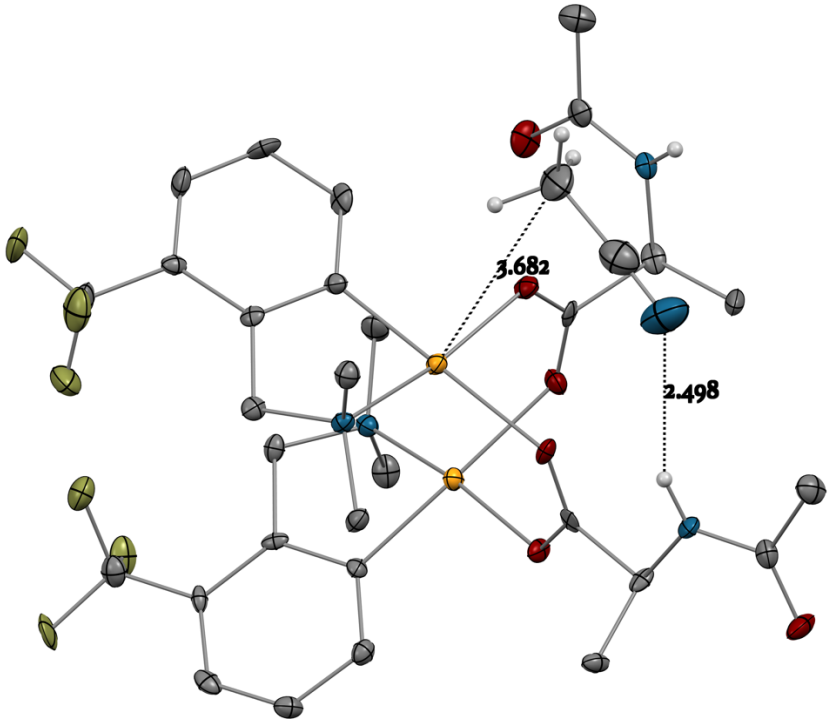

unit cell complex_6b with hydrogen bonding network

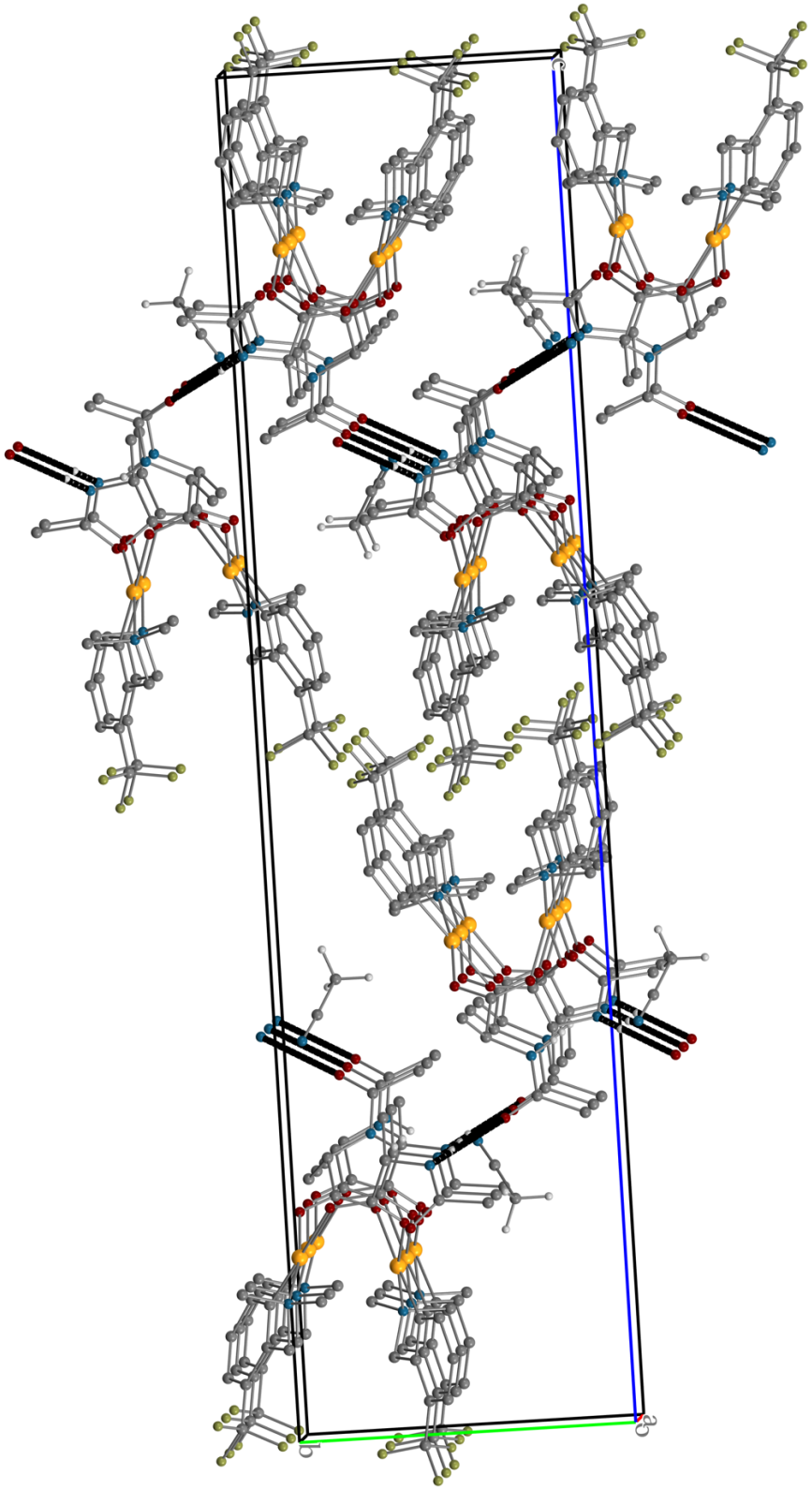

Table 1 Crystal data and structure refinement for complex_6b.

Identification code	complex_6b
Empirical formula	$C_{32}H_{41}F_6N_5O_6Pd_2$
Formula weight	918.50
Temperature/K	100(2)
Crystal system	orthorhombic
Space group	$P2_12_12_1$
a/Å	9.3180(4)
b/Å	9.8627(4)
c/Å	40.0507(19)
α/°	90
β/°	90
γ/°	90
Volume/Å^3	3680.7(3)
Z	4
ρ_{calc}g/cm^3	1.658
μ/mm^{-1}	1.056
F(000)	1848.0
Crystal size/mm^3	0.34 × 0.16 × 0.14
Radiation	MoKα (λ = 0.71073)
2Θ range for data collection/°	4.254 to 52.728
Index ranges	$-11 \le h \le 11$, $-11 \le k \le 12$, $-44 \le l \le 49$
Reflections collected	39996
Independent reflections	6909 [R_{int} = 0.0715, R_{sigma} = 0.0850]
Data/restraints/parameters	6909/45/475
Goodness-of-fit on F^2	1.046
Final R indexes [I>=2σ (I)]	R_1 = 0.0435, wR_2 = 0.0576
Final R indexes [all data]	R_1 = 0.0728, wR_2 = 0.0620
Largest diff. peak/hole / e Å^{-3}	0.67/-0.75
Flack parameter	0.008(14)

$R_{int} = \Sigma \mid F_o^2 - \langle F_o^2 \rangle \mid / \Sigma \mid F_o^2 \mid$

$R1 = \Sigma \mid \mid F_o \mid - \mid F_c \mid \mid / \Sigma \mid F_o \mid$

$wR2 = [\Sigma [w (F_o^2 - F_c^2)^2] / \Sigma [w (F_o^2)^2]]^{1/2}$

Goodness-of-fit = $[\Sigma [w (F_o^2 - F_c^2)^2] / (n-p)]^{1/2}$

n: number of independent reflections; p: number of refined parameters

Table 2 Fractional Atomic Coordinates (×104) and Equivalent Isotropic Displacement Parameters (Å2×103) for complex_6b. U_{eq} **is defined as 1/3 of of the trace of the orthogonalised** U_{IJ} **tensor.**

Atom	*x*	*y*	*z*	U(eq)
Pd1	6673.5(5)	4489.8(5)	3614.3(2)	14.37(13)
Pd2	5832.8(5)	1617.5(5)	3721.4(2)	14.13(13)
O1	4982(4)	4453(5)	3290.3(10)	17.3(10)
O2	4574(4)	2196(4)	3299.6(10)	16.0(11)
O3	1787(6)	3112(4)	2324.5(11)	27.0(12)
O4	7965(4)	3473(5)	3257.1(10)	18.5(11)
O5	7493(5)	1304(4)	3400.9(11)	17.1(11)
O6	10869(5)	1046(5)	3424.2(12)	28.4(12)
N1	8350(6)	4864(5)	3936.6(13)	15.1(13)
N2	2989(6)	2259(6)	2759.8(14)	16.3(14)
N3	4183(6)	1588(5)	4062.3(12)	13.7(11)
N4	9567(5)	399(6)	2981.5(13)	15.1(14)
C1	5577(6)	5491(6)	3951.7(15)	13.0(15)
C2	4211(7)	6058(6)	3913.0(17)	17.1(15)
C3	3592(7)	6742(6)	4176.2(16)	18.4(16)
C4	4279(8)	6891(6)	4475.6(17)	18.6(16)
C5	5639(7)	6345(6)	4522.7(15)	12.9(15)
C6	6292(6)	5629(6)	4257.5(15)	12.2(15)
C7	7726(7)	4941(7)	4277.8(16)	16.5(17)
C8	6417(7)	6518(7)	4841.8(17)	22.2(16)
C9	8949(7)	6198(6)	3847.9(17)	23.0(18)
C10	9502(7)	3858(7)	3930.0(17)	25.4(19)
C11	4411(6)	3386(8)	3189.6(15)	15.9(15)
C12	3282(7)	3572(6)	2915.1(15)	15.1(15)
C13	1951(6)	4205(6)	3069.5(16)	17.6(16)
C14	2300(8)	2139(7)	2469.1(17)	19.1(18)
C15	2185(7)	736(6)	2328.7(17)	24.9(18)
C16	6923(7)	1031(6)	4111.3(16)	14.5(16)
C17	8267(7)	423(7)	4106.4(16)	21.1(16)
C18	8947(7)	70(6)	4405.2(18)	24.5(18)
C19	8285(7)	315(7)	4705.2(16)	22.8(16)
C20	6946(7)	890(6)	4715.7(16)	14.4(16)
C21	6250(6)	1247(6)	4414.9(16)	13.0(16)
C22	4804(7)	1913(6)	4392.5(16)	15.7(17)
C23	6230(8)	1118(8)	5042.1(17)	26(2)
C24	3597(7)	195(6)	4066.9(17)	20.5(18)
C25	2971(6)	2526(6)	3987.7(16)	18.1(17)
C26	8076(7)	2215(7)	3227.3(15)	14.4(15)

C27	8965(7)	1726(7)	2928.0(15)	17.8(16)
C28	8022(8)	1737(7)	2621.5(16)	26.4(18)
C29	10476(7)	164(7)	3234.8(18)	20.5(18)
C30	10955(8)	-1299(6)	3271.9(18)	30.1(19)
F1	5677(5)	7206(4)	5072.3(9)	31.8(11)
F2	7666(4)	7193(4)	4803.1(9)	28.6(10)
F3	6785(4)	5330(4)	4985.0(9)	27.7(10)
F4	5840(5)	2417(4)	5087.4(10)	40.7(12)
F5	7050(4)	783(4)	5302.0(9)	39.8(12)
F6	5018(4)	381(5)	5075(1)	39.3(11)
N5	4461(7)	-687(8)	2906(2)	56(2)
C31	5232(9)	-1163(8)	3086(2)	42(2)
C32	6262(9)	-1742(8)	3333.2(19)	46(2)

Table 3 Anisotropic Displacement Parameters (Å2×103) for complex_6b. The Anisotropic displacement factor exponent takes the form: $-2\pi^2[h^2a^{*2}U_{11}+2hka^*b^*U_{12}+\ldots]$.

Atom	U_{11}	U_{22}	U_{33}	U_{23}	U_{13}	U_{12}
Pd1	15.1(3)	15.2(3)	12.9(3)	-2.8(2)	-2.3(2)	0.7(3)
Pd2	13.3(2)	16.7(3)	12.4(3)	3.1(2)	0.3(2)	1.3(3)
O1	23(2)	12(2)	16(3)	-5(2)	-10(2)	0(2)
O2	17(3)	20(3)	11(3)	3(2)	-5(2)	0(2)
O3	40(3)	17(3)	24(3)	2(2)	-17(3)	4(3)
O4	22(3)	19(3)	15(3)	-3(2)	5(2)	1(2)
O5	18(3)	16(3)	17(3)	6(2)	2(2)	1(2)
O6	28(3)	29(3)	28(3)	-5(2)	-10(3)	-12(3)
N1	16(3)	14(3)	16(3)	-1(2)	1(3)	1(3)
N2	22(4)	15(3)	12(4)	4(3)	-1(3)	3(3)
N3	11(3)	15(3)	15(3)	2(3)	0(3)	0(3)
N4	17(3)	14(3)	14(3)	-2(3)	1(2)	-5(3)
C1	17(4)	9(3)	13(4)	-2(3)	-1(3)	0(3)
C2	19(4)	16(3)	16(4)	0(3)	-4(3)	-2(3)
C3	15(4)	15(4)	25(4)	-2(3)	-2(3)	2(3)
C4	23(4)	10(4)	23(4)	-4(3)	5(4)	-2(3)
C5	20(4)	11(4)	8(4)	-2(3)	1(3)	-6(3)
C6	9(4)	8(3)	20(4)	5(3)	0(3)	-1(3)
C7	17(4)	19(4)	13(4)	1(3)	-1(3)	-5(3)
C8	19(4)	28(4)	19(4)	-1(3)	3(3)	-4(3)
C9	19(4)	28(4)	22(4)	-2(3)	0(3)	-8(3)
C10	16(4)	38(5)	22(4)	-4(3)	1(3)	9(3)
C11	11(4)	25(4)	11(4)	-2(4)	8(3)	5(4)
C12	20(3)	9(3)	16(4)	5(3)	-6(3)	-5(4)
C13	16(4)	14(4)	23(4)	-5(3)	-8(3)	4(3)
C14	22(4)	21(4)	14(5)	-2(3)	2(3)	-2(4)
C15	24(4)	23(4)	27(5)	-7(4)	-5(3)	-1(4)
C16	14(4)	14(3)	16(4)	2(3)	1(3)	2(3)
C17	24(4)	24(4)	15(4)	7(3)	9(3)	-5(4)
C18	18(4)	24(4)	32(5)	8(3)	-8(4)	8(3)
C19	28(4)	31(4)	10(4)	4(3)	-1(4)	0(4)
C20	14(4)	11(4)	19(4)	-3(3)	-3(3)	1(3)
C21	14(4)	9(3)	16(4)	4(3)	1(3)	-2(3)
C22	17(4)	13(4)	18(4)	-1(3)	-3(3)	-2(3)
C23	30(5)	37(5)	12(5)	1(4)	-6(4)	0(4)
C24	20(4)	22(4)	19(4)	0(3)	-1(3)	-1(3)
C25	16(4)	23(4)	15(4)	6(3)	0(3)	2(3)
C26	13(4)	23(4)	7(4)	0(3)	-7(3)	-1(3)
C27	21(4)	14(4)	18(4)	-1(3)	4(3)	-11(3)

C28	45(5)	25(4)	10(4)	1(4)	-2(3)	12(4)
C29	18(4)	26(4)	18(4)	3(3)	8(3)	0(3)
C30	26(4)	25(4)	39(5)	-2(4)	1(4)	4(4)
F1	40(3)	42(3)	13(2)	-17.3(19)	1(2)	5(2)
F2	29(2)	35(2)	22(3)	-6.1(19)	-3.1(19)	-16(2)
F3	32(2)	32(2)	19(2)	5(2)	-4(2)	-2(2)
F4	62(3)	32(2)	28(3)	-7(2)	5(3)	17(3)
F5	47(3)	60(3)	12(2)	2(2)	-8(2)	17(2)
F6	38(3)	58(3)	22(3)	7(2)	8(2)	-9(3)
N5	44(5)	57(5)	68(6)	16(4)	-8(4)	11(4)
C31	42(5)	34(5)	50(6)	-3(4)	6(4)	0(4)
C32	68(7)	39(5)	33(5)	15(4)	9(4)	8(5)

Table 4 Bond Lengths for complex_6b.

Atom	Atom	Length/Å	Atom	Atom	Length/Å
Pd1	O1	2.042(4)	C3	C4	1.367(9)
Pd1	O4	2.121(4)	C4	C5	1.390(9)
Pd1	N1	2.060(5)	C5	C6	1.413(8)
Pd1	C1	1.961(6)	C5	C8	1.479(9)
Pd2	O2	2.134(4)	C6	C7	1.501(8)
Pd2	O5	2.034(4)	C8	F1	1.337(7)
Pd2	N3	2.056(5)	C8	F2	1.350(7)
Pd2	C16	1.951(6)	C8	F3	1.349(8)
O1	C11	1.246(8)	C11	C12	1.533(8)
O2	C11	1.263(8)	C12	C13	1.520(8)
O3	C14	1.219(8)	C14	C15	1.497(9)
O4	C26	1.251(8)	C16	C17	1.389(9)
O5	C26	1.260(7)	C16	C21	1.385(9)
O6	C29	1.211(8)	C17	C18	1.398(9)
N1	C7	1.487(8)	C18	C19	1.372(9)
N1	C9	1.472(7)	C19	C20	1.372(9)
N1	C10	1.462(8)	C20	C21	1.413(8)
N2	C12	1.463(8)	C20	C23	1.485(9)
N2	C14	1.335(8)	C21	C22	1.501(8)
N3	C22	1.479(8)	C23	F4	1.343(8)
N3	C24	1.479(8)	C23	F5	1.333(7)
N3	C25	1.490(7)	C23	F6	1.350(8)
N4	C27	1.440(8)	C26	C27	1.535(8)
N4	C29	1.342(8)	C27	C28	1.510(9)
C1	C2	1.398(9)	C29	C30	1.517(9)
C1	C6	1.401(8)	N5	C31	1.120(10)
C2	C3	1.378(9)	C31	C32	1.493(11)

Table 5 Bond Angles for complex_6b.

Atom	Atom	Atom	Angle/°	Atom	Atom	Atom	Angle/°
O1	Pd1	O4	90.04(16)	F1	C8	F2	105.9(5)
O1	Pd1	N1	170.72(19)	F1	C8	F3	106.2(5)
N1	Pd1	O4	94.41(18)	F2	C8	C5	112.3(5)
C1	Pd1	O1	92.6(2)	F3	C8	C5	113.0(6)
C1	Pd1	O4	176.7(2)	F3	C8	F2	104.9(5)
C1	Pd1	N1	82.7(2)	O1	C11	O2	128.3(6)
O5	Pd2	O2	87.66(16)	O1	C11	C12	115.1(6)
O5	Pd2	N3	170.3(2)	O2	C11	C12	116.4(6)
N3	Pd2	O2	96.80(18)	N2	C12	C11	109.1(5)
C16	Pd2	O2	177.6(2)	N2	C12	C13	112.6(5)
C16	Pd2	O5	93.7(2)	C13	C12	C11	108.5(5)
C16	Pd2	N3	81.6(2)	O3	C14	N2	122.2(6)
C11	O1	Pd1	123.4(4)	O3	C14	C15	121.4(6)
C11	O2	Pd2	126.2(4)	N2	C14	C15	116.4(6)
C26	O4	Pd1	125.5(4)	C17	C16	Pd2	125.9(5)
C26	O5	Pd2	124.6(4)	C21	C16	Pd2	114.9(5)
C7	N1	Pd1	106.8(4)	C21	C16	C17	119.2(6)
C9	N1	Pd1	107.2(4)	C16	C17	C18	120.3(6)
C9	N1	C7	108.9(5)	C19	C18	C17	120.1(6)
C10	N1	Pd1	115.1(4)	C20	C19	C18	120.6(6)
C10	N1	C7	109.8(5)	C19	C20	C21	119.6(6)
C10	N1	C9	108.9(5)	C19	C20	C23	119.9(6)
C14	N2	C12	122.7(6)	C21	C20	C23	120.5(6)
C22	N3	Pd2	107.3(4)	C16	C21	C20	120.2(6)
C22	N3	C25	110.0(5)	C16	C21	C22	114.9(5)
C24	N3	Pd2	107.3(4)	C20	C21	C22	124.9(6)
C24	N3	C22	109.5(5)	N3	C22	C21	108.1(5)
C24	N3	C25	107.4(5)	F4	C23	C20	112.6(6)
C25	N3	Pd2	115.1(4)	F4	C23	F6	105.9(6)
C29	N4	C27	121.0(6)	F5	C23	C20	113.1(6)
C2	C1	Pd1	126.8(5)	F5	C23	F4	106.6(6)
C2	C1	C6	119.4(6)	F5	C23	F6	105.7(6)
C6	C1	Pd1	113.8(4)	F6	C23	C20	112.4(6)
C3	C2	C1	119.5(6)	O4	C26	O5	128.3(6)
C4	C3	C2	121.9(6)	O4	C26	C27	115.5(6)
C3	C4	C5	120.2(6)	O5	C26	C27	116.1(6)
C4	C5	C6	119.0(6)	N4	C27	C26	112.3(5)
C4	C5	C8	121.2(6)	N4	C27	C28	110.8(5)
C6	C5	C8	119.8(6)	C28	C27	C26	108.5(5)
C1	C6	C5	120.1(5)	O6	C29	N4	122.7(6)

C1	C6	C7	115.3(5)	O6	C29	C30	122.2(6)
C5	C6	C7	124.6(6)	N4	C29	C30	115.1(6)
N1	C7	C6	108.8(5)	N5	C31	C32	177.6(10)

Complex_6a

molecular structure complex_6a with 40% ellipsoids

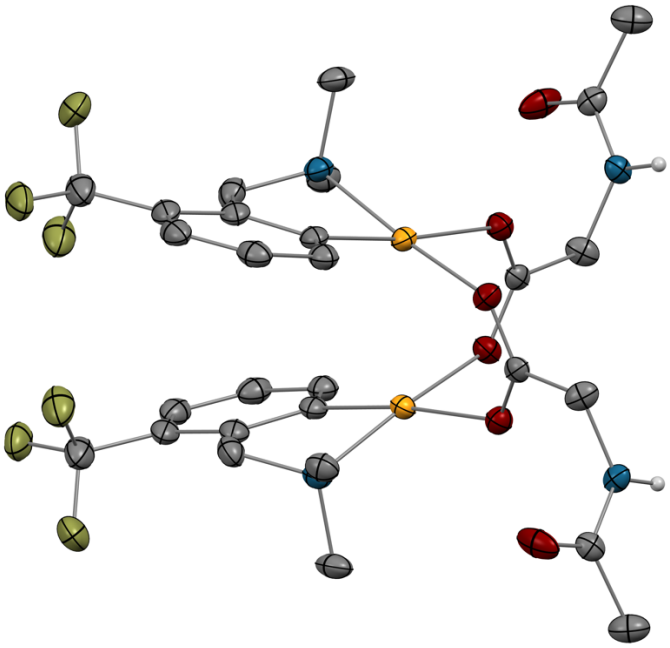

asymmetric unit complex_6a with 40% ellipsoids

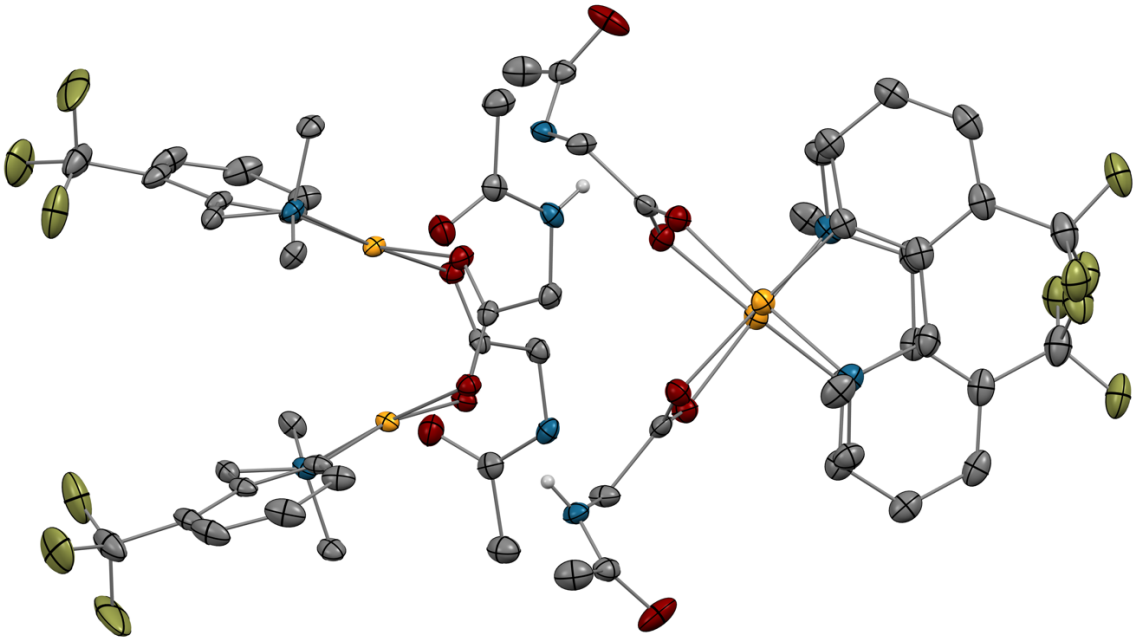

unit cell complex_6a with hydrogen bonding

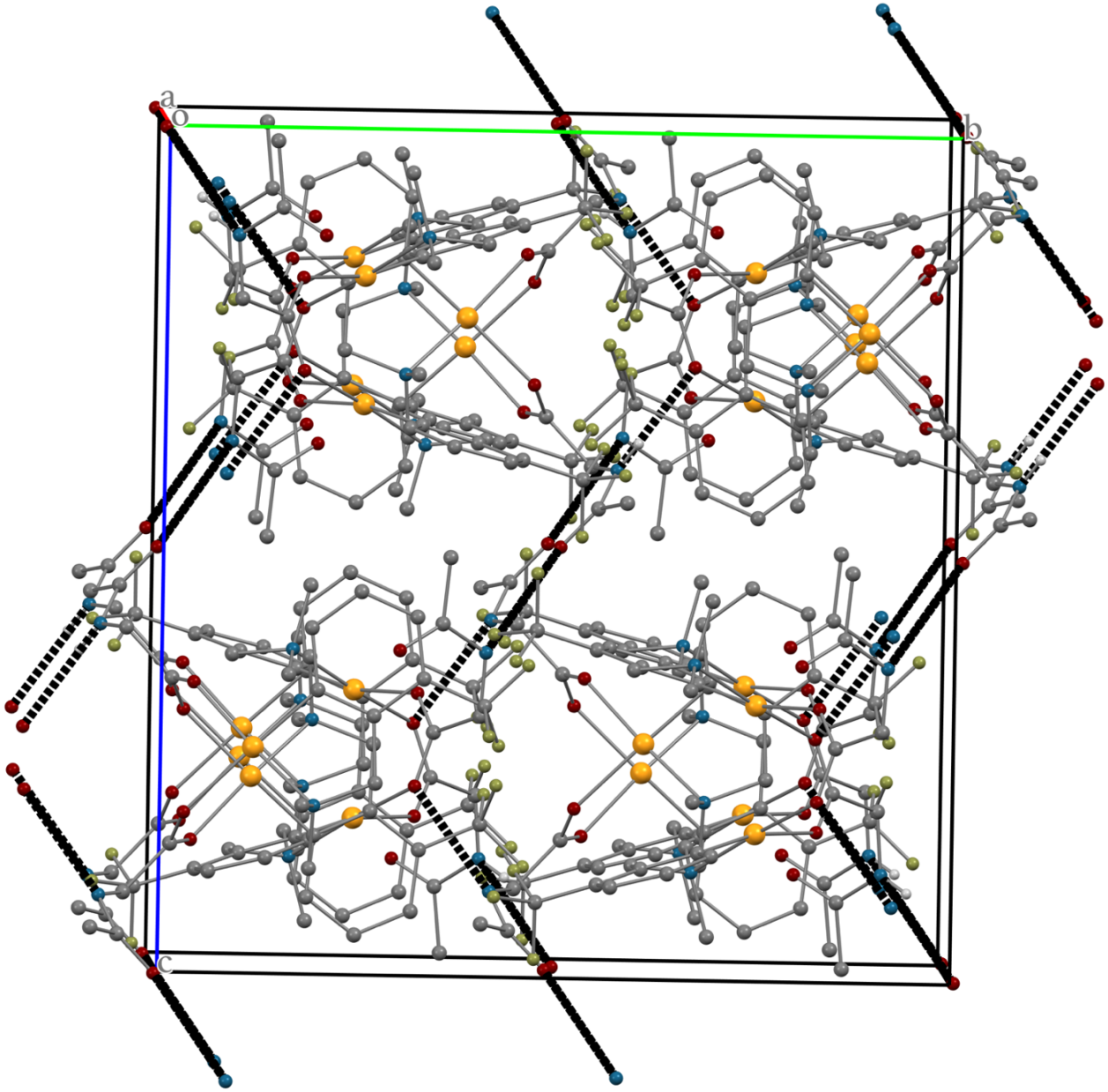

Table 1 Crystal data and structure refinement for complex_6a.

Identification code	complex_6a
Empirical formula	$C_{28}H_{34}F_6N_4O_6Pd_2$
Formula weight	849.39
Temperature/K	100(2)
Crystal system	monoclinic
Space group	C2/c
a/Å	19.2283(14)
b/Å	17.6933(14)
c/Å	18.9065(15)
α/°	90
β/°	93.545(3)
γ/°	90
Volume/Å^3	6419.9(9)
Z	8
ρ_{calc}g/cm^3	1.758
μ/mm^{-1}	1.202
F(000)	3392.0
Crystal size/mm^3	0.17 × 0.15 × 0.11
Radiation	MoKα (λ = 0.71073)
2Θ range for data collection/°	4.244 to 53.616
Index ranges	$-24 \le h \le 24$, $-22 \le k \le 22$, $-23 \le l \le 23$
Reflections collected	86726
Independent reflections	6867 [R_{int} = 0.0293, R_{sigma} = 0.0133]
Data/restraints/parameters	6867/0/429
Goodness-of-fit on F^2	1.073
Final R indexes [I>=2σ (I)]	R_1 = 0.0213, wR_2 = 0.0497
Final R indexes [all data]	R_1 = 0.0265, wR_2 = 0.0522
Largest diff. peak/hole / e Å^{-3}	0.81/-0.46

$R_{int} = \Sigma \mid F_o^2 - \langle F_o^2 \rangle \mid / \Sigma \mid F_o^2 \mid$

$R1 = \Sigma \mid \mid F_o \mid - \mid F_c \mid \mid / \Sigma \mid F_o \mid$

$wR2 = [\Sigma [w (F_o^2 - F_c^2)^2] / \Sigma [w (F_o^2)^2]]^{1/2}$

Goodness-of-fit = $[\Sigma [w (F_o^2 - F_c^2)^2] / (n-p)]^{1/2}$

n: number of independent reflections; p: number of refined parameters

Table 2 Fractional Atomic Coordinates (×104) and Equivalent Isotropic Displacement Parameters (Å2×103) for complex_6a. U_{eq} **is defined as 1/3 of of the trace of the orthogonalised** U_{IJ} **tensor.**

Atom	*x*	*y*	*z*	U(eq)
Pd1	5239.9(2)	2507.3(2)	6747.3(2)	17.22(4)
F1	6424.3(8)	-789.6(9)	5981.5(10)	59.8(5)
F2	5693.0(14)	-264.4(10)	5236.0(9)	93.5(8)
F9	5409.9(8)	-525.2(8)	6273.7(10)	59.5(5)
O1	5972.6(7)	3273.2(7)	7150.3(7)	21.1(3)
O2	5591.6(7)	3296.7(8)	8241.1(7)	22.7(3)
O3	7297.0(8)	3043.5(8)	8780.8(8)	33.5(3)
N1	4592.4(8)	1716.3(9)	6266.3(8)	19.2(3)
N2	6707.7(9)	4134.3(10)	8757.2(9)	22.5(3)
C1	5960.4(10)	1782.0(11)	6524.7(9)	21.2(4)
C2	6669.4(10)	1936.8(13)	6507.1(11)	27.9(4)
C3	7124.9(11)	1381.7(15)	6303.1(12)	36.9(5)
C4	6884.8(12)	667.5(15)	6130.4(12)	37.1(6)
C5	6181.8(11)	506.1(13)	6139.4(10)	29.3(5)
C6	5710.5(10)	1065.5(11)	6323(1)	22.0(4)
C7	4938.4(10)	959.8(11)	6342(1)	22.4(4)
C8	5932.9(14)	-258.5(14)	5914.5(13)	42.0(6)
C9	4502.7(10)	1931.5(12)	5505.9(10)	25.2(4)
C10	3890.8(10)	1660.7(12)	6549.7(11)	24.9(4)
C11	5993.7(9)	3499.4(10)	7789.6(10)	19.5(4)
C12	6555.5(10)	4078.0(11)	8003(1)	23.3(4)
C13	7076.5(10)	3583.5(12)	9099.1(11)	24.7(4)
C14	7215.5(13)	3666.5(14)	9887.1(12)	35.9(5)
Pd2	4242.6(2)	6154.7(2)	7310.7(2)	23.06(5)
F4	4217.8(8)	9251.3(8)	7247.9(9)	51.3(4)
F6	3666.4(7)	9608.5(8)	6280.8(9)	48.1(4)
F8	3109.9(7)	9114.0(8)	7113.7(9)	47.8(4)
O4	4528.3(7)	5402.1(8)	6557.3(7)	26.8(3)
O5	5661.6(7)	5292.4(8)	6907.5(7)	26.9(3)
O6	6197.6(8)	4936(1)	5008.7(9)	43.1(4)
N3	3833.1(8)	6923.6(10)	7982.1(9)	27.0(4)
N4	5885.9(9)	4232(1)	5919.0(9)	23.8(4)
C15	4050.6(10)	6960.0(12)	6619.2(11)	25.8(4)
C16	4020.9(10)	6875.9(13)	5885.6(11)	28.8(4)
C17	3882.3(11)	7493.3(13)	5445.9(13)	33.4(5)
C18	3779.7(11)	8201.5(13)	5733.7(13)	33.9(5)
C19	3802.2(11)	8292.5(12)	6463.2(13)	32.3(5)
C20	3925.9(10)	7670.1(12)	6912.0(12)	28.5(4)

C21	3964.0(12)	7698.6(12)	7707.9(12)	31.9(5)
C22	3700.6(12)	9060.5(14)	6773.7(15)	40.9(6)
C23	4104.1(11)	6878.3(13)	8729.6(11)	32.2(5)
C24	3069.8(11)	6767.9(15)	7963.2(13)	37.1(5)
C25	5132.2(10)	5132.8(11)	6523.6(10)	22.5(4)
C26	5198.4(11)	4550.2(13)	5940.1(10)	27.4(4)
C27	6343.9(10)	4468.7(12)	5470.9(10)	25.6(4)
C28	7055.9(12)	4115.6(16)	5559.3(13)	39.0(5)

Table 3 Anisotropic Displacement Parameters (Å2×103) for complex_6a. The Anisotropic displacement factor exponent takes the form: $-2\pi^2[h^2a^{*2}U_{11}+2hka^*b^*U_{12}+\ldots]$.

Atom	U_{11}	U_{22}	U_{33}	U_{23}	U_{13}	U_{12}
Pd1	15.42(7)	20.27(8)	15.64(7)	-2.50(5)	-1.66(5)	3.77(5)
F1	54.7(10)	40.5(9)	84.1(12)	-9.8(8)	3.5(9)	31.3(7)
F2	179(2)	47.1(10)	47.4(10)	-26.3(8)	-52.3(12)	22.8(12)
F9	44.7(9)	30.9(8)	101.8(14)	-19.9(8)	-4.5(9)	7.2(7)
O1	21.1(7)	23.3(7)	18.8(6)	0.2(5)	-0.8(5)	-0.7(5)
O2	22.7(7)	24.7(7)	20.3(7)	1.7(5)	-0.8(5)	-8.3(6)
O3	36.8(9)	25.5(8)	37.8(9)	-4.2(7)	-0.9(7)	2.9(7)
N1	17.3(7)	22.1(8)	17.7(7)	-4.2(6)	-1.9(6)	5.3(6)
N2	19.9(8)	22.1(8)	25.7(9)	-6.2(7)	1.1(7)	-3.5(7)
C1	18.9(9)	30.6(10)	14.0(8)	-1.8(7)	-1.4(7)	7.5(8)
C2	19.0(9)	41.6(12)	22.7(10)	-1.7(9)	-1.3(8)	4.3(9)
C3	18.8(10)	61.2(16)	30.4(11)	-8.2(11)	-1.4(9)	10.3(10)
C4	27.8(11)	54.9(15)	28.0(11)	-12.2(10)	-3.2(9)	23.0(11)
C5	32.0(11)	36.1(12)	18.8(9)	-7.3(8)	-5.5(8)	14.9(9)
C6	22.6(9)	29.4(10)	13.6(8)	-3.3(7)	-3.4(7)	8.5(8)
C7	24.5(10)	21.7(9)	20.5(9)	-4.2(7)	-2.8(7)	5.3(8)
C8	48.0(15)	37.8(13)	38.5(13)	-13.6(11)	-12.8(11)	22.4(12)
C9	25.9(10)	29.7(10)	19.1(9)	-2.6(8)	-6.0(8)	5.1(8)
C10	17.2(9)	28(1)	29.4(10)	-7.7(8)	1.8(8)	0.5(8)
C11	17.4(9)	17.9(9)	22.6(9)	2.9(7)	-3.4(7)	-0.2(7)
C12	22.5(10)	21.7(9)	25.8(10)	1.8(8)	1.3(8)	-5.3(8)
C13	19.9(9)	26.5(10)	27.6(10)	-1.4(8)	1.7(8)	-8.5(8)
C14	37.8(13)	42.4(13)	27.2(11)	1.8(10)	0.1(9)	-4.7(10)
Pd2	19.21(8)	23.31(8)	26.87(8)	1.52(6)	2.96(6)	3.03(6)
F4	44.3(8)	36.2(8)	70.5(11)	-4.7(7)	-19.9(8)	0.5(6)
F6	43.4(8)	27.2(7)	72.5(10)	14.0(7)	-6.9(7)	1.0(6)
F8	40.5(8)	33.6(7)	69.7(10)	0.3(7)	6.0(7)	11.0(6)
O4	27.1(7)	27.3(7)	26.2(7)	1.1(6)	3.1(6)	5.2(6)
O5	26.2(7)	26.5(7)	28.1(7)	-2.9(6)	3.2(6)	0.1(6)
O6	30.9(8)	59.9(11)	38.0(9)	27.9(8)	-1.6(7)	-8.6(8)
N3	19.8(8)	29.9(9)	31.1(9)	-2.8(7)	1.2(7)	2.9(7)
N4	26.7(9)	27.3(9)	17.5(8)	4.6(7)	1.8(7)	5.1(7)
C15	15.7(9)	27.2(10)	34.2(11)	3.6(9)	-0.2(8)	1.6(8)
C16	20.4(10)	31.6(11)	34.3(11)	3.4(9)	1.1(8)	-0.2(8)
C17	22.6(10)	41.9(13)	35.2(12)	8.7(10)	-1.9(9)	-2.1(9)
C18	21.4(10)	33.7(12)	46.2(13)	13.3(10)	-2.5(9)	1.1(9)
C19	18.7(10)	27.8(11)	49.9(14)	5.1(10)	-3.3(9)	2.5(8)
C20	16.8(9)	29.3(11)	38.8(12)	2.4(9)	-3.2(8)	1.4(8)
C21	29.0(11)	25.9(11)	39.9(12)	-2.8(9)	-4.4(9)	5.7(9)

C22	31.3(12)	30.2(12)	59.8(16)	7.0(11)	-7.4(11)	2(1)
C23	29.3(11)	37.7(12)	29.8(11)	-3.8(9)	3.4(9)	3.1(9)
C24	19.8(10)	47.9(14)	43.9(13)	-11.1(11)	4.9(9)	2.1(10)
C25	25.2(10)	22.5(10)	20.5(9)	7.1(8)	5.8(8)	1.0(8)
C26	28.1(10)	36.9(12)	17.1(9)	0.4(8)	1.4(8)	5.9(9)
C27	26.4(10)	29.3(11)	20.7(9)	-1.9(8)	-1.0(8)	-3.9(8)
C28	25.6(11)	57.0(15)	34.6(12)	1.6(11)	2.6(9)	3.0(11)

Table 4 Bond Lengths for complex_6a.

Atom	Atom	Length/Å	Atom	Atom	Length/Å
Pd1	O1	2.0661(13)	Pd2	O4	2.0497(14)
Pd1	O2[1]	2.1239(13)	Pd2	O5[1]	2.1244(14)
Pd1	N1	2.0485(16)	Pd2	N3	2.0506(17)
Pd1	C1	1.9534(18)	Pd2	C15	1.954(2)
F1	C8	1.333(3)	F4	C22	1.340(3)
F2	C8	1.336(3)	F6	C22	1.344(3)
F9	C8	1.334(3)	F8	C22	1.342(3)
O1	C11	1.272(2)	O4	C25	1.260(2)
O2	C11	1.240(2)	O5	C25	1.245(2)
O3	C13	1.219(3)	O6	C27	1.223(3)
N1	C7	1.498(2)	N3	C21	1.493(3)
N1	C9	1.487(2)	N3	C23	1.478(3)
N1	C10	1.485(2)	N3	C24	1.491(3)
N2	C12	1.441(3)	N4	C26	1.440(3)
N2	C13	1.347(3)	N4	C27	1.327(3)
C1	C2	1.393(3)	C15	C16	1.393(3)
C1	C6	1.400(3)	C15	C20	1.399(3)
C2	C3	1.386(3)	C16	C17	1.388(3)
C3	C4	1.378(4)	C17	C18	1.385(3)
C4	C5	1.383(3)	C18	C19	1.387(3)
C5	C6	1.400(3)	C19	C20	1.402(3)
C5	C8	1.488(3)	C19	C22	1.498(3)
C6	C7	1.499(3)	C20	C21	1.503(3)
C11	C12	1.524(3)	C25	C26	1.521(3)
C13	C14	1.504(3)	C27	C28	1.505(3)

[1]1-X,+Y,3/2-Z

Table 5 Bond Angles for complex_6a.

Atom	Atom	Atom	Angle/°	Atom	Atom	Atom	Angle/°
O1	Pd1	O2[1]	93.52(5)	O4	Pd2	O5[1]	90.09(6)
N1	Pd1	O1	173.57(6)	O4	Pd2	N3	172.24(6)
N1	Pd1	O2[1]	90.95(6)	N3	Pd2	O5[1]	93.78(6)
C1	Pd1	O1	91.93(7)	C15	Pd2	O4	93.23(7)
C1	Pd1	O2[1]	168.11(6)	C15	Pd2	O5[1]	173.83(7)
C1	Pd1	N1	82.83(7)	C15	Pd2	N3	82.33(8)
C11	O1	Pd1	122.55(12)	C25	O4	Pd2	124.62(13)
C11	O2	Pd1[1]	134.37(12)	C25	O5	Pd2[1]	126.94(13)
C7	N1	Pd1	108.30(11)	C21	N3	Pd2	108.36(13)
C9	N1	Pd1	106.57(12)	C23	N3	Pd2	115.45(13)
C9	N1	C7	110.22(14)	C23	N3	C21	108.96(17)
C10	N1	Pd1	115.20(11)	C23	N3	C24	107.52(17)
C10	N1	C7	108.33(15)	C24	N3	Pd2	106.12(13)
C10	N1	C9	108.19(15)	C24	N3	C21	110.37(17)
C13	N2	C12	119.58(17)	C27	N4	C26	122.75(18)
C2	C1	Pd1	125.75(16)	C16	C15	Pd2	125.66(16)
C2	C1	C6	119.43(18)	C16	C15	C20	119.50(19)
C6	C1	Pd1	114.67(14)	C20	C15	Pd2	114.83(16)
C3	C2	C1	120.2(2)	C17	C16	C15	120.4(2)
C4	C3	C2	120.5(2)	C18	C17	C16	120.2(2)
C3	C4	C5	120.0(2)	C17	C18	C19	119.9(2)
C4	C5	C6	120.3(2)	C18	C19	C20	120.3(2)
C4	C5	C8	118.8(2)	C18	C19	C22	119.9(2)
C6	C5	C8	120.8(2)	C20	C19	C22	119.8(2)
C1	C6	C7	115.48(16)	C15	C20	C19	119.5(2)
C5	C6	C1	119.41(19)	C15	C20	C21	115.29(19)
C5	C6	C7	125.09(19)	C19	C20	C21	125.1(2)
N1	C7	C6	108.73(16)	N3	C21	C20	108.54(17)
F1	C8	F2	106.6(2)	F4	C22	F6	106.54(19)
F1	C8	F9	104.7(2)	F4	C22	F8	106.1(2)
F1	C8	C5	113.6(2)	F4	C22	C19	112.41(19)
F2	C8	C5	111.6(2)	F6	C22	C19	112.6(2)
F9	C8	F2	105.0(2)	F8	C22	F6	105.95(18)
F9	C8	C5	114.54(19)	F8	C22	C19	112.7(2)
O1	C11	C12	116.33(16)	O4	C25	C26	114.30(17)
O2	C11	O1	125.37(17)	O5	C25	O4	127.38(19)
O2	C11	C12	118.29(17)	O5	C25	C26	118.32(17)
N2	C12	C11	113.93(16)	N4	C26	C25	113.78(17)
O3	C13	N2	121.26(19)	O6	C27	N4	122.5(2)
O3	C13	C14	121.3(2)	O6	C27	C28	121.8(2)

N2	C13	C14	117.43(19)	N4	C27	C28	115.67(19)

Complex_S5.1

complex_S5.1 with 50% ellipsoids

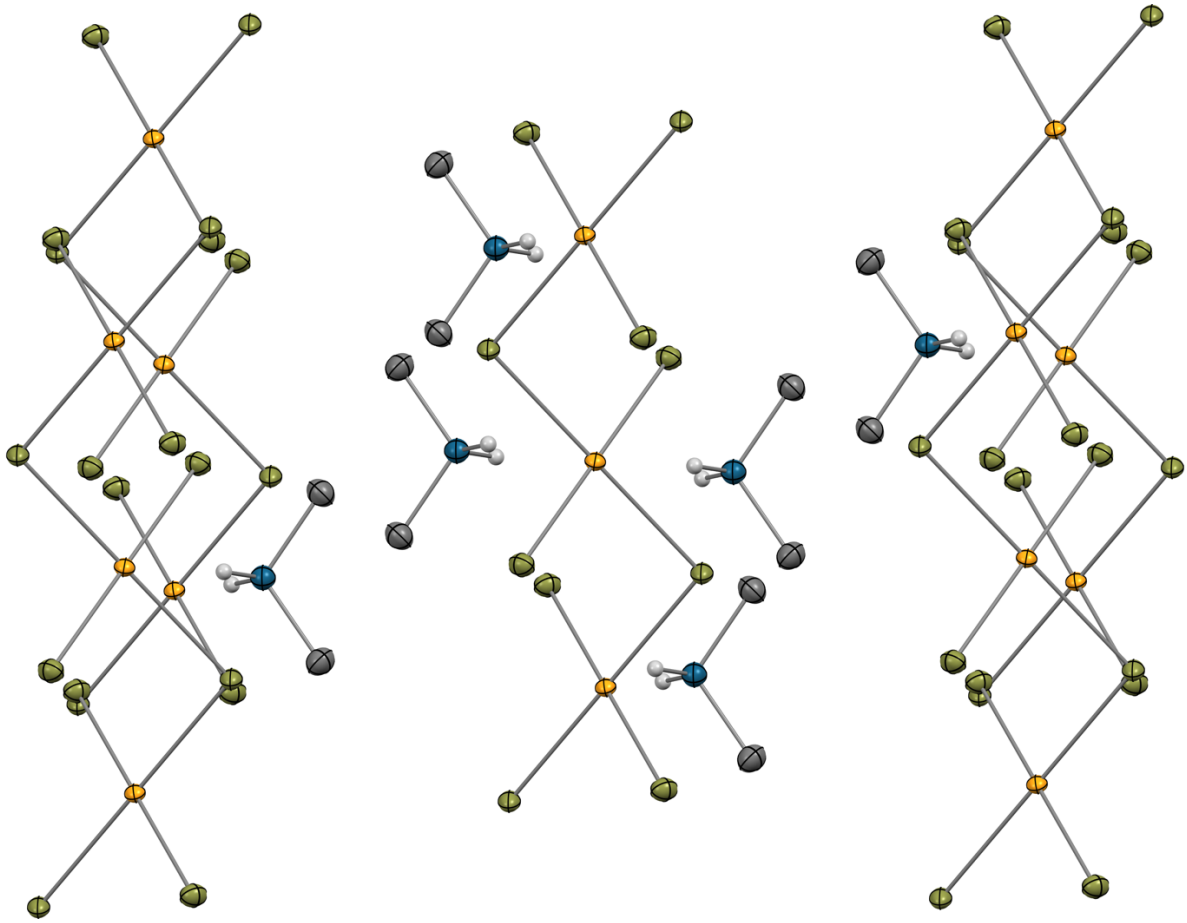

complex_S5.1 with 50% ellipsoids and short contacts

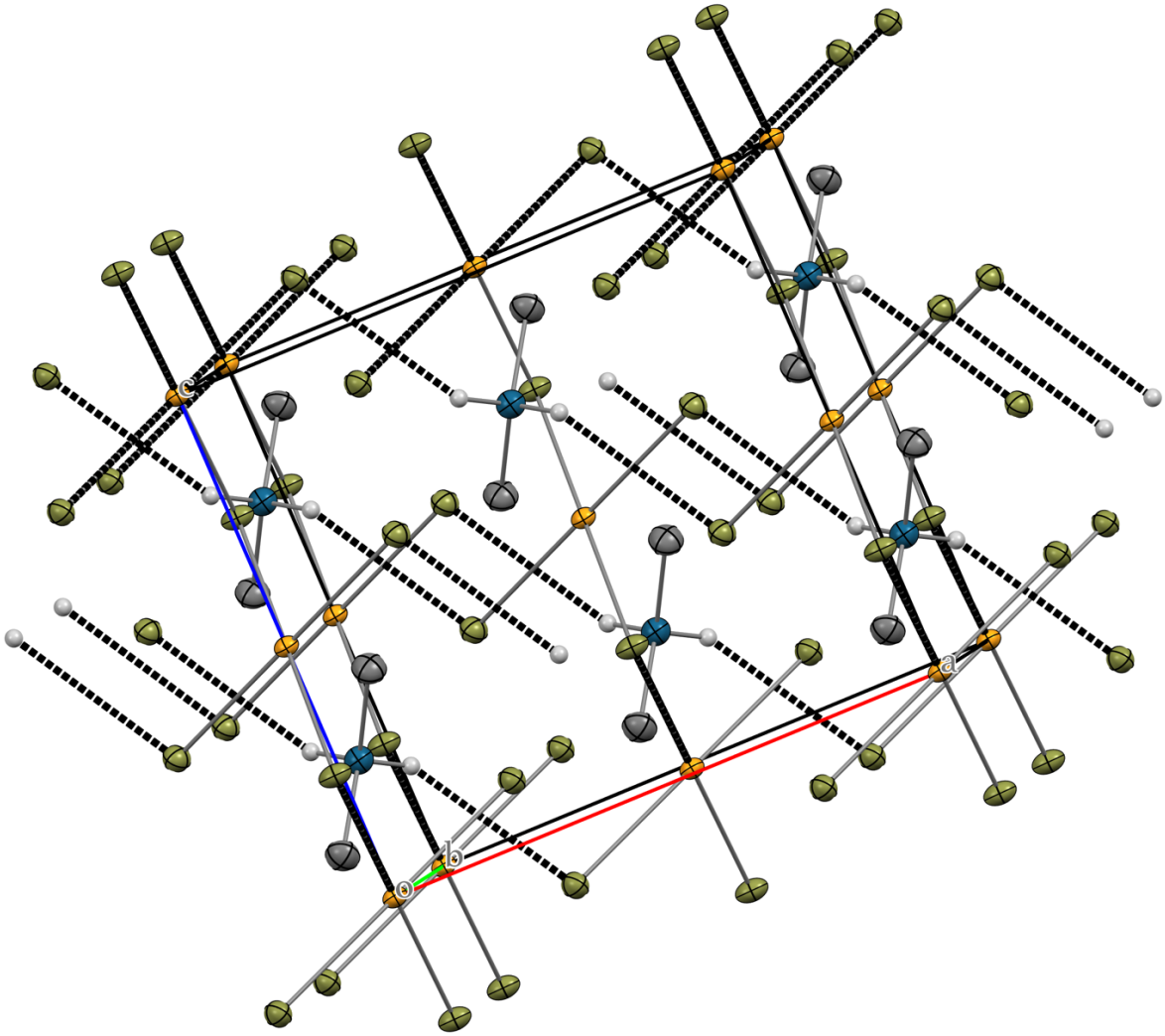

Table 1 Crystal data and structure refinement forcomplex_S5.1.

Identification code	complex_S5.1
Empirical formula	$C_4H_{16}Cl_6N_2Pd_2$
Formula weight	517.69
Temperature/K	100(2)
Crystal system	monoclinic
Space group	C2/c
a/Å	7.6908(5)
b/Å	13.0776(8)
c/Å	7.1107(4)
α/°	90
β/°	90.8831(14)
γ/°	90
Volume/Å^3	715.09(8)
Z	2
ρ_{calc}g/cm^3	2.404
μ/mm^{-1}	3.603
F(000)	496.0
Crystal size/mm^3	0.32 × 0.12 × 0.11
Radiation	MoKα (λ = 0.71073)
2Θ range for data collection/°	6.146 to 67.494
Index ranges	$-11 \le h \le 12$, $-20 \le k \le 20$, $-11 \le l \le 11$
Reflections collected	17218
Independent reflections	1435 [R_{int} = 0.0231, R_{sigma} = 0.0103]
Data/restraints/parameters	1435/0/40
Goodness-of-fit on F^2	1.137
Final R indexes [I>=2σ (I)]	R_1 = 0.0115, wR_2 = 0.0247
Final R indexes [all data]	R_1 = 0.0137, wR_2 = 0.0253
Largest diff. peak/hole / e Å^{-3}	0.44/-0.53

$R_{int} = \Sigma \mid F_o^2 - \langle F_o^2 \rangle \mid / \Sigma \mid F_o^2 \mid$

$R1 = \Sigma \mid \mid F_o \mid - \mid F_c \mid \mid / \Sigma \mid F_o \mid$

$wR2 = [\Sigma [w (F_o^2 - F_c^2)^2] / \Sigma [w (F_o^2)^2]]^{1/2}$

Goodness-of-fit = $[\Sigma [w (F_o^2 - F_c^2)^2] / (n-p)]^{1/2}$

n: number of independent reflections; p: number of refined parameters

Table 2 Fractional Atomic Coordinates (×104) and Equivalent Isotropic Displacement Parameters (Å2×103) for complex_S5.1. **U_{eq} is defined as 1/3 of of the trace of the orthogonalised U_{IJ} tensor.**

Atom	*x*	*y*	*z*	U(eq)
Pd1	5000	5000	5000	8.92(3)
Cl2	5000	6125.4(2)	7500	13.04(6)
Cl1	7531.7(3)	4269.7(2)	6140.8(3)	13.99(5)
N1	10000	3741.7(10)	2500	13.7(2)
C2	10836.2(14)	3104.0(9)	3990.8(16)	18.68(19)

Table 3 Anisotropic Displacement Parameters (Å2×103) for complex_S5.1. **The Anisotropic displacement factor exponent takes the form: $-2\pi^2[h^2a^{*2}U_{11}+2hka^*b^*U_{12}+\ldots]$.**

Atom	U_{11}	U_{22}	U_{33}	U_{23}	U_{13}	U_{12}
Pd1	10.95(4)	9.04(4)	6.78(4)	0.39(3)	0.67(3)	−0.14(3)
Cl2	20.35(15)	10.51(13)	8.29(12)	0	0.62(10)	0
Cl1	13.53(9)	15.53(10)	12.86(9)	0.15(8)	−0.98(7)	2.40(8)
N1	14.9(5)	13.1(5)	13.2(5)	0	0.6(4)	0
C2	20.1(5)	17.7(5)	18.2(5)	3.1(4)	−1.2(4)	2.2(4)

Table 4 Bond Lengths for complex_S5.1.

Atom	Atom	Length/Å	Atom	Atom	Length/Å
Pd1	Cl2	2.3079(2)	Pd1	Cl1[1]	2.3049(3)
Pd1	Cl2[1]	2.3079(2)	N1	C2	1.4872(13)
Pd1	Cl1	2.3049(3)	N1	C2[2]	1.4872(13)

[1]1-X,1-Y,1-Z; [2]2-X,+Y,1/2-Z

Table 5 Bond Angles for complex_S5.1.

Atom	Atom	Atom	Angle/°	Atom	Atom	Atom	Angle/°
Cl2	Pd1	Cl2[1]	180.0	Cl1[1]	Pd1	Cl2	89.818(7)
Cl1[1]	Pd1	Cl2[1]	90.182(7)	Cl1	Pd1	Cl1[1]	180.0
Cl1	Pd1	Cl2	90.183(7)	Pd1	Cl2	Pd1[2]	100.756(13)
Cl1	Pd1	Cl2[1]	89.817(7)	C2	N1	C2[3]	111.79(12)

Complex_17

molecular structure complex_17 with 40% ellipsoids

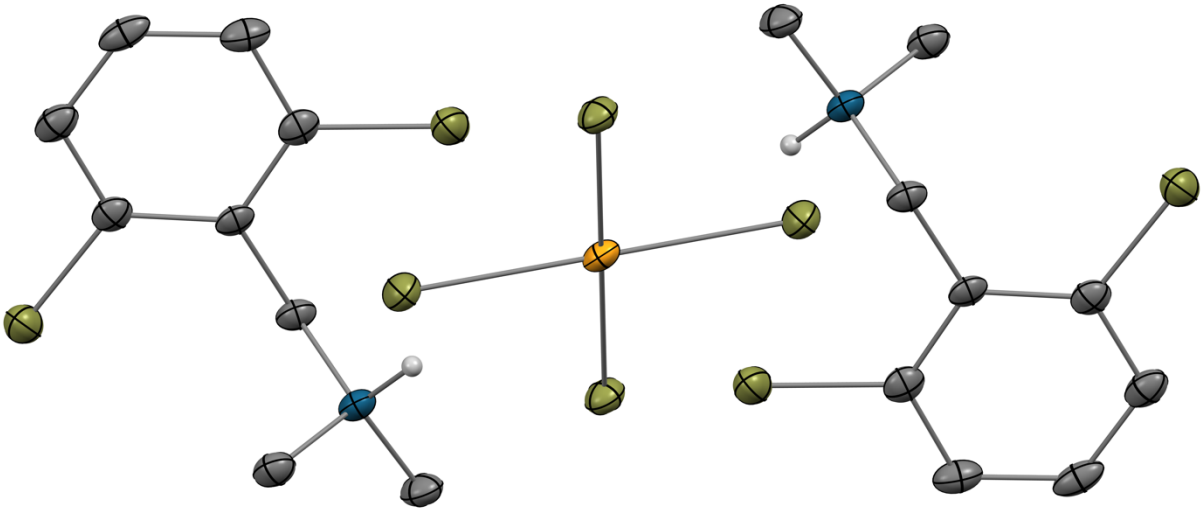

unit cell complex_17 with 40% ellipsoids and short contacts

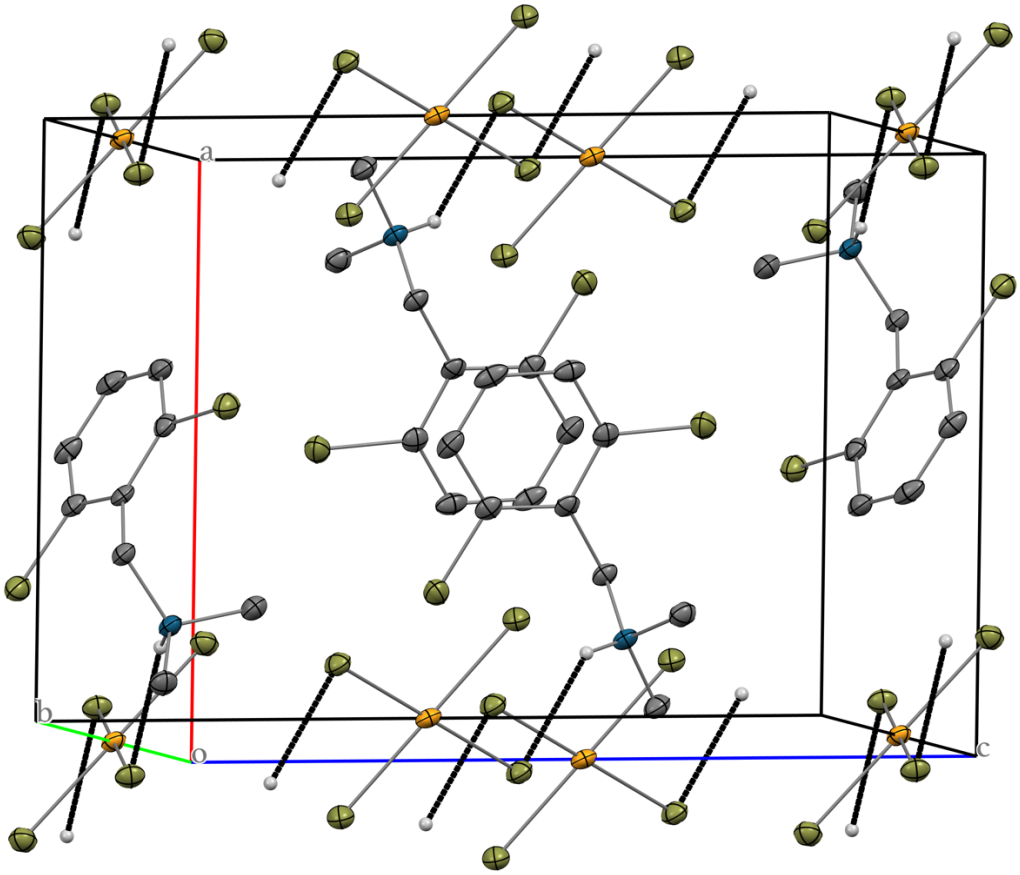

Table 1 Crystal data and structure refinement for complex_17.

Identification code	complex_17
Empirical formula	$C_{18}H_{24}Cl_8N_2Pd$
Formula weight	658.39
Temperature/K	100(2)
Crystal system	monoclinic
Space group	$P2_1/c$
a/Å	10.3725(10)
b/Å	8.0905(8)
c/Å	14.2505(13)
α/°	90
β/°	90.468(2)
γ/°	90
Volume/Å^3	1195.8(2)
Z	2
ρ_{calc}g/cm^3	1.828
μ/mm^{-1}	1.680
F(000)	656.0
Crystal size/mm^3	0.22 × 0.09 × 0.06
Radiation	MoKα (λ = 0.71073)
2Θ range for data collection/°	5.718 to 52.862
Index ranges	$-12 \le h \le 12$, $-9 \le k \le 10$, $-17 \le l \le 17$
Reflections collected	15065
Independent reflections	2444 [R_{int} = 0.0536, R_{sigma} = 0.0425]
Data/restraints/parameters	2444/1/138
Goodness-of-fit on F^2	1.096
Final R indexes [I>=2σ (I)]	R_1 = 0.0435, wR_2 = 0.1038
Final R indexes [all data]	R_1 = 0.0677, wR_2 = 0.1154
Largest diff. peak/hole / e Å^{-3}	1.82/-0.40

$R_{int} = \Sigma \mid F_o^2 - \langle F_o^2 \rangle \mid / \Sigma \mid F_o^2 \mid$

$R1 = \Sigma \mid \mid F_o \mid - \mid F_c \mid \mid / \Sigma \mid F_o \mid$

$wR2 = [\Sigma [w (F_o^2 - F_c^2)^2] / \Sigma [w (F_o^2)^2]]^{1/2}$

Goodness-of-fit = $[\Sigma [w (F_o^2 - F_c^2)^2] / (n-p)]^{1/2}$

n: number of independent reflections; p: number of refined parameters

Table 2 Fractional Atomic Coordinates (×104) and Equivalent Isotropic Displacement Parameters (Å2×103) for complex_17. U_{eq} is defined as 1/3 of of the trace of the orthogonalised U_{IJ} tensor.

Atom	*x*	*y*	*z*	U(eq)
Pd1	0	0	5000	20.30(17)
Cl1	1625.2(11)	94.6(15)	6119.7(9)	28.4(3)
Cl2	740.2(11)	2392.3(15)	4309.2(9)	26.3(3)
Cl3	5189.4(12)	4788.5(16)	7413.7(9)	31.5(3)
Cl4	2322.6(12)	6660.9(16)	4414.8(8)	30.2(3)
N1	1598(4)	5492(5)	6598(3)	20.3(9)
C1	2735(4)	4649(6)	6158(3)	22.4(11)
C2	1944(5)	6343(6)	7490(3)	27.1(11)
C3	566(5)	4255(6)	6767(4)	26.8(11)
C4	3797(4)	5826(6)	5900(3)	20.8(10)
C5	3704(4)	6789(6)	5091(3)	23.2(10)
C6	4692(5)	7828(6)	4801(4)	26.9(11)
C7	5812(5)	7917(6)	5324(4)	28.3(12)
C8	5956(5)	6973(6)	6131(4)	26.8(11)
C9	4961(4)	5955(6)	6404(3)	23.5(11)

Table 3 Anisotropic Displacement Parameters (Å2×103) for complex_17. The Anisotropic displacement factor exponent takes the form: $-2\pi^2[h^2a^{*2}U_{11}+2hka^*b^*U_{12}+\ldots]$.

Atom	U_{11}	U_{22}	U_{33}	U_{23}	U_{13}	U_{12}
Pd1	14.8(3)	22.3(3)	23.8(3)	−1.5(2)	5.79(19)	−2.2(2)
Cl1	22.6(6)	34.1(7)	28.4(7)	2.3(5)	0.2(5)	−4.6(5)
Cl2	21.8(6)	26.1(6)	31.1(7)	4.3(5)	4.1(5)	−3.7(5)
Cl3	28.1(7)	41.7(8)	24.8(7)	2.6(6)	1.3(5)	6.0(6)
Cl4	26.3(6)	39.8(7)	24.7(7)	2.9(6)	2.5(5)	6.0(5)
N1	17(2)	22(2)	22(2)	−1.1(16)	5.5(16)	0.1(16)
C1	20(2)	23(3)	23(3)	−2.2(19)	6.5(19)	1.3(19)
C2	23(3)	33(3)	26(3)	−3(2)	6(2)	1(2)
C3	23(3)	30(3)	28(3)	0(2)	6(2)	−7(2)
C4	17(2)	23(3)	22(3)	−3(2)	7.2(19)	5.0(19)
C5	22(2)	22(2)	26(3)	−4(2)	7(2)	4(2)
C6	29(3)	21(2)	31(3)	2(2)	13(2)	1(2)
C7	25(3)	19(2)	42(3)	−7(2)	15(2)	−2(2)
C8	20(2)	28(3)	32(3)	−10(2)	7(2)	−2(2)
C9	23(2)	24(3)	23(3)	−4(2)	5.6(19)	6(2)

Table 4 Bond Lengths for complex_17.

Atom	Atom	Length/Å	Atom	Atom	Length/Å
Pd1	Cl1[1]	2.3129(12)	N1	C3	1.486(6)
Pd1	Cl1	2.3129(12)	C1	C4	1.504(6)
Pd1	Cl2[1]	2.3058(12)	C4	C5	1.394(7)
Pd1	Cl2	2.3059(12)	C4	C9	1.403(7)
Cl3	C9	1.736(5)	C5	C6	1.391(7)
Cl4	C5	1.724(5)	C6	C7	1.377(8)
N1	C1	1.504(6)	C7	C8	1.387(7)
N1	C2	1.486(6)	C8	C9	1.379(7)

[1]-X,-Y,1-Z

Table 5 Bond Angles for complex_17.

Atom	Atom	Atom	Angle/°	Atom	Atom	Atom	Angle/°
Cl1[1]	Pd1	Cl1	180.0	C5	C4	C9	115.7(4)
Cl2[1]	Pd1	Cl1[1]	91.34(4)	C9	C4	C1	123.4(4)
Cl2	Pd1	Cl1	91.34(4)	C4	C5	Cl4	118.7(4)
Cl2	Pd1	Cl1[1]	88.66(4)	C6	C5	Cl4	118.8(4)
Cl2[1]	Pd1	Cl1	88.66(4)	C6	C5	C4	122.5(5)
Cl2[1]	Pd1	Cl2	180.00(5)	C7	C6	C5	119.4(5)
C2	N1	C1	112.4(4)	C6	C7	C8	120.3(4)
C3	N1	C1	109.3(4)	C9	C8	C7	119.1(5)
C3	N1	C2	110.1(4)	C4	C9	Cl3	119.7(4)
C4	C1	N1	113.2(4)	C8	C9	Cl3	117.5(4)
C5	C4	C1	120.7(4)	C8	C9	C4	122.9(5)

Complex_16

molecular structure complex_16 with 40% ellipsoids

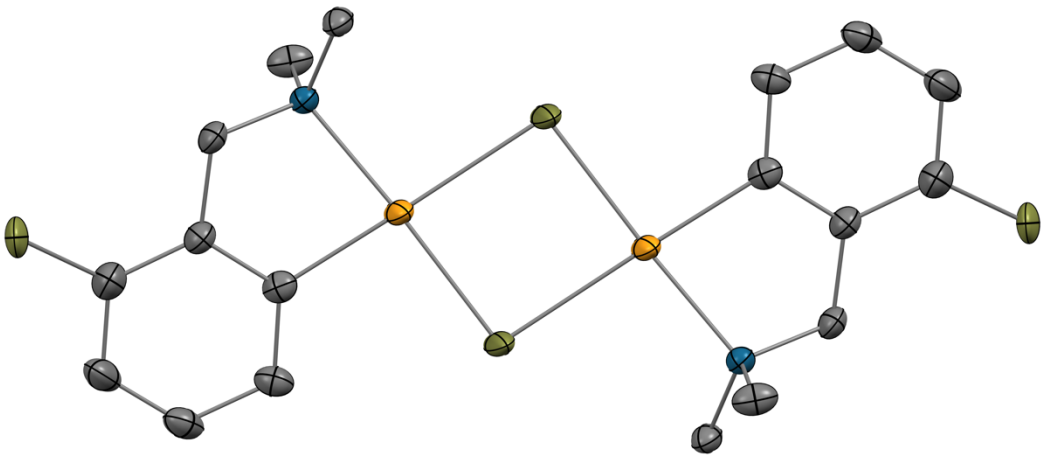

unit cell complex_16 with 30% ellipsoids

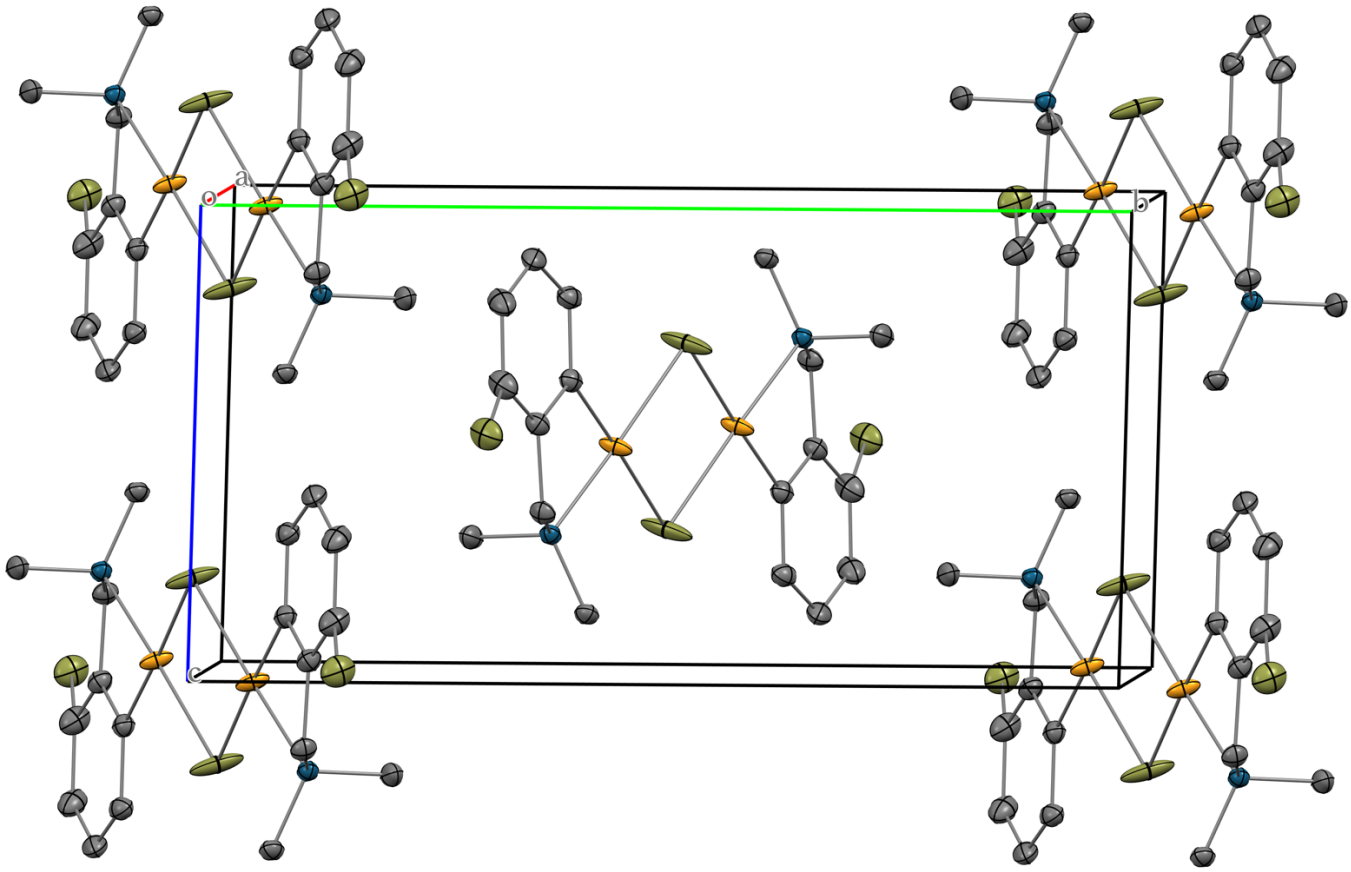

Table 1 Crystal data and structure refinement for complex_16.

Identification code	complex_16
Empirical formula	$C_{18}H_{23.6}Cl_{2.4}N_2Pd_2$
Formula weight	565.87
Temperature/K	100(2)
Crystal system	monoclinic
Space group	$P2_1/c$
a/Å	7.8606(4)
b/Å	15.7100(9)
c/Å	8.3499(4)
α/°	90
β/°	108.6070(13)
γ/°	90
Volume/Å^3	977.23(9)
Z	2
ρ_{calc}g/cm^3	1.923
μ/mm^{-1}	2.171
F(000)	557.0
Crystal size/mm^3	0.34 × 0.24 × 0.18
Radiation	MoKα (λ = 0.71073)
2Θ range for data collection/°	5.186 to 64.492
Index ranges	$-11 \le h \le 11$, $-23 \le k \le 23$, $-12 \le l \le 12$
Reflections collected	54669
Independent reflections	3456 [R_{int} = 0.0442, R_{sigma} = 0.0186]
Data/restraints/parameters	3456/0/120
Goodness-of-fit on F^2	1.290
Final R indexes [I>=2σ (I)]	R_1 = 0.0419, wR_2 = 0.0876
Final R indexes [all data]	R_1 = 0.0529, wR_2 = 0.0907
Largest diff. peak/hole / e Å^{-3}	1.63/-0.80

$R_{int} = \Sigma \mid F_o^2 - \langle F_o^2 \rangle \mid / \Sigma \mid F_o^2 \mid$

$R1 = \Sigma \mid \mid F_o \mid - \mid F_c \mid \mid / \Sigma \mid F_o \mid$

$wR2 = [\Sigma [w (F_o^2 - F_c^2)^2] / \Sigma [w (F_o^2)^2]]^{1/2}$

Goodness-of-fit = $[\Sigma [w (F_o^2 - F_c^2)^2] / (n-p)]^{1/2}$

n: number of independent reflections; p: number of refined parameters

Table 2 Fractional Atomic Coordinates (×104) and Equivalent Isotropic Displacement Parameters (Å2×103) for complex_16. **U_{eq} is defined as 1/3 of of the trace of the orthogonalised U_{IJ} tensor.**

Atom	*x*	*y*	*z*	U(eq)
Pd1	3158.6(3)	585.3(2)	143.0(3)	30.69(9)
Cl1	6121.8(13)	118.2(11)	2006.0(12)	64.8(4)
Cl2	-3532(6)	1737(4)	-385(7)	46.7(12)
N1	2415(3)	1232.3(16)	1971(3)	21.7(5)
C1	823(4)	1002(2)	-1334(4)	25.9(6)
C2	233(5)	1024(2)	-3101(4)	30.4(7)
C3	-1444(5)	1356(2)	-3970(4)	36.5(8)
C4	-2552(6)	1648(3)	-3109(5)	42.5(9)
C5	-1979(5)	1628(3)	-1354(5)	40.2(8)
C6	-288(4)	1308(2)	-466(4)	28.4(6)
C7	406(4)	1252(2)	1426(4)	27.6(6)
C8	3128(6)	2108(2)	2065(4)	34.9(8)
C9	3104(5)	844(2)	3665(4)	27.0(6)

Table 3 Anisotropic Displacement Parameters (Å2×103) for complex_16. **The Anisotropic displacement factor exponent takes the form: $-2\pi^2[h^2a^{*2}U_{11}+2hka^*b^*U_{12}+\ldots]$.**

Atom	U_{11}	U_{22}	U_{33}	U_{23}	U_{13}	U_{12}
Pd1	20.00(11)	53.76(18)	19.35(11)	-12.73(11)	7.75(8)	0.36(11)
Cl1	27.3(4)	135.3(12)	26.0(4)	-36.7(6)	0.3(3)	24.4(6)
Cl2	32(2)	57(3)	49(3)	-5(2)	11.1(19)	16(2)
N1	24.2(11)	22.2(12)	20.6(11)	-1.7(9)	9.9(9)	-1.9(9)
C1	26.9(14)	26.0(15)	25.5(14)	-1.8(11)	9.3(11)	-5.2(12)
C2	33.8(16)	31.6(17)	25.6(14)	-3.3(12)	9.1(12)	-7.6(13)
C3	44(2)	30.1(17)	27.0(15)	-2.8(13)	-1.0(14)	-4.4(15)
C4	38.7(19)	40(2)	37.5(19)	-7.3(16)	-3.4(15)	8.0(17)
C5	31.1(17)	47(2)	39.5(19)	-9.0(17)	7.3(15)	6.2(16)
C6	28.5(15)	30.3(16)	27.5(14)	-2.8(12)	10.6(12)	-0.4(13)
C7	27.0(14)	32.1(16)	27.0(14)	-3.0(12)	13.3(12)	3.0(12)
C8	50(2)	28.0(17)	28.3(15)	-2.0(13)	15.0(15)	-12.1(15)
C9	33.0(16)	29.7(15)	20.9(13)	-0.6(11)	12.4(12)	3.6(13)

Table 4 Bond Lengths for complex_16.

Atom	Atom	Length/Å	Atom	Atom	Length/Å
Pd1	Cl1[1]	2.3257(9)	C1	C2	1.399(4)
Pd1	Cl1	2.4641(10)	C1	C6	1.386(4)
Pd1	N1	2.068(2)	C2	C3	1.387(5)
Pd1	C1	1.969(3)	C3	C4	1.373(6)
Cl2	C5	1.674(6)	C4	C5	1.389(6)
N1	C7	1.497(4)	C5	C6	1.394(5)
N1	C8	1.478(4)	C6	C7	1.500(4)
N1	C9	1.475(4)			

[1]1-X,-Y,-Z

Table 5 Bond Angles for complex_16.

Atom	Atom	Atom	Angle/°	Atom	Atom	Atom	Angle/°
Cl1[1]	Pd1	Cl1	86.10(3)	C2	C1	Pd1	126.7(3)
N1	Pd1	Cl1	96.50(7)	C6	C1	Pd1	113.9(2)
N1	Pd1	Cl1[1]	177.38(8)	C6	C1	C2	119.4(3)
C1	Pd1	Cl1[1]	94.74(10)	C3	C2	C1	120.1(3)
C1	Pd1	Cl1	177.88(10)	C4	C3	C2	120.5(3)
C1	Pd1	N1	82.65(12)	C3	C4	C5	119.9(4)
Pd1[1]	Cl1	Pd1	93.91(3)	C4	C5	Cl2	117.8(4)
C7	N1	Pd1	107.75(18)	C4	C5	C6	120.1(4)
C8	N1	Pd1	107.74(19)	C6	C5	Cl2	119.9(4)
C8	N1	C7	110.0(3)	C1	C6	C5	120.0(3)
C9	N1	Pd1	113.64(19)	C1	C6	C7	116.9(3)
C9	N1	C7	109.2(2)	C5	C6	C7	123.1(3)
C9	N1	C8	108.5(3)	N1	C7	C6	108.4(2)

Complex_6c

NAc-Leu and primary coordination sphere with 30% ellipsoids

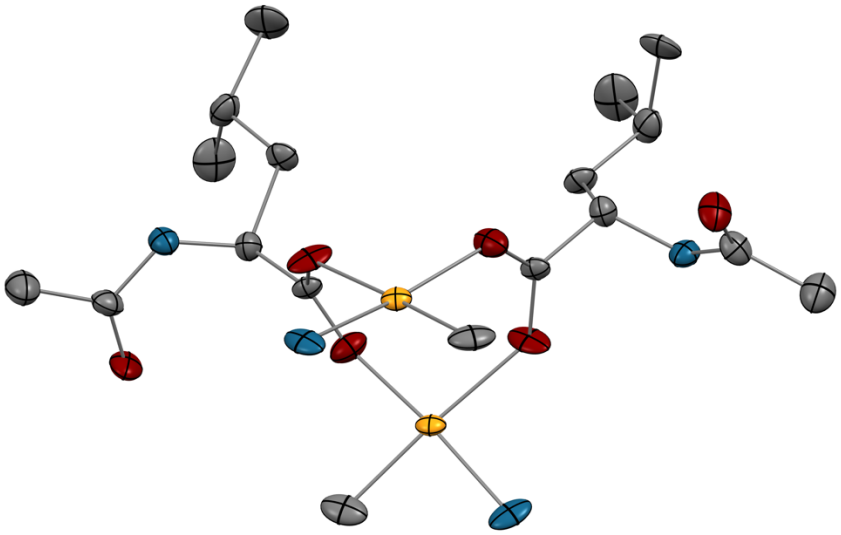

molecular structure complex_6c with 30% ellipsoids on MPAA; dmba disorder masked

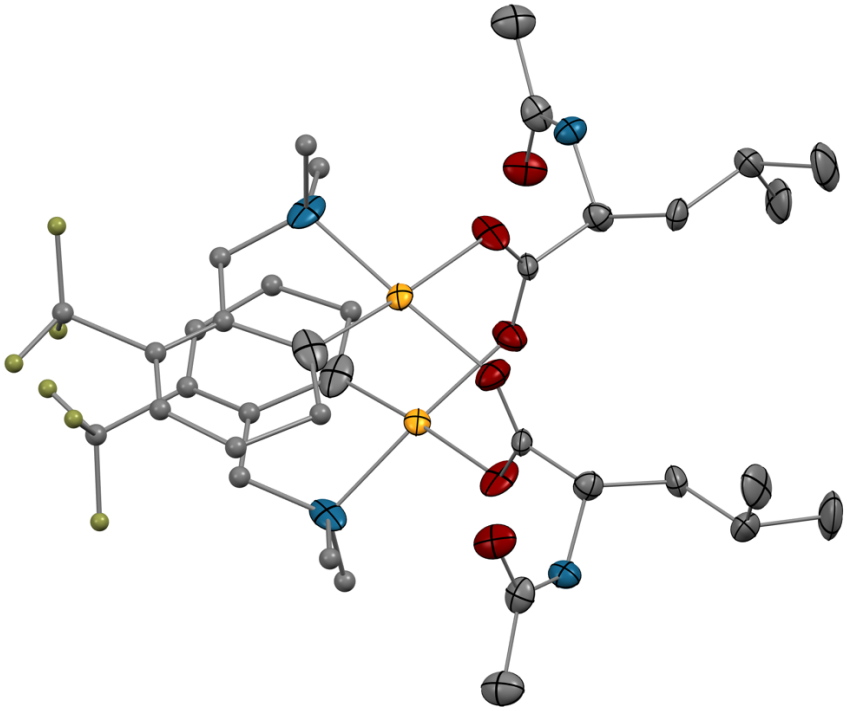

molecular structure complex_6c with disorder over dmba shown

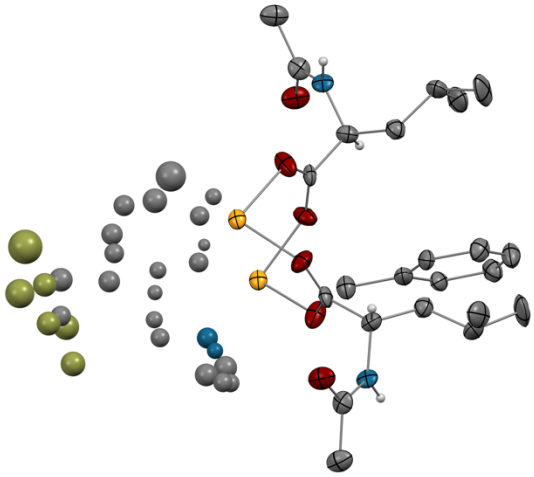

unit cell_6c with hydrogen bonding emphasized and dmba disorder masked

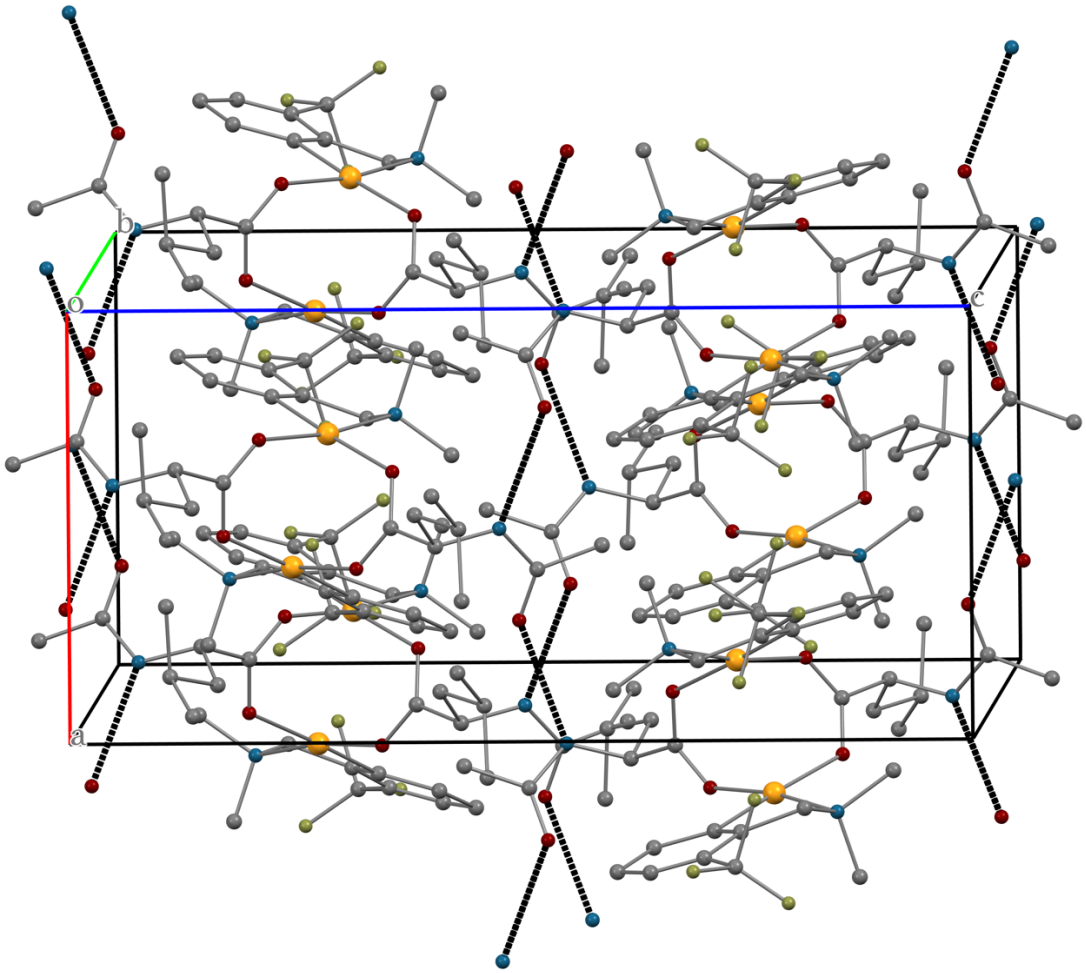

Table 1 Crystal data and structure refinement for complex_6c.

Identification code	complex_6c
Empirical formula	$C_{43}H_{58}F_6N_4O_6Pd_2$
Formula weight	1053.73
Temperature/K	100(2)
Crystal system	orthorhombic
Space group	$C222_1$
a/Å	9.2657(11)
b/Å	29.630(4)
c/Å	19.311(3)
α/°	90
β/°	90
γ/°	90
Volume/Å^3	5301.8(12)
Z	4
ρ_{calc}g/cm^3	1.320
μ/mm^{-1}	0.742
F(000)	2152.0
Crystal size/mm^3	0.28 × 0.14 × 0.08
Radiation	MoKα (λ = 0.71073)
2Θ range for data collection/°	4.6 to 50.04
Index ranges	$-10 \le h \le 10$, $-34 \le k \le 29$, $-20 \le l \le 22$
Reflections collected	21110
Independent reflections	4174 [R_{int} = 0.0712, R_{sigma} = 0.0778]
Data/restraints/parameters	4174/105/271
Goodness-of-fit on F^2	1.050
Final R indexes [I>=2σ (I)]	R_1 = 0.0650, wR_2 = 0.1400
Final R indexes [all data]	R_1 = 0.0899, wR_2 = 0.1490
Largest diff. peak/hole / e Å^{-3}	2.10/-0.90
Flack parameter	0.017(19)

$R_{int} = \Sigma \mid F_o^2 - \langle F_o^2 \rangle \mid / \Sigma \mid F_o^2 \mid$

$R1 = \Sigma \mid \mid F_o \mid - \mid F_c \mid \mid / \Sigma \mid F_o \mid$

$wR2 = [\Sigma [w (F_o^2 - F_c^2)^2] / \Sigma [w (F_o^2)^2]]^{1/2}$

Goodness-of-fit = $[\Sigma [w (F_o^2 - F_c^2)^2] / (n-p)]^{1/2}$

n: number of independent reflections; p: number of refined parameters

Table 2 Fractional Atomic Coordinates (×104) and Equivalent Isotropic Displacement Parameters (Å2×103) for complex_6c. U_{eq} **is defined as 1/3 of of the trace of the orthogonalised** U_{IJ} **tensor.**

Atom	*x*	*y*	*z*	U(eq)
Pd1	1538.1(10)	6728.9(3)	7702.0(5)	35.5(3)
O1	1496(12)	7217(3)	6969(5)	51(2)
O2	-741(10)	7191(3)	6559(6)	59(3)
O3	2682(10)	7262(4)	5159(5)	57(3)
N2	512(11)	7579(4)	5366(6)	38(3)
C1	982(16)	7247(6)	4255(8)	59(4)
C2	1470(16)	7369(4)	4962(7)	44(3)
C3	-480(20)	8955(5)	6034(10)	93(7)
C4	1991(19)	8656(6)	5717(9)	75(6)
C5	380(20)	8543(5)	5766(8)	61(5)
C6	114(16)	8144(4)	6243(8)	46(4)
C7	897(15)	7705(5)	6062(7)	42(3)
C8	521(14)	7342(4)	6578(7)	37(3)
C19	5000	7357(6)	7500	48(6)
C20	5000	7860(6)	7500	48(5)
C21	3748(13)	8115(3)	7531(7)	45(4)
C22	3677(13)	8582(3)	7547(8)	53(4)
C23	5000	8800(6)	7500	63(7)
C16	3370(20)	6295(9)	8738(15)	38(7)
C17	880(30)	6309(10)	9091(13)	43(7)
N1	1851(19)	6256(6)	8495(12)	30(7)
C15	1650(30)	5814(6)	8205(15)	41(7)
C9	2310(30)	6225(7)	7188(16)	44(9)
C10	2770(30)	6283(10)	6492(14)	43(7)
C11	3250(40)	5910(11)	6095(17)	68(9)
C12	3130(30)	5504(9)	6456(16)	52(8)
C13	2750(30)	5427(6)	7144(14)	53(7)
C14	2220(20)	5816(6)	7495(17)	26(6)
C18	2740(20)	4970(6)	7485(10)	47(7)
F1	1411(15)	4896(4)	7759(8)	64(5)
F2	3704(17)	4977(5)	8017(9)	69(5)
F3	3070(20)	4643(6)	7024(10)	96(7)
C16A	3540(30)	6269(14)	8490(20)	61(13)
C17A	1120(40)	6170(14)	8909(18)	58(13)
N1A	2010(30)	6204(9)	8278(16)	50(12)
C15A	1880(30)	5783(8)	7911(17)	33(9)
C9A	2280(30)	6297(8)	6970(15)	17(8)
C10A	2660(30)	6430(11)	6285(15)	32(8)

C11A	3110(60)	6083(15)	5830(20)	104(19)
C12A	3110(40)	5646(11)	6101(19)	50(10)
C13A	2790(30)	5507(8)	6770(17)	44(9)
C14A	2300(30)	5869(7)	7190(20)	33(9)
C18A	2730(30)	5020(9)	6997(15)	63(11)
F1A	1386(19)	4918(6)	7230(11)	63(6)
F3A	2900(30)	4759(10)	6433(16)	133(12)
F2A	3770(20)	4968(7)	7489(13)	76(8)

Table 3 Anisotropic Displacement Parameters (Å2×103) for complex_6c. The Anisotropic displacement factor exponent takes the form: $-2\pi^2[h^2a^{*2}U_{11}+2hka^*b^*U_{12}+\ldots]$.

Atom	U_{11}	U_{22}	U_{33}	U_{23}	U_{13}	U_{12}
Pd1	21.9(4)	34.2(5)	50.4(6)	-1.0(5)	-4.7(5)	1.5(5)
O1	38(5)	59(6)	57(6)	21(5)	-15(6)	-5(6)
O2	29(5)	53(6)	94(9)	28(6)	-18(5)	-14(5)
O3	32(5)	86(8)	52(6)	-6(5)	9(4)	19(5)
N2	16(5)	52(7)	46(6)	1(5)	-9(5)	3(4)
C1	47(9)	84(12)	46(8)	1(8)	9(6)	20(8)
C2	26(6)	51(8)	55(7)	0(6)	7(6)	13(6)
C3	150(20)	29(9)	95(15)	-5(9)	36(15)	27(10)
C4	100(16)	53(10)	71(11)	15(8)	7(10)	-32(10)
C5	100(15)	47(9)	36(10)	8(8)	-2(10)	-1(9)
C6	45(8)	42(7)	51(10)	4(7)	-6(6)	0(6)
C7	40(8)	51(8)	35(7)	5(6)	0(6)	5(6)
C8	33(8)	20(7)	58(9)	-2(6)	-5(8)	-6(6)
C19	36(10)	39(9)	68(18)	0	-3(9)	0
C20	73(12)	38(9)	34(13)	0	0(9)	0
C21	53(8)	34(6)	47(9)	1(5)	-7(6)	-13(5)
C22	46(8)	47(7)	66(11)	-11(7)	-6(7)	13(6)
C23	62(11)	37(11)	90(20)	0	-26(12)	0

Table 4 Bond Lengths for complex_6c.

Atom	Atom	Length/Å	Atom	Atom	Length/Å
Pd1	Pd1[1]	2.9552(19)	C15	C14	1.47(3)
Pd1	O1	2.024(8)	C9	C10	1.42(3)
Pd1	O2[1]	2.113(10)	C9	C14	1.35(3)
Pd1	N1	2.095(19)	C10	C11	1.42(3)
Pd1	C9	1.93(2)	C11	C12	1.39(4)
Pd1	N1A	1.96(3)	C12	C13	1.39(4)
Pd1	C9A	2.03(2)	C13	C14	1.42(3)
O1	C8	1.234(16)	C13	C18	1.51(2)
O2	C8	1.252(15)	C18	F1	1.360(18)
O3	C2	1.228(17)	C18	F2	1.359(19)
N2	C2	1.335(16)	C18	F3	1.350(17)
N2	C7	1.441(17)	C16A	N1A	1.48(3)
C1	C2	1.48(2)	C17A	N1A	1.48(3)
C3	C5	1.55(2)	N1A	C15A	1.44(3)
C4	C5	1.53(3)	C15A	C14A	1.47(4)
C5	C6	1.518(18)	C9A	C10A	1.42(3)
C6	C7	1.529(18)	C9A	C14A	1.34(3)
C7	C8	1.508(18)	C10A	C11A	1.41(3)
C19	C20	1.49(2)	C11A	C12A	1.40(4)
C20	C21	1.385(8)	C12A	C13A	1.39(4)
C20	C21[2]	1.385(8)	C13A	C14A	1.42(3)
C21	C22	1.386(8)	C13A	C18A	1.51(3)
C22	C23	1.388(8)	C18A	F1A	1.36(2)
C16	N1	1.49(2)	C18A	F3A	1.34(3)
C17	N1	1.47(3)	C18A	F2A	1.37(2)
N1	C15	1.44(3)			

[1]-X,+Y,3/2-Z; [2]1-X,+Y,3/2-Z

Table 5 Bond Angles for complex_6c.

Atom	Atom	Atom	Angle/°	Atom	Atom	Atom	Angle/°
O1	Pd1	Pd1[1]	78.3(3)	C10	C9	Pd1	120.2(19)
O1	Pd1	O2[1]	90.2(4)	C14	C9	Pd1	116(2)
O1	Pd1	N1	172.5(6)	C14	C9	C10	123(2)
O1	Pd1	C9A	88.2(9)	C9	C10	C11	121(3)
O2[1]	Pd1	Pd1[1]	80.9(3)	C12	C11	C10	112(3)
N1	Pd1	Pd1[1]	109.0(5)	C13	C12	C11	130(2)
N1	Pd1	O2[1]	89.3(7)	C12	C13	C14	114(2)
C9	Pd1	Pd1[1]	102.8(9)	C12	C13	C18	124.4(19)
C9	Pd1	O1	101.5(10)	C14	C13	C18	121(2)
C9	Pd1	O2[1]	168.2(10)	C9	C14	C15	115.7(18)
C9	Pd1	N1	78.9(11)	C9	C14	C13	120(3)
N1A	Pd1	O1	165.3(10)	C13	C14	C15	124(2)
N1A	Pd1	O2[1]	102.1(10)	F1	C18	C13	108.6(16)
N1A	Pd1	C9A	79.6(13)	F2	C18	C13	108.3(17)
C9A	Pd1	O2[1]	178.3(10)	F2	C18	F1	107.7(15)
C8	O1	Pd1	131.0(9)	F3	C18	C13	110.9(16)
C8	O2	Pd1[1]	122.5(9)	F3	C18	F1	110.0(16)
C2	N2	C7	120.1(11)	F3	C18	F2	111.3(17)
O3	C2	N2	123.2(13)	C16A	N1A	Pd1	106(2)
O3	C2	C1	120.1(12)	C17A	N1A	Pd1	113(2)
N2	C2	C1	116.7(13)	C17A	N1A	C16A	108(3)
C4	C5	C3	110.6(15)	C15A	N1A	Pd1	113(2)
C6	C5	C3	109.0(13)	C15A	N1A	C16A	109(3)
C6	C5	C4	111.7(14)	C15A	N1A	C17A	107(2)
C5	C6	C7	116.4(13)	N1A	C15A	C14A	107(2)
N2	C7	C6	108.5(11)	C10A	C9A	Pd1	123.9(19)
N2	C7	C8	111.9(11)	C14A	C9A	Pd1	112(2)
C8	C7	C6	110.3(11)	C14A	C9A	C10A	123(2)
O1	C8	O2	126.5(12)	C11A	C10A	C9A	117(3)
O1	C8	C7	116.7(11)	C12A	C11A	C10A	116(3)
O2	C8	C7	116.8(12)	C13A	C12A	C11A	128(3)
C21	C20	C19	123.0(8)	C12A	C13A	C14A	112(3)
C21[2]	C20	C19	123.0(8)	C12A	C13A	C18A	124(2)
C21[2]	C20	C21	113.9(16)	C14A	C13A	C18A	123(3)
C20	C21	C22	125.8(13)	C9A	C14A	C15A	117(2)
C21	C22	C23	114.9(13)	C9A	C14A	C13A	123(3)
C22	C23	C22[2]	124.6(16)	C13A	C14A	C15A	120(3)
C16	N1	Pd1	108.1(14)	F1A	C18A	C13A	110(2)
C17	N1	Pd1	114.6(15)	F1A	C18A	F2A	113(2)
C17	N1	C16	109(2)	F3A	C18A	C13A	108(2)

C15	N1	Pd1	107.8(16)	F3A	C18A	F1A	104(2)
C15	N1	C16	108.6(18)	F3A	C18A	F2A	115(2)
C15	N1	C17	108.7(19)	F2A	C18A	C13A	106(2)
N1	C15	C14	108.2(17)				

Complex_S1.4

molecular structure complex_S1.4 with 30% ellipsoids

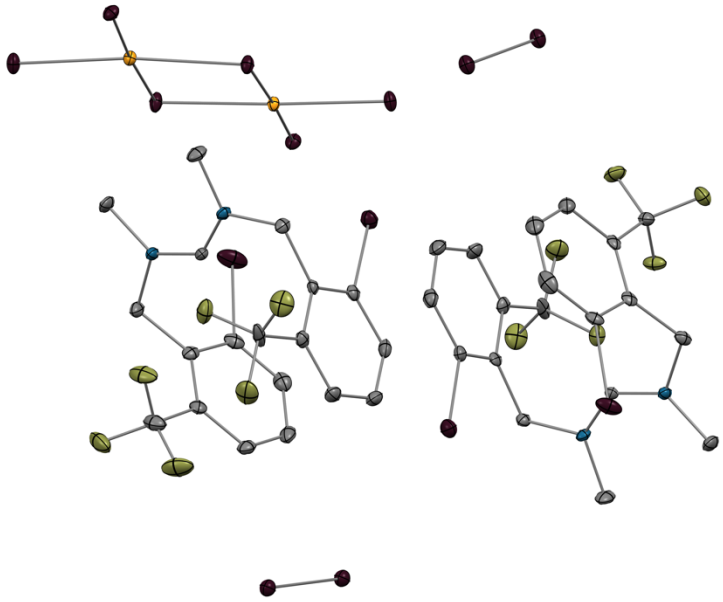

organic formamidinium fragment in complex_S1.4 with 50% ellipsoids

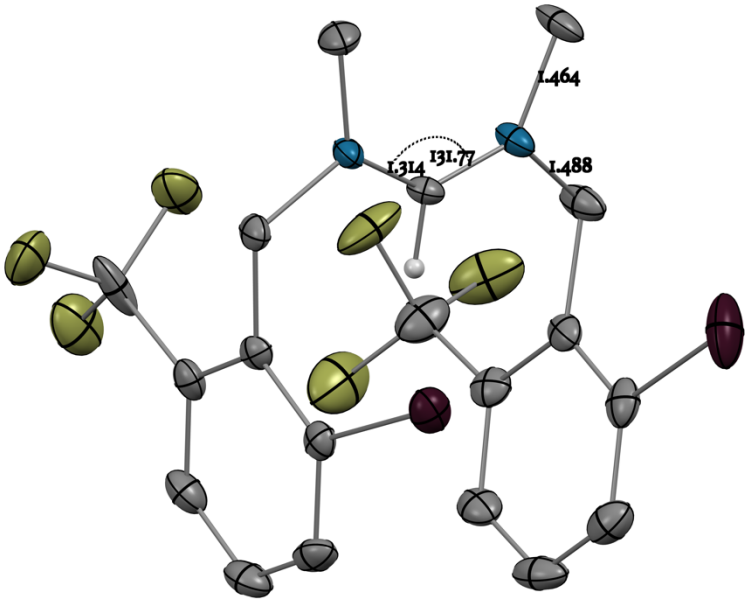

inorganic iodopalladate fragment in complex_S1.4 with 50% ellipsoids

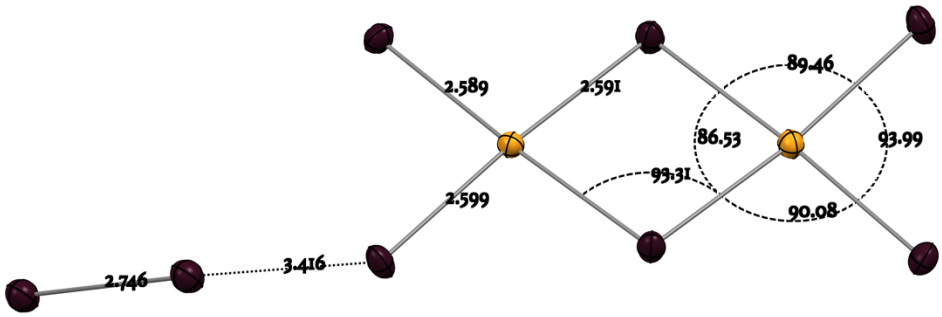

unit cell complex_S1.4 with 30% ellipsoids

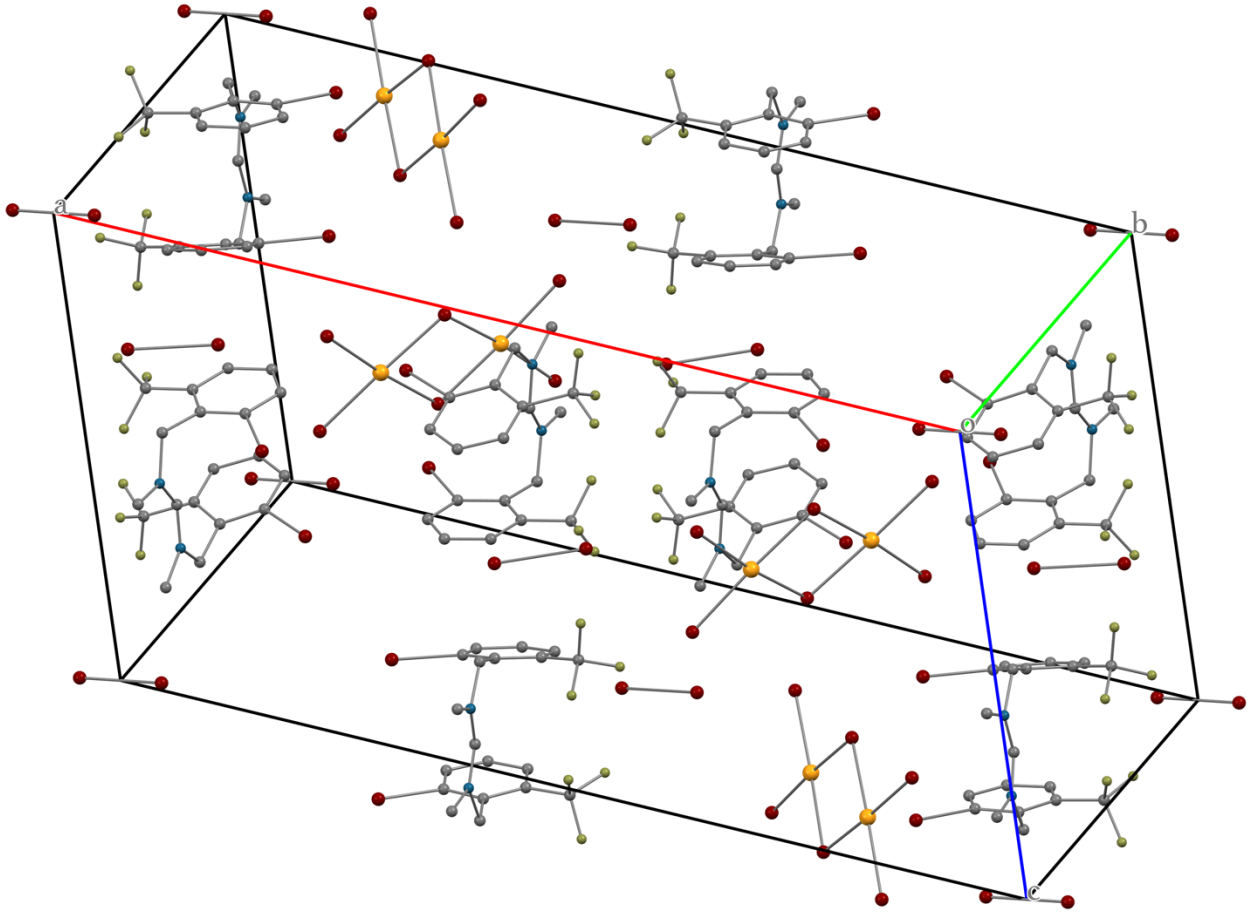

iodine/iodide networks in complex_S1.4

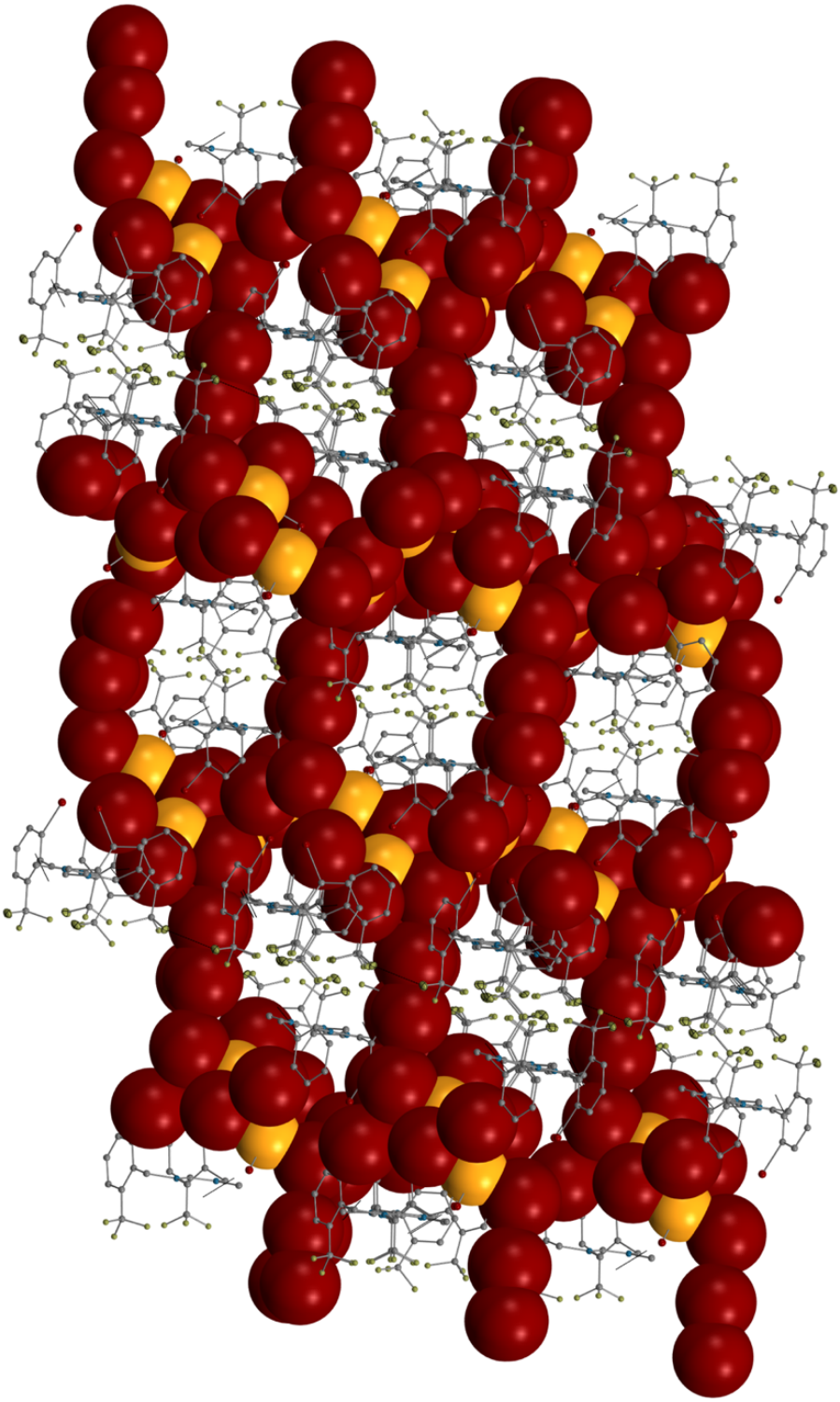

Table 1 Crystal data and structure refinement for complex_S1.4.

Identification code	complex_S1.4
Empirical formula	$C_{38}H_{34}F_{12}I_{12}N_4Pd_2$
Formula weight	2510.29
Temperature/K	100(2)
Crystal system	monoclinic
Space group	$P2_1/c$
a/Å	28.337(5)
b/Å	13.971(3)
c/Å	14.982(3)
α/°	90
β/°	102.276(5)
γ/°	90
Volume/Å^3	5795.8(19)
Z	4
ρ_{calc}g/cm^3	2.877
μ/mm^{-1}	7.083
F(000)	4504.0
Crystal size/mm^3	0.32 × 0.21 × 0.14
Radiation	MoKα (λ = 0.71073)
2Θ range for data collection/°	4.414 to 54.392
Index ranges	-36 ≤ h ≤ 36, -17 ≤ k ≤ 17, -19 ≤ l ≤ 19
Reflections collected	155125
Independent reflections	12881 [R_{int} = 0.0515, R_{sigma} = 0.0247]
Data/restraints/parameters	12881/0/617
Goodness-of-fit on F^2	1.069
Final R indexes [I>=2σ (I)]	R_1 = 0.0279, wR_2 = 0.0562
Final R indexes [all data]	R_1 = 0.0406, wR_2 = 0.0603
Largest diff. peak/hole / e Å^{-3}	2.70/-1.12

$R_{int} = \Sigma \mid F_o^2 - \langle F_o^2 \rangle \mid / \Sigma \mid F_o^2 \mid$

$R1 = \Sigma \mid \mid F_o \mid - \mid F_c \mid \mid / \Sigma \mid F_o \mid$

$wR2 = [\Sigma [w (F_o^2 - F_c^2)^2] / \Sigma [w (F_o^2)^2]]^{1/2}$

Goodness-of-fit = $[\Sigma [w (F_o^2 - F_c^2)^2] / (n-p)]^{1/2}$

n: number of independent reflections; p: number of refined parameters

Table 2 Fractional Atomic Coordinates (×104) and Equivalent Isotropic Displacement Parameters (Å2×103) for complex_S1.4. U_{eq} is defined as 1/3 of the trace of the orthogonalised U_{IJ} tensor.

Atom	*x*	*y*	*z*	U(eq)
Pd1	2009.6(2)	3579.0(2)	4787.8(2)	14.11(7)
Pd2	3007.0(2)	1736.0(2)	5091.6(2)	14.97(7)
I1	1328.3(2)	4063.9(2)	3420.0(2)	19.23(7)
I2	1718.5(2)	4736.2(2)	5918.3(2)	20.49(7)
I3	2336.7(2)	2366.8(2)	3758.0(2)	21.40(7)
I4	2703.5(2)	3004.4(2)	6105.4(2)	19.00(7)
I5	3310.0(2)	609.4(2)	3953.9(2)	23.29(7)
I6	3650.2(2)	1163.6(2)	6489.6(2)	20.08(7)
I7	491.6(2)	4875.2(2)	5227.0(2)	23.55(7)
I8	4519.6(2)	10239.9(2)	4719.7(2)	23.39(7)
I9	2136.2(2)	10632.3(3)	6170.0(2)	33.42(9)
I10	2155.9(2)	9166.7(2)	3732.9(2)	26.88(8)
F1	64.3(11)	8390(2)	2026(2)	39.1(8)
F2	-150.9(11)	7805(2)	3202(2)	38.1(7)
F3	90.9(10)	9253(2)	3206.6(18)	26.9(6)
F4	241.9(9)	9087(2)	5102.8(18)	27.2(6)
F5	228(1)	8843(2)	6510.6(19)	30.9(7)
F6	261.2(10)	7657.3(19)	5613(2)	32.0(7)
N1	1002.1(13)	10435(2)	3482(2)	14.8(7)
N2	959.4(13)	10828(2)	5013(2)	15.7(8)
C1	163.5(19)	8389(4)	2901(4)	32.3(13)
C2	683.9(17)	8038(3)	3300(3)	19.5(10)
C3	752.8(19)	7127(3)	3651(3)	25.2(11)
C4	1218(2)	6793(3)	4005(3)	29.3(12)
C5	1610.4(18)	7379(3)	4018(3)	25.0(11)
C6	1538.4(17)	8306(3)	3661(3)	18.9(9)
C7	1081.8(16)	8650(3)	3279(3)	16.6(9)
C8	1013.7(16)	9623(3)	2845(3)	16.8(9)
C9	983(2)	11371(3)	3031(3)	31.0(12)
C10	991.4(15)	10261(3)	4335(3)	14.0(8)
C11	919(2)	11880(3)	4998(3)	27.9(11)
C12	974.1(17)	10403(3)	5925(3)	19.2(10)
C13	1222.6(16)	9436(3)	6076(3)	17.2(9)
C14	1724.5(16)	9396(3)	6257(3)	20.5(10)
C15	1966.8(18)	8540(4)	6454(3)	31.4(12)
C16	1711.1(19)	7698(4)	6471(3)	30.4(12)
C17	1215.9(18)	7710(4)	6270(3)	25.0(11)
C18	973.0(16)	8574(3)	6069(3)	18.2(9)

C19	431.2(17)	8540(3)	5830(3)	21.3(10)
I11	2879.7(2)	6109.8(2)	6320.2(2)	25.93(7)
I12	2739.9(2)	5050.6(3)	3722.3(2)	44.12(11)
F7	4989.0(11)	6588(2)	7878(2)	42.0(8)
F8	5211.1(11)	7267(2)	6767(2)	43.1(8)
F9	4939.6(10)	5835(2)	6634(2)	35.4(7)
F10	4862.2(12)	7291(3)	4328(3)	52.1(10)
F11	4760.9(11)	5852(2)	4740(2)	43.3(9)
F12	4747.0(12)	6152(3)	3338(2)	47.2(9)
N3	3940.2(14)	4397(3)	4801(2)	18.5(8)
N4	4016.9(13)	4724(2)	6392(2)	15.9(8)
C20	4884.7(18)	6676(4)	7012(4)	32.3(13)
C21	4374.3(17)	7076(3)	6663(3)	19.6(10)
C22	4320.4(18)	8016(3)	6357(3)	24.6(11)
C23	3864.8(19)	8406(3)	6076(3)	26.9(11)
C24	3461.6(18)	7867(3)	6082(3)	23.9(11)
C25	3516.7(16)	6907(3)	6382(3)	17.7(9)
C26	3966.5(16)	6507(3)	6688(3)	15.3(9)
C27	4021.9(17)	5501(3)	7071(3)	18.9(9)
C28	4083.7(19)	3777(3)	6818(3)	26.3(11)
C29	3962.2(15)	4935(3)	5521(3)	15.0(9)
C30	3949(2)	3351(3)	4754(3)	28.1(12)
C31	3910.3(19)	4858(3)	3895(3)	24.6(11)
C32	3747.9(17)	5892(3)	3848(3)	19.9(10)
C33	3259.1(18)	6118(4)	3724(3)	24.2(11)
C34	3103.2(19)	7062(4)	3647(3)	28.0(11)
C35	3428(2)	7787(4)	3690(3)	30.4(12)
C36	3914.1(19)	7596(3)	3832(3)	25.1(11)
C37	4077.3(17)	6658(3)	3913(3)	21.6(10)
C38	4607.3(19)	6488(4)	4073(4)	32.9(12)

Table 3 Anisotropic Displacement Parameters (Å2×103) for complex_S1.4. The Anisotropic displacement factor exponent takes the form: $-2\pi^2[h^2a^{*2}U_{11}+2hka^*b^*U_{12}+\ldots]$.

Atom	U_{11}	U_{22}	U_{33}	U_{23}	U_{13}	U_{12}
Pd1	15.01(17)	15.08(16)	12.10(15)	-1.06(12)	2.52(13)	2.00(13)
Pd2	15.33(17)	13.94(16)	15.56(16)	-1.11(13)	3.10(13)	1.73(13)
I1	22.70(16)	19.01(15)	14.38(14)	1.05(11)	0.33(11)	3.79(12)
I2	16.35(15)	27.29(16)	17.93(14)	-7.13(12)	3.90(11)	4.40(12)
I3	24.62(16)	23.28(15)	14.72(14)	-4.50(11)	0.66(12)	8.64(13)
I4	20.33(15)	20.71(15)	14.42(14)	-3.07(11)	0.28(11)	5.69(12)

I5	20.10(15)	25.61(16)	24.17(16)	-8.67(13)	4.74(12)	4.92(13)
I6	21.58(16)	17.34(14)	19.69(15)	2.43(11)	0.75(12)	2.93(12)
I7	21.46(16)	29.39(16)	20.17(15)	-2.27(13)	5.26(12)	2.02(13)
I8	25.60(16)	21.75(15)	23.61(16)	-1.91(12)	6.97(13)	-1.03(13)
I9	26.71(18)	49.1(2)	22.41(16)	4.06(15)	0.59(13)	-17.74(16)
I10	21.93(16)	29.13(17)	31.20(17)	0.44(14)	9.29(13)	1.63(13)
F1	37.0(18)	48(2)	26.4(16)	-6.0(14)	-6.8(14)	4.4(15)
F2	26.8(16)	34.8(17)	52(2)	-7.0(15)	5.8(14)	-10.8(14)
F3	22.6(15)	28.2(15)	29.0(15)	-6.6(12)	3.6(12)	3.2(12)
F4	20.7(15)	28.9(15)	29.5(15)	12.8(12)	-0.3(12)	-3.6(12)
F5	28.1(16)	35.7(17)	33.8(16)	1.4(13)	17.9(13)	1.9(13)
F6	29.8(16)	20.0(14)	45.8(18)	4.4(13)	7.0(14)	-6.8(13)
N1	19.6(19)	10.6(17)	12.9(17)	2.6(14)	0.8(15)	0.5(15)
N2	21(2)	12.1(17)	15.2(18)	-0.9(14)	5.5(15)	-2.9(15)
C1	37(3)	28(3)	40(3)	-30(2)	25(3)	-21(2)
C2	27(3)	18(2)	14(2)	-6.8(18)	4.2(18)	-1(2)
C3	33(3)	15(2)	29(3)	-4(2)	10(2)	-5(2)
C4	46(3)	16(2)	28(3)	4(2)	12(2)	5(2)
C5	27(3)	26(3)	22(2)	2(2)	6(2)	10(2)
C6	24(2)	18(2)	17(2)	-2.8(18)	8.6(19)	1.2(19)
C7	27(2)	17(2)	8.4(19)	-2.2(16)	8.1(18)	-1.2(19)
C8	23(2)	16(2)	12(2)	1.0(17)	4.6(18)	-0.4(18)
C9	57(4)	19(2)	19(2)	8(2)	13(2)	1(2)
C10	13(2)	14(2)	15(2)	0.2(17)	4.0(17)	-1.0(17)
C11	46(3)	12(2)	28(3)	-3(2)	14(2)	-3(2)
C12	23(2)	22(2)	13(2)	-2.4(18)	4.6(18)	-7.3(19)
C13	23(2)	23(2)	6.3(19)	1.3(17)	3.3(17)	-0.6(19)
C14	21(2)	28(3)	12(2)	4.4(19)	3.1(18)	-4(2)
C15	19(3)	51(3)	24(3)	5(2)	2(2)	8(2)
C16	38(3)	31(3)	24(3)	8(2)	8(2)	12(2)
C17	31(3)	24(2)	21(2)	5(2)	8(2)	6(2)
C18	23(2)	24(2)	9(2)	3.3(17)	6.9(18)	4(2)
C19	26(3)	18(2)	21(2)	2.5(19)	9(2)	-3(2)
I11	20.53(16)	28.77(17)	29.23(17)	-3.70(13)	6.94(13)	-1.86(13)
I12	43.3(2)	60.5(3)	25.69(18)	-1.31(17)	0.85(16)	-31.3(2)
F7	28.1(17)	51(2)	39.6(19)	-0.7(16)	-7.9(14)	4.8(15)
F8	24.1(16)	46(2)	60(2)	-10.5(17)	11.5(15)	-10.5(15)
F9	24.3(16)	32.9(17)	48.6(19)	-12.9(14)	7.0(14)	5.0(13)
F10	33.0(19)	48(2)	71(2)	19.3(19)	2.8(17)	-15.7(17)
F11	26.2(17)	53(2)	49(2)	33.0(17)	4.5(14)	7.6(15)
F12	39.8(19)	59(2)	52(2)	21.6(18)	29.7(17)	17.0(17)
N3	29(2)	11.2(18)	17.2(19)	-1.2(15)	10.3(16)	-1.9(16)

N4	21(2)	11.0(17)	15.1(18)	−1.5(14)	2.3(15)	−1.9(15)
C20	25(3)	34(3)	44(3)	−29(3)	21(2)	−16(2)
C21	22(2)	20(2)	17(2)	−7.1(18)	5.2(18)	−2.3(19)
C22	31(3)	18(2)	27(3)	−5(2)	10(2)	−7(2)
C23	39(3)	14(2)	29(3)	1(2)	12(2)	−1(2)
C24	29(3)	23(2)	20(2)	−0.2(19)	7(2)	12(2)
C25	21(2)	21(2)	11(2)	−2.0(17)	4.8(18)	0.4(19)
C26	18(2)	17(2)	12(2)	−2.3(17)	6.0(17)	2.3(18)
C27	27(3)	17(2)	11(2)	−1.0(17)	1.1(18)	−0.4(19)
C28	37(3)	17(2)	22(2)	5.9(19)	0(2)	2(2)
C29	18(2)	10(2)	18(2)	0.8(17)	6.4(18)	0.7(17)
C30	48(3)	11(2)	28(3)	−5.7(19)	15(2)	−3(2)
C31	44(3)	16(2)	17(2)	−1.2(18)	13(2)	2(2)
C32	30(3)	18(2)	11(2)	2.2(17)	2.8(19)	−1(2)
C33	27(3)	32(3)	12(2)	2.7(19)	1.8(19)	−6(2)
C34	27(3)	36(3)	22(2)	5(2)	5(2)	8(2)
C35	50(3)	21(3)	24(3)	7(2)	15(2)	13(2)
C36	38(3)	18(2)	20(2)	5.4(19)	7(2)	−1(2)
C37	27(3)	23(2)	15(2)	5.5(19)	6.5(19)	1(2)
C38	31(3)	36(3)	33(3)	15(2)	9(2)	0(2)

Table 4 Bond Lengths for complex_S1.4.

Atom	Atom	Length/Å	Atom	Atom	Length/Å
Pd1	I1	2.5891(5)	C14	C15	1.379(7)
Pd1	I2	2.5994(5)	C15	C16	1.384(8)
Pd1	I3	2.5916(5)	C16	C17	1.371(7)
Pd1	I4	2.5996(5)	C17	C18	1.390(6)
Pd2	I3	2.6004(5)	C18	C19	1.502(6)
Pd2	I4	2.5965(5)	I11	C25	2.106(5)
Pd2	I5	2.5967(5)	I12	C33	2.095(5)
Pd2	I6	2.5934(5)	F7	C20	1.273(6)
I7	I7[1]	2.7460(8)	F8	C20	1.348(6)
I8	I8[2]	2.7560(8)	F9	C20	1.329(5)
I9	C14	2.104(5)	F10	C38	1.345(6)
I10	C6	2.107(5)	F11	C38	1.340(6)
F1	C1	1.281(6)	F12	C38	1.332(6)
F2	C1	1.355(6)	N3	C29	1.305(5)
F3	C1	1.322(5)	N3	C30	1.463(5)
F4	C19	1.346(5)	N3	C31	1.489(6)
F5	C19	1.341(5)	N4	C27	1.486(5)

F6	C19	1.338(5)	N4	C28	1.464(5)
N1	C8	1.487(5)	N4	C29	1.314(5)
N1	C9	1.467(5)	C20	C21	1.535(7)
N1	C10	1.308(5)	C21	C22	1.389(6)
N2	C10	1.306(5)	C21	C26	1.410(6)
N2	C11	1.473(5)	C22	C23	1.382(7)
N2	C12	1.483(5)	C23	C24	1.370(7)
C1	C2	1.549(7)	C24	C25	1.414(6)
C2	C3	1.375(6)	C25	C26	1.378(6)
C2	C7	1.421(6)	C26	C27	1.513(6)
C3	C4	1.393(7)	C31	C32	1.513(6)
C4	C5	1.376(7)	C32	C33	1.394(7)
C5	C6	1.400(6)	C32	C37	1.410(6)
C6	C7	1.385(6)	C33	C34	1.388(7)
C7	C8	1.501(6)	C34	C35	1.362(7)
C12	C13	1.517(6)	C35	C36	1.373(7)
C13	C14	1.391(6)	C36	C37	1.387(6)
C13	C18	1.396(6)	C37	C38	1.489(7)

[1]-X,1-Y,1-Z; [2]1-X,2-Y,1-Z

Table 5 Bond Angles for complex_S1.4.

Atom	Atom	Atom	Angle/°	Atom	Atom	Atom	Angle/°
I1	Pd1	I2	93.815(18)	C17	C18	C19	117.3(4)
I1	Pd1	I3	90.043(18)	F4	C19	C18	112.7(4)
I1	Pd1	I4	176.602(17)	F5	C19	F4	105.9(4)
I2	Pd1	I4	89.471(18)	F5	C19	C18	113.0(4)
I3	Pd1	I2	176.015(17)	F6	C19	F4	105.4(4)
I3	Pd1	I4	86.656(18)	F6	C19	F5	106.6(4)
I4	Pd2	I3	86.536(18)	F6	C19	C18	112.6(4)
I5	Pd2	I3	89.453(18)	C29	N3	C30	128.1(4)
I5	Pd2	I4	174.013(17)	C29	N3	C31	119.2(4)
I6	Pd2	I3	176.518(17)	C30	N3	C31	112.7(3)
I6	Pd2	I4	90.075(18)	C28	N4	C27	112.3(3)
I6	Pd2	I5	93.988(19)	C29	N4	C27	119.8(3)
Pd1	I3	Pd2	93.401(18)	C29	N4	C28	127.8(4)
Pd2	I4	Pd1	93.305(18)	F7	C20	F8	108.2(4)
C9	N1	C8	112.9(3)	F7	C20	F9	109.1(5)
C10	N1	C8	119.5(3)	F7	C20	C21	112.4(4)
C10	N1	C9	127.5(4)	F8	C20	C21	109.6(5)
C10	N2	C11	127.7(4)	F9	C20	F8	106.0(4)

C10	N2	C12	118.7(4)	F9	C20	C21	111.3(4)
C11	N2	C12	113.6(3)	C22	C21	C20	119.1(4)
F1	C1	F2	109.0(4)	C22	C21	C26	120.6(4)
F1	C1	F3	109.7(5)	C26	C21	C20	120.3(4)
F1	C1	C2	112.3(4)	C23	C22	C21	120.2(5)
F2	C1	C2	108.7(4)	C24	C23	C22	120.6(4)
F3	C1	F2	105.8(4)	C23	C24	C25	119.2(4)
F3	C1	C2	111.2(4)	C24	C25	I11	116.9(3)
C3	C2	C1	119.2(4)	C26	C25	I11	121.6(3)
C3	C2	C7	121.1(4)	C26	C25	C24	121.5(4)
C7	C2	C1	119.7(4)	C21	C26	C27	121.0(4)
C2	C3	C4	120.0(5)	C25	C26	C21	117.9(4)
C5	C4	C3	120.2(4)	C25	C26	C27	121.1(4)
C4	C5	C6	119.5(5)	N4	C27	C26	115.7(3)
C5	C6	I10	117.2(3)	N3	C29	N4	131.8(4)
C7	C6	I10	121.1(3)	N3	C31	C32	114.4(4)
C7	C6	C5	121.8(4)	C33	C32	C31	120.4(4)
C2	C7	C8	121.7(4)	C33	C32	C37	117.5(4)
C6	C7	C2	117.3(4)	C37	C32	C31	122.1(4)
C6	C7	C8	121.0(4)	C32	C33	I12	121.1(4)
N1	C8	C7	115.6(3)	C34	C33	I12	117.7(4)
N2	C10	N1	131.8(4)	C34	C33	C32	121.1(5)
N2	C12	C13	114.6(3)	C35	C34	C33	120.2(5)
C14	C13	C12	119.2(4)	C34	C35	C36	120.6(5)
C14	C13	C18	117.5(4)	C35	C36	C37	120.1(5)
C18	C13	C12	123.3(4)	C32	C37	C38	121.4(4)
C13	C14	I9	120.8(3)	C36	C37	C32	120.5(4)
C15	C14	I9	117.9(4)	C36	C37	C38	118.1(4)
C15	C14	C13	121.3(4)	F10	C38	C37	112.1(5)
C14	C15	C16	120.1(5)	F11	C38	F10	105.8(4)
C17	C16	C15	120.1(5)	F11	C38	C37	112.5(4)
C16	C17	C18	119.6(5)	F12	C38	F10	107.0(4)
C13	C18	C19	121.3(4)	F12	C38	F11	106.0(4)
C17	C18	C13	121.4(4)	F12	C38	C37	113.0(4)

Complex_15

molecular structure complex_15 with 40% ellipsoids

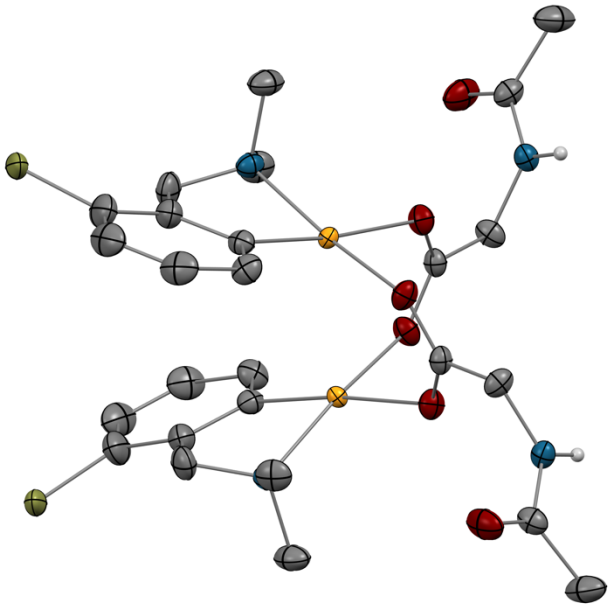

asymmetric unit complex_15 with 40% ellipsoids

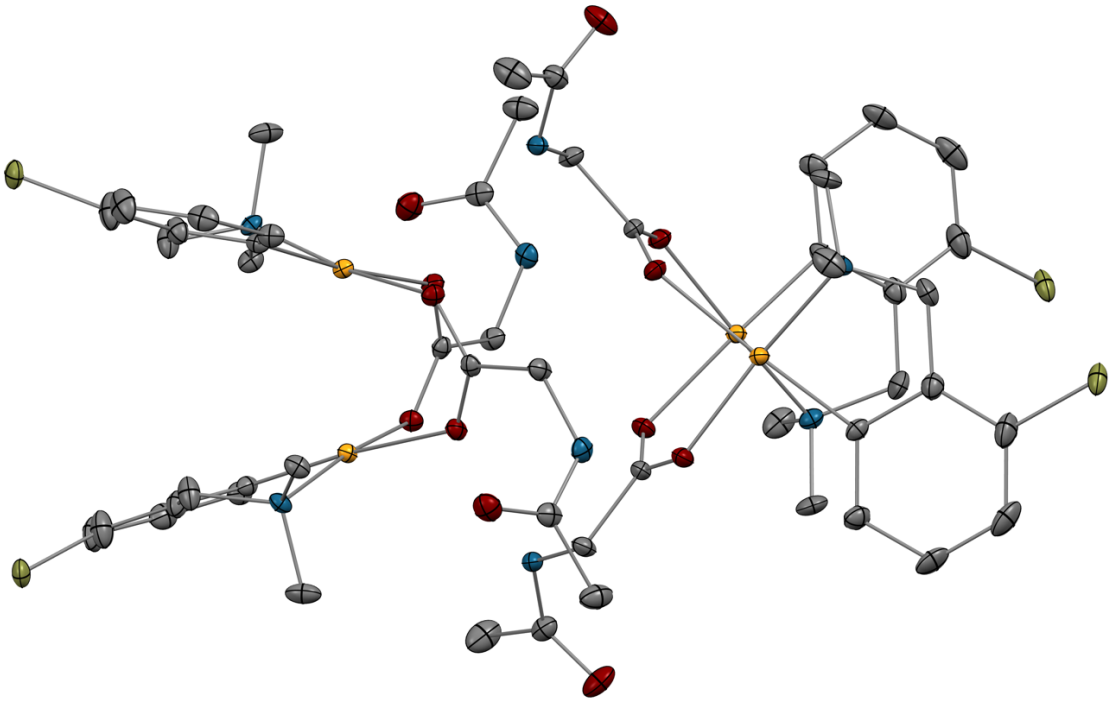

unit cell complex_15 with hydrogen bonding network

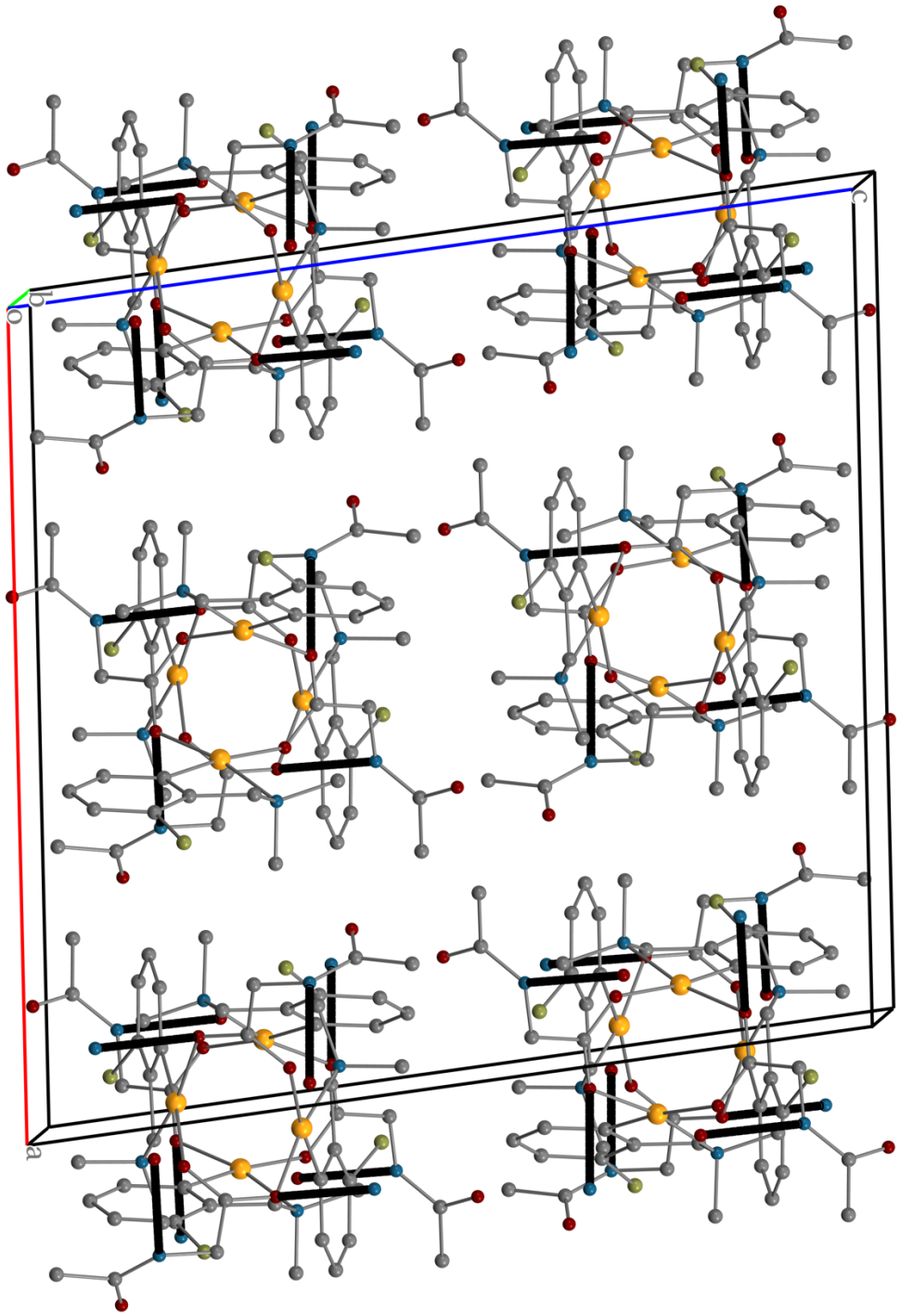

Table 1 Crystal data and structure refinement for complex_15.

Identification code	complex_15
Empirical formula	$C_{26}H_{35}ClN_4O_6Pd_2$
Formula weight	747.83
Temperature/K	100(2)
Crystal system	monoclinic
Space group	C2/c
a/Å	19.2982(5)
b/Å	16.4180(5)
c/Å	19.7030(6)
α/°	90
β/°	96.7390(10)
γ/°	90
Volume/Å^3	6199.5(3)
Z	8
ρ_{calc}g/cm^3	1.602
μ/mm^{-1}	1.630
F(000)	3008.0
Crystal size/mm^3	0.04 × 0.03 × 0.02
Radiation	synchrotron (λ = 0.41328)
2Θ range for data collection/°	2.172 to 37.75
Index ranges	-29 ≤ h ≤ 22, -25 ≤ k ≤ 25, -30 ≤ l ≤ 30
Reflections collected	85500
Independent reflections	12148 [R_{int} = 0.1001, R_{sigma} = 0.0708]
Data/restraints/parameters	12148/2/373
Goodness-of-fit on F^2	1.022
Final R indexes [I>=2σ (I)]	R_1 = 0.0402, wR_2 = 0.0831
Final R indexes [all data]	R_1 = 0.0663, wR_2 = 0.0921
Largest diff. peak/hole / e Å^{-3}	1.06/-1.09

$R_{int} = \Sigma \mid F_o^2 - \langle F_o^2 \rangle \mid / \Sigma \mid F_o^2 \mid$

$R1 = \Sigma \mid \mid F_o \mid - \mid F_c \mid \mid / \Sigma \mid F_o \mid$

$wR2 = [\Sigma [w (F_o^2 - F_c^2)^2] / \Sigma [w (F_o^2)^2]]^{1/2}$

Goodness-of-fit = $[\Sigma [w (F_o^2 - F_c^2)^2] / (n-p)]^{1/2}$

n: number of independent reflections; p: number of refined parameters

Table 2 Fractional Atomic Coordinates (×104) and Equivalent Isotropic Displacement Parameters (Å2×103) for complex_15. U_{eq} is defined as 1/3 of of the trace of the orthogonalised U_{IJ} tensor.

Atom	*x*	*y*	*z*	U(eq)

Pd1	5750.2(2)	8700.1(2)	7345.5(2)	17.32(5)
Cl1	6622.9(7)	11856.6(8)	6981.1(8)	31.5(3)
O1	5322.9(10)	7951.3(11)	6573.3(9)	24.0(4)
O2	4263.4(10)	7737.3(11)	6911.3(9)	23.8(4)
O3	3494.0(12)	7254.4(14)	4900.7(11)	39.7(5)
N1	6330.3(11)	9460.9(14)	8022.3(11)	22.3(4)
N2	3928.9(12)	6621.3(14)	5872.9(11)	20.7(4)
C1	5861.9(14)	9592.5(16)	6703.4(13)	21.9(5)
C2	5738.5(15)	9553.3(19)	5989.3(14)	28.9(6)
C3	5849.8(18)	10245(2)	5601.5(17)	38.5(8)
C4	6091.5(18)	10955(2)	5905.5(19)	44.5(9)
C5	6229.3(18)	10992(2)	6620.1(19)	40.7(8)
C6	6104.6(16)	10319.5(17)	7016.1(15)	28.3(6)
C7	6196.9(18)	10312.6(17)	7784.4(15)	32.6(7)
C8	7074.5(15)	9249(2)	7987.7(17)	35.8(7)
C9	6188.8(16)	9393(2)	8745.9(13)	31.1(6)
C10	4724.3(14)	7620.3(15)	6526.7(12)	19.7(5)
C11	4593.0(14)	7036.9(17)	5927.5(13)	24.1(5)
C12	3423.2(15)	6766.9(18)	5358.5(14)	26.7(6)
C13	2773.1(17)	6259(2)	5364.8(19)	43.4(9)
Pd2	5256.5(2)	4768.6(2)	8238.6(2)	15.86(5)
Cl2	5616.9(8)	1568.2(8)	9091.4(7)	27.5(3)
O4	6018.1(9)	5519.0(11)	7933.7(9)	20.8(4)
O5	5498.8(9)	5737.7(11)	6862.4(9)	20.2(4)
O6	7042.9(11)	5777.3(13)	6091.7(11)	33.5(5)
N3	4595.1(11)	3993.8(13)	8677.3(10)	19.1(4)
N4	6496.3(12)	6810.0(14)	6577.4(12)	23.2(5)
C14	5914.1(13)	3861.7(16)	8424.6(12)	19.5(5)
C15	6638.5(13)	3890.3(17)	8425.2(13)	23.0(5)
C16	7034.1(15)	3185.6(19)	8560.0(15)	30.8(6)
C17	6719.1(17)	2457.2(19)	8708.7(18)	38.9(8)
C18	6001.1(17)	2437.1(19)	8728.1(19)	39.8(8)
C19	5597.6(15)	3126.9(17)	8577.7(15)	26.5(6)
C20	4820.1(15)	3140.7(17)	8552.8(17)	31.8(7)
C21	3840.3(13)	4072.3(17)	8443.3(13)	22.4(5)
C22	4702.1(15)	4175(2)	9421.1(13)	32.4(7)
C23	5968.3(13)	5850.9(15)	7346.4(12)	18.7(5)
C24	6561.2(14)	6436.2(17)	7244.9(13)	23.2(5)
C25	6711.3(14)	6419.2(18)	6036.8(14)	25.5(6)
C26	6550.9(17)	6849(2)	5360.9(15)	36.8(7)

Table 3 Anisotropic Displacement Parameters (Å2×103) for complex_15. The Anisotropic displacement factor exponent takes the form: $-2\pi^2[h^2a^{*2}U_{11}+2hka^*b^*U_{12}+\ldots]$.

Atom	U_{11}	U_{22}	U_{33}	U_{23}	U_{13}	U_{12}
Pd1	20.33(10)	18.37(9)	13.29(8)	-0.04(6)	2.13(6)	-2.21(7)
Cl1	27.0(7)	16.4(6)	48.3(9)	6.8(6)	-6.7(6)	-2.3(5)
O1	31.4(11)	23.6(9)	17.0(8)	-3.9(7)	2.4(7)	-6.0(8)
O2	30.4(11)	22.7(9)	18.8(9)	-5.5(7)	4.5(7)	-0.7(8)
O3	33.6(13)	46.0(14)	39.6(12)	22.5(11)	4.2(9)	7.1(10)
N1	20.4(11)	26.2(11)	19.9(10)	-3.8(9)	0.6(8)	-1.6(9)
N2	25.3(12)	20.1(11)	16.1(10)	0.7(8)	0.6(8)	-2.9(8)
C1	19.8(13)	24.2(13)	22.0(12)	5.5(10)	4.6(9)	-0.5(10)
C2	30.4(16)	33.2(15)	24.0(13)	4.8(11)	6.6(11)	-4.8(12)
C3	36.4(18)	50(2)	30.7(16)	19.2(14)	11.1(13)	-3.2(15)
C4	38.5(19)	44(2)	52(2)	26.9(17)	10.8(16)	-4.4(15)
C5	41(2)	25.2(16)	55(2)	10.1(14)	2.0(16)	-7.6(13)
C6	29.2(16)	22.9(14)	32.5(15)	2.5(11)	1.7(12)	-3.2(11)
C7	43.1(18)	20.2(14)	33.9(16)	-9.0(11)	1.6(13)	-4.5(12)
C8	19.4(14)	47.2(19)	40.6(17)	-13.4(15)	2.4(12)	-0.2(13)
C9	33.7(16)	43.5(18)	15.7(12)	-9.3(11)	0.9(11)	-2.1(13)
C10	27.2(14)	16.9(11)	14.9(10)	-2.0(9)	1.7(9)	-0.9(9)
C11	27.3(14)	28.2(14)	16.9(11)	-6.1(10)	3.4(10)	-5.4(11)
C12	26.0(14)	29.7(15)	24.9(13)	4.8(11)	5.5(11)	4.1(11)
C13	24.0(17)	59(2)	46(2)	17.3(17)	-1.1(14)	-6.8(15)
Pd2	14.57(9)	18.14(9)	15.10(8)	1.40(6)	2.74(6)	2.53(6)
Cl2	32.4(7)	14.5(6)	36.2(7)	0.7(5)	6.1(6)	4.7(5)
O4	19.0(9)	23.5(9)	20.5(9)	0.9(7)	4.7(7)	-1.4(7)
O5	19.3(9)	21.7(9)	19.7(8)	-1.9(7)	2.9(7)	-6.3(7)
O6	32.1(12)	35.3(12)	34.7(11)	-4.6(9)	11.0(9)	-1.0(9)
N3	16.1(10)	21.7(10)	19.4(10)	5.3(8)	1.3(8)	2.5(8)
N4	19.8(11)	22.6(11)	27.7(11)	0.9(9)	5.0(9)	-6.3(8)
C14	17.7(12)	23.5(12)	16.9(11)	-2.5(9)	-0.1(9)	5.8(9)
C15	16.9(13)	29.5(14)	22.6(12)	-1(1)	2.7(9)	4.5(10)
C16	21.3(14)	39.9(17)	30.2(14)	-4.2(13)	-0.8(11)	10.6(12)
C17	32.1(18)	27.4(16)	55(2)	-3.8(14)	-3.9(14)	14.4(13)
C18	29.5(17)	24.5(15)	64(2)	3.1(15)	-0.7(15)	4.2(12)
C19	23.9(14)	21.5(13)	32.8(15)	-2.8(11)	-1.4(11)	5.3(10)
C20	20.7(14)	20.4(13)	52.3(19)	1.6(13)	-4.7(12)	-0.5(10)
C21	15.3(12)	28.1(14)	23.7(12)	4.8(10)	2.1(9)	1.1(10)
C22	25.8(15)	54(2)	17.6(12)	4.5(12)	2.4(10)	-7.4(13)
C23	19.2(12)	17.0(11)	20.8(11)	-2.1(9)	6.6(9)	-0.2(9)
C24	22.4(14)	26.8(14)	20.9(12)	-2.1(10)	4.3(10)	-8.5(10)
C25	19.7(14)	32.3(15)	24.8(13)	-0.8(11)	3.6(10)	-10.4(11)

C26	31.0(17)	52(2)	26.9(15)	5.5(14)	1.8(12)	-9.9(14)

Table 4 Bond Lengths for complex_15.

Atom	Atom	Length/Å	Atom	Atom	Length/Å
Pd1	Pd1[1]	3.0279(4)	Pd2	Pd2[1]	2.9621(4)
Pd1	O1	2.0522(18)	Pd2	O4	2.0606(18)
Pd1	O2[1]	2.1571(17)	Pd2	O5[1]	2.1512(17)
Pd1	N1	2.060(2)	Pd2	N3	2.063(2)
Pd1	C1	1.964(3)	Pd2	C14	1.963(2)
Cl1	C5	1.724(4)	Cl2	C18	1.795(4)
O1	C10	1.270(3)	O4	C23	1.272(3)
O2	C10	1.249(3)	O5	C23	1.250(3)
O3	C12	1.225(3)	O6	C25	1.231(4)
N1	C7	1.487(4)	N3	C20	1.495(4)
N1	C8	1.487(4)	N3	C21	1.481(3)
N1	C9	1.487(3)	N3	C22	1.486(3)
N2	C11	1.445(3)	N4	C24	1.443(3)
N2	C12	1.343(3)	N4	C25	1.350(4)
C1	C2	1.401(4)	C14	C15	1.399(4)
C1	C6	1.398(4)	C14	C19	1.401(4)
C2	C3	1.399(4)	C15	C16	1.394(4)
C3	C4	1.367(5)	C16	C17	1.388(5)
C4	C5	1.403(5)	C17	C18	1.391(5)
C5	C6	1.389(4)	C18	C19	1.387(4)
C6	C7	1.503(4)	C19	C20	1.496(4)
C10	C11	1.518(3)	C23	C24	1.525(3)
C12	C13	1.508(4)	C25	C26	1.507(4)

[1]1-X,+Y,3/2-Z

Table 5 Bond Angles for complex_15.

Atom	Atom	Atom	Angle/°	Atom	Atom	Atom	Angle/°
O1	Pd1	Pd1[1]	80.71(5)	O4	Pd2	Pd2[1]	83.18(5)
O1	Pd1	O2[1]	91.63(7)	O4	Pd2	O5[1]	91.70(7)
O1	Pd1	N1	169.72(8)	O4	Pd2	N3	171.35(8)
O2[1]	Pd1	Pd1[1]	77.02(5)	O5[1]	Pd2	Pd2[1]	76.37(5)
N1	Pd1	Pd1[1]	109.26(6)	N3	Pd2	Pd2[1]	105.06(6)
N1	Pd1	O2[1]	93.09(8)	N3	Pd2	O5[1]	92.80(8)
C1	Pd1	Pd1[1]	108.02(8)	C14	Pd2	Pd2[1]	108.53(7)

C1	Pd1	O1	91.96(10)	C14	Pd2	O4	92.32(9)
C1	Pd1	O2[1]	174.23(10)	C14	Pd2	O5[1]	174.01(9)
C1	Pd1	N1	82.65(10)	C14	Pd2	N3	82.66(10)
C10	O1	Pd1	126.35(16)	C23	O4	Pd2	122.73(16)
C10	O2	Pd1[1]	126.20(17)	C23	O5	Pd2[1]	127.10(16)
C7	N1	Pd1	107.77(16)	C20	N3	Pd2	107.64(16)
C7	N1	C8	109.7(2)	C21	N3	Pd2	116.76(15)
C7	N1	C9	109.1(2)	C21	N3	C20	108.9(2)
C8	N1	Pd1	106.45(17)	C21	N3	C22	107.9(2)
C8	N1	C9	108.3(2)	C22	N3	Pd2	105.58(17)
C9	N1	Pd1	115.37(17)	C22	N3	C20	109.9(2)
C12	N2	C11	122.1(2)	C25	N4	C24	121.0(2)
C2	C1	Pd1	126.4(2)	C15	C14	Pd2	126.8(2)
C6	C1	Pd1	114.2(2)	C15	C14	C19	119.3(2)
C6	C1	C2	119.4(2)	C19	C14	Pd2	113.88(19)
C3	C2	C1	119.5(3)	C16	C15	C14	119.8(3)
C4	C3	C2	121.3(3)	C17	C16	C15	120.8(3)
C3	C4	C5	119.4(3)	C16	C17	C18	119.2(3)
C4	C5	Cl1	118.2(3)	C17	C18	Cl2	119.3(2)
C6	C5	Cl1	121.3(3)	C19	C18	Cl2	119.1(3)
C6	C5	C4	120.3(3)	C19	C18	C17	120.7(3)
C1	C6	C7	115.5(2)	C14	C19	C20	116.2(2)
C5	C6	C1	120.1(3)	C18	C19	C14	120.1(3)
C5	C6	C7	124.3(3)	C18	C19	C20	123.7(3)
N1	C7	C6	108.7(2)	N3	C20	C19	108.6(2)
O1	C10	C11	113.2(2)	O4	C23	C24	114.3(2)
O2	C10	O1	126.6(2)	O5	C23	O4	126.9(2)
O2	C10	C11	120.2(2)	O5	C23	C24	118.8(2)
N2	C11	C10	114.9(2)	N4	C24	C23	113.7(2)
O3	C12	N2	122.5(3)	O6	C25	N4	122.8(3)
O3	C12	C13	122.1(3)	O6	C25	C26	122.0(3)
N2	C12	C13	115.3(2)	N4	C25	C26	115.1(3)

References

(1) Powers, D. C.; Ritter, T. *Nature Chemistry* **2009**, *1* (4), 302.
(2) Jones, T. C.; Nielson, A. J.; Rickard, C. E. *Australian Journal of chemistry* **1984**, *37*, 2179.
(3) Cope, A. C.; Friedrich, E. C. *J. Am. Chem. Soc.* **1968**, *90* (4), 909.
(4) Pfeffer, M. *Inorganic Syntheses* **1989**, *26*, 211.
(5) Diaz-de-Villegas. *Journal of Organometallic Chemistry* **1995**, *490*, 35.
(6) Hiraki, K.; Fuchita, Y.; Pfeffer, M. Inorganic Syntheses. Vol. 26, **1989**, pp 208-211.
(7) Milani, J.; Pridmore, N. E.; Whitwood, A. C.; Fairlamb, I. J. S.; Perutz, R. N. *Organometallics* **2015**, *34* (17), 4376.
(8) Tayama, E.; Kimura, H. *Angew. Chem. Int. Ed.* **2007**, *46* (46), 8869.
(9) Deprez, N. R.; Sanford, M. S. *J. Am. Chem. Soc.* **2009**, *131* (31), 11234.
(10) Powers, D. C.; Xiao, D. Y.; Geibel, M. A. L.; Ritter, T. *J. Am. Chem. Soc.* **2010**, *132* (41), 14530.
(11) Ryabov, A. D. *Inorg. Chem.* **1987**, *26*, 1252.
(12) Laurence, C.; Legros, J.; Nicolet, P.; Vuluga, D.; Chantzis, A.; Jacquemin, D. *J Phys Chem B* **2014**, *118* (27), 7594.
(13) Bakhmutov, V. I.; Berry, J. F.; Cotton, F. A.; Ibragimov, S. *Dalton Trans.* **2005**, 1989-1992.
(14) Powers, D. C.; Geibel, M. A. L.; Klein, J. E. M. N.; Ritter, T. *J. Am. Chem. Soc.* **2009**, *131* (47), 17050.
(15) Powers, D. C.; Benitez, D.; Tkatchouk, E.; Goddard, W. A., III; Ritter, T. *J. Am. Chem. Soc.* **2010**, *132* (40), 14092.
(16) Cai, G.; Fu, Y.; Li, Y.; Wan, X.; Shi, Z. *J. Am. Chem. Soc.* **2007**, *129* (24), 7666.
(17) Pregosin, P.G., Kumar, A. Fernandez, I. Chem. Rev. **2005,** 105, 2977–2998